THE UNIVERSITY LIBRARY

PROTECTION OF AUTHOR'S COPYRIGHT

SEDIMENTOLOGY, STRATIGRAPHY AND STRUCTURAL GEOLOGY OF THE BURWOOD SUB-BASIN, MOUNT HAMILTON - MARAROA RIVER AREA, WESTERN SOUTHLAND, NEW ZEALAND

MICHAEL PETER M^{C}DONNELL

A thesis submitted for the degree of
Master of Science at the
University of Otago,
Dunedin, New Zealand

9 June 2003

ABSTRACT

Structural and sedimentological evolution of the Burwood sub-Basin has resulted in the formation of a range of depositional environments in the Mount Hamilton - Mararoa River area in western Southland, New Zealand. The basement rock in the area is Triassic Murihiku Supergroup sediments (siltstone, sandstone, conglomerate and tuff). The basement is unconformably overlain by a series of sedimentary units that represent a range of depositional environments - from braided alluvial plain through to deep marine basin. With the initiation of extension during the Eocene, the Nightcaps Group began to accumulate; the Beaumont Formation was deposited by a braided river system that flowed from the southwest carrying Median Tectonic Zone and Takitimu Group detritus. Subsequent to this the Orauea Mudstone accumulated in a large lake that covered much of western Southland. During the early-mid Oligocene the tectonic regime became transtensional and the basin continued to subside, forming a sequence of marine units (Waiau Group). The early Whaingaroan Spear Peak Formation was deposited first, as a small, debris flow-dominated, proximal submarine ramp or fan. Detritus contained in this unit is derived from the Takitimu Group and Murihiku Supergroup to the southeast. As sediment supply rapidly decreased, the hemi-pelagic mudstone of the Waicoe Formation was deposited, giving way temporarily to a turbidite-dominated, outer submarine fan (Weydon Formation), flowing from the northeast, carrying Caples Terrane material, before another period of Waicoe Formation deposition. The Waitakian Haycocks Formation was then deposited as a thick, turbidite-dominated outer fan. The sediment is derived from the Caples Terrane and was transported by currents flowing from the north. Deposition of the Waiau Group reflects the change from early-mid Oligocene transtension to early Miocene transpression that continued and increased until the late Miocene, resulting in deformation in the area.

Following deposition of the Tertiary units, all the units in the area have been folded and faulted, with orientation of minor structures controlled by the regional Moonlight Fault System and Southland Syncline. Faulting in the southern part of the area parallels the north-south axis of the Southland Syncline, while in the west is parallel to the northeast-southwest Moonlight Fault System. Folding of the units is often disharmonic: the Beaumont and Spear Peak Formations are tightly folded, while the overlying units are more broadly folded. Fold axes in the west are orientated 20° from the Moonlight Fault System, suggesting that they have formed as a result of transpressional strain related to movement on this fault system. Structural analysis indicates that 30% shortening and 5km dextral shear across the area is compatible with the relative orientations of folds and faults. Comparison of bedding orientation above and below the unconformity reveals that the western limb of the Southland Syncline was sub-horizontal until the late Miocene, while the east limb dipped approximately 40°.

The structural and sedimentary record of the Burwood sub-Basin throughout the Tertiary parallels that of the other western Southland Basins, with a number sedimentary units deposited in a subsiding basin that trended north-south and was bounded by the regionally extensive Moonlight Fault System. The structure in the area also shows evidence for distributed late Cenozoic deformation that resulted in the bending of the South Island terranes.

Mount Hamilton looking west from the base of Centre Hill

ACKNOWLEDGEMENTS

I wish to thank my supervisor Richard Norris, for organising this project, reading drafts and discussing ideas, his help was very much appreciated. Thanks also to the staff in the Geology Department who have helped with various aspects of this project: Steve Read (computing), Damian Walls (geochem and crashed computers), Ewan Fordyce (microfossils), Andrew Grebneff (macro fossils), James White (discussing aspects of sedimentary geology), and John Williams and Adrien Dever for keeping the department running smoothly.

Access to land provided freely by Paul Ewing (Haycocks Station) and Chris Thompson (Burwood Station) was much appreciated, and special thanks to Barry Stevenson for providing access to Mount Hamilton Station and a bed to sleep in (and a hot shower) at the shearing quarters. Thank to the shearers and possum trappers who provided me beer and an occasional fed after a long day in the field.

Special thanks to Abby and Andy C. for reading over various drafts and fixing up the many grammatical errors. A big shout out goes to the students in the Geology Department (Anton, Simone, Izzy, J.D, Damo, Carolyn, Travis, Shaun, Allan and the rest of the geology massive) who have made writing this thesis a lot easier, with the generally non-geology related tea room conversations and after hours support.

TABLE OF CONTENTS

Appendices

TABLE OF FIGURES

LIST OF TABLES

1 INTRODUCTION

1.1 AIMS OF THE STUDY

The geology of the Mt Hamilton-Mararoa River area in western Southland has not previously been studied in detail. It is known that the study area is part of the Burwood sub-Basin (Turnbull, Uruski et al, 1993) and that it contains the lower part of the stratigraphic sequence of this basin. The main structural features of the area are also known to be associated with the regionally important Moonlight Fault System (Carter and Norris, 1977b; Norris and Carter, 1982; Turnbull, Uruski et al, 1993).

The primary aim this study of is to make a detailed geological map of the area. Using the information gained from field mapping together with previous work, I will endeavour to establish a stratigraphic sequence for the area, and fully describe the sedimentology and provenance of each rock unit. I will also attempt to map, describe and interpret geological structures in the area, and investigate their relationship with the Moonlight Fault System.

While most of the stratigraphic units in the area have been previously described (Harrington, 1982; Kirby, 1989; Turnbull, Uruski et al, 1993) there is little detailed work published on the sedimentology of the units. Therefore a major objective of this thesis, is to present detailed descriptions and interpretations of the sedimentary units in the field area.

Ultimately I am to link all the stratigraphic and structural interpretations together to form a detailed geological history of field area. This interpretation will describe how this part of the basin changed has evolved in the context of other areas in the Te Anau Basin and western Southland as a whole.

1.2 AREA COVERED

The study area encompasses 130km^2 of farmland between Mossburn and Te Anau in northwest Southland. The eastern side is bounded by Mt Hamilton, the western by the Mararoa River with Princhester Creek to the south (figure 1.2.1).

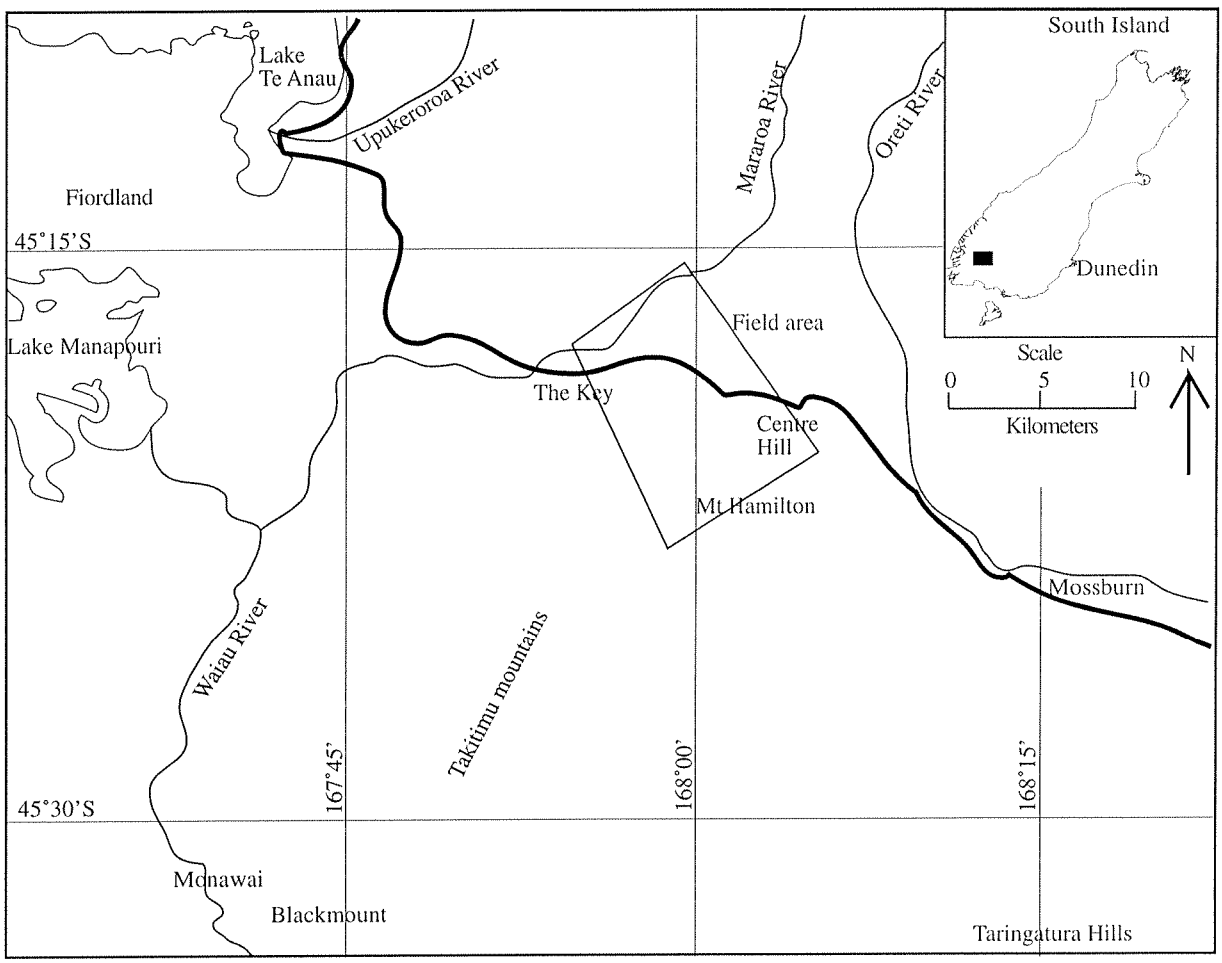

Figure 1.2.1 Location map of the South Island of New Zealand (inset) showing part of northwestern Southland. The main map of the northwestern Southland area shows the field area and other areas that are mentioned in the report.

1.3 PREVIOUS WORK

This section only records the previous geological work that relates directly to the field area. A more extensive list of the geological work done in western Southland can be found in Turnbull, Uruski et al (1993) and Turnbull (2000). Previous literature associated with the stratigraphic units in the area will be reviewed in the sections of the report that are related to those units.

The first reconnaissance geological work in the western Southland area was done in the mid-late nineteenth century by Hector (1863 and 1864), Hutton (1871) and Cox (1878). The first detailed geological report of the western Southland area was by Park (1921). Detailed studies of the Mt Hamilton-Mararoa River area were carried out by McCraw (1947), who mapped the area, described the units and attempted to date and correlate them with other units in southern New Zealand. Wood (1962) incorporated work from a number of different sources to construct the 1:250 000 Wakatipu map sheet.

No further studies were published until 1970 when Force et al, wrote a paper on Quaternary warping at Gorge Saddle, suggesting that this had resulted in changes to drainage in the area. Throughout the 1970's, mapping continued as part of the University of Otago's geology field school. The mapping done on these field camps, was included in the field guide for the Geological Society of New Zealand trip to western Southland by Carter and Norris (1977b).

In the 1970's and 1980's the geology of the basins of western Southland was extensively studied as part of a hydroelectric scheme development, and also as a potential source of hydrocarbons. McKellar (1973) studied the Quaternary geology in the Te Anau Basin as part of the hydroelectric dam investigation, including the western part of the study area.

During the 1980's a number of BSc (Hons) projects were undertaken, focusing on the stratigraphy and structure, incorporating minor work on dating and deducing the provenance of the units. Harrington (1982) worked on an area mainly west of the Mararoa River but part of the area included the Haycocks in the northwest corner of the study area. Kirby (1989) and Hall (1989) worked at Princhester Creek and Elmwood Station respectively. Amoco shot a suite of seismic refection profiles in the 1980's during regional hydrocarbon exploration. None of these covered the map area, although several were immediately to the west in the central Te Anau Basin.

Turnbull et al (1989) gave descriptions of the different units from western Southland including those in the study area that had not previously been described. Turnbull, Uruski et al (1993) published a monograph that included a lot of information about the sedimentary basins of western Southland, including maps of the study area and stratigraphic sections of the

units in the Burwood sub-Basin. The latest report with information on the study area is the Qmap of the Wakatipu area, which contains much of the available material resulting from previous work in the area (Turnbull, 2000).

1.4 REGIONAL GEOLOGY OF WESTERN SOUTHLAND

1.4.1 BASEMENT GEOLOGY

INTRODUCTION

Western Southland contains a number of different types of basement rocks. Many of these basement units are separate terranes that have been accreted together to form the southern part of New Zealand (Coombs et al, 1976; Bishop et al, 1985; Landis et al, 1999). In addition to these terranes there are the Western Province rocks, onto which the terranes have been accreted (Coombs et al, 1976; Bishop et al, 1985; Landis et al, 1999). The basement rocks in the western Southland area are important with respect to this project, as they are a possible source for the sediment observed in the field area. For this reason, a brief description of the basement rock types will be given in this chapter. Basement rocks that outcrop in the study area are discussed further in chapter two.

WESTERN PROVINCE

The basement rocks that underlie and form the southern and western parts of western Southland are part of the Western Province (see figure 1.4.1).

The Western Province is made up of metasediments that vary in metamorphic grade from sub greenschist facies in the southwest block to the granulite and amphibolite facies rocks of the Western Fiordland Orthogneiss (Ward, 1984; Bishop, 1986; Mattinson et al, 1986; Bradshaw, 1990). These metasediments have been intruded at various stages in their metamorphic history (Mortimer et al, 1999) by plutons dating from the mid Palaeozoic through to the Jurassic and Cretaceous (Bishop, 1986; Mattison et al, 1986; Bradshaw, 1990). These plutonic rocks outcrop over the greatest area of the Western Province (Mortimer et al, 1999). In the Western Fiordland block, the intrusions have undergone different degrees of metamorphism prior to and during the main regional metamorphic event (Mattison et al, 1986; Bradshaw, 1990).

The major rock types of the Western Province are the metasediments, plutonic and meta-plutonic rocks with mineral compositions ranging from granite to gabbro (Mattison et al, 1986; Bradshaw, 1990). In Eastern Fiordland, small amounts of arc volcanic rocks such as andesite and rhyolite are present (King et al, 1985; Turnbull, 1985).

Median Tectonic Zone (MTZ)

The Median Tectonic Zone (MTZ), as described by Kimbrough et al (1993), is made up of Mesozoic plutonic, volcanic and sedimentary rocks. The contacts between the MTZ and both Western Province and Brook Street Terrane are either faulted or intruded (Mortimer et al, 1999) (figure 1.4.1). Owing to the fact that the contacts with the plutonic rocks of the Western Province are mainly intrusive, Mortimer et al (1999) grouped the rocks of the MTZ with the plutonic rocks of the Western Province and called it the Median Tectonic Batholith. The use of the MTZ is retained for the purpose of this study as it has a different provenance signature to the Western Province, having not been metamorphosed to the same degree.

The MTZ rocks are generally subduction related I-type plutonics, ranging in composition from granite to gabbro (Kimbrough et al, 1994). Initially they intruded volcanic and sedimentary sequences during the Triassic, but these rocks were subsequently intruded by the intrusions that now dominate the MTZ (Kimbrough et al, 1994).

Brook Street Terrane

The Brook Street Terrane is faulted against the MTZ to the west, and the Murihiku Terrane to the east (Coombs et al, 1976; Bishop et al, 1985; Landis et al, 1999) (figure 1.4.1). The Brook Street Terrane comprises three main groups: the Longwood Complex (Challis and Lauder, 1977; Cowden et al, 1990), the Takitimu Group (Houghton, 1981; Houghton and Landis, 1989), and the Alabaster Group (Nauman, 1973; Bishop et al, 1990).

The Longwood Complex is made up of Permian basic plutonic rocks that have been intruded by granitoids possibly as young as Jurassic (Challis and Lauder, 1977; Cowden et al, 1990; Mortimer et al, 1999). These plutonic rocks form the roots of the arc volcanoes represented by the arc volcanic rocks of the Takitimu Group (Houghton, 1981; Houghton and Landis, 1989)

The Takitimu Group contains arc volcanics that are generally basaltic to andesitic in composition, while more silicic rocks such as ryo-dacite are locally abundant (Houghton, 1981). Sediments derived directly from these volcanics formed basins around the Brook Street arc, and are also present in the Takitimu Group (Houghton and Landis, 1989). The Takitimu Group is metamorphosed from zeolite to prehnite-pumpellyite facies (Houghton, 1981).

The Alabaster Group comprises the Eglinton and Skippers sub-Groups. The Eglinton sub-Group is made up of andesite-basalt volcanics and volcaniclastics (Grindley, 1958; Lindsay, 1980; Turnbull, 1986). The Skippers sub-Group contains volcaniclastics with minor schist and ultrabasic rocks (Nauman, 1973; Begg and Ballard, 1991). The rocks of the Alabaster Group have been metamorphosed from prehnite-pumpellyite facies to greenschist facies (Turnbull, 1986).

Murihiku Terrane

The Murihiku Terrane is faulted between the Takitimu Group and the Dun Mountain - Maitai Terrane (Coombs et al, 1976; Bishop et al, 1985; Landis et al, 1999) (figure 1.4.1), and consists of volcaniclastic sediments, tuffs and conglomerates (Coombs, 1950; Campbell and Coombs, 1966; Boles, 1974; Ballance and Campbell, 1993; Roser et al, 2002). Sediments have undergone zeolite metamorphism, particularly evident in the tuff beds where the glass is easily altered to zeolites (Coombs 1954; Roser et al, 2002). The Murihiku Terrane is generally thought to have acted as part of the Takitimu basement block after the Cretaceous terrane accretion (Norris and Carter, 1982; Turnbull, Uruski et al, 1993). This terrane is the main basement unit in the field area and a more detailed description of this unit is given in section 2.3.

Dun Mountain - Maitai Terrane

The Dun Mountain - Maitai Terrane lies to the north of the Murihiku Terrane and is separated by a fault that formed during the accretion of the terranes in the late Cretaceous (Coombs et al, 1976) (figure 1.4.1). This terrane is made up two distinct rock associations: the Dun Mountain Ophiolite, and the Maitai volcanics and sediments (Blake and Landis, 1973; Coombs et al, 1976).

The Dun Mountain Ophiolite exhibits the classic ophiolite sequence of ultramafics, gabbros, basaltic dykes and pillow lavas and is interpreted to be part of the Permian sea floor (Blake and Landis, 1973; Coombs et al, 1976). Towards the east the ophiolite sequence is broken up and serpentinised into a zone of serpentinite melange, hence outcrop is minimal (Coombs et al, 1976).

The Maitai Group sediments include volcaniclastic sandstone, conglomerate, siltstone, tuff and minor limestone (Aitchison et al, 1988). Fossil and radiometric dating indicate that this terrane formed in the Permian-mid Triassic (Landis, 1974; Aitchison et al, 1988). The sediments are interpreted as having been deposited on the ocean floor, now forming part of the Dun Mountain Ophiolite Belt (Landis, 1974; Coombs et al, 1976).

Caples Terrane

The Caples Terrane lies to the north of the Dun Mountain - Maitai Terrane and is separated from it by the Livingstone Fault (Coombs et al, 1976) (figure 1.4.1). The Caples Terrane is made up of a thick sequence of volcanic rocks (Kawachi, 1974) and volcaniclastic sediments (Turnbull, 1979). The volcanic rocks are predominantly basaltic pillow lava, breccia and tuff (Kawachi, 1974) while the volcaniclastics include mudstone, siltstone, sandstone and conglomerates (Turnbull, 1979). Rare fossils in the sediments indicate that the Caples Terrane was deposited in the late Permian - early Triassic (Turnbull, 1979).

The metamorphic grade of the Caples Terrane increases progressively to the north, from prehnite-pumpellyite facies near the Livingstone Fault to greenschist facies in the middle of the schist (Mortimer and Roser, 1992) (figure 1.4.1), and metamorphism is thought to have occurred in the early Jurassic - mid Cretaceous (Adams et al, 1985). The rocks in the Caples Terrane collided with the Rakaia Terrane during accretion at the Gondwana margin (Coombs et al, 1976), causing the zone between the two terranes to be metamorphosed to form the Haast Schist (Coombs et al, 1976; Mortimer and Roser, 1992). Lawsonite-albite-chlorite facies metamorphism is also present and relict blue amphibole occurs locally (Kawachi, 1974; Turnbull, 1979).

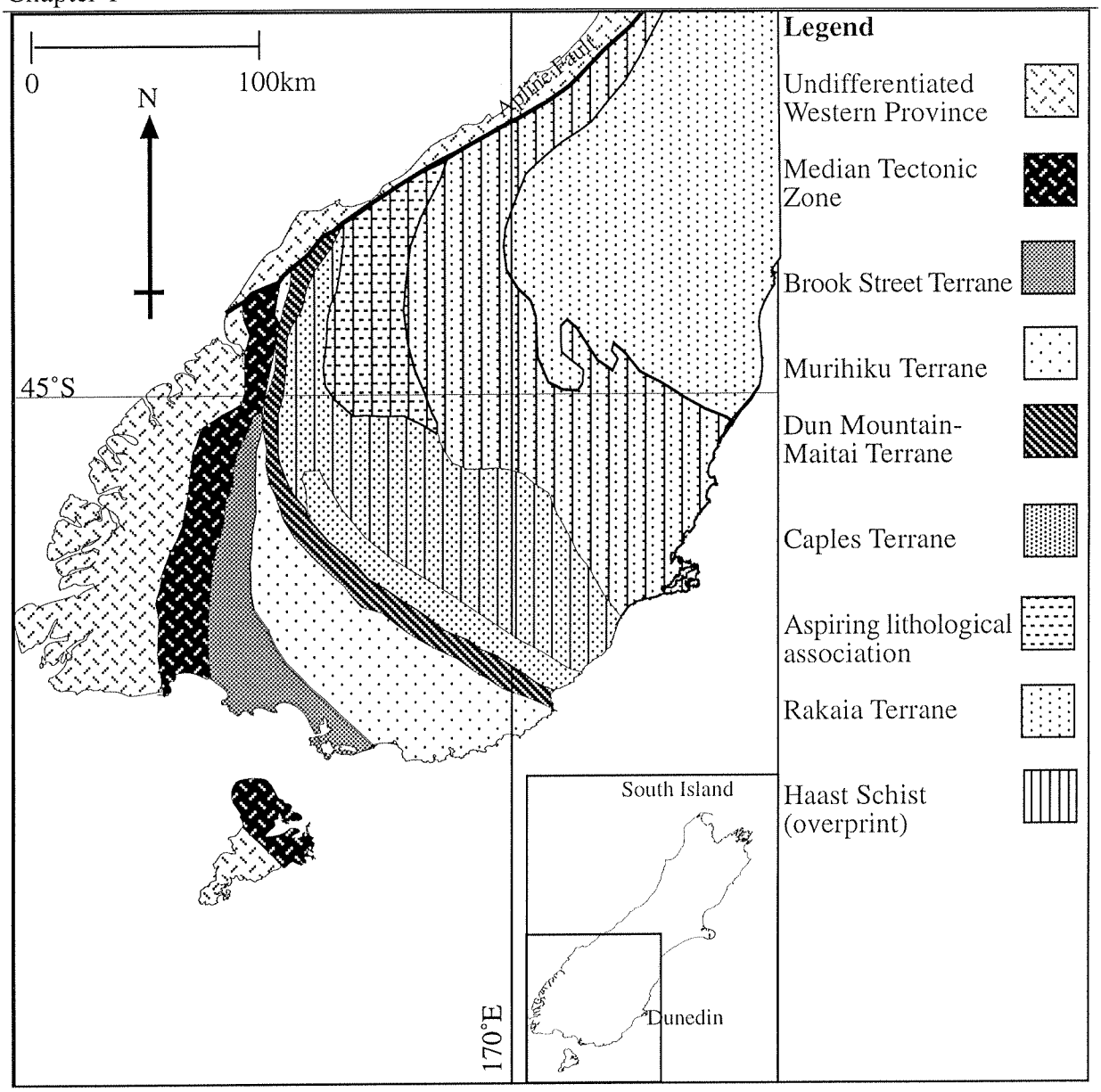

Figure 1.4.1 Map of the southern South Island showing the basement rocks in the area. Figure after Landis et al (1999).

1.4.2 CRETACEOUS-CENOZOIC GEOLOGY

Western Southland is covered by a number of sedimentary basins that contain Cretaceous-Cenozoic rocks (Carter and Norris, 1976; Norris et al, 1978; Norris and Carter, 1980; Norris and Carter, 1982; Turnbull, Uruski et al, 1993; Norris and Turnbull, 1993). The two main onshore basins are the Te Anau and Waiau Basins, while the two main offshore basins are the Solander and the Balleny Basins (Norris and Carter, 1980; Turnbull, Uruski et al, 1993) (figure 1.4.2).

The oldest sediments in the western Southland basins are the mid-late Cretaceous non-marine fluvial and lacustrine sequences and coal measures (Field and Browne et al, 1989). These sediments were deposited in an extensional environment that was related to rifting associated with the opening of the Tasman Sea (Carter and Norris, 1976; Norris et al, 1978; Norris and Carter, 1980; Norris and Carter, 1982; Laird, 1993). The Cretaceous sediments are not regionally common in western Southland and outcrop only in small area for example the Ohai Group at Ohai (Bowen, 1964; Turnbull, Uruski et al, 1993).

Cretaceous sediments in western Southland underwent a period of erosion, resulting in a regional unconformity during the Paleocene and early Eocene (Bowen, 1964; Turnbull, Uruski et al, 1993). At approximately 45 Ma (mid Eocene) a spreading ridge opened up to the southwest of the South Island (Sutherland, 1995). This extension caused discontinuities inherited from the early Cretaceous terrane accretion to be reactivated, forming the sedimentary basins that are now preserved in western Southland (Carter and Norris, 1976; Norris and Turnbull, 1993). These were infilled by mainly non-marine sediments, that were deposited in a variety of different depositional environments (Carter and Norris, 1976; Norris and Turnbull, 1993; Turnbull, Uruski et al, 1993).

During the Oligocene, plate dynamics in western Southland changed so that there was oblique dextral normal motion in the area (Carter and Norris, 1976; Sutherland, 1995), leading to the initiation of major movement along the Moonlight Fault System (Carter and Norris, 1976; Norris and Carter, 1982; Sutherland, 1995). At about this time a marine transgression occurred in response to the extension that was taking place (Carter and Norris, 1976; Norris et al, 1978; Norris and Carter, 1980; Norris and Carter, 1982; Norris and Turnbull, 1993; Turnbull, Uruski et al, 1993) resulting in a number of different depositional environments for sediments in the basins of western Southland (Turnbull, Uruski et al, 1993). These ranged from fan-deltas and submarine fans to open basin areas of low sedimentation (Turnbull, Uruski et al, 1993).

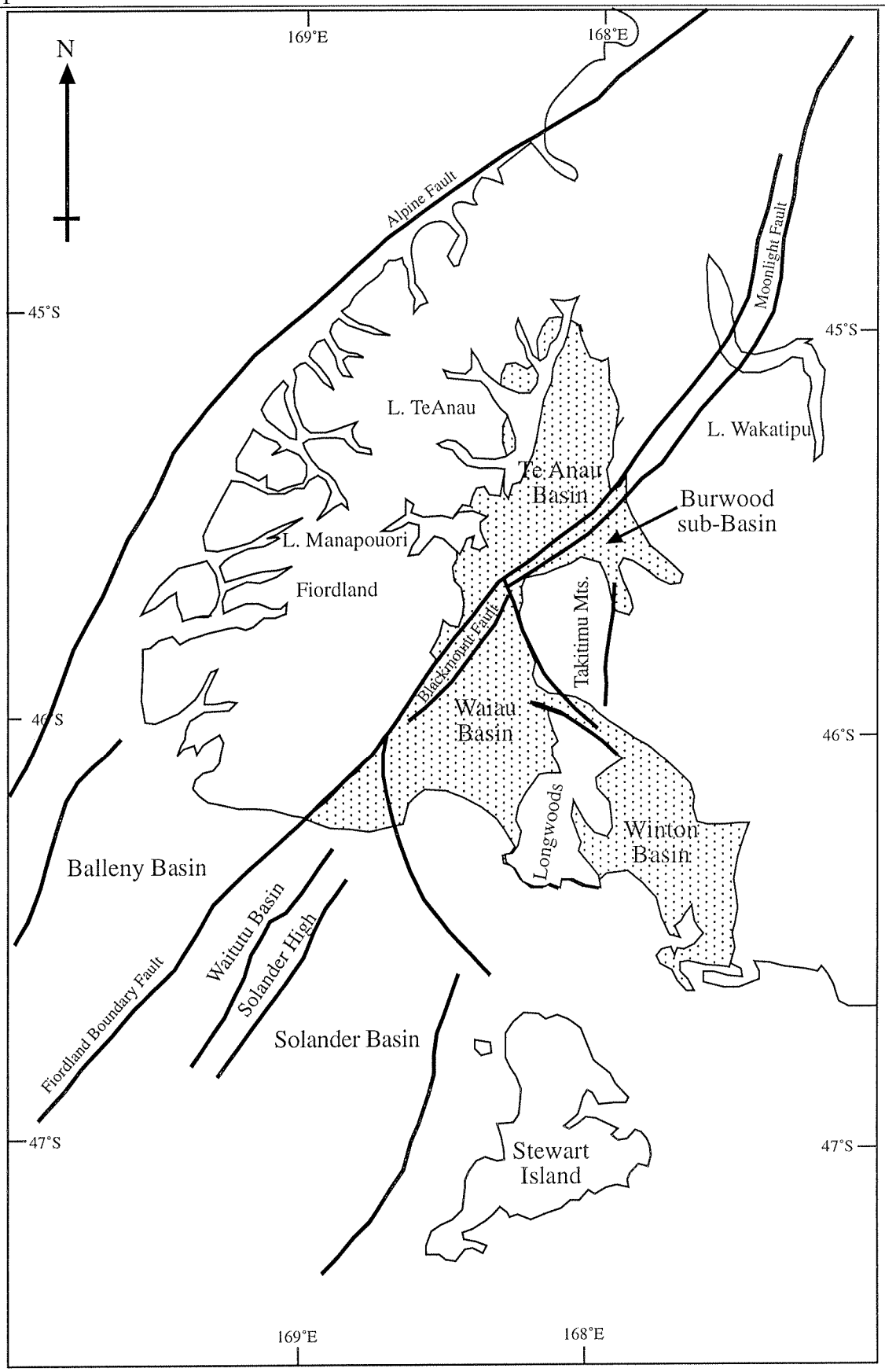

Figure 1.4.2 Map of western Southland showing the onshore sedimentary basins and some of the important Cenozoic structures in the area. Figure after Norris and Turnbull (1993).

Plate motion became more oblique throughout the Oligocene and by the early Miocene the plate boundary though New Zealand was predominantly transform in nature (Carter and Norris, 1976; Norris et al, 1978; Norris and Carter, 1980; Norris and Carter, 1982; Norris and Turnbull, 1993; Sutherland, 1995). During the Miocene (25-10 Ma) the Alpine Fault was formed as a transform feature, but by the mid-late Miocene (6 Ma) convergence began generating uplift of the Southern Alps (Carter and Norris, 1976; Carter and Norris, 1976; Norris et al, 1978; Norris and Carter, 1980; Norris and Carter, 1982; Norris et al, 1990; Norris and Turnbull, 1993).

In the early-mid Miocene submarine basin sedimentation continued, however the source of sediment started to change as more of the Caples Terrane to the north was uplifted (Norris and Turnbull, 1993). In the mid-late Miocene, as the rate of uplift in the north increased, the Te Anau Basin ceased being a marine depocentre (Turnbull, Uruski et al, 1993). Subsequently the predominantly non-marine, fluvial sediments of the Prospect Formation flooded the Te Anau Basin and the top part of the Waiau Basin, resulting in the formation of local unconformities (Turnbull, Uruski et al, 1993; Norris and Turnbull, 1993; Manville, 1994).

Finally a combination of Pliocene - Pleistocene uplift along the Alpine Fault and glaciation resulted in the deposition of non-marine sediments across the western Southland basins (Turnbull, Uruski et al, 1993; Norris and Turnbull, 1993).

1.5 METHODS

1.5.1 INTRODUCTION

A number of different investigative methods were carried out on samples collected in the field, in order to fulfil the aims of the study. These included mapping, X-ray florescence spectroscopy, heavy mineral analysis, paleocurrent investigations, modal analysis of sandstone thin sections, microfossil investigations and vitrinite reflectance studies of coal. These methods are described in this section

1.5.2 MAPPING TECHNIQUES

Standard geological mapping techniques were used to map the area, with geological observations and structural measurements made at every outcrop in the field area. Outcrops were located using GPS and logged as a waypoint, along with a number that correlated to that of the field notebook. The grid reference data was downloaded into a table using the program waypoint+ and the associated structural measurements were manually typed into the table. The structural data were then plotted onto a map of the study area using the GIS program MapInfo. The structures and geological units were mapped manually onto a paper map and then digitised. Each unit, as well as the different types of structures are saved as separate layers when all the layers are combined a complete geological map of the area is formed.

The sedimentary units described in Turnbull et al (1989) and Turnbull, Uruski et al (1993) were considered most suitable for use in this mapping project (figure 1.7.1).

1.5.3 X-RAY FLORESCENCE SPECTROSCOPY

Samples of the Tertiary sandstones in the area were analysed using x-ray florescence to determine the major and trace element concentrations. Samples of at least 200g were collected from representitive outcrops in the study area, and then crushed in a tungsten carbide swing mill for around thirty seconds. Analysis of each sample was carried out using the Philips PW1410 spectrometer. Major element analysis was done using fused glass disks while trace element concentrations were determined using pressed powder discs. Loss on ignition was determined by firing the samples for at least one hour in air at 1100°C. The data used in this report have been recalculated to 100% LOI free.

Discrimination plots have been used to determine the provenance of the sandstones. Two plots from Roser and Korsch (1988) have been used to analyse the major elements. These plots discriminate between active continental margin (ACM, P3 and P4) and arc (Arc, P1 and P2) environments. These graphs can be used as an indicator of provenance, with rocks derived from Western Province and Median Tectonic Zone plotting in the ACM, P3 and P4 fields while rocks derived from the Eastern Province may plot in the Arc, P1 and P2 fields.

The simplest classification diagram is the silica versus K_2O/Na_2O graph. Rocks that plot to the right of the line are high in silica and potassium, typical of an ACM environment. Low silica and high sodium rocks plot to the left of the line and are typical of arc environments.

Another plot using major element analysis is the discriminant function plot; this plot uses most of the major elements. F1 and F2 are calculated using the formula in Roser and Korsch (1988), which involves multiplying most of the major elements by a coefficient and adding a constant. The fields on the diagram represent differing maturity of the sediments with P1 being derived from mafic igneous rocks, P2 derived from intermediate igneous rocks, P3 derived from acid igneous rocks and P4 being recycled sediments.

The trace element data is analysed using the La/Y versus Ce/V plot of Mortimer and Roser (1992). The plot discriminates between the La and Ce enriched ACM derived rocks and the Y and V enriched arc-derived sediments.

Owing to the fact that most of the rocks in the area are not made up of first cycle sediments, using these discrimination plots involves making the assumption that no fractionation has occurred during the erosion and sedimentation processes. Petrographic studies of the sandstones and heavy minerals have helped to discriminate between sediments that have undergone a lot of fractionation and those that have not.

1.5.4 HEAVY MINERAL ANALYSIS

Heavy mineral samples from all the Cenozoic sandstones in the study area were analysed and compared with the surrounding basement rocks in order to determine the provenance of the sands.

About 500 g of each of the sandstone samples were analysed. Initially the samples had to be disaggregated by crushing them using a mortar and pestle. Crushing was done in a number of steps, with the samples being sieved between 2.5 ø and 4 ø sieves. The sample that was left in the 2.5 ø sieve was then re-crushed until the entire sample was finer than 2.5ø. The crushed samples were then washed in a boiling solution of sodium hexameta-phosphate to break down any mud and matrix material that was left on the grains. The boiled sample was washed through a 4 ø wet sieve, leaving the clean disaggregated grains to be dried.

The heavy minerals were separated using heavy liquid polytungstate (LST) with specific gravity of 2.71-2.76 g/cm^3. The technique used to separate the heavy minerals from the rest of the grains is described by Carver (1971) and Lindholm (1987).

Heavy mineral grains were mounted on glass slides as thin sections, ground to approximately 30 μm and analysed using a petrographic microscope.

1.5.5 CURRENT DIRECTION MEASUREMENTS

Current direction indictors have been used in many studies to accurately recreate the flow patterns that deposited sediments and slope directions in the basin (e.g Potter and Pettijohn, 1977). A number of different current direction indicators were present in the field area, reflecting the various types of depositional environments that existed during formation. The most common indicators were cross-beds, ripple marks and imbrication of pebbles. Less common were flutes, channels and parting lineations.

Measurement of the current direction indicators was carried out in the manner described in Hoyt (1971), and Potter and Pettijohn (1977). For the cross-beds, ripple marks and imbrication, the strike and dip of the sedimentary structure was measured. For the flutes, channels and parting lineations the plunge and plunge direction was measured. In the case of the parting lineation and channel measurements, the lineation shows only the orientation of the flow, and not the direction. This meant that other direction-specific data from the outcrop were required.

At each outcrop where detailed paleocurrent analysis was undertaken, as many measurements as possible were taken, in order that an average flow direction could be obtained. Owing to the fact that most of the strata in the study area are dipping, bedding was rotated to horizontal using a stereonet to give the true original current direction (High Jr and Picard, 1971). For sedimentary structures that were measured using strike and dip, the current direction is 90° from the strike of the structure. It is oriented in the dip direction in the case of cross-beds and in the opposite direction to the dip direction in the case of imbrication (Potter and Pettijohn, 1977).

1.5.6 THIN SECTION POINT COUNTING

Thin sections of representitive samples of the Cenozoic sandstones from the area were point counted in order to get an accurate modal analysis of the constituent grains in the sandstones. The technique that was used is described in Galehouse (1971) and Harwood (1988). Four hundred points per slide were counted, resulting in a probable error of 5% or less (Galehouse, 1971). The mechanical stage was set up so that no grain was counted more than once, each point was 0.33 mm apart, and the rows were 0.66 mm apart. In lithic grains with constituents larger than 0.2 mm, the point was counted as the constituent rather than as a lithic grain in a manner similar to that of Ingersoll et al (1984).

1.5.7 MICROFOSSIL ANALYSIS

Microfossils were used in order to find the age and depth of deposition of the sedimentary units in the study area. Due to the fact that many of the sandy sediments were deposited in a turbulent manner, samples from these sediments tend to contain microfossils that had been transported, and in most cases, broken. Therefore microfossil analysis samples were only taken from the grey calcareous mudstones that are thick enough to be mapped as Waicoe Formation, as this unit is interbedded with all the other marine units in the area (Turnbull et al, 1989; Turnbull, Uruski et al, 1993) (figure 1.7.1, map and cross-section in appendix H).

In the field, samples were collected from representative outcrops at sites where the stratigraphy was well known. This ensured that information gained from the study could be applied to units on either side of that part of the Waicoe Formation. Outcrops that were sampled were tested with 10% hydrochloric acid to ensure that the rock was calcareous. Fresh samples were obtained by digging into the outcrop until the mudstone was quite hard. Most samples were about 1 kg although generally only 500 g was processed further. The rest was kept as a backup sample.

In order to extract the microfossils from the rock it first had to be disaggregated. The first step in the disaggregation process was to use the kerosene method described in Hornibrook et al (1989). The samples were then boiled for up to 4 hours in a solution that contained sodium hexameta-phosphate at a concentration of at least 10g per litre of water. In the case of samples that did not disaggregate by using the method described, 10ml of hydrogen peroxide was also added to the solution.

Once the rock was disaggregated the sample was sieved in a 4 ø wet sieve, and only material that was left in the sieve was filtered and dried. Microfossils were picked from the dried sample using a brush under microscope and then glued to a slide ready for optical identification.

1.5.8 VITRINITE REFLECTANCE OF COAL

Vitrinite reflectance of carbonaceous material determines the grade of the coal. In this study the main purpose of the vitrinite reflectance work was to determine the depth of burial of the samples. Owing to the fact that the grade of coal is directly related to burial depth, vitrinite reflectance can indicate burial depth, although other factors also affect coal grade and vitrinite reflectance (Thomas, 1992).

Samples to be analysed were collected from the Beaumont Formation, as this was the only unit in the area that contained abundant coal. Samples were chosen based on coal grade, rather than seeking representative samples. This was done crudely by choosing the coal that appeared most shiny at each outcrop, in an attempt to give the highest coal rank, as opposed to the average rank. The coal was then broken into pieces approximately 1cm in diameter and mounted in a briquette. Analysis was done on a Zeiss reflected light microscope and photometer and calibrated against five different Zeiss glass reflectance standards for coal. All measurements were made using oil immersion (RI=1.518) in green light (=510 μm). Ten spots were analysed on each of the standards before the coal was analysed and each briquette was analysed forty times.

Average measured Ro values from each standard were plotted against the known Ro values for the standards, and a best-fit line added. The averages of each coal briquette were then added to the line to find the actual value of reflectance for the samples.

1.6 UNIT DESCRIPTIONS AND INTERPRETATIONS

One of the main aims of this study was to investigate and make detailed sedimentological descriptions and interpretations of the sedimentary units in the study area. Detailed descriptions of the lithofacies within the sedimentary formations were made in the field by

using measured sections and detailed outcrop descriptions. All lithofacies for each sedimentary formation present in the study area have been described.

Lithofacies descriptions are used to infer the environment of deposition for each sedimentary unit. Current direction data gathered during the lithofacies investigations were also used to determine the flow and slope direction of the basin where sediments were deposited (see section 1.5.5). A combination of all the lithofacies data gives a good idea of how the basin evolved though time and how this affected the sediments that were being deposited in the area.

Rocks from the different formations in the study area were studied petrographically (see section 1.5.6). The petrology of the formations was used to further define the units and also to assess the provenance of the sediments. Some petrological aspects of the sediments can also be used to investigate the sedimentary processes that deposited the sediments in the area.

Finally a combination of sedimentology and sedimentary petrology is used to build up a description and interpretation of each sedimentary unit in the study area. Interpretation of each unit will include the mode and environment of deposition of the sediment, and sediment provenance. This information can then be used along with age data to recreate the sedimentary history of the basin.

1.7 SEDIMENTARY UNITS

The sedimentary units that were used in the study were those of Turnbull, Uruski et al (1993). Similar units are also used in a later 1:250,000 geological map of the area published in Turnbull (2000). Figure 1.7.1 is a stratigraphic section for the study area and is an adaptation of the stratigraphic column that was published in Turnbull, Uruski et al (1993).

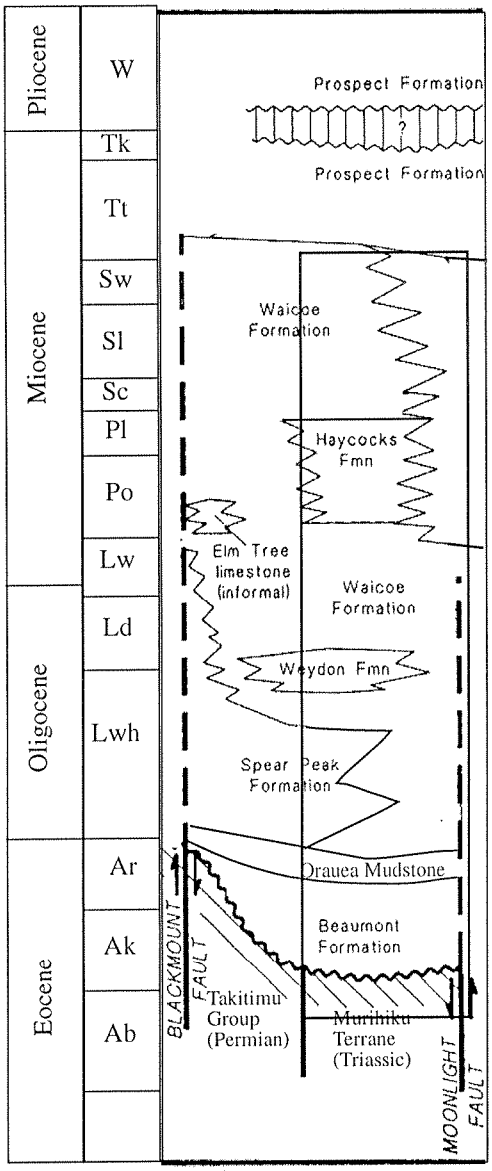

Figure 1.7.1 Stratigraphic section of the Burwood sub-Basin after Turnbull, Uruski et al (1993). This section and the appropriate units were used throughout the study. The rectangle represents the approximate stratigraphy of the study area.

2 MURIHIKU SUPERGROUP

2.1 INTRODUCTION

The Murihiku Terrane forms the basement in the study area, and is present from Mount Hamilton to Princhester Creek and at Centre Hill in the southern part of the area, it is also found across a large part of Southland and South Otago (Coombs et al, 1976; Bishop et al, 1985; Landis et al, 1999; Roser et al, 2002) (figure 1.4.1). The Murihiku Terrane is offset by the Alpine Fault, reappearing in Nelson, and continuing up the west side of the North Island, possibly extending as far as New Caledonia (Coombs et al, 1976; Bishop et al, 1985; Ballance and Campbell, 1993; Landis et al, 1999; Roser et al, 2002).

The main component of the Murihiku Terrane is the Murihiku Supergroup, which is composed of over 15 km of volcanic-derived sediments (Ballance and Campbell, 1993). The volcanic arc that fed the basin is thought to have been part of Gondwana that lay to the southwest of its present location (Ballance and Campbell, 1993). The thick sedimentary sequence of the Murihiku Terrane was deposited in what is interpreted to have been a fore-arc basin from the late Permian until the early Cretaceous (Coombs et al, 1976; Carter et al, 1978, Ballance and Campbell, 1993; Roser et al, 2002), although the Park volcanics within the Murihiku Terrane have a back-arc signature (Coombs et al, 1996). The sedimentary environments that were present during the deposition of the Murihiku Terrane sediments include non-marine fluvial floodplains, deltas, shelf and submarine fans (Ballance and Campbell, 1993).

Prior to terrane accretion during the early Cretaceous, these sediments were metamorphosed to zeolite facies (Coombs, 1959; Boles and Coombs, 1977). For a unit thickness of up to 15km, metamorphism to such a low grade is unusual in that sediments buried to that depth should have undergone greenschist facies metamorphism (Landis et al, 1999; Roser et al, 2002). During accretion the Murihiku Terrane was folded into a broad series of synclines and anticlines (Balance and Campbell, 1993), the largest being the Southland Syncline (Campbell and Coombs, 1966). This is an extensive regional structure that can be traced across Southland and South Otago, as well as through Nelson, where it has been offset some 480 km by the Alpine Fault (Coombs et al, 1976; Bishop et al, 1985; Landis, 1999). Both

limbs of the Southland Syncline are exposed in the study area. Campbell and Coombs (1966) defined a number of different groups of rocks that make up the Murihiku Terrane in Southland and South Otago, and attempts have been made to extend these units into other areas. However, due to the fact that the units are often laterally discontinuous, correlation can be difficult.

2.2 LITHOFACIES DESCRIPTION AND INTERPRETATION

INTRODUCTION

Lithofacies present within the Murihiku Supergroup sediments were investigated using measured sections through the unit, with detailed observations of the sediments being made along the line of section. The sections were measured where the unit was well exposed and contained a number of its characteristic lithofacies. This enabled the relationship between the different lithofacies to be studied. Two detailed sections were made that concentrated on small scale sedimentary features seen within the beds. These are at G.R. 2126960 5502180 (figure 2.2.2) and 2126580 5502850 (figure 2.2.3). A larger summary section through most of the unit shows the stratigraphic order of the different lithofacies and was measured between G.R. 2120500 5502500 and 2121000 5503000 (figure 2.2.1).

Three different lithofacies were recognised while mapping the area. They can be recognised on both sides of the Southland Syncline in similar stratigraphic order. In the stratigraphically lowest part of the Murihiku Supergroup a conglomerate lithofacies is common and can be traced along strike throughout the area, although the individual beds are probably not continuous (figure 2.2.1 and 2.2.2). Tuff beds are common in parts of the Murihiku Supergroup within 100 m above the top of the conglomerates (figure 2.2.1). The dominant lithofacies in the Murihiku Supergroup is siltstone and fine sandstone with sporadically interbedded medium-coarse sandstone and mudstone (figure 2.2.1, 2.2.2 and 2.2.3).

CONGLOMERATES DESCRIPTION

Conglomerates occur at the base of the Murihiku Supergroup where it is exposed in the study area (figure 2.2.1 and 2.2.2). These conglomerates are usually found to be discontinuous and in some places they form lenses that are often quite resistant and form high standing outcrops (e.g. G.R. 2120400 5487400, figure 2.2.4), of up to 1 – 5 m at maximum thickness (figure 2.2.1 and 2.2.2).

The conglomerates contain very well rounded plutonic (granite - grano-diorite) and volcanic (andesite-rhyolite) clasts (appendix C, OU 73314 - 73318) (figure 2.2.4 and 2.2.5). Sorting in the conglomerate outcrops is very poor, with clast size ranging from pebbles a few centimetres in diameter to cobbles 20 cm in diameter (e.g. G.R. 2120400 5487400, figure 2.2.4 and 2.2.5). Hard, black, angular claystone chips are also found within the conglomerate lenses, as well as in the surrounding sediments (e.g. G.R. 2120400 5487400). A siltstone matrix supports the clasts in the conglomerates (e.g. G.R. 2126960 55028100) and in some outcrops the pebbles are "floating" in the matrix, with pebbles up to 30 cm apart (figure 2.2.2, 2.2.4 and 2.2.5). As the clasts are matrix-supported there is no imbrication of the pebbles. Few sedimentary features can be seen in the conglomerate lenses, although crude normal (e.g. G.R. 2121230 5486400) (figure 2.2.4) and reverse (e.g G.R. 2126960 5502810) grading is occasionally present.

Conglomerate Interpretation

The high degree of rounding of the clasts indicate that they have been redeposited from a higher energy environment (Walker, 1975; Carter and Norris, 1977a; Carter et al, 1978; Lowe, 1982). The fact that the conglomerate clasts are all matrix-supported and have both normal and reverse graded bedding suggests that they have been deposited by mass flow processes (Boggs, 2001). This type of depositional mechanism is suggested by Ricci-Lucchi (1975) for facies A deposits. Carter and Norris (1977a) and Lowe (1982) suggest that these type of deposits form as traction carpets in high density turbidity currents, however Shanmugam (2000) shows that these are in fact debris flows rather than turbidity currents.

Tuff Description

Although tuffs are only a minor part of the Murihiku Supergroup in the study area, they form conspicuous beds that are very noticeable in outcrop. The tuffs in the study area are normally found near the base of the exposed section, and are always higher in the sequence than the dominant conglomerate layers (Figure 2.2.1).

Generally the beds have an orange or white weathered surface, although a fresh section shows that the rock is actually grey in colour with small weathered fractures running through it (figure 2.2.6). Tuffs range in grain size from silt up to fine sand (figure 2.2.7). Petrographic

investigation reveals that the grains are dominantly glass shards and plagioclase crystals, with fractures and cement consisting of heulandite (appendix C, OU 73312, 73313) (figure 2.2.7).

Tuff outcrops are usually more eroded than the surrounding siltstone, due to the pervasive fracturing causing them to break up into small pieces. The unfractured tuff is very well indurated and hard to break with a hammer (figure 2.2.6). The tuffs are usually interbedded with the siltstones with beds ranging in width from 10 cm up to a few meters, the contacts with the siltstone are sharp at the base and the top of the beds (figure 2.2.1). Tuff beds appeared to be massive and no graded bedding was seen, this may have been due to the fact that they are fine grained. Rare coarser layers are present in the fine-grained tuff beds although the grain size within any given bed is usually quite similar. Tuff outcrops in the study area were quite continuous and could usually be traced between ridges not displaced by faulting.

Tuff Interpretation

The lack of recognizable sedimentary structures within the tuffs of the Murihiku Supergroup in the study area makes interpretation of the depositional mechanism difficult. The lack of sedimentary structures could be due to the compaction and metamorphism that they have undergone, or there may simply never have been any sedimentary structures. The association with other deep water units indicates that the tuffs were also deposited in deep water. Whether any transport occurred after the initial deposition of these tuffs is impossible to tell due to the lack of sedimentary structures within the unit, although the bottom currents that have acted on the surrounding siltstone would have also affected the tuff.

Siltstone Description

The dominant lithofacies in the Murihiku Supergroup in the study area is grey resistant siltstone. The siltstone is lithic arkose made up of dominantly andesine feldspar and lithic grains in a matrix of crushed grains and mud (appendix C, OU 73310, 73311). Siltstone is found throughout the Murihiku Supergroup and near the top it becomes almost the only lithology present (figure 2.2.1, 2.2.2 and 2.2.3).

The siltstone ranges from well sorted to poorly sorted sandy siltstone (appendix C). Some siltstone also contains hard black mudstone chips that are generally a few centimetres in length.

Siltstone usually forms beds that are up to 5 m thick. Thin (<10 cm) mudstone and mottled lithic arkose sandstone layers separate the siltstone layers as well as the other lithofacies that are described. The contacts between the siltstone and other sediments are generally sharp (figure 2.2.1, 2.2.2 and 2.2.3). However, crude beds with occasional pebbles and cobbles occur within the siltstone, with gradational contacts between the pebbly and pebble-free layers. The siltstone also contains occasional interbedded sandstone-mudstone 'packets' a few meters thick (figure 2.2.3). These packets often show turbidite features, such as normal grading.

Within the siltstone layers no sedimentary structure or grading is observed, apart from fine lamination (mm scale). In some siltstone layers fossils are distributed through the layer (e.g G.R. 2126580 5502850), or concentrated as a shell bed between layers (e.g G.R. 2120700 5502700).

SILTSTONE INTERPRETATION

It is difficult to determine the depositional environment of the siltstone facies in the Murihiku Supergroup due to the lack of sedimentary structure. It is likely that the bulk of the siltstone in the Murihiku Supergroup in the study area was deposited as muddy contourites. Evidence for this is: the fine grain size of the sediment, its poor sorting, the presence of clay chips, the lack of sedimentary structure, except for lamination (some of which was probably destroyed by bioturbation), and the fossil layers (possibly lag deposits) (table 2.2.1). All these features are present in the muddy contourite facies of Stow and Lovell (1979) and Stow et al (1998). The apparent thickness of the beds is probably due to the amalgamation of numerous smaller beds, also a common occurrence in muddy contourites (Stow and Lovell, 1979).

Stow et al (1998) warn against interpreting sediments as contourites unless many of the features in their facies model are recognized. While many contourite features are present in the Murihiku Supergroup siltstones, these features tend to be subtle (table 2.2.1). However interpretation that the siltstones are contourites is also supported by the fact that the sediments

show no features considered to be indicative of any of the turbidite facies (e.g Ricci-Lucchi, 1975), yet Shanmugam (2000) suggests that not enough is known about contourites to apply facies models to ancient sediments.

Stow et al. 1998	Murihiku Supergroup
Muddy, bioturbated, trace lamination	Common
Silty-muddy mottled irregular layers, bioturbated	Present
Sandy, bioturbated, trace lamination	Rare
Micro-brecciated shale-chip layer in muddy contourite	Present
Gravel-lag, irregular, poorly sorted, reverse graded ± muddy ± Fe Mn crust	Present

Table 2.2.1 The similarities between the clastic countourite model and the sediments in the Murihiku Supergroup in the study area are shown in this table. Note the most common features in the Murihiku Supergroup are the finer grained parts of the facies.

While most of the siltstone in the Murihiku Supergroup was probably deposited as contourites, the interbedded sandstone and mudstone units (figure 2.2.3) that are present within the siltstone are likely to be turbidite deposits. The flysch within the Murihiku Supergroup siltstones is part of facies E of Ricci-Lucchi (1975) (E1 chapter 4).

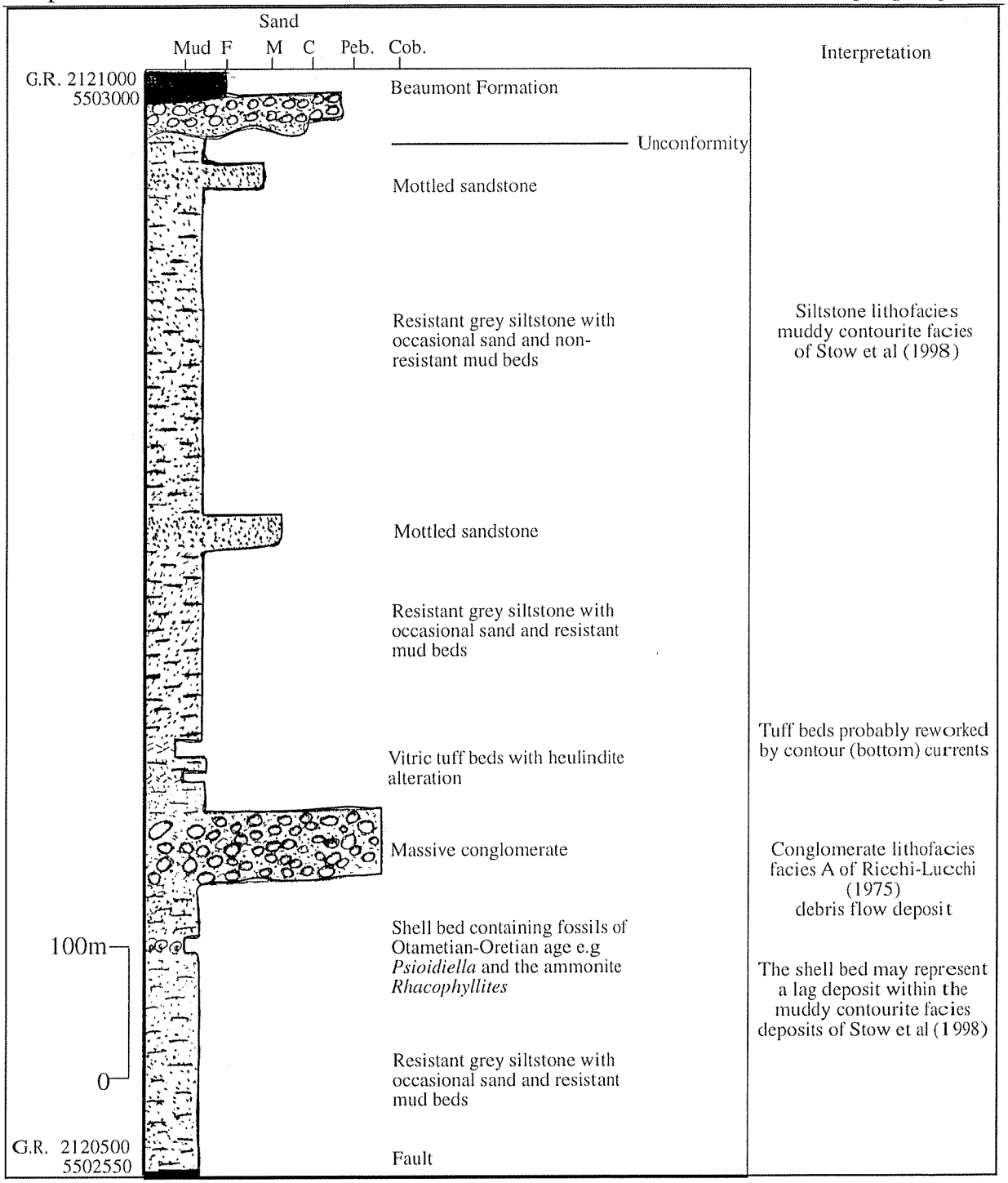

Figure 2.2.1. Summary section through the Murihiku Supergroup in the study area extending from the faulted base up to the unconformable contact with the Beaumont Formation. This section shows the main lithofacies present in the Murihiku Supergroup and their interpretations.

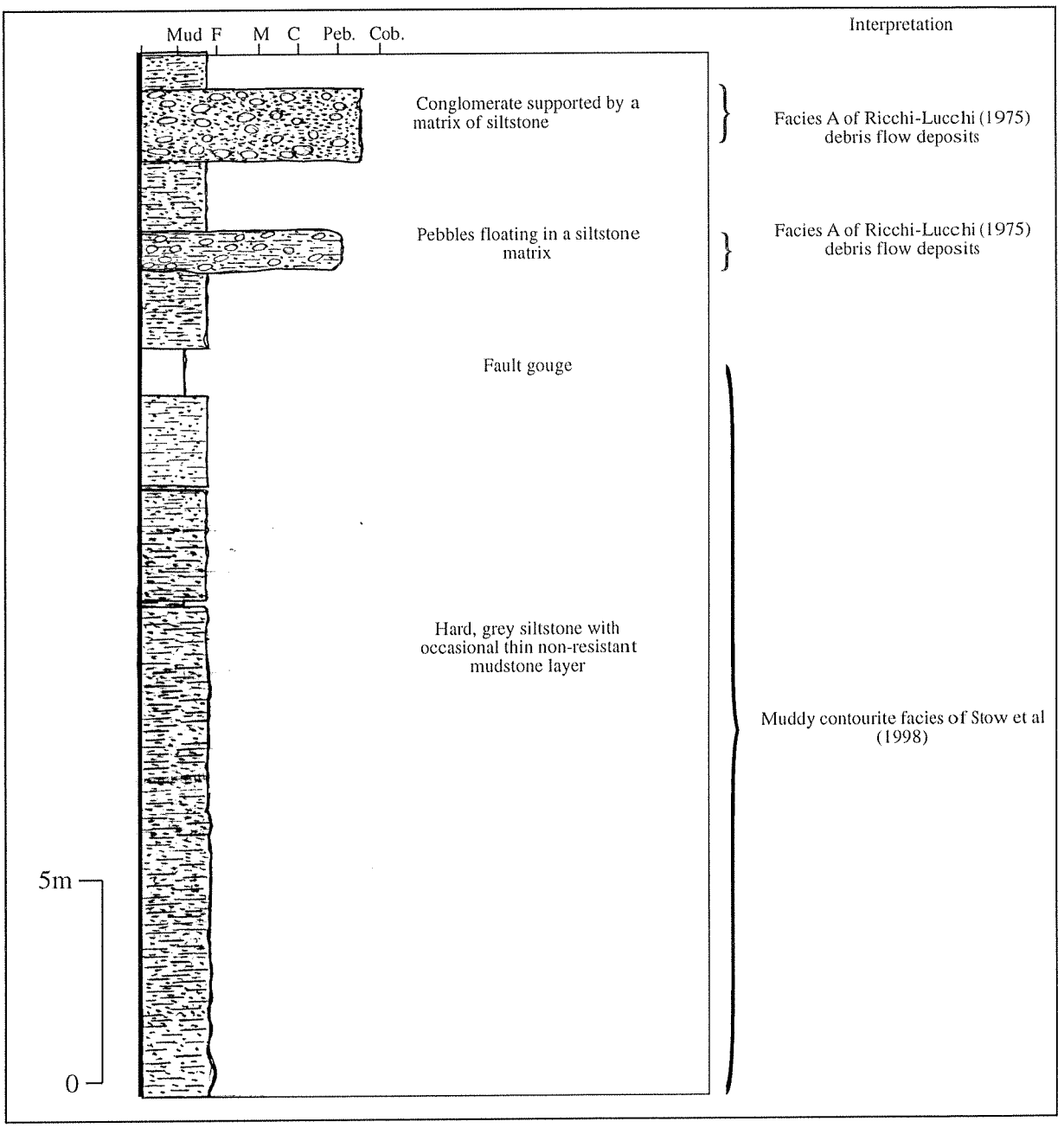

Figure 2.2.2 Measured section through the Murihiku Supergroup at G.R. 2126960 5502180, showing the lithofacies that are present and their interpretation.

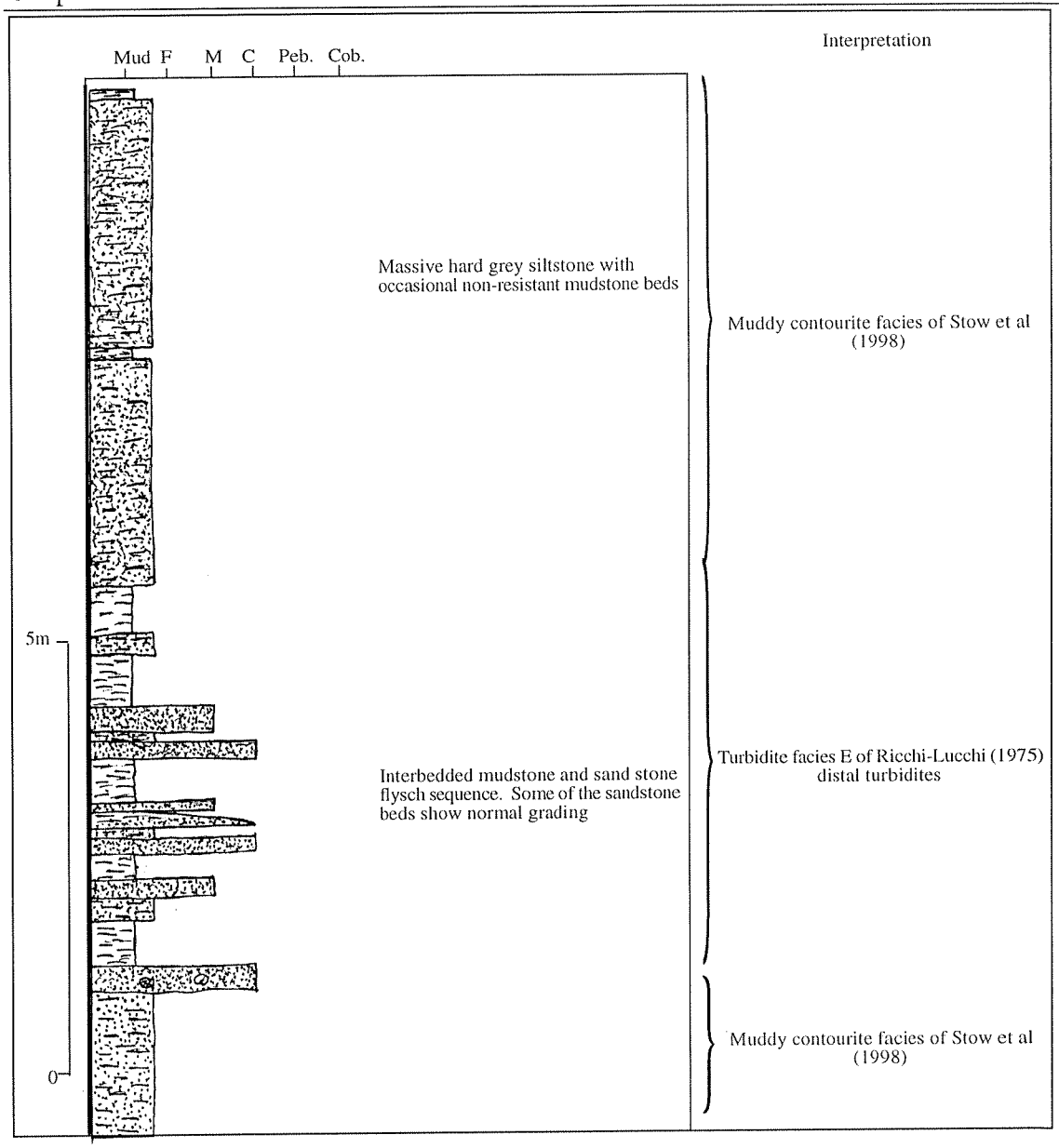

Figure 2.2.3 Measured section of the Taringatura Group at G.R. 2126580 5502850. This section shows the lithofacies that are present as well as the interpretations of the facies. Note the difference between the lithofacies that are interpreted as contourites from those that are turbidites.

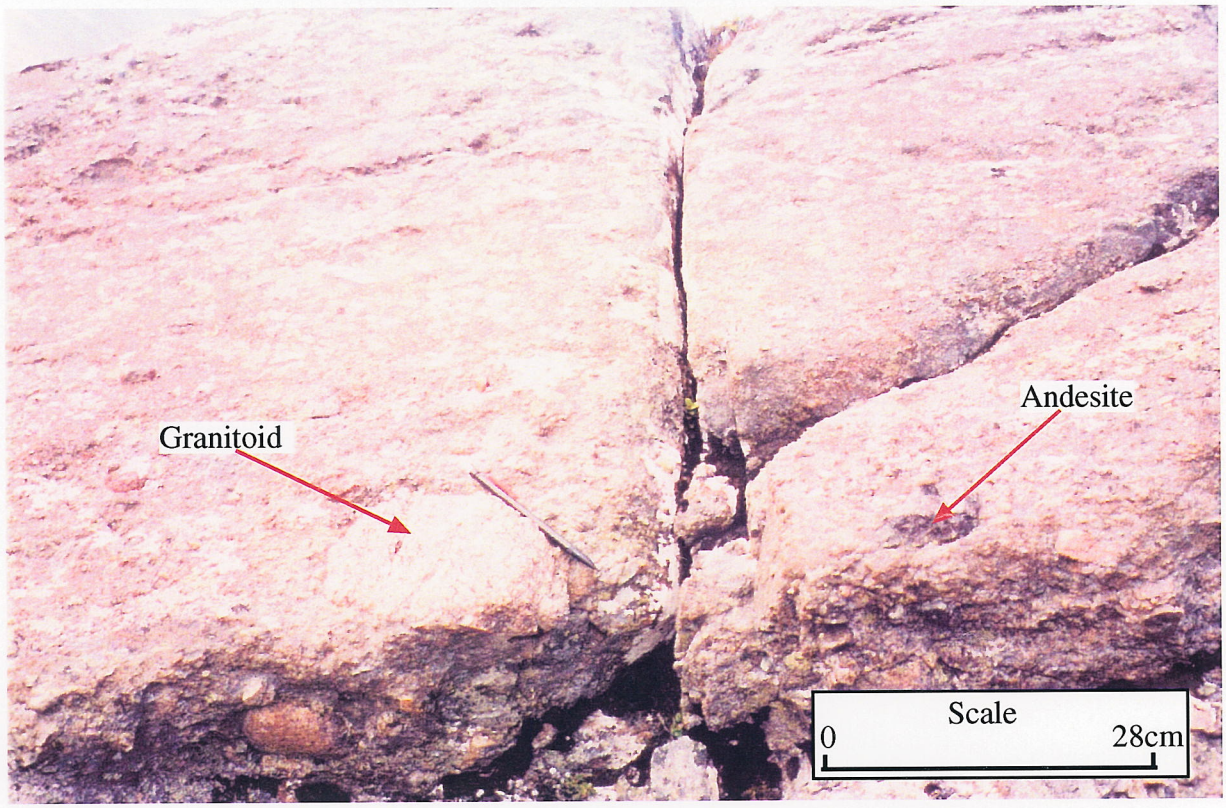

Figure 2.2.4 Taringatura Group conglomerate at G.R. 2120400 5487400 showing the two most abundant clasts types. Note the matrix supported nature of the conglomerate and the crude stratification.

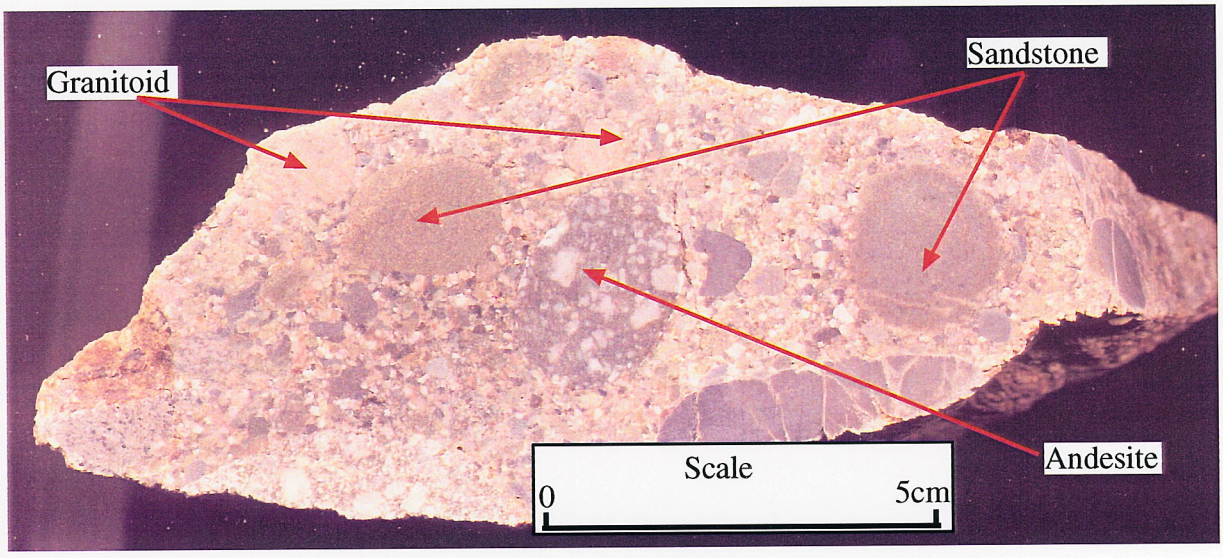

Figure 2.2.5 Handspecimen from the outcrop shown in figure 2.2.4 showing the main constituents of the Murihiku Supergroup conglomerates. Note the well rounded nature of the clasts.

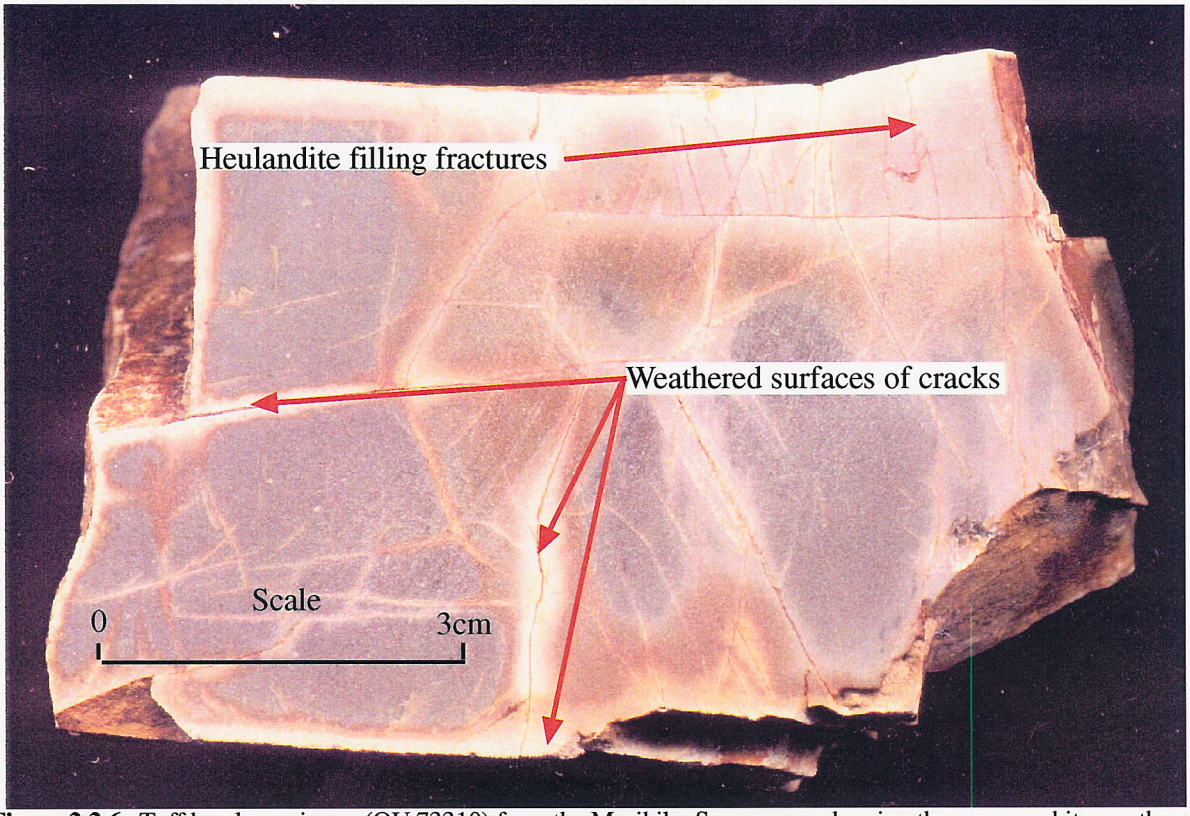

Figure 2.2.6. Tuff hand specimen (OU 73310) from the Murihiku Supergroup showing the orange-white weathered surfaces of the fractures in what is a grey rock when unweathered. Heulandite fillings can be seen in some of the cracks.

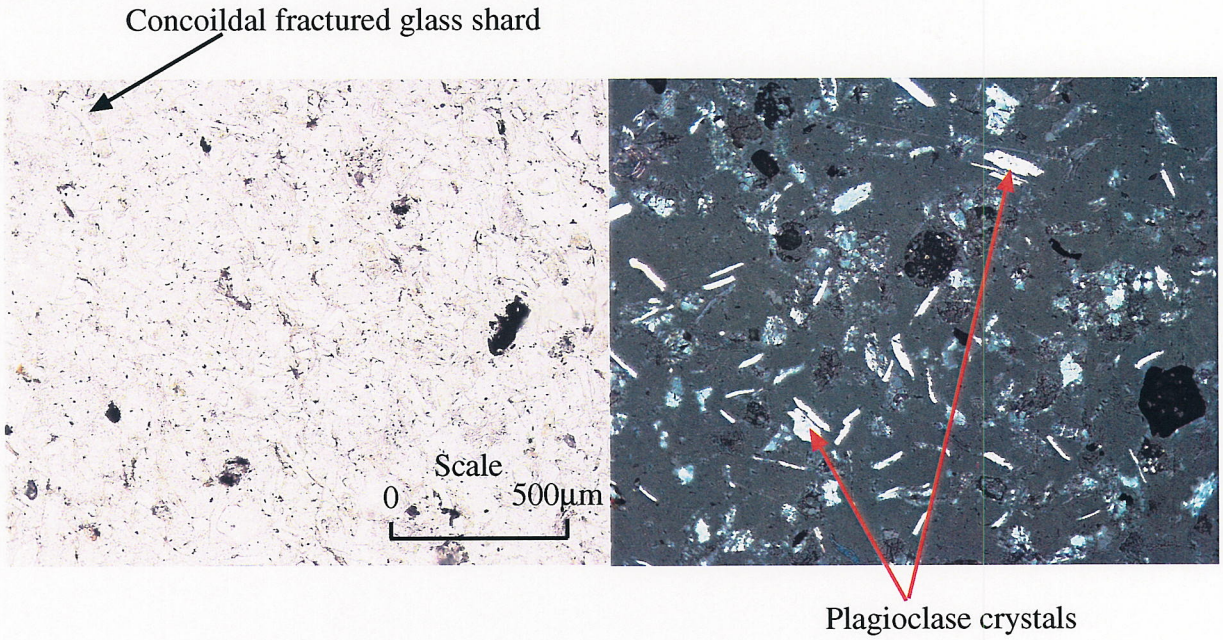

Figure 2.2.7 Photomicrographs of the tuff (OU 73310) (plane-polarised light on the left, cross-polarised light on the right) in figure 2.2.7, showing the large proportion of glass shards in the rock as well as the plagioclase crystals. Note that the edges of the glass grains are altered to zeolite.

2.3 AGE AND FOSSIL OCCURRENCE

Fossils within the Murihiku Supergroup are not common in the study area, however a few important fossil localities exist that give a good idea of the age of the unit. Fossils were collected when found during field mapping. No attempt has been made, however, to search the area for new localities, or to systematically collect large samples. Most of the fossil information that relates to the Murihiku Supergroup has been gathered from the University of Otago Geology Department fossil collection. The fossils in the area give constraints on the age of the Murihiku Supergroup, that can be used to correlate across the Southland Syncline and also between the study area and regions to the southeast.

WEST LIMB OF THE SOUTHLAND SYNCLINE

Kirby (1989) found the regionally important *Manticula problematica* shell bed, which marks the top of the Oretian stage at G.R. 2117800 5501600. Another fossil locality found by Kirby (1989) was at G.R. 2119400 5502200, where a number of different fossils were identified, including the brachiopods *Dielasma* and *Rynchonella* and a Ptreroid that was probably *Halobia*. An outcrop at G.R. 2120700 5502550 (figure 2.2.2) has been known to contain fossils since the late 1960s, and Dr J.D. Campbell made a number of collections from this outcrop during the 1970s and 1980s. Fossils collected included *Maoririty nchia mackayi* and the ammonite *Rhacophyllites*. Samples taken in this study established that while most of the fossils were quite broken, a number of them could be identified as *Psioidiella* (identification by A. Grebneff).

From all the fossils that have been collected from the west limb of the Southland Syncline in the study area, it is apparent that the age of the Murihiku in this area is Oretian-Otametian. The best evidence for this is the *Manticula problematica* bed, which occurs throughout the Murihiku Terrane and marks the boundary at the top of the Oretian stage. Most of the other fossils in the area fit into the Oretian-Otametian stages although some also occur in the Kahikuan stage.

EAST LIMB OF THE SOUTHLAND SYNCLINE

Two fossil localities have been found on the eastern limb of the Southland Syncline in the study area. Dr J.D Campbell collected a number of fossils from an outcrop near the road at

G.R. 2126600 5504600, including *Alipunctifera, Rhynchonellide, Dielasama* and *Retzia*. Field mapping revealed another fossil locality at G.R. 2126500 5502800 (figure 2.2.3). Which contains a lot of shell fragments and some complete fossils in a well-indurated siltstone. The toughness of the rock lead to many fossils being broken during collection, but one complete fossil and some fragments were identified as *Psioidiella* (identification by A. Grebneff).

The fossils that were collected by Dr J.D Campbell indicate an Etalian age for that the part of the Taringatura Group, while fossils collected during fieldwork for this study indicate an age of Oretian-Otamitian.

2.4 SUMMARY

STATUS OF THE TARINGATURA GROUP IN THE STUDY AREA

One of the formations defined by Campbell and Coombs (1966) was the Taringatura Group, whose type locality is the Taringatura Hills to the southeast of the study area (figure 1.2.1 and 2.4.1). Here the Taringatura Group encompasses "Mesozoic rocks exposed in the Taringatura Hills from the granite-bearing conglomerate immediately overlying the North Range Group upward" (Campbell and Coombs, 1966). Boles (1974) extended the Taringatura Group to the southeast in the Hokonui Hills despite the lack of the granite-bearing conglomerate (figure 2.4.1 and 2.4.2). Boles (1974) redefined the base of the Taringatura Group into the Hokonui Hills as the "first ridge forming, prominent, medium to coarse sandstones above the North Range Group." Begg (1981) extended the Taringatura Group to the Wairaki Hills between the Taringatura Hills and the study area (figure 2.4.1 and 2.4.2).

In the study area the Murihiku Terrane rocks have been faulted so that only a section with a maximum thickness of approximately 2 km is preserved. Projecting the strike of the formations described in Campbell and Coombs (1966) and Begg (1981) into the study area suggests that the Taringatura Group should be present if it is continuous along strike (figure 2.4.1 and 2.4.2). The basis for the correlation between the Taringatura Group to the southeast of the area and the Murihiku Supergroup in the study area is based on the lithology and the age of the rocks.

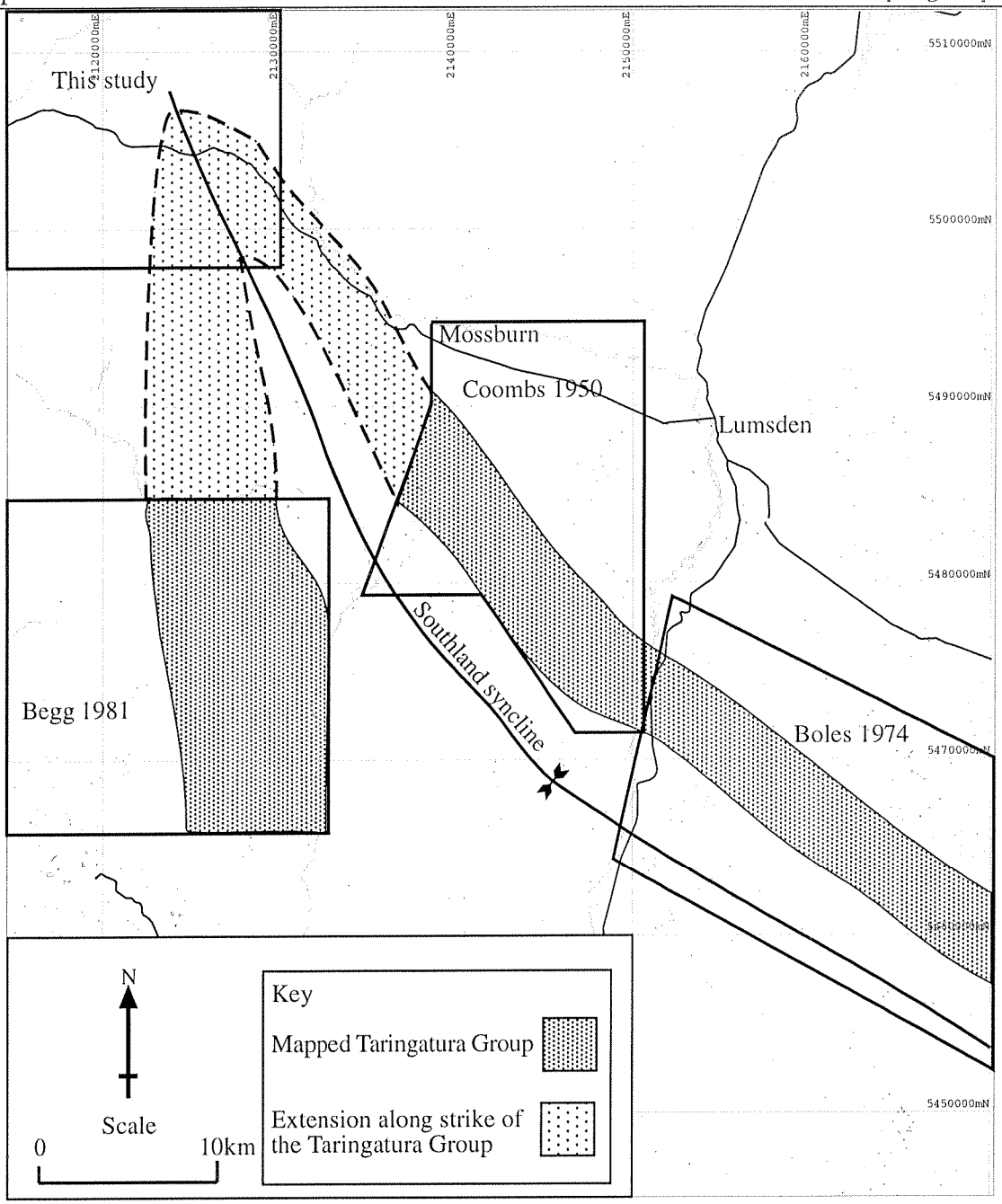

Figure 2.4.1 Map showing other areas where the Taringatura Group has been mapped in the past and the likely extension of the group to the north. The likely extension is based on structural measurements from the mapped areas.

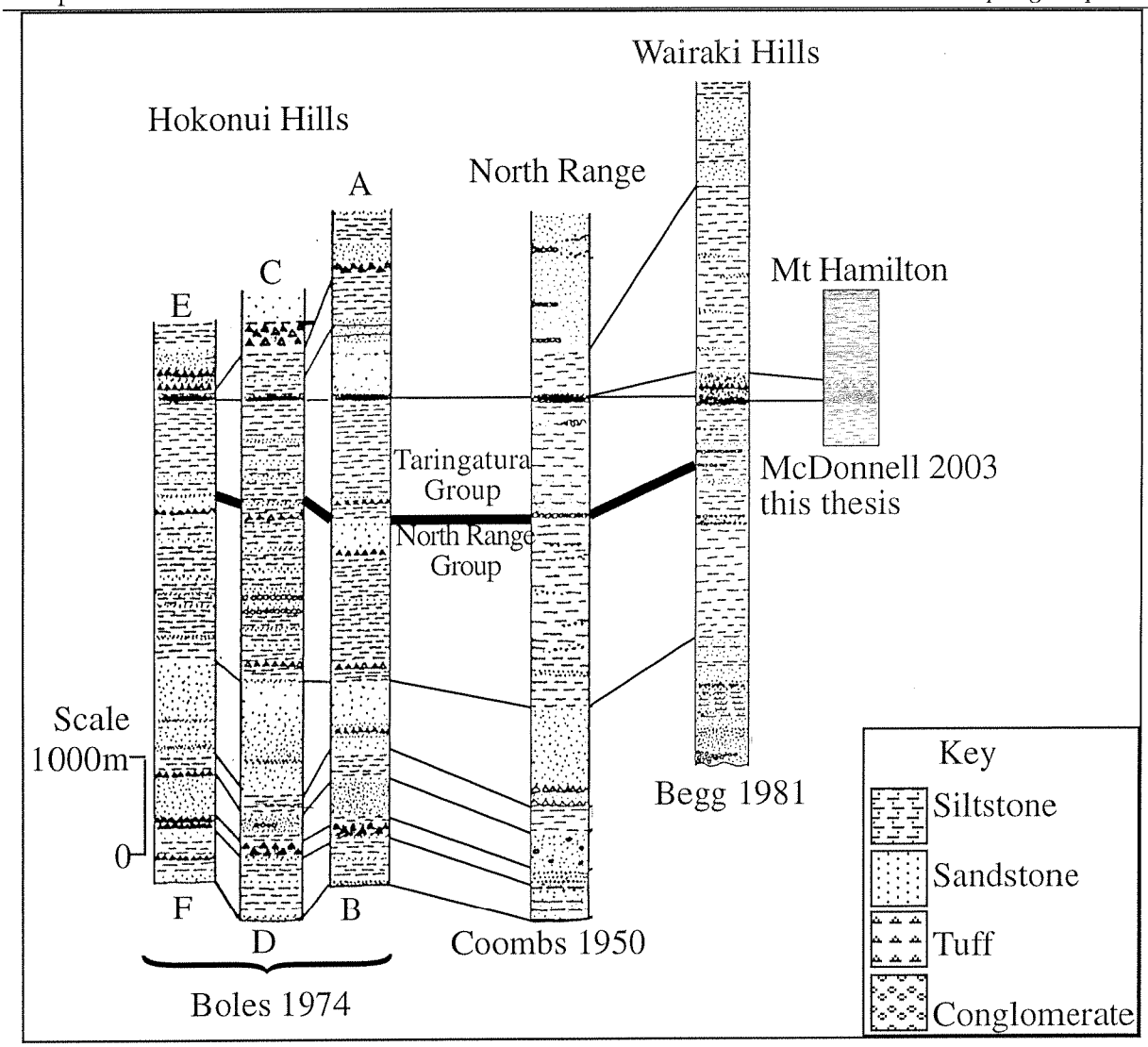

Figure 2.4.2 Comparison of sections through the Murihiku in different areas. The boundary between the North Range and Taringatura Group is shown in bold, showing that the study area has stratigraphy that is similar to the Taringatura Group in other areas.

The age, stratigraphy, lithofacies and petrography of the Murihiku Supergroup rocks in the field area are all consistent with the descriptions of the Taringatura Group given in Campbell and Coombs (1966), Boles (1974) and Begg (1981). The Kaihikuan - Otamitian age of the Murihiku Supergroup in the area is the same as that of the Taringatura Group in the other areas (Campbell and Coombs, 1966; Boles, 1974; Begg, 1981). The stratigraphy is shown to be similar in the sections in figure 2.4.2. All of the above authors described the same types of lithofacies in their descriptions of the Taringatura Group as those present in the study area. The petrography of the clasts in the conglomerates in the study area showed that some of the clasts were granitic in composition. The definition of Campbell and Coombs (1966) requires the conglomerates within the Taringatura Group to contain granite while the North Range

Group contains no granite. All the evidence gathered from the Murihiku rocks in the area indicate that this unit is part of the Taringatura Group.

Environment of deposition of the Taringatura Group

The lithofacies that are present in the Taringatura Group are all marine units formed in deep water. The conglomerates formed as debris flows, with the clasts being redeposited from their original source, as shown by the reverse grading and matrix supported nature of the clasts (Shanmugam, 2000). The massive siltstones in the siltstone lithofacies are probably contourites formed by slope-parallel deep ocean bottom currents, as shown by the similarities to the contourite model of Stow et al, (1998). The tuffs in the study area are also likely to have been reworked by contour currents as they are interbedded with the siltstone, although they do not have recognisable sedimentary structures themselves. The interbedded sandstone and mudstone beds within the siltstone lithofacies are most likely distal turbidites as they show normal grading and the rhythmic sandstone-mudstone partings typical of turbidite deposition (e.g Bouma, 1964; Ricci-Lucchi, 1975; Shanmugam, 2000). The petrography of the conglomerate clasts indicates that the Taringatura Group formed in a basin that was receiving sediment from a dissected arc, as both plutonic and volcanic clasts are present (eg Carter et al, 1978; Ballance and Campbell, 1993).

Carter et al (1978) placed all the Murihiku Supergroup rocks described by Campbell and Coombs (1966) into their facies association 2, which contained sediments that are identical to those found in the study area. The interpretation of Carter et al (1978) was that the sediments were mainly deposited as contourites, with turbidites and redeposited conglomerate channels also present, all in the context of an upper trench slope environment.

The sedimentology of the units in the study area is consistent with the interpretation of Carter et al (1978). The redeposited conglomerates, contourites and tuffs are all consistent with an upper trench slope environment (Carter et al, 1978; Rupke, 1978; Mitchell and Reading, 1978). However, a major problem with the interpretation of the Taringatura Group and North Range Group deposits as trench deposits (Carter et al, 1978) is that the thickness of the sediment far exceeds that of any modern trench (Rupke, 1978).

3 NIGHTCAPS GROUP

INTRODUCTION

The Nightcaps Group is an Eocene terrestrial unit that overlies the basement rocks and Ohai Group in the Waiau Basin and around the edges of the Takitimu Mountains (Turnbull, Uruski et al, 1993). The type section for this group is along the Waiau River from G.R. D45/012428 to D45/038492 (Bowen, 1964; Turnbull et al, 1989). The Nightcaps Group is made up of two formations, the Beaumont Formation and the Orauea Mudstone, both of which are represented in the type section (Bowen, 1964 and Turnbull et al, 1989).

The lower Nightcaps Group is made up of the Beaumont Formation cross-bedded sandstone and conglomerate, with carbonaceous mud and coal (Turnbull et al, 1989; Turnbull, Uruski et al, 1993) (section 3.1). Overlying the Beaumont Formation is the brown, massive, sparsely carbonaceous mudstone of the Orauea Mudstone (Turnbull et al, 1989; Turnbull, Uruski et al, 1993) (section 3.2).

The Nightcaps Group unconformably overlies the Murihiku Supergroup in the study area. The unconformity is angular with a smaller angular discordance on the west limb of the Southland Syncline than on the east (see chapter 6, map and cross-section in appendix H).

3.1 BEAUMONT FORMATION

3.1.1 INTRODUCTION

The Beaumont Formation outcrops along the flanks of the Takitimu Mountains and is present along the eastern edge of the Waiau Basin, extending southward to Orepuki (Turnbull et al, 1989). The Beaumont Formation is interpreted to extend westwards into the western Southland basins and to grade into Eocene units in the west such as the Earl Mountains Sandstone (Turnbull, Uruski et al, 1993). In the study area the Beaumont Formation forms a band around the flanks of Mount Hamilton and Centre Hill (see map appendix H). Infaulted slivers of Beaumont Formation are also present in the Mount Hamilton area (see map appendix H).

Most previous work on the Beaumont Formation has been done in the Ohai region, as this area has been extensively mined for coal (Bowen, 1964; Sykes, 1988). Bowen (1964) first recognised that the Beaumont Formation was different from the Ohai coal measures and that the two were separated by an unconformity. Bowen (1964) also described the content of the Beaumont Formation and dated it in the Ohai area. Sykes (1988) studied the lithofacies that are present in the Beaumont Formation at Ohai and also carried out detailed studies on the coal. In the study area the Beaumont Formation was originally informally called the Princhester Formation by Fitzharris (1967) and Carter and Norris (1977b). Turnbull et al (1989) abandoned the Princhester Formation name in favour of the Beaumont Formation.

The type section for the Beaumont Formation is drillhole 166 (G.R. D45/ 160 633) (Bowen, 1964). The base of the type section is defined on palynological grounds, with the top marked by the transition to the massive mudstone of the Orauea Mudstone (Turnbull et al, 1989 and references therein). The Beaumont Formation ranges in thickness from a few hundred meters at Ohai to over 500 m in the Waiau Basin subsurface (Bowen, 1964; Turnbull et al, 1989). In the study area the Beaumont Formation is at least 600 m thick, assuming that the formation is not internally faulted, which would cause repetition of the sequence (map and cross-section in appendix H).

3.1.2 AGE AND FOSSIL OCCURRENCE

Owing to the fact that the Beaumont Formation is a terrestrial unit, fossils are scarce. One shelly fossil was found in mud-rich Beaumont Formation at G.R. 2120200 5499700. The fossil was an impression of a shell that looked like a mussel and is probably a fresh water species. The other fossils that were found in the sandstone at G.R. 2126100 5502700 were leaf impressions that are probably *Nothofagus*.

The age of the Beaumont Formation has been determined prior to this study using pollen dating (Bowen, 1964; Sykes, 1988; Pocknall and Turnbull, 1989). Results of this dating were deemed sufficient for the purposes of this report, hence no further age analysis was carried out.

Two floral zones are present in the Beaumont Formation in the type section. The older is the middle Eocene, *Nothofagus flemingii* zone, while the younger is the upper Eocene *N. mataurаensis* zone (Bowen, 1964; Pocknall and Turnbull, 1989). In the area around the north of the Takitimu Mountains and in Princhester Creek, the Beaumont Formation has been dated as late Eocene (Kaiatan-Runangan) due to the presence of *N. mataurаennsis* (Turnbull et al, 1989; Turnbull, Uruski et al, 1993). The study area is close to the areas from where the northern Takitimu samples were taken, therefore it is assumed that a Kaiatan-Runangan (upper Eocene) age is appropriate for the area.

3.1.3 LITHOFACIES DESCRIPTION AND INTERPRETATION

Three different lithologies are recognised in the study area, which are discontinuous in most cases, with no set stratigraphic order apparent. Sandstone is the dominant lithology in the Beaumont Formation, with conglomerate often present as interbedded layers. Mudstone/siltstone does not form resistant outcrops and is usually confined to slumps and boggy areas.

Descriptions of the conglomerate and the sandstone have been divided into separate lithofacies. This was based on differing sedimentary structures being indicative of different environments of deposition, despite a continuum in grain size. Lithofacies of Miall (1977) have been used for comparison with the lithofacies in the study area. The mixed coarse sediment in the Beaumont Formation is typical of a braided river system (Collinson, 1996),

so this comparison is well founded, since Miall (1977) based his facies on braided river systems. Interpretations of the different facies are based on published information and consider aspects covered in the facies of Miall (1977), as well as features that are seen in the study area but not in the original facies descriptions. Although only one detailed section has been done in this study relationships between the different facies were recognised during field mapping, and have been used to understand the facies associations. Problems with comparing facies in ancient sediments with present day environments (see chapter 4) are not as important in the study of alluvial sediments, as modern day examples can be studied, as they form in river systems.

Conglomerate Facies Gp Description

Gp facies conglomerates are present throughout the Beaumont Formation sequence (figure 3.1.1). The conglomerates generally form lenses that are 1-10 m wide and up to about 5 m thick. The bases of the conglomerate beds are erosional, and the beds commonly fine upwards.

Tabular cross-bedding is common within the Gp conglomerate layers, with beds up to 1 m high and original dip angles of 20-30° (figure 3.1.1, 3.1.4). The results of cross-bed measurements are shown in figure 3.1.2 and appendix E1.

The Gp conglomerates are clast supported with a small amount of matrix present between the clasts i.e high clast/matrix ratio. The conglomerates are moderately sorted with clasts all falling within the pebble size range (1-5 cm) with a matrix of medium-coarse sand (figure 3.1.4).

Conglomerate Facies Gp Interpretation

This lithofacies is interpreted as being deposited by stream flow as a linguoid bar, the deposits of which are characterised by lenses of stratified sediments with well developed cross-beds (Miall, 1978; Boggs, 2001). The high clast/matrix ratio and moderate sorting is also a feature of linguoid bars and the clast supported nature of the sediment is typical of stream flow and is due to the fines remaining in suspension after discharge, leaving the coarser sediment to settle out (Collinson, 1978a; 1996). Linguoid bars are attached to the side of a braided river

channel, and the cross beds are formed as slip faces on the downstream side of the bar (Collinson, 1978a; 1996).

Conglomerate Facies Gm Description

Facies Gm conglomerates are also present throughout the Beaumont Formation, forming beds that are more continuous than facies Gp and range in thickness from 10 cm up to 3 m (figure 3.1.1). Beds often have a crude horizontal stratification that is formed by different sized clasts. No other sedimentary structures are present and, stratification is not present at all in the thinner beds. The Gm conglomerates are clast supported with matrix also present between the clasts, and have a clast/matrix ratio lower than that of the Gp conglomerates. Sorting of the Gm conglomerates is generally poor with clast sizes ranging from a few centimetres up to about 10 cm. In the crudely stratified part of the unit moderate sorting of clasts defines the layers. The matrix of the Gm conglomerates is medium sand to granule in size.

Conglomerate Facies Gm interpretation

This facies is interpreted as being deposited by stream flow as a longitudinal bar, which are characterized by crude horizontal bedding with a lower clast/matrix ratio, and are more poorly sorted than the Gp deposits (Miall, 1978; Nemec and Postma, 1993; Boggs, 2001). Longitudinal bars form in the middle of braided river systems where the coarsest sediments are deposited due to the stream losing power (Boggs, 2001). This waning of the stream flow does not allow the sediments to be sorted, thus leaving a low clast/matrix ratio and little internal structure (Collinson, 1978a; 1996).

Sandstone Facies St description

Sandstones of facies St are common in the Beaumont Formation and are present in the measured section figure 3.1.1. This facies is made up of mainly lens-shaped sand layers that are generally a few decimetres thick and commonly discontinuous. The bases of the beds or lenses are erosional downward concave surfaces. Layers are composed of a number of lenses stacked together, and can therefore be many meters thick (figure 3.1.1). Sedimentary structures in this facies consist of trough cross-beds, identified as pi cross-beds of Allen (1963). Cross-beds are generally 5-20 cm high although some can reach almost 1 m. The St facies sandstones in the study area are made up of medium sandstone that is well sorted.

SANDSTONE FACIES ST INTERPRETATION

Sand grain size and the presence of pi cross-beds is the reason for describing this facies as St (Miall, 1977), forming due to the migration of dunes under lower flow regime conditions (Allen, 1963; Miall, 1977; Miall, 1978; Collinson, 1978a; 1996). These types of deposits are formed in the transition to upper plane phase beds (Collinson, 1996).

SANDSTONE FACIES SH DESCRIPTION

This facies is widespread throughout the Beaumont Formation and is well represented in the measured section (figure 3.1.1). Beds are up to 4 m thick, and are continuous with have parallel edges. Pervasive lamination on the millimetre scale is the most obvious sedimentary structure; cross-beds are rare but do occur. The Sh facies is poorly to moderately well sorted. Some beds are made up of moderately well sorted sandstone while others are made up of sandstone with randomly oriented pebbles floating in it. The grain size ranges from medium sand up to pebbles 5 cm in diameter.

SANDSTONE FACIES SH INTERPRETATION

The grain size and lamination in this facies is the reason for interpreting it as Sh (Miall, 1978). The Sh facies is formed by planar flow under lower or upper flow regime conditions (Miall, 1978; Collinson, 1978a; 1996). Sykes (1988) split the Sh facies into Shu (upper flow regime) and Shl (lower flow regime), based on the presence (Shu) or absence (Shl) of pebbles in the sand (Sykes, 1988). Both of these facies are present in the Beaumont Formation in the study area (figure 3.1.1). The presence of small cross-beds in this facies is probably related to preservation of upper flow regime standing waves (Collinson, 1996).

MUDSTONE AND SILTSTONE FACIES FSC, FCF AND C DESCRIPTION

These lithofacies generally occur in lower parts of the Beaumont Formation in the study area and are usually separate from the other facies described above e.g G.R. 2119500 5501500 (figure 3.1.5), although small layers of muddy sediments are also present within the coarser part of the unit (figure 3.1.1). This unit is generally massive grey mudstone or siltstone (facies Fsc) with interbedded coal lenses and carbonaceous mud (facies C). Due to the mud-rich composition of this facies, it is often slumped and outcrops poorly (figure 3.1.5). One example of a fresh water mollusc was also found in the massive mud in the study area (facies Fcf).

MUDSTONE AND SILTSTONE FACIES FSC, FCF AND C INTERPRETATION

The facies Fsc massive mud-siltstone and facies C coal and carbonaceous mud suggests that this muddy part of the Beaumont Formation was formed in backswamp and swamp conditions (Miall, 1978). The freshwater mollusc shows that facies Fcf backswamp ponds were present in the area at the time of deposition (Miall, 1978). The grey colour of the mud indicates that it was water saturated (Collinson, 1996), which is also evidence for a swamp type environment. All these types of environments occur in flood plain areas where sediment is deposited from suspension during floods and bioturbated by plants (Collinson, 1996).

LITHOFACIES DISCUSSION

The vertical and horizontal relationships between the different lithofacies that are present in the Beaumont Formation differ across the study area. On the slopes of Mount Hamilton (G.R. 2119500 5501500) the basal part of the Beaumont Formation is always made up of facies Fsc, Fcf and C. This mud and coal layer ranges in thickness from a few meters up to over 100 m (figure 3.1.3). Above the muddy facies the conglomerate (Gm, Gp) and sandstone (Sh, St) rich facies abound and the muddy facies are scarcely seen (figure 3.1.3 and 3.1.5). This facies association shows that the region initially formed as a swampy flood plane area receiving minor suspended material during floods, while vegetation on the plain destroyed sedimentary structures and deposited coal seams. After some time the major channels of the braided river system migrated into the area, depositing the coarser detritus, characteristic of a braided river plain environment.

Large scale lateral facies changes are not recognised in the study area, although they must exist, as the floodplain seen at the base of the Beaumont Formation would have had a river adjacent to it in order for the sediment to be deposited.

PALEOCURRENT ANALYSIS

Cross-beds from lithofacies Gt and St were measured using the technique described in section 1.5.5. The results of this analysis are shown in figure 3.1.2 as rose diagrams in the positions where the outcrops are located, showing that the currents depositing the Beaumont Formation flowed in a southwest to northeast direction, roughly parallel to the present basin margins (appendix E1).

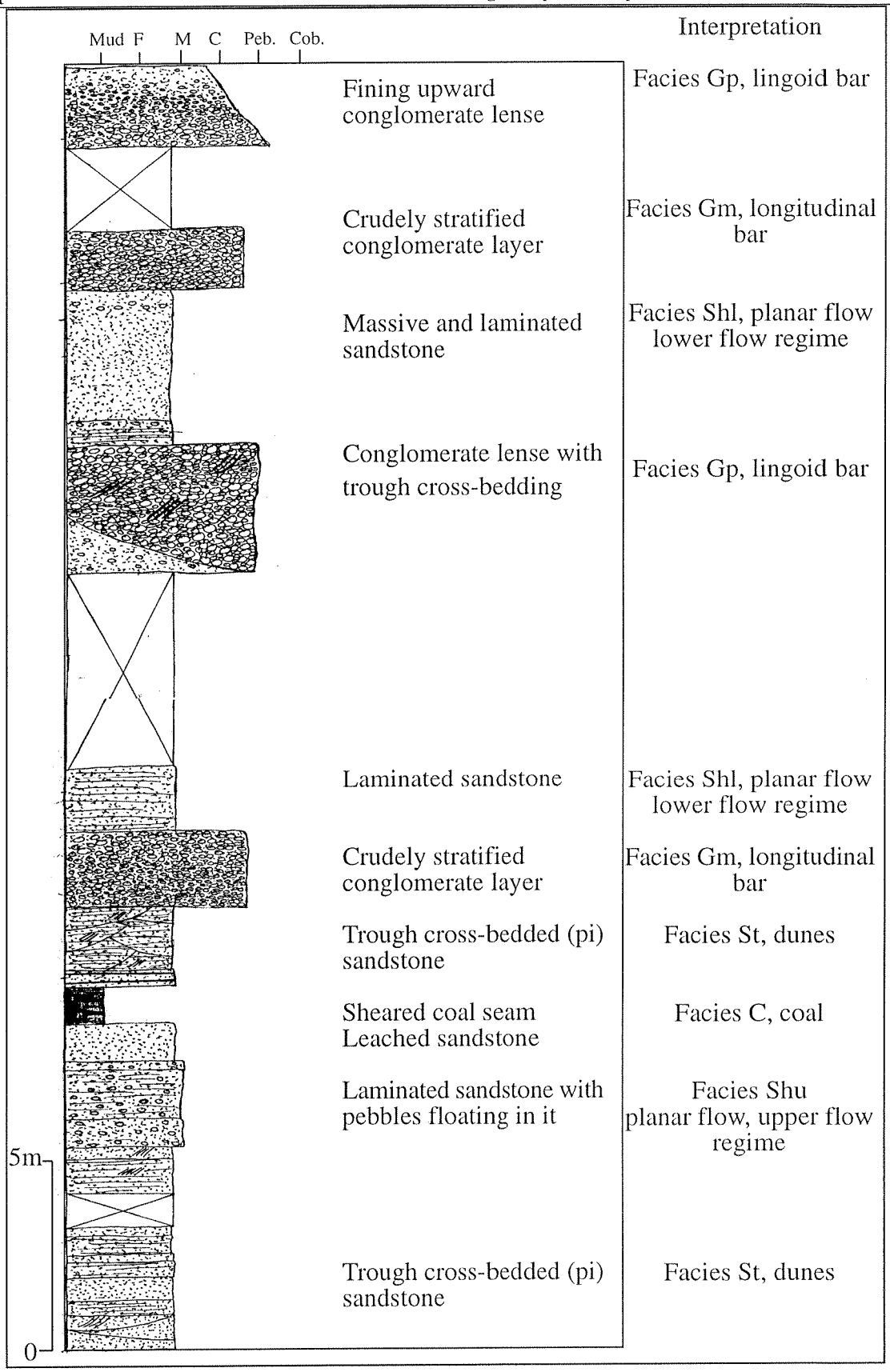

Figure 3.1.1 Measured section through the Beaumont Formation at G.R. 2121190 5503030. The section is about 50 m above the base of the unit. The section shows lithofacies that are present in the Beaumont Formation and gives an interpretation of their facies (see text for description of facies).

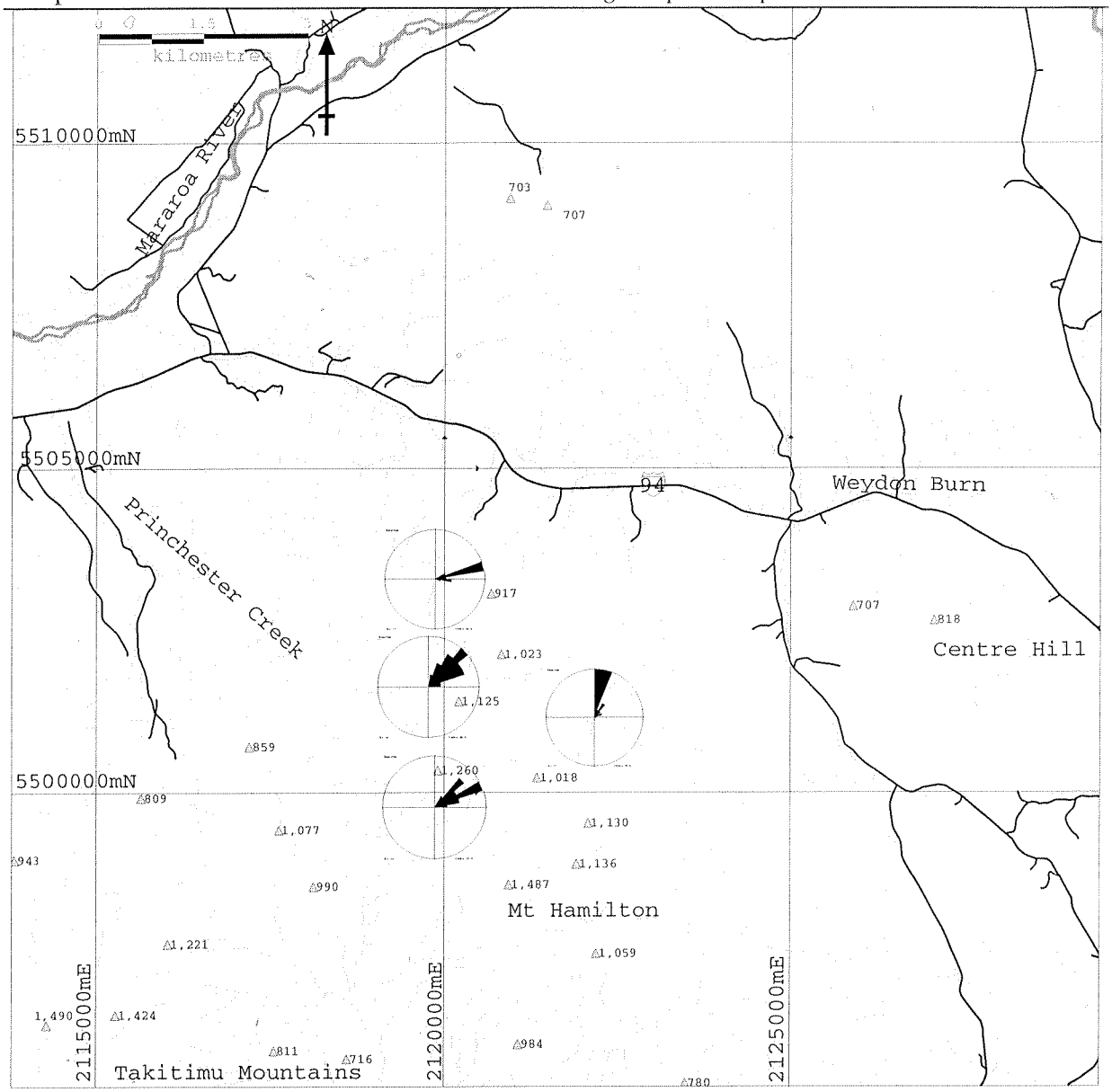

Figure 3.1.2 Rose diagrams representing the current directions measured from cross-beds in the Beaumont Formation. The diagrams are located at the position of the outcrop that was measured.

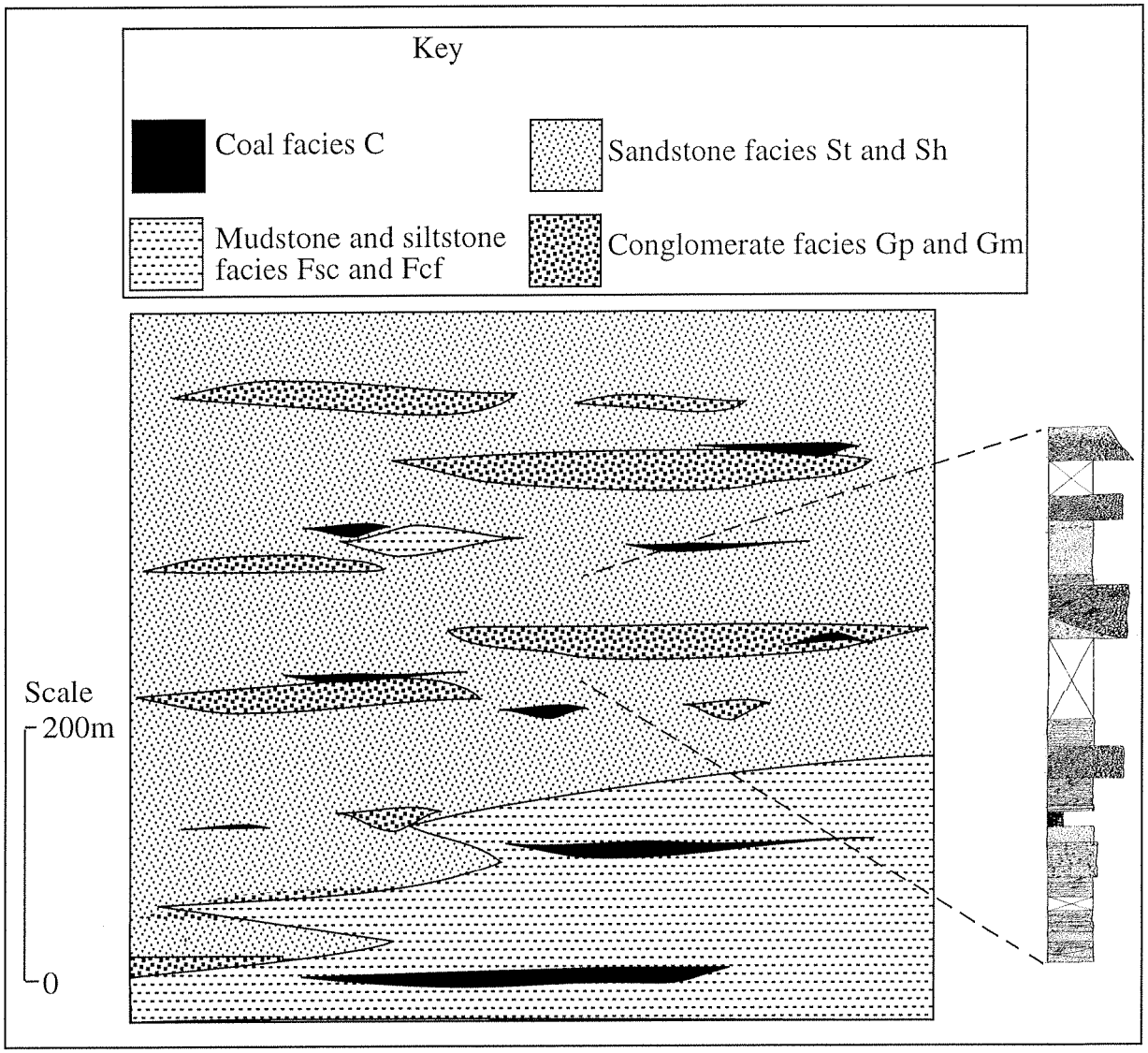

Figure 3.1.3 Facies associations in the Beaumont Formation showing the floodplain deposited mud and coal rich base of the formation overlain by the coarser sandstone and conglomerate facies deposited in a braided river plain environment.

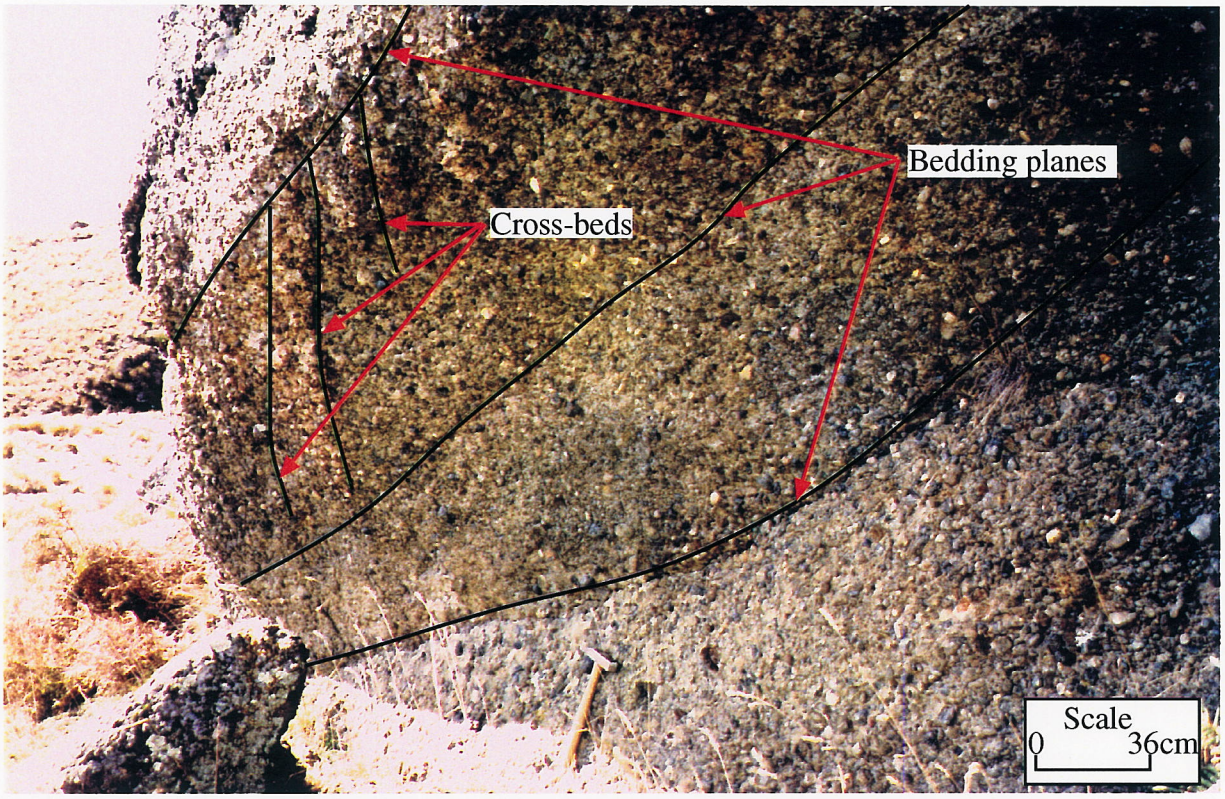

Figure 3.1.4 Beaumont Formation facies Gp conglomerate (G.R. 2120300 5502700) showing the lensoid nature of the beds and cross-beds (note that the strike of the cross-beds is at an oblique angle to the plane of the photograph).

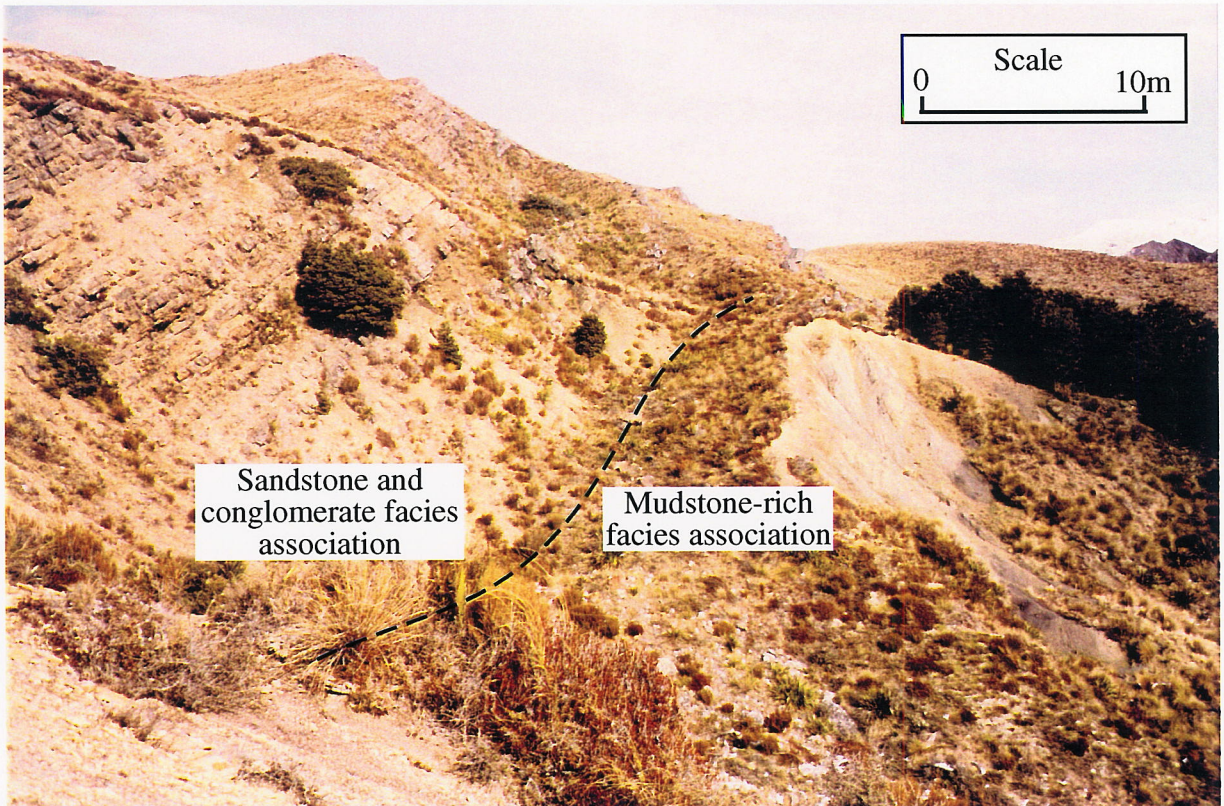

Figure 3.1.5 The mudstone-rich facies association is seen here (G.R. 2120200 5501500) where it is most abundant underlying the sandstone and conglomerate facies association.

3.1.4 PETROLOGY

INTRODUCTION

A number of different petrological techniques were used to analyse rocks of the Beaumont Formation in an attempt to determine the provenance and depth of burial of the unit, as well as aid interpretation of the sedimentary processes that formed it. Petrography of the sandstone, conglomerate clasts, and heavy mineral samples were combined with whole rock geochemical analysis to infer the provenance of the Beaumont Formation. Vitrinite reflectance of the coal in the Beaumont Formation was carried out to give an approximate depth of burial of the unit.

SANDSTONE PETROGRAPHY

Three sandstone slides from the Beaumont Formation were analysed using the point count method described in section 1.5.6 to determine the modal proportions of the grains (appendix B, OU 73289-73291). Grains in the Beaumont Formation sandstones are angular, with grain size ranging from 0.15-0.4 mm in diameter. The sand is moderately well sorted, and grains are clast supported with muddy matrix infilling the pore space.

The sandstone is quartz-rich, with quartz accounting for 50-60% of the rock (figure 3.1.7). Lithic fragments are the second most prominent mode in the sandstone, comprising 17-20% of the rock(figure 3.1.7). Sedimentary lithics are the most common (12-17%), with volcanic lithics making up 3-5% of the rock. 10-20% of the sandstone is feldspar with both plagioclase and potassium feldspar present (figure 3.1.7). The sandstone contains 7-10% matrix, and is therefore classed as an arenite according to Pettijohn et al (1987). Minor amounts (<1%) of heavy minerals, mica and metamorphic lithics are also present.

The average Q:F:L ratio for the Beaumont Formation sandstone is 60:20:20. Figure 3.1.6 is a Q:F:L plot of the data from this study as well as that of Kirby (1989) and Hall (1989). Data from this study and petrofacies 1 of Kirby (1989) all fit into the subarkose and sublitharenite fields of Pettijohn et al (1987). According to Pettijohn et al (1987) samples of Hall (1989) are arkose while petrofacies 2 sandstones of Kirby (1989) fit into the arkose arenite and litharenite fields.

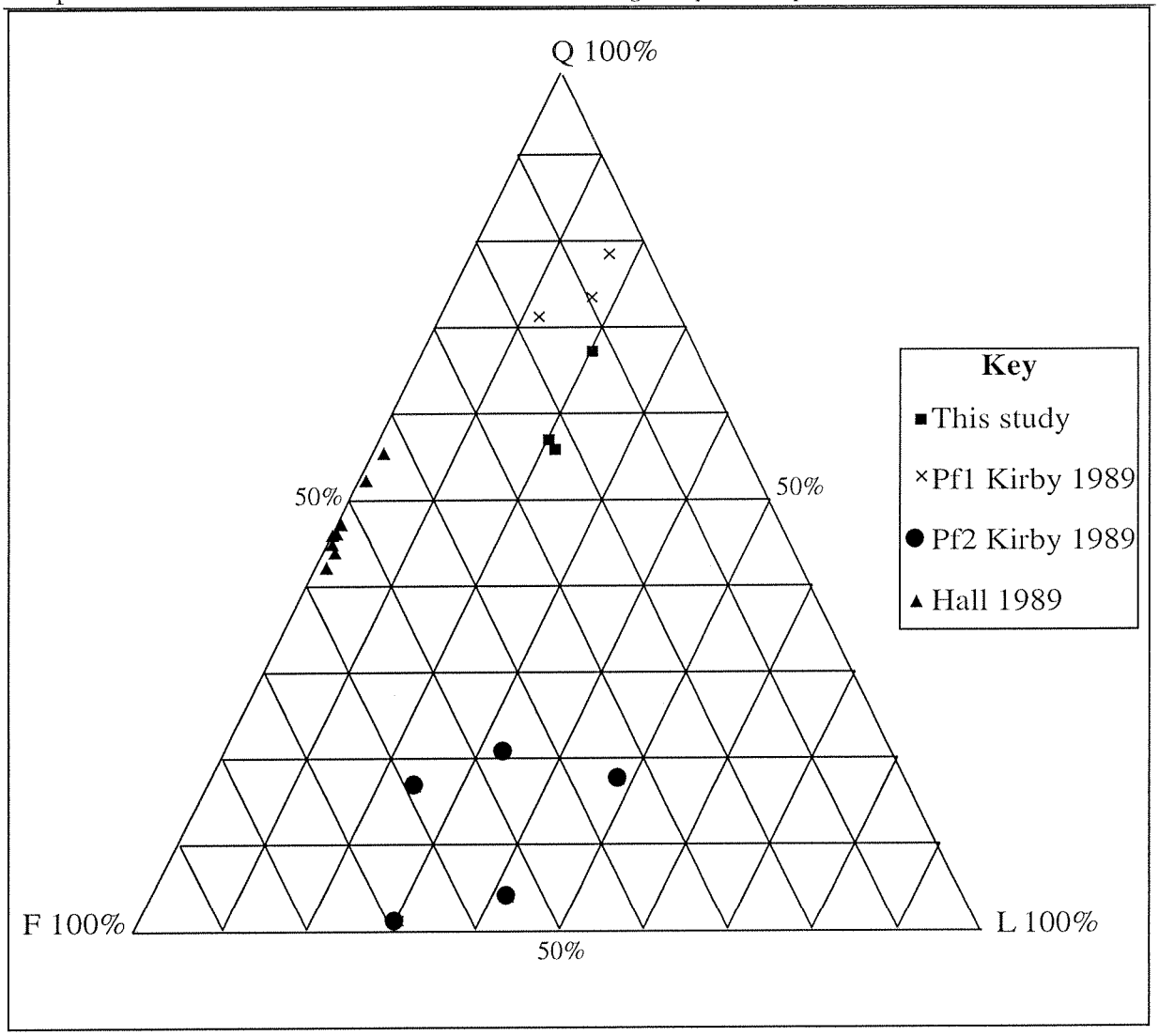

Figure 3.1.6 Q:F:L diagram for the Beaumont Formation sandstone from this study as well as Kirby (1989) and Hall (1989). This shows that the data from this study are similar to petrofacies 1 (Pf1) of Kirby (1989). The sandstones from Hall (1989) have less lithic grains than this study, while petrofacies 2 (Pf2) of Kirby (1989) is much more lithic rich.

CONGLOMERATE PETROGRAPHY

Clast types that have been identified in hand specimen and thin section from outcrops of Beaumont Formation include Murihiku Supergroup hard grey siltstone and auto-cannibalised Beaumont Formation brown sandstone (appendix C). These clast types, along with green-grey sandstones represented by OU 73322, often make up over 50% of the clasts near the top of the unit and decrease towards the base. Granitoid clasts (OU 73319, 73322) make up over 50% of the clast total in the lower part of the unit, becoming less abundant toward the top. The other clast type seen in the Beaumont Formation is porphyritic andesite (OU 73320) accounting for up to 10% of the clasts throughout the unit.

HEAVY MINERALS

A thin-section of the heavy mineral sample (OU 73328) taken from the Beaumont Formation sandstone (for separation techniques see section 1.5.4) was investigated petrographically in order to identify minerals present in the heavy mineral fraction of the sandstone (figure 3.1.8). Opaques are the most common (60%), and are all altered to varying degrees. Titanite is the main alteration mineral, while the original minerals appear to be ilmenite and magnetite as well as titanite. 30% of the heavy fraction is zircon some of which is prismatic. Other grains include hornblende and spinel (2-3% each), while the final 5% of the sample was unable to be identified due to intense alteration.

GEOCHEMISTRY OF THE SANDSTONE

Major and trace element geochemistry of the sandstone from the Beaumont Formation has been analysed using discrimination plots (see section 1.5.3, appendix D, OU 73289-73291). Data from Hall (1989) is also plotted on the graphs to see if the same geochemical patterns are present throughout the Beaumont Formation.

Major element data from this study and Hall (1989) all plot in the ACM field of the silica versus K_2O/Na_2O graph of Roser and Korsch (1988) (figure 3.1.9A). On the discriminant function plot of Roser and Korsch (1988) most of the samples plot in the P3 and P2 fields (figure 3.1.9B).

Trace elements from both Hall (1989) and those of this study all plot of the arc section in the La/Y versus Ce/V plot of Mortimer and Roser (1992) (figure 3.1.10).

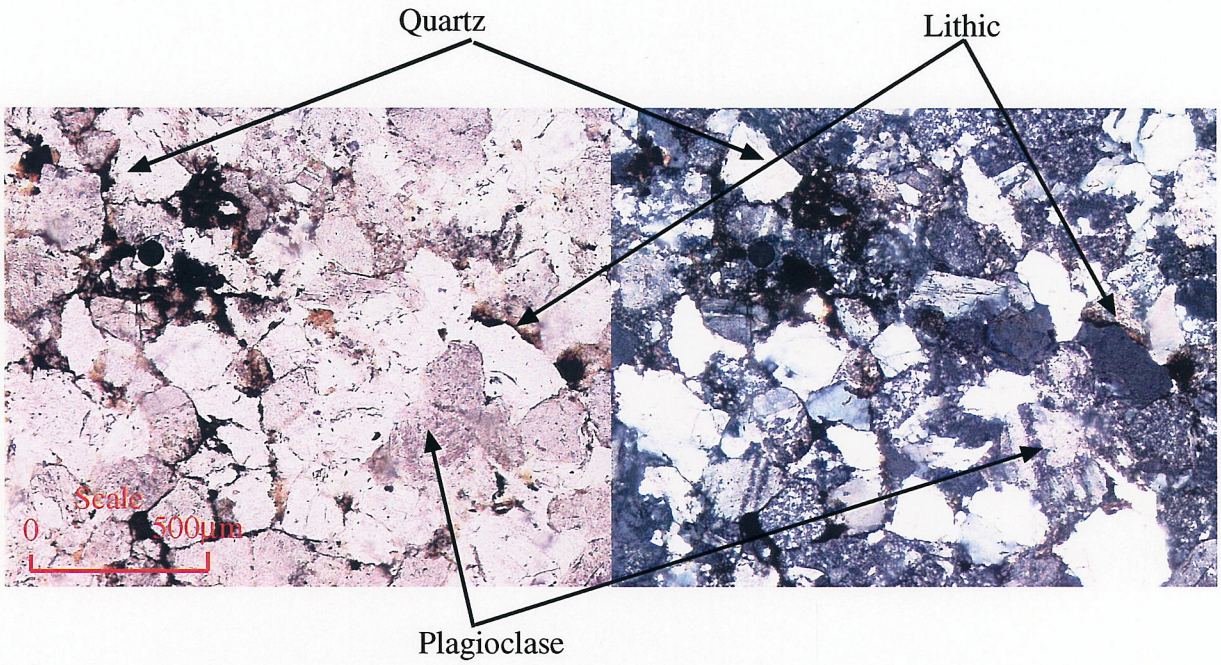

Figure 3.1.7 Photomicrograph of the Beaumont Formation sandstone (OU 73290) (plane-polarised light on the left, cross-polarised light on the right) showing the major constituents, note the clean nature of the quartz compared with the altered plagioclase and lithic grains.

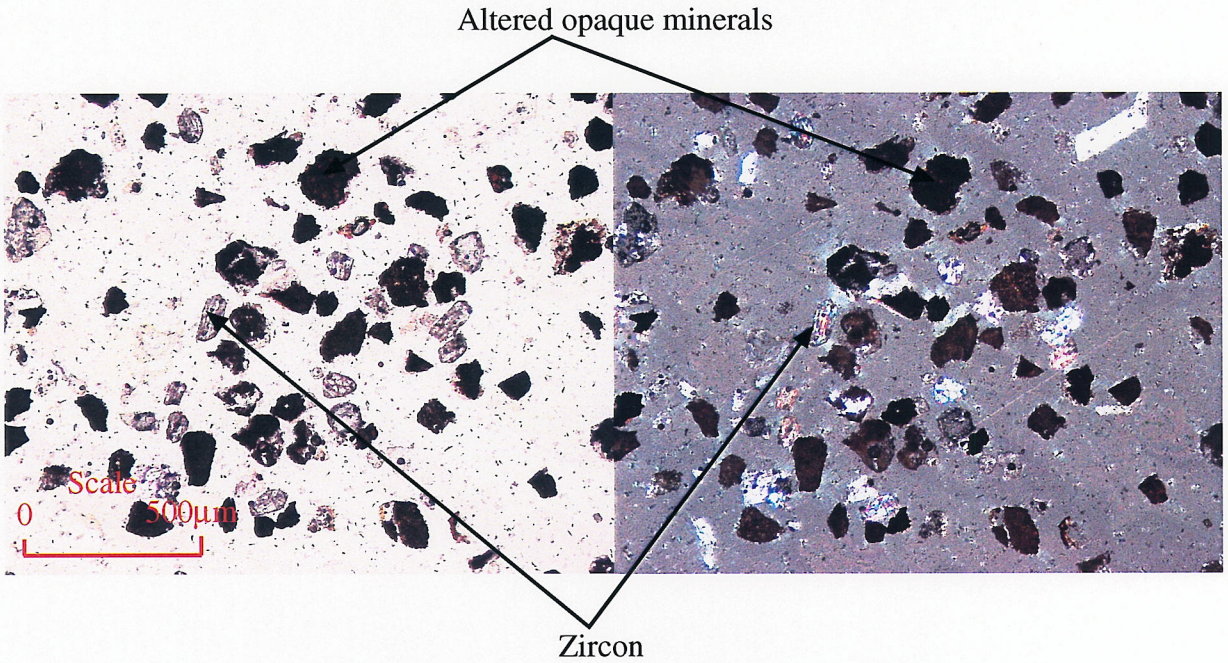

Figure 3.1.8 Photomicrograph of the heavy mineral sample from the Beaumont Formation sandstone (OU 73328) (plane-polarised light on the left, cross-polarised light on the right) the majority of the grains are altered opaque minerals that are hard to identify, the other grains are zircons some of which have a prismatic shape indicating that they are first cycle sediments.

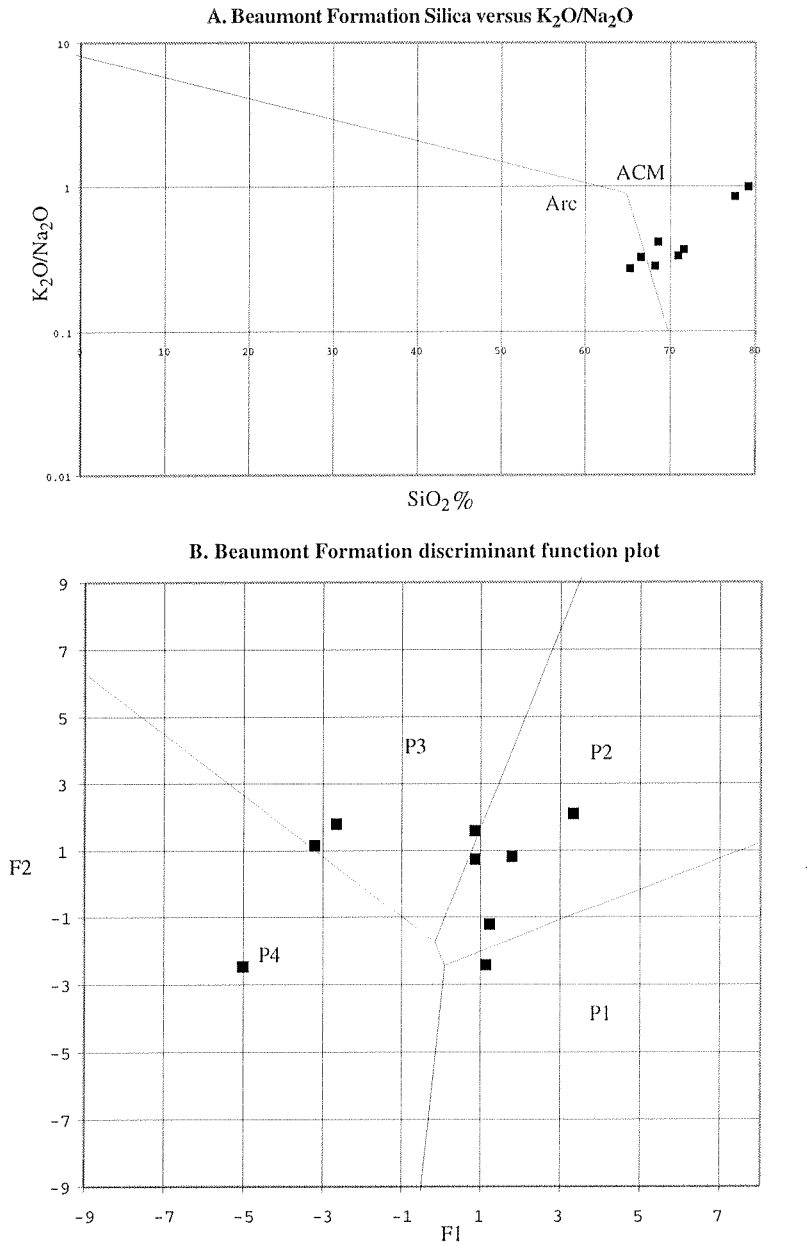

Figure 3.1.9 Major element discrimination plots. Figure **A** shows that the simple SiO_2 vs K_2O/Na_2O plot indicates an active continental margin derived origin for the Beaumont Formation sandstone. The more complex discriminant function plot in **B** shows that the source of the sediment may range from intermediate igneous to felsic igneous, with some samples falling in or close to the recycled field.

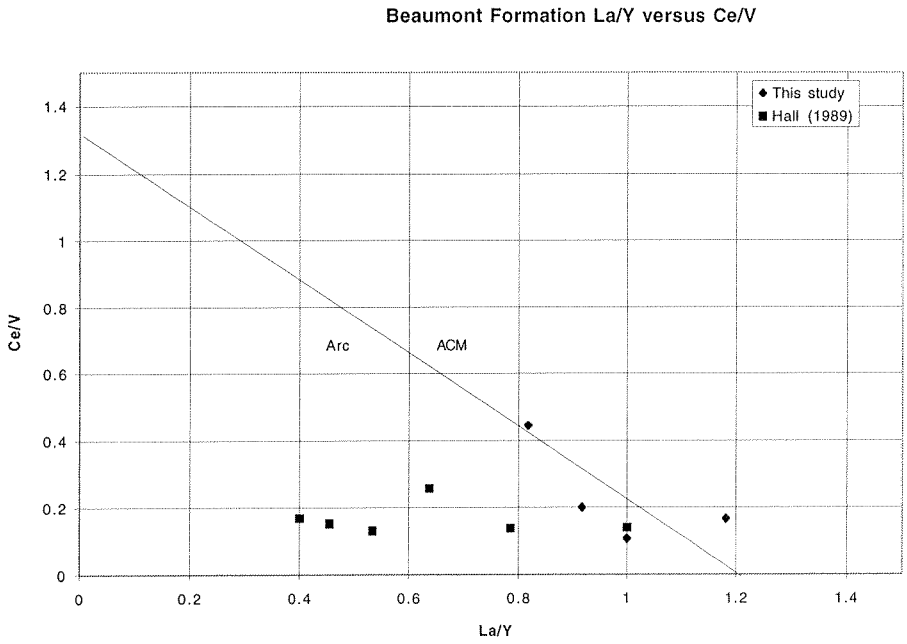

Figure 3.1.10 Trace element discrimination plot. The La/Y vs Ce/V plot shows that the Beaumont Formation sandstones are derived from an arc type source with two samples falling into the ACM section of the graph.

VITRINITE REFLECTANCE

Vitrinite reflectance studies of the coal in the Beaumont Formation were carried out in order to find the maximum depth of burial of the basin in the study area. The VR_o data from this study have been plotted together with depth data from other New Zealand basins, namely the Solander Basin to the south of the study area, and the western platform and Taranaki Graben in the Taranaki Basin. The study area was related to both of these basins before the late Cenozoic movement on the Alpine Fault (Carter and Norris, 1976). The Moonlight Fault that bounds the western Southland basins is probably equivalent to the Taranaki Fault in the north (Carter and Norris, 1976).

The coal in the study has VR_o values that range from 0.3 up to 0.5. This range of values gives a wide depth range when compared to the other areas. When compared to the Solander-1 data VR_{omax} is equivalent to a depth of 2000 m, whereas if the Taranaki Graben data is used VR_{omax} gives a depth of almost 3000 m, while 3800 m is the result obtained using the western platform data (figure 3.1.11).

A lack of other information on the burial conditions in the area such as geothermal gradient makes any interpretation of burial depth difficult. Other factors that affect the vitrinite reflectance independent of burial depth include the sedimentary environment that the coal was deposited in and the amount of deformation that has occurred.

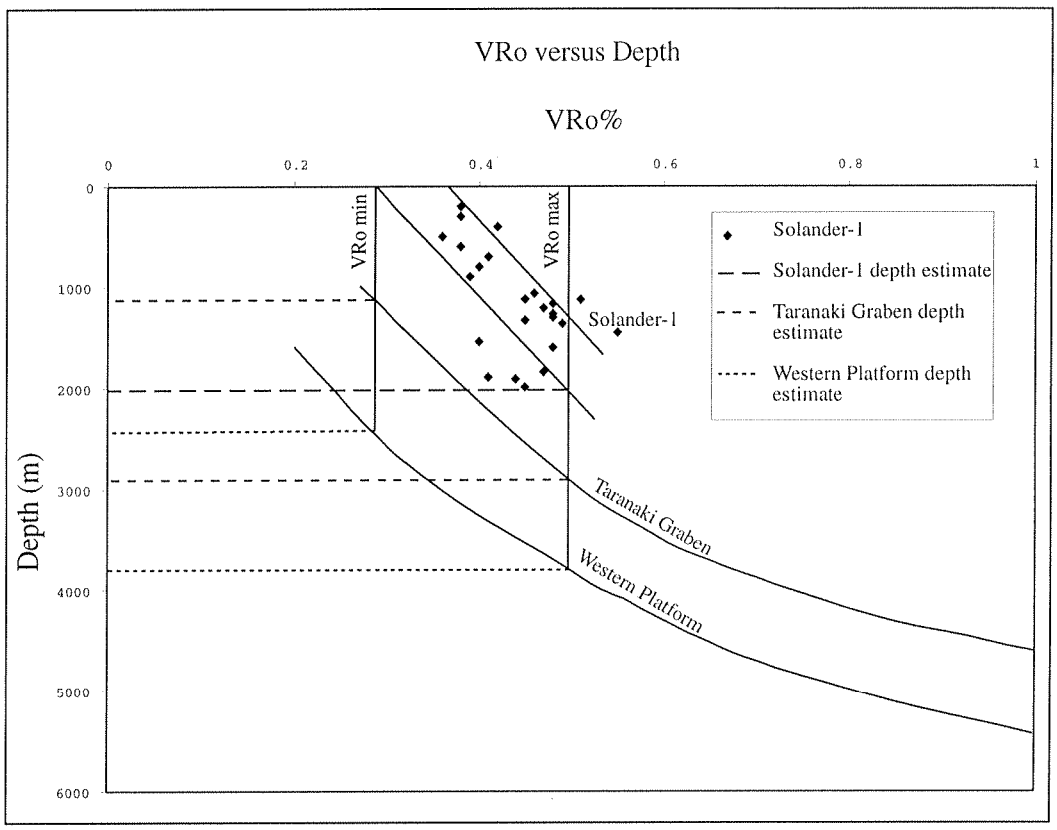

Figure 3.1.11 Vitrinite reflectance versus depth graph of the Solander Basin and two drill holes in the Taranaki Basin. The VR_{omax} and VR_{omin} values from this study are also compared in order to find the depth of burial of the Beaumont Formation in the study area. Solander-1 data is from Turnbull, Uruski et al, (1993); Taranaki data is from Pilaar and Wakefield (1984).

3.1.5 SUMMARY

Environment of deposition of the Beaumont Formation

Lithofacies present in the Beaumont Formation give a good idea of the two different types of environment that were present when the unit was deposited. The first sediments were deposited in a backswamp environment on a floodplain, while the upper part of the unit has been deposited by a braided river system on a river plain that migrated into the area over time.

The mud and siltstone facies (Fsc, Fcf and C of Miall (1978)) forming the bottom part of the Beaumont Formation in the study area, suggests a backswamp-swamp environment (Miall, 1978). This indicates that the main channels of the river system that deposited the upper part of the unit were not present in the study area in the early stages of the deposition, although flood waters affected the area depositing fine-grained sediment.

The upper part of the Beaumont Formation is predominantly conglomerate (facies Gm and Gp) and sandstone facies (St and Sh) units. Minor muddy and carbonaceous units are also present. These facies are typical of the Donjek type facies assemblage of Miall (1977). The Donjek type facies assemblage indicates that the sediment was deposited as part of a braided river system at some distance from the source (Miall, 1977). Coarse sediments that are deposited by stream flow, with no input from debris flows, also indicate that the river is some distance from the source in the middle part of an alluvial fan (Collinson, 1996). Paleocurrent data from the Beaumont Formation shows that the river flowed from the southwest to the northeast.

Provenance of the Beaumont Formation

Petrography of the Beaumont Formation suggests that the sediments within it are derived from at least two different sources. One source is the Median Tectonic Zone plutonic rocks, while the other is volcanic derived sediments of the Takitimu Group and volcaniclastics of the Murihiku Supergroup.

Evidence for a Median Tectonic Zone provenance

The Beaumont Formation sandstone petrography from Hall (1989), Kirby (1989) petrofacies 1, and this study all suggest that the sediment is very mature. The major element geochemistry of the sandstone shows that some of the sediments are derived from an active continental margin or similar source. This is shown in the silica versus K_2O/Na_2O plot and the P3 section of the discriminant function plot.

The presence of granitoid pebbles (OU 73321, 73319), and the results of heavy mineral analysis suggest a plutonic source for the sandstone, but the sediment lacks the high-grade metamorphic minerals such as the garnets present in the Western Province. The prismatic nature of the zircons in the sample confirms that the sediment is not recycled.

Both the petrography and major element geochemistry of the sandstone indicate that the sediments are derived from either the high-grade meta-plutonic rocks of the Western Province or the plutonic rocks of the Median Tectonic Zone. The granitoid pebbles and the heavy mineral analysis are both indicative of the plutonic rocks in the Median Tectonic Zone indicating that part of the Beaumont Formation is derived from this source. Median Tectonic Zone rocks were probably uplifted between the Waiau and Te Anau Basins at this time (Zink, 2000).

Evidence for a Takitimu Group Province

Petrofacies 2 of Kirby (1989) is immature sediment containing many lithic grains. Some of the major element geochemistry from Hall (1989) plots in the P2 field indicating an arc type provenance, as does trace element geochemistry from both Hall (1989) and this study. Field observations and petrology of the pebbles in the conglomerate indicate that there are intermediate volcanic (Takitimu Group), green volcaniclastic (Takitimu Group), and grey siltstone (Murihiku Supergroup) pebbles in the Beaumont Formation. All this evidence indicates that part of the Beaumont Formation was derived from the Takitimu Group and Murihiku Supergroup that makes up the Takitimu Mountains.

Depth of burial

The vitrinite reflectance study of the Beaumont Formation suggests a burial depth of 3000 m, but geological observation shows that this is far too shallow an estimate. In the area between G.R. 2121000 5502800 and 2123300 5503800 the Eocene-late Oligocene sequence is exposed at the surface with little or no repetition of the sequence. In this area the thickness of the sediment is about 4000 m (see map and cross-section, appendix H), but this area does not include the Miocene Haycocks Formation that is at least 2000 m thick. Most of this sediment was deposited before the Miocene compressive phase (Carter and Norris, 1976; Turnbull, Uruski et al, 1993; Sutherland, 1995) began to uplift the units in the area. This means that the Beaumont Formation was covered by up to 6000 m of sediment prior to uplift, showing that the vitrinite reflectance study was not representative in determining the maximum burial depth for the sediments in the basin.

A number of factors could have affected the vitrinite reflectance of the coals in the Beaumont Formation including: sedimentary environment, geothermal gradient, burial time and uplift rates. If the Beaumont Formation was uplifted before the coal had fully crystallised the vitrinite reflectance number would be lower.

3.2 ORAUEA MUDSTONE

3.2.1 INTRODUCTION

The Orauea Mudstone was first described by Bowen (1964) in the Ohai area, and mentioned by Sykes (1988), although no lithofacies studies were carried out. In the study area a mudstone unit was known to overlie the Beaumont Formation (Carter and Norris, 1977b), but was not officially named until 1989 when Turnbull et al included it in the Orauea Mudstone.

The Orauea Mudstone conformably overlies the Beaumont Formation, and is present along the east side of the Waiau Basin, in the Ohai area and around the northern Takitimu Mountains (Turnbull et al, 1989; Turnbull, Uruski et al, 1993). In the study area the unit is present above the Beaumont Formation, and around the edges of Mount Hamilton and Centre Hill (map and cross-section, appendix H), although outcrop is poor due to the mud rich nature of the unit. The type locality for the Orauea Mudstone as defined by Turnbull et al (1989), is in Ohai Stream (G.R. D45/120620) (Arafin, 1982). The base and top of the unit have separate reference sections at drillhole 364 (G.R. D45/157625) 100-161 m, and on the banks of the Waiau River (G.R. D45/037485 to D45/038492) respectively. The Orauea Mudstone is up to 500 m thick in the Ohai area (Bowen, 1964; Sykes, 1988; and Turnbull et al, 1989) and in the study area is 300-400 m thick.

3.2.2 AGE AND FOSSIL OCCURENCE

No fossils were found in the Orauea Mudstone, so unit age has been determined by the fact that it conformably overlies the Runangan aged Beaumont Formation, and is conformably overlain by the early Whaingaroan, Spear Peak Formation and Waicoe Formation. This has lead to the conclusion that the age of the Orauea Mudstone is late Eocene-early Oligocene (Runangan-early Whaingaroan), an age which is consistent with the palynological data of Pocknall and Turnbull (1989) in the Waiau Basin, where the Runangan *Nothofagidites mataurаensis* was found in the bottom part of the unit.

3.2.3 LITHOFACIES DESCRIPTION AND INTERPRETATION

FACIES DESCRIPTIONS

Laminated mudstone is the main lithofacies in the Orauea Mudstone, with minor lithofacies represented by sandstone layers. The mudstone is brown and contains abundant fine-grained carbonaceous material. The sandstone layers are approximately 10 cm thick, have flat bases and tops and consist of medium sand grade material.

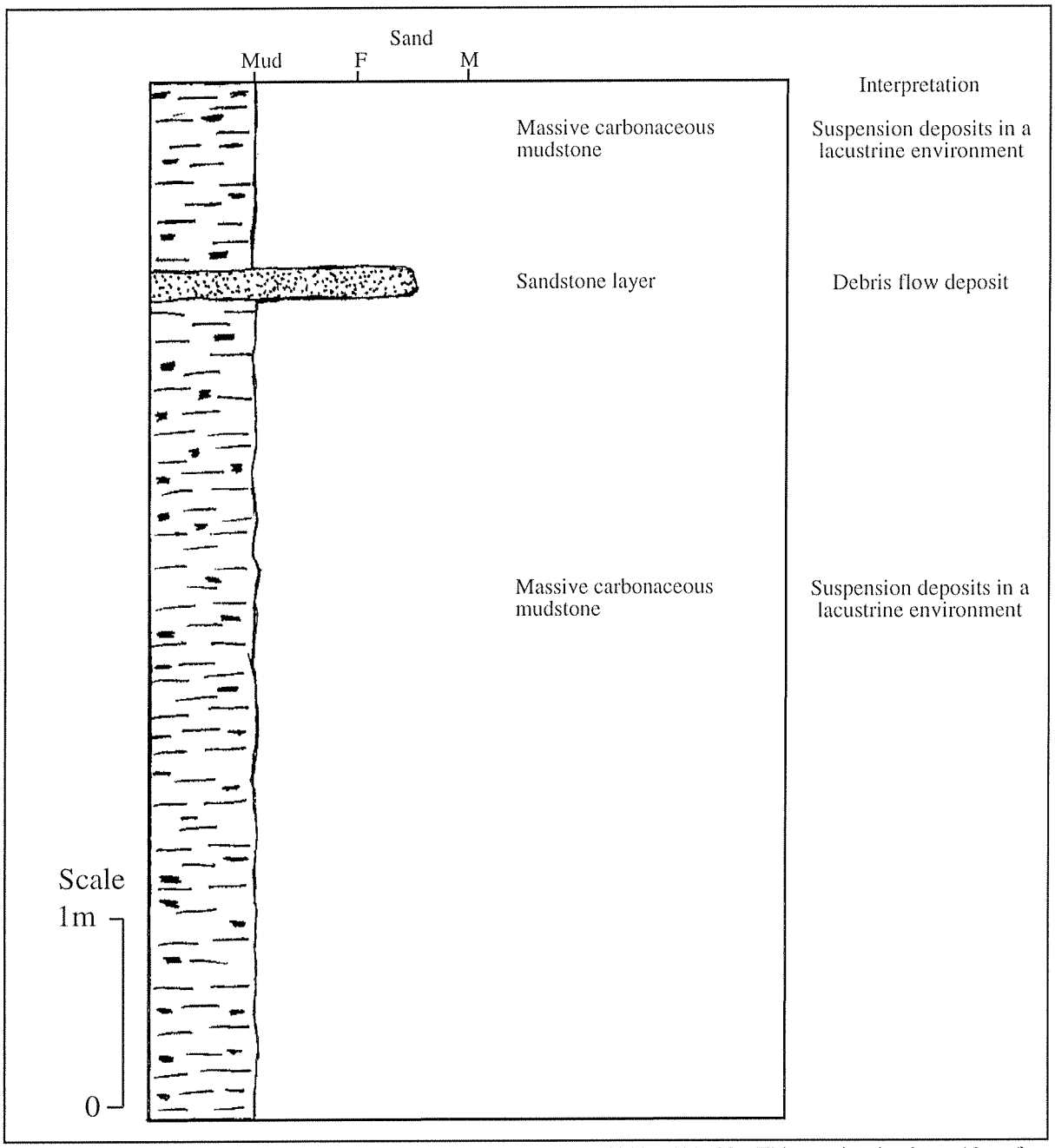

Figure 3.2.1 Orauea Mudstone measured section from G.R. 2124900 5502700. This section is about 10 m from the base of the overlying Waicoe Formation that is exposed nearby. The section shows the predominant carbonaceous mudstone in the formation as well as the sandstone layers that are present.

3.2.4 SUMMARY

ENVIRONMENT OF DEPOSITION

The presence of mudstone indicates that most of the sediment was deposited from suspension, and the carbonaceous material contained in the Orauea Mudstone suggests that the unit was formed in a terrestrial environment (Collinson, 1978b). This evidence leads to the interpretation of the Orauea Mudstone as a lacustrine deposit. Sandstone layers in the Orauea Mudstone probably represent fan deposits formed by debris flows (Collinson, 1978b).

4 WAIAU GROUP

INTRODUCTION

Conformably overlying the Nightcaps Group are the marine sediments of the Waiau Group, which range in age from Oligocene to Pliocene (Landis, 1974), and are present in both the Waiau and Te Anau Basins, where the sediments may exceed 5000 m in thickness (Turnbull et al, 1989; Turnbull, Uruski et al, 1993). The Waiau Group consists of various marine units including: hemipelagic mudstone (Waicoe Formation), flysch sandstone (e.g Haycocks Formation), breccia (e.g Spear Peak Formation), and shelf limestone and sandstone (e.g Clifden sub-Group) (Turnbull et al, 1989; Turnbull, Uruski et al, 1993). Sediments of the Waiau Group vary dramatically throughout the basins, and for this reason a number of different type sections are allocated to represent the different units that are present. Unfortunately, none of these type sections include units within the study area (Turnbull et al, 1989).

In the study area the Waiau Group is dominantly made up of the Waicoe Formation, which has been flooded by three major Oligocene-Miocene submarine fan deposits: the Spear Peak Formation, the Weydon Formation, and the Haycocks Formation (Carter and Norris, 1977b; Turnbull et al, 1989; Turnbull, Uruski et al, 1993; Turnbull, 2000). These fan deposits are sand and gravel-rich as opposed to the mud-rich Waicoe Formation in which they are interbedded (figure 1.7.1).

SUBMARINE FANS AND TURBIDITE FACIES

Since turbidites were first proposed by Kuenen and Migliorini (1950) they have become the favoured model for the transport of sediment from shelf areas to submarine fans (e.g Bouma, 1964; Mutti and Ricci-Lucchi, 1972; Ricci-Lucchi, 1975; Walker, 1978; Stow and Shanmugam, 1980; Lowe, 1982). Most of the submarine fan models are based on outcrop observations of interbedded sandstone and mudstone, however Shanmugam (2000) suggests that these models are flawed and that they do not relate to formation of present day submarine fans. Observations of drill core from submarine fans often show that the sedimentary features predicted by turbidite facies models occur only rarely in many fans (Shanmugam, 2000).

One of the problems with submarine facies models is that since their inception most deep water sandstone-mudstone sequences have been interpreted as turbidites, with new models being developed to suit the situation. Features that don't fit the turbidite model are often over-looked or added to the new model (Shanmugam, 2000). Shanmugam (2000) suggests that many of the sequences previously described as turbidites are in fact debris flow deposits. Stow and Mayall (2000) and Stow and Johansson (2000) show some of the complexities that can be expected in the transport and deposition processes in submarine gravity driven processes. Most often, submarine fan deposits are likely to have been transported by both laminar flow and turbulent flow processes, with the sedimentary structures preserved in the rock only recording the last part of this transport (Stow and Mayall, 2000).

Despite the trend to abandon some of the turbidite facies models that were used for almost twenty years (Normark, 1991; Walker, 1992), Basu and Bouma (2000) show the relationship between ancient turbidite emplaced sediments of Tanqua Karoo and sediment from fans drilled in the ocean drilling program. Miall (1999) suggests that facies models are still applicable in modern sedimentology so long as their limitations are realized and they are only used as guides for the identification of facies.

The problems associated with submarine fan deposits are very important in regard to this project as the Waiau Group is made up of a number of these fans. In an attempt to discriminate between debris flow and turbidite deposits a number of key criteria have been applied to facies that are recognised in the study area (table 4.1). The facies used in this study are similar to those described by Ricci-Lucchi (1975) and Stow et al (1996) (figure 4.1). These facies were originally designed to represent turbidite facies. The nature of the sedimentary relationships has not changed, although some of the interpretations may be different (figure 4.1). While these models form a base for the study, observations of aspects of the sediment in the study area that differ from the model are investigated in order to interpret the types of processes that resulted in the deposition of the unit.

In this report "*a turbidity current is a sediment gravity-flow with Newtonian rheology and turbulent state from which deposition occurs through suspension settling*" (Shanmugam, 2000), and "*a debris flow is a sediment-gravity flow with plastic rheology and laminar state from which deposition occurs through freezing*" (Shanmugam, 2000).

	Turbidites	Debris flow
Grading	Normal	Normal, reverse or non-graded
Cross-beds	No	Yes
Lamination	Yes (T_b, T_c, T_d)	Possibly
Floating clasts	No	Yes
Armoured mud-ball	No	Yes
Nature of beds	Channels-sheet	Channels-sheets (composed of amalgamated channels)
Bouma sequences	Yes	No
Flow type	Newtonian flow	Bingham plastic flow

Table 4.1 Some of the criteria that can be used to discriminate between turbidites and debris flows based on sedimentary structures that can be seen in outcrop. The information in the table is from Shanmugam (2000).

	1 Turbidite	2 Debris flow
A	 Gravel-pebbly sandstone Normal graded Poor sorting No floating clasts, armoured mud balls, cross beds Some horizontal stratification Sand(gravel)/pelite=very high(>>1) Facies A2.5 and A2.3 of Stow et al (1996)	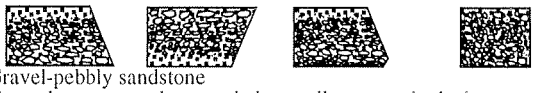 Gravel-pebbly sandstone Normal, reverse and un-graded as well as some beds that are reverse graded at the base and normally graded at the top Poor sorting Lense shaped beds Beds up to 15 meters thick Floating clasts, armoured mud-balls and cross-beds common Some horizontal stratification Sand(gravel)/pelite=very high(>>1) All facies A except D2.3 and D2.5 of Stow et al (1996)
B	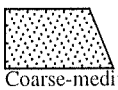 Coarse-medium sandstone with some small pebbles at the base of beds Normal graded Better sorting than A1 Lenticular beds over scales of 10s of metres Beds 300-2000 millimetres Sand/pelite=high(>1) Facies B2.5 of Stow et al (1996)	 Coarse-medium sandstone with some small pebbles at the base of beds Normal, reverse and un-graded Better sorting than A1 Lenticular beds over scales of 10s of metres Beds 300-2000 millimetres Floating clasts, armoured mud-balls and cross-beds common Sand/pelite=high(>1) All facies B except D2.5 of Stow et al (1996)
C	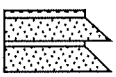 Normal graded sandstone interbedded with mudstone Poor-well sorted sediment Even parallel beds over 10s to 100s of metres Beds 500-5000 millimetres Sand/pelite=high(>1) Abundant sole marks Bouma sequence Facies C2 of Stow et al (1996)	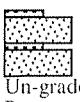 Un-graded sandstone interbedded with mudstone Poor-well sorted sediment Even parallel beds over tens to hundreds of metres Beds 500-5000 millimetres Sand/pelite=high(>1) Bouma sequence absent Facies C1 of Stow et al (1996)
D	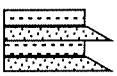 Normal graded sandstone interbedded with mudstone Well sorted sediment Even parallel beds over 100s of metres to kilometres Beds 30-500 millimetres Sand/pelite=low(≤1) Lamination, ripples and convolute bedding common Bouma sequence Facies D2.1 of Stow et al (1996)	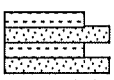 Un-graded sandstone interbedded with mudstone Moderate-well sorted sediment Even parallel beds over 100s of metres to kilometres Beds 30-500 millimetres Sand/pelite=low(<1) Bouma sequence absent All facies D sediments except D2.1 of Stow et al (1996)
E	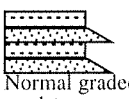 Normal graded fine sandstone or siltstone interbedded with mudstone Well sorted sediment Lenticular beds or parallel only for a few meters Beds 30-500 millimetres Sand/pelite=low(<1) Lamination common Bouma sequence Facies E2.1, 2.2 & 2.3 of Stow et al (1996)	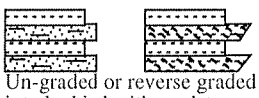 Un-graded or reverse graded fine sandstone or siltstone interbedded with mudstone Moderately sorted sediment Lenticular beds or parallel only for a few metres Beds 30-500 millimetres Sand/pelite=low(<1) Broken shell layers common All facies E except E2.1, 2.2 & 2.3 of Stowet al (1996)

Figure 4.1 The sedimentary facies used in this study based on those of Ricci-Lucchi (1975) and Stow et al (1996). The facies are divided into turbidite and debris flow, based on some of the criteria from Shanmugam (2000), shown in table 4.1. Facies F and G discussed in the text are used in the same way as Ricci-Lucchi (1975).

4.1 SPEAR PEAK FORMATION

4.1.1 INTRODUCTION

TYPE SECTION

Two type sections are given for this unit, reflecting the changes in lithology that occur along strike within it. The main reference section is from (G.R. D43/186021) to (G.R. D43/194058) while the secondary section is at G.R. D43/215032 where it cuts the breccia facies (Turnbull et al, 1989). Both of these sections are within the study area.

DISTRIBUTION AND THICKNESS

The Spear Peak Formation (Turnbull et al, 1989) has been mapped around the north end of the Takitimu Mountains, from Elm Tree Creek (Fitzharris, 1967) to the upper Weydon Burn in the study area (Turnbull et al, 1989) (map and cross-sections in appendix H). Thickness of the formation varies along strike from 650 m in Princhester Creek, to 0 m where it pinches out at either end (Turnbull et al, 1989) (map and cross-sections in appendix H).

PREVIOUS WORK

Very little detailed work has been carried out on the Spear Peak Formation, and most studies in the area have concentrated on mapping the units rather than describing detailed sedimentology. The unit was first mapped by McCraw (1947) as "Duntroonian sandstones and conglomerates", based on the unit being lithologicaly distinct from the other Tertiary rocks in the area. Carter and Norris (1977b) and Beanland (1980) interpreted the sediments of the Spear Peak Formation as being derived from the Takitimu Mountains. Kirby (1989) split the formation up into two lithofacies: lithofacies 1 contains Takitimu type detritus while lithofacies 2 contains MTZ or Western Province type detritus. The name Spear Peak Formation was formalized by Turnbull et al (1989), these authors and Kirby (1989) both interpreting the unit as being deposited in a proximal submarine fan complex.

4.1.2 AGE AND FOSSIL OCCURRENCE

The only fossils seen in the Spear Peak Formation in this study were those described by Kirby (1989) within the unit she named the Davaar Limestone Member of the Weydon Formation. This algal limestone contains the algae *Lithothamnium* sp and *Lithophyllum* sp (Kirby, 1989) and is considered in this study to be part of the Speak Peak Formation. The minimum age of this formation was determined from microfossils in the Waicoe Formation directly overlying it (section 4.2.2), a lower Whaingaroan age being obtained from this sample. A maximum age for the Spear Peak Formation can be inferred from the age of the underlying Orauea Mudstone that has been dated Kaiatan-Whaingaroan (Pocknall and Turnbull, 1989). This information indicates that the Spear Peak Formation is lower Whaingaroan in age as suggested by Carter and Norris (1977b) and Turnbull et al (1989).

4.1.3 LITHOFACIES DESCRIPTION AND INTERPRETATION

The Spear Peak Formation consists of a number of different lithologies, namely graded mudstone and sandstone, conglomerate, breccia and olistoliths. Graded sandstone and mudstone are the dominant lithologies, with lenses and channels of other lithologies locally abundant and often forming prominent outcrops. These lithologies have been divided in order to determine the environment of deposition of the Spear Peak Formation, with each lithofacies based on those of Ricci-Lucchi (1975) and Stow (1996) (figure 4.1).

LITHOFACIES A2 DESCRIPTION

Facies A2 sediments are abundant in the Spear Peak Formation. This facies is dominated by conglomerate and pebbly sandstone with occasional coarse sandstone layers representing a minor constituent. Clasts range in size from 1 cm up to 80 cm in diameter, and vary from well rounded to sub angular (figures 4.1.1, 4.16 and 4.1.7). The conglomerates are generally clast-supported although matrix-supported lenses also occur. Sorting is generally poor, although some lenses display moderate sorting (figures 4.1.1, 4.16 and 4.1.7).

Facies A2 conglomerates form both small channels within B2 and C facies sediments (figure 4.1.7), and large channels that are up to 500 m wide and 50 m thick. Bedding within these channels dips 10-20° more steeply than in the surrounding sediments. The channels are made up of smaller lenses that are up to 5 m thick and 20 m wide (figure 4.1.1). The bases of both

the major channel and the smaller lenses are erosional, with local unconformities formed within the Spear Peak Formation and between the Spear Peak Formation and the Orauea Mudstone at G.R. 2121500 5503400, where a channel cuts into the underlying unit.

Sedimentary structures present in this facies include cross-beds, imbrication, rip up clasts and crude lamination (figures 4.1.6 and 4.1.7). Tabular cross-beds that are up to 1 m high and dip at about 20-30° occur in some lenses in this facies; these fore-sets have smaller cross-beds preserved on the fronts of them that dip in the opposite direction. Large cross-beds similar to those found in the study area are not well documented in the ancient record, but have been seen using sonar in recent sediments (Piper and Kontopoulos, 1994). Some lenses have abundant imbrication with the long axis of the clasts generally pointing down current (figure 4.1.6). Rip up clasts in this facies are rare, but where present they are in the form of tabular clasts up to 1 m wide and 15 cm thick, with smeared out edges, and a calcite cement causing them to be very hard (figure 4.1.8). Generally the conglomerates show a crude horizontal lamination. Reverse graded bedding is common in this facies and minor amounts of normal grading are also present. The bases of some beds are reverse graded with the top parts becoming normally graded (figure 4.1.7).

LITHOFACIES A2 INTERPRETATION

The lenses and channels that make up this facies suggest that it formed in the feeder channels of a submarine fan (Walker, 1975; Nemec and Steel, 1988; Morris and Busby-Spera, 1990; Reading and Richards, 1994). The conglomeratic nature and the angularity of the sediments suggest that they have been deposited close to their source (Reading and Richards, 1994). The rip up clasts that are present in this facies have probably been transported only a matter of metres, as the mudstone that they are made of would break up quickly if it was transported further. These clasts represent hemi-pelagic mudstone that must have been accumulating near the channels at the time they were forming.

These types of channels have been documented from fan-deltas (Nemec and Steel, 1988) and submarine fans (Morris and Busby-Spera, 1990; Reading and Richards, 1994). The sedimentary structures that are present in this facies are identical to those described in Walker (1975) as slope deposits. These types of deposits would presumably form between a fan delta

and a submarine fan, with the more disorganised parts of the facies forming closer to the land than the organised parts.

The imbrication in the conglomerates has the long axis of the clasts facing downstream, suggesting that they were deposited as mass flow type deposits (Boggs, 2000). Reverse grading in this facies is indicative of debris flow deposition (see table 4.1). The cross-beds are also indicative of debris flow deposition, as they are deposited from bed-load rather than suspended-load. The interpretation of this type of deposit as being deposited by debris flows is at odds with the facies model of Walker (1975) who suggested that these types of deposits are deposited by turbidity currents.

LITHOFACIES B2 (INTERBEDDED SANDSTONE AND MUDSTONE) DESCRIPTION

This lithofacies is dominated by interbedded sandstone and mudstone with some of the sandstone layers containing small pebbles (<2 cm diameter) floating in the sand. The sandstone ranges from coarse to medium sand and has siltstone partings. Pebble conglomerates occasionally occur in the coarse part of graded beds and are matrix supported (figure 4.1.2 and 4.1.7). Sorting ranges from poorly sorted coarse sandstone to moderately well sorted siltstones and mudstones.

This facies consists of layers that are relatively parallel but pinch out over 1-10 metres, and within the facies, coarse sandstone forms small channels (<1 m in width and tens of centimetres deep) (figure 4.1.7). The beds range in thickness from a few centimetres up to 50 cm, with a sandstone/siltstone ratio of about 1:1 (figure 4.1.8). Some of the beds have been amalgamated into larger beds that reach thicknesses of up to 2 m. The beds are commonly graded normally, although reverse grading is also present (figure 4.1.2). Overall this facies fines upwards; at the base it is interbedded with coarse A2 pebbly sandstones and at the top it is interbedded with C facies sandstone and mudstone, this latter transition taking place over only 25 m (figures 4.1.2 and 4.1.8).

Sedimentary structures other than graded bedding are not common in this facies, the major structure is the lamination that is present in the silt to mud parts of the unit. Load casts, rip-up clasts (similar to those described in facies A2) and fluid escape structures are also present although these are not common (figures 4.1.2 and 4.1.8).

LITHOFACIES B2 INTERPRETATION

This lithofacies is indicative of dominantly debris flow deposition in a submarine fan environment. The presence of floating pebbles, some reverse grading and rip-up clasts, all fit into the debris flow facies and eliminate the possibility of turbidite deposition (figure 4.1). Some of the features within the siltstone, such as the lamination, have possibly resulted from suspension settling from a turbid layer. This may suggest that the flows were made up of a basal zone transported as a debris flow with a zone of turbidity above it. This type of deposit has in the past been referred to as a turbidite, despite the fact that the base is not a turbidite (e.g Postma et al, 1988). Shanmugam (2000) prefers the base part to be called a sandy debris flow and the top portion to be called a turbidite.

The fining upwards of the sequence, and the lenticular nature of the facies B deposits, suggests that this part of the fan was proximal to the feeder channels (Ricci-Lucchi, 1975; Reading and Richards, 1994; Stow, 1996). The proximal nature of the facies is also shown by the fact that it is interbedded with the A2 deposits at the base. The tabular nature of the rip-up clasts indicate that these have not been transported a great distance.

LITHOFACIES C1 (INTERBEDDED SANDSTONE AND MUDSTONE) DESCRIPTION

This facies is similar to facies B in that it consists of interbedded sandstone and siltstone, but it differs in that the beds are more continuous and the siltstone partings are thicker (figure 4.1.2). The sandstone is well sorted and of medium to coarse grainsize.

The beds are continuous over large distances much greater than outcrop scale, although they are less than 30 cm thick (mostly 10-20 cm). Beds are often, but not universally, normally graded (figure 4.1.2), and the sand/siltstone ratio is about 0.75. No amalgamated beds were seen in association with this facies (figure 4.1.2). The fining upward trend of the unit continues, with the base of this facies being interbedded with the facies B2 sediments, and the upper part of this facies presumably grading into the hemi-pelagic Waicoe Formation (figure 4.1.2).

Apart from pervasive lamination of the sandstone beds and the graded bedding, sedimentary structures were not seen in this facies.

LITHOFACIES C1 INTERPRETATION

The more continuous nature of this facies, combined with the lack of any pebble-sized material and the presence of pervasive lamination and normal grading, indicates that it has been deposited by turbidites (figure 4.1). Some of the beds in the facies are ungraded and may represent debris flow deposits. A lack of coarse material and the continuous nature of the beds suggest that this facies was deposited in a mid fan type environment and that it is more distal from the feeder channels than the facies B2 sediments (Ricci-Lucchi, 1975; Reading and Richards, 1994; Stow, 1996).

LITHOFACIES F1 (BRECCIA AND OLISTOLITHS) DESCRIPTION

Olistoliths and chaotic debris are present in the Spear Peak Formation. These are composed of very poorly sorted, angular clasts of volcaniclastics, diorite and volcanic breccia that can reach up to 20 m in diameter (figure 4.1.5). The olistoliths form lenticular beds up to 50 m long, and overlie the facies B sandstone beds where the contact is seen.

The limestone unit at G.R. 2115900 5504200 is made up of brecciated volcaniclastics in a matrix that consists of algal limestone, with minor foraminifera, brachiopods and other shells constituting the remainder of the limestone (Kirby, 1989). Kirby (1989) referred to the limestone as the Davaar Limestone Member of the Weydon Formation, although mapping during this study has shown that it is part of the Spear Peak Formation and that it grades into the facies B sediments of this formation.

This facies is usually chaotic with few sedimentary structures present, although occasional reverse grading is present in the finer sediments. Shear zones and brecciated areas are common in this facies, especially between the larger clasts (figure 4.1.5).

LITHOFACIES F1 (BRECCIA AND OLISTOLITHS) INTERPRETATION

The coarse angular nature of the sediment, in combination with the structures within this facies, suggest that it formed by mass movement type processes. Reverse grading in some of the unit is indicative of debris flow deposits, while the larger blocks suggest a slump or block fall type of deposition. Due to the fact that these sediments have been emplaced in the fan deposits and include limestone, they must have been formed in a submarine environment.

The nature of the sediment indicates that they have been deposited adjacent to the source, which could have been a fault scarp or an over-steepened submarine canyon wall.

LITHOFACIES DISCUSSION

Lithofacies within the Spear Peak Formation do not form regular cycles, instead tending to form inter-fingering relationships that have a general fining upward nature (figure 4.1.3). Considered as a whole, the depositional system that formed the Spear Peak Formation is most similar to the type 2 system of Mutti (1985), or the multiple-source gravel rich submarine ramp of Reading and Richards (1994). The facies F1 deposits represent scarp deposits caused by the erosion of the basin margin, and channels are represented by facies A2, while facies B2 and C1 formed the inner and middle part of the fan respectively. These deposits and their inter-fingering nature are all consistent with the fan systems of Mutti (1985) and Reading and Richards (1994). The dominant depositional mechanism was debris flow, with minor turbidity currents concentrated in the top part of the unit, consistent with the gravel-rich submarine ramp Reading and Richards (1994).

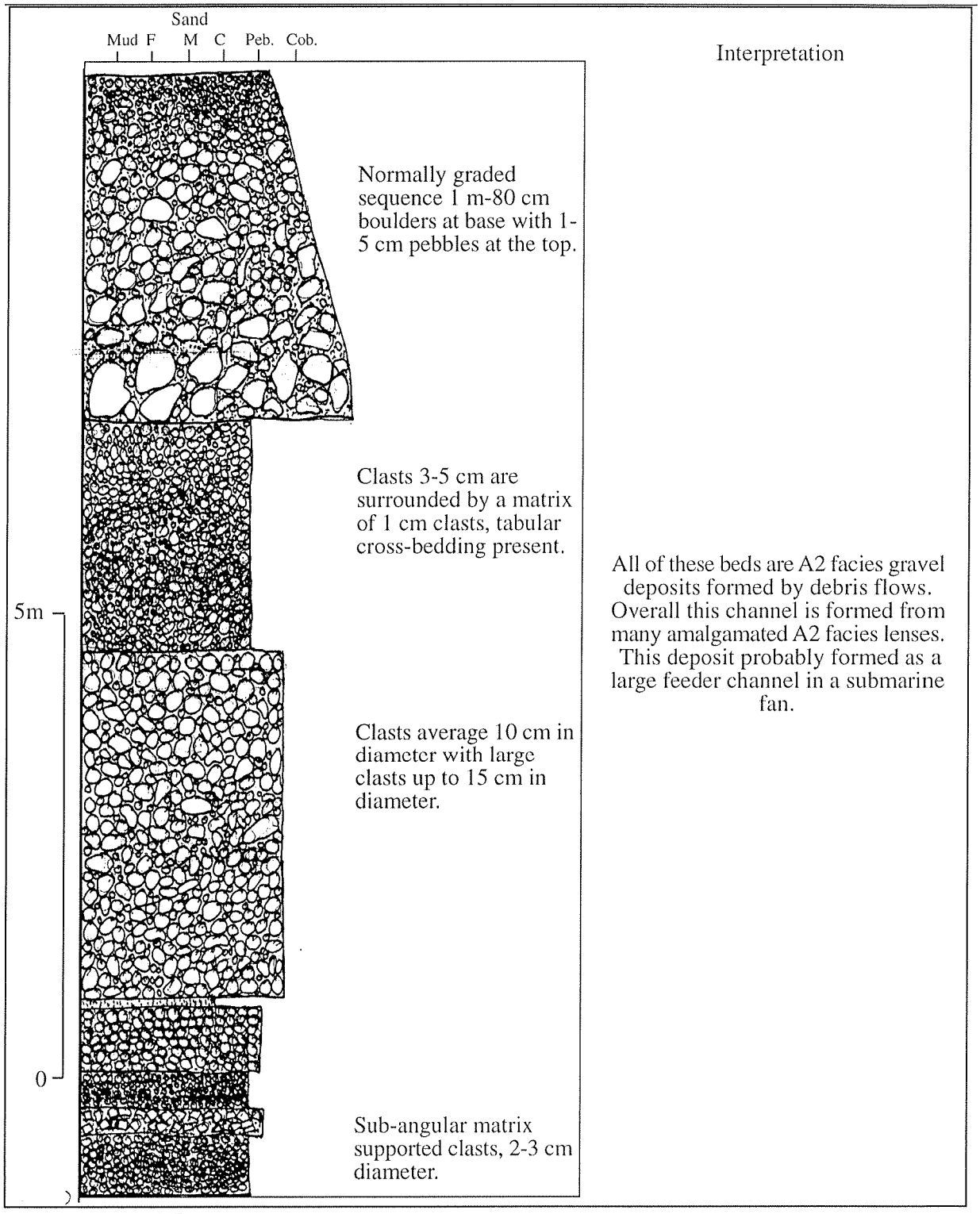

Figure 4.1.1 Section through the channel at G.R. 2121500 5503400, showing the amalgamated A2 conglomerate beds that form in the channel deposits. All beds shown in the section are lenses that are up to 20 m wide.

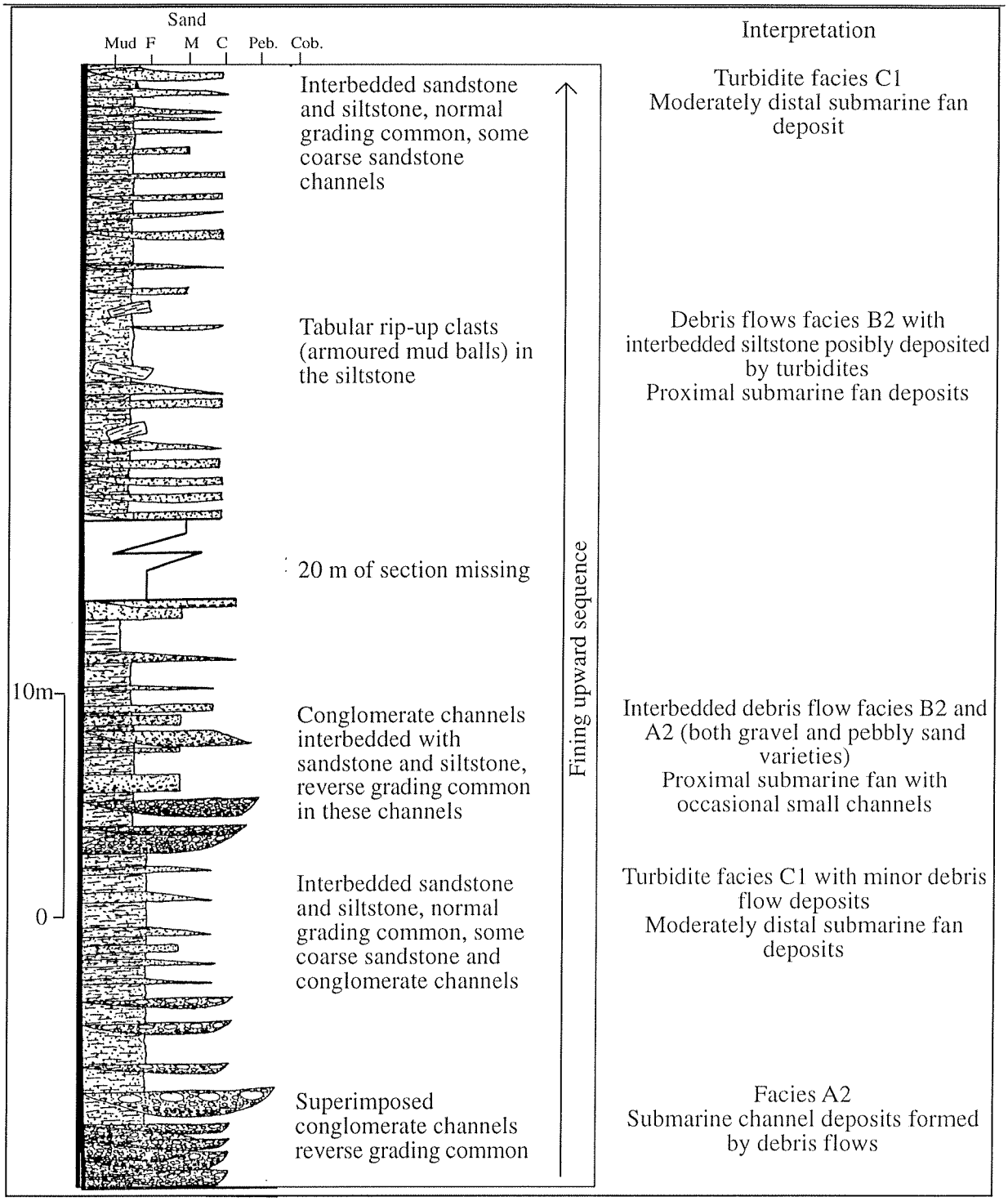

Figure 4.1.2 This section between G.R. 2117300 5505900 and 2117400 5505900 shows most of the lithofacies that are present in the Spear Peak Formation. The fining upward sequence and the related change in lithofacies is seen in this section, with the coarser grained, less mature facies at the base, and the finer grained more mature facies at the top. This section is about 50 m above a large channel deposit similar to that shown in figure 4.1.1

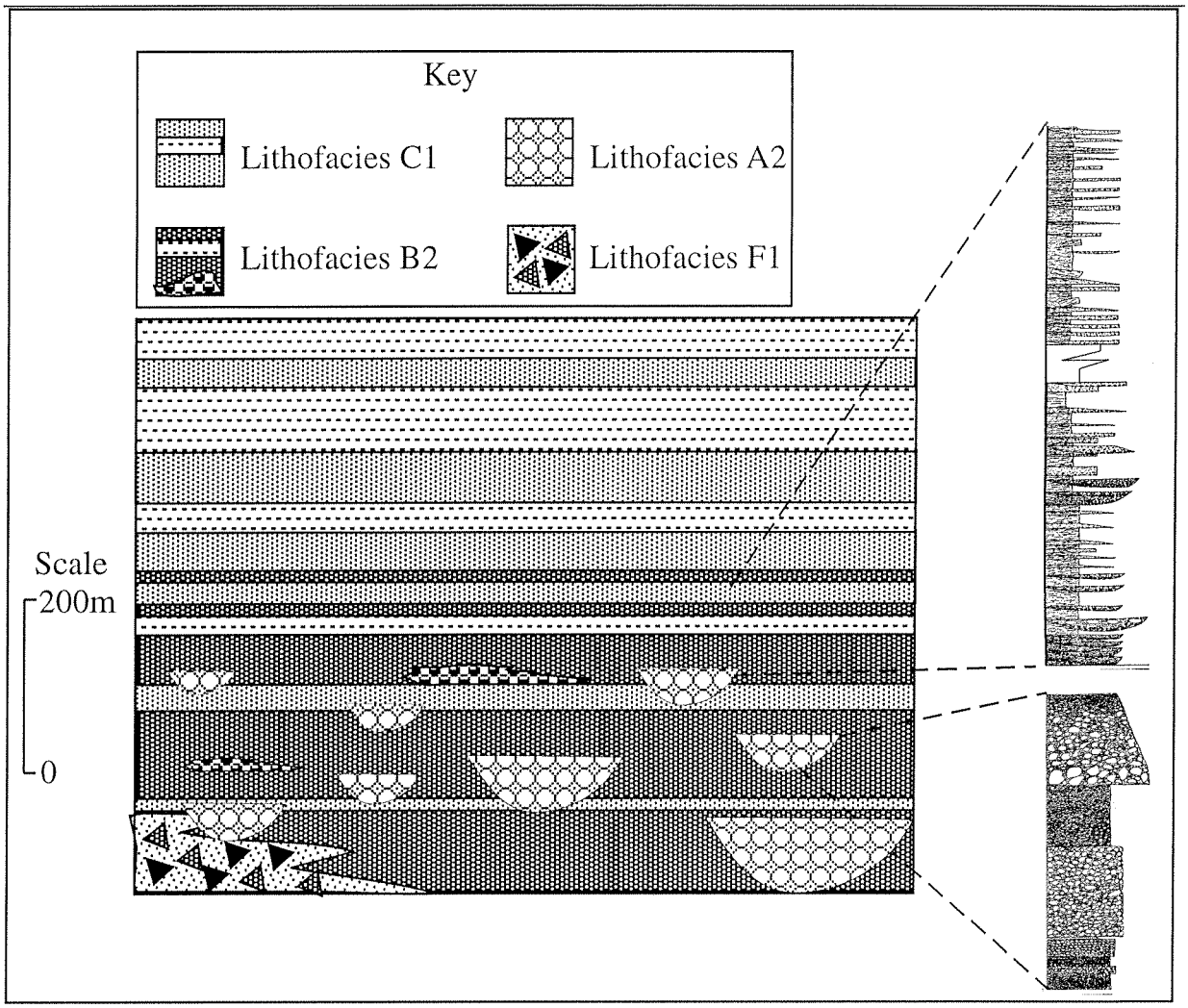

Figure 4.1.3 Schematic section through the Spear Peak Formation, showing the lithofacies associations that occur in the unit. The unit generally fines and thins upwards due to the change from facies B to facies C sediments. Conglomerates and breccias of facies A and F1 occur as interfingering layers. Sections from figure 4.1.1 and 4.1.2 are also shown.

PALEOCURRENT ANALYSIS

Cross-beds and imbrication of the pebbles were measured in the Spear Peak Formation within the A2 facies conglomerates using techniques described in section 1.5.5. The results shown in figure 4.1.4 indicate that the currents that deposited this unit flowed approximately from the south to the north (appendix E2).

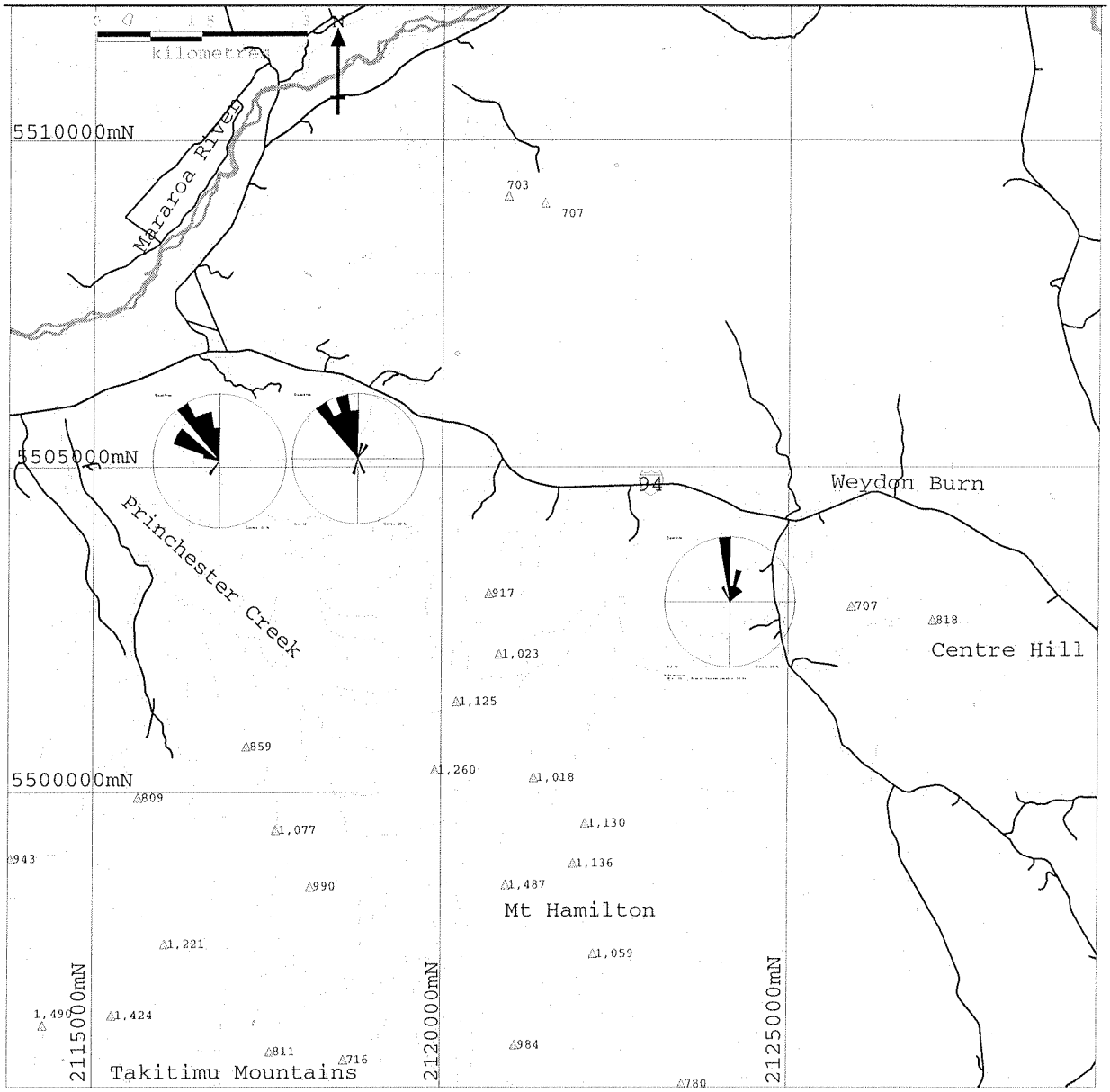

Figure 4.1.4 Current direction map of the A2 facies channels in the Spear Peak Formation, showing that the currents flowed in a broadly south to north direction.

Figure 4.1.5 Breccia in the Spear Peak Formation (G.R. 2117100 5503500) made up of large angular clasts of Takitimu Group derived material. Above this breccia is a 30 m wide olistolith (facies F1), also composed of intact Takitimu Group volcanic sediment.

Figure 4.1.6 Facies A2 conglomerate in the Spear Peak Formation at G.R. 2118700 5504900. Sedimentary structures such as cross-beds and imbrication were used to determine the current direction.

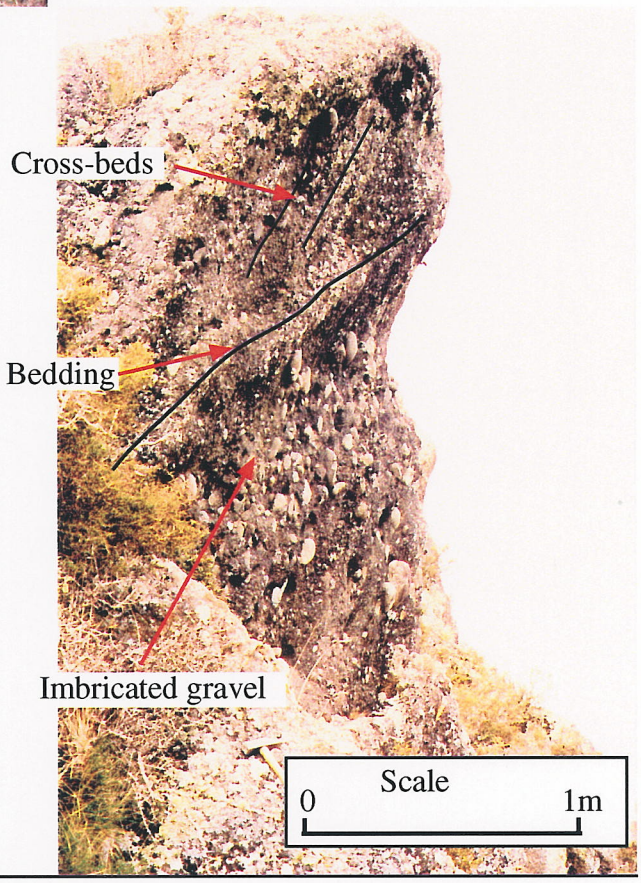

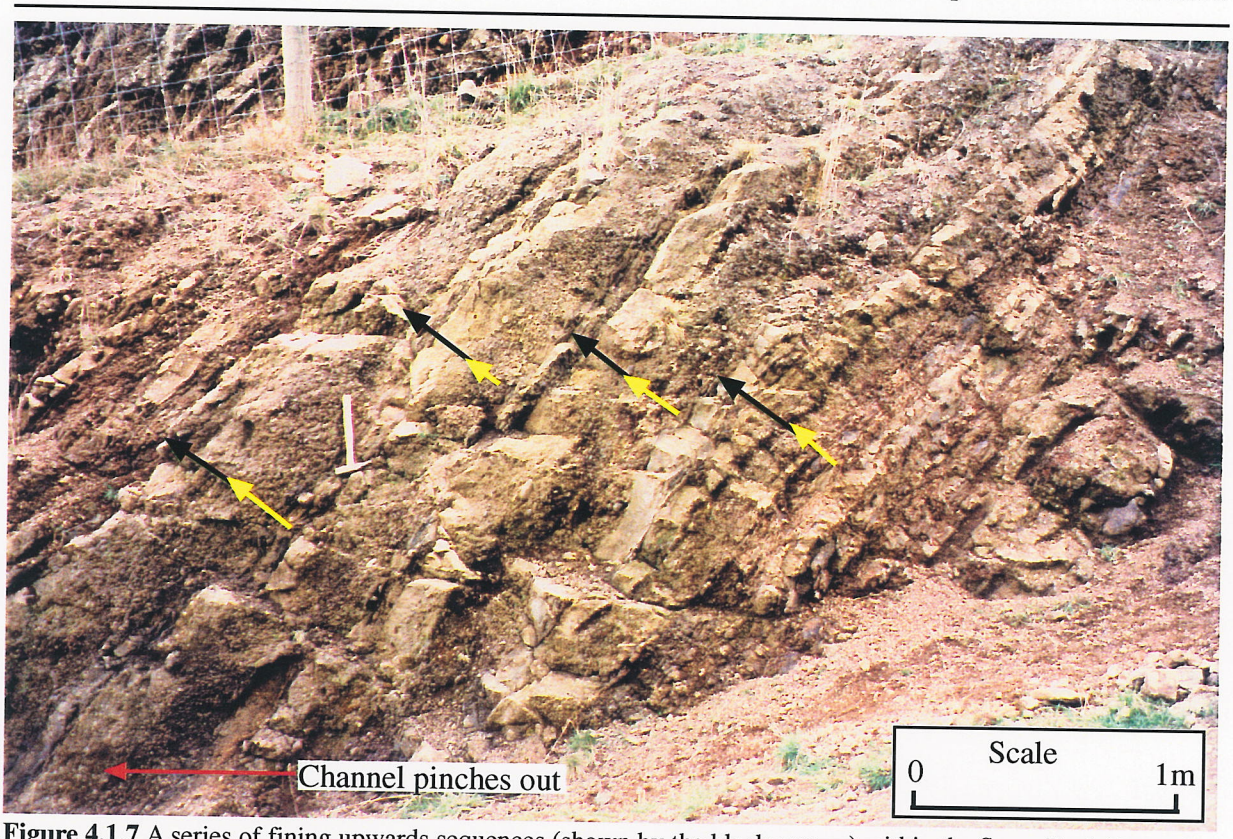

Figure 4.1.7 A series of fining upwards sequences (shown by the black arrows) within the Spear Peak Formation at G.R. 2117600 5506500 occur in the facies B2 sandstones; within this facies floating pebbles are common. The bases of these sequences are conglomerates (facies A2), and these coarsen upwards (yellow arrows). The coarsest parts of the beds are lenticular and are generally only a few metres wide.

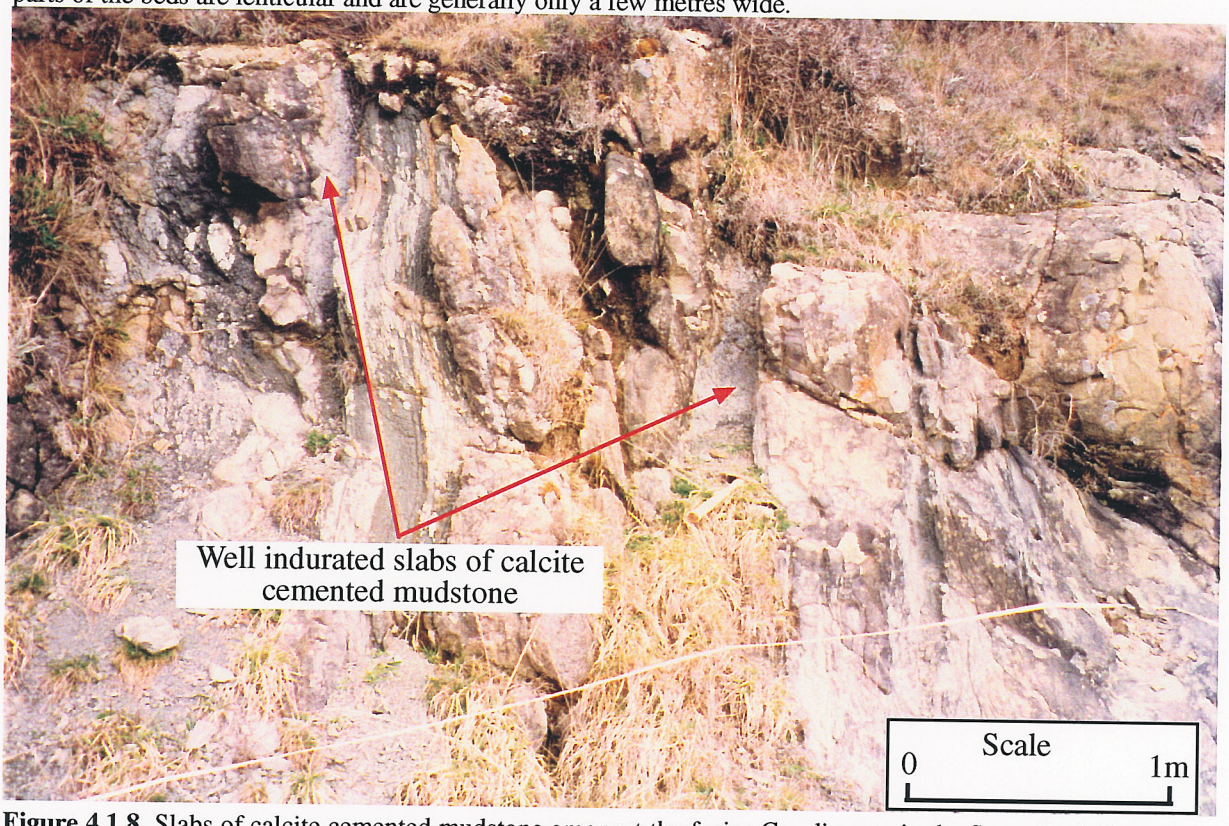

Figure 4.1.8 Slabs of calcite cemented mudstone amongst the facies C sediments in the Spear Peak Formation; (G.R. 2117600 5506400), these slabs are up to 1 m wide and the edges are generally eroded while the bulk of the slab is coherent and well indurated.

4.1.4 PETROLOGY

INTRODUCTION

Petrological techniques were used in order to find the provenance, and identify sedimentary processes that formed the Spear Peak Formation. In the field, observations of hand specimens were used to identify clasts in the facies A2 conglomerates, supported by petrography of clasts that could not be accurately identified. Other methods used were sandstone petrography, heavy mineral analysis, and whole rock geochemistry.

SANDSTONE PETROGRAPHY

Three sandstone slides from the Spear Peak Formation were point-counted in this study using the method described in section 1.5.6 (appendix B, OU 73292, OU 73293, OU 73307). Grains in the sandstone are angular, with grain size ranging from 0.1-0.5 mm in diameter. The sand is poorly sorted, and grains are clast supported with matrix and psuedomatrix infilling pore spaces.

Sandstone in this unit is lithic-rich, with lithics accounting for 50-65% of the grains (figure 4.1.10). The lithics are dominantly sedimentary and low grade metamorphic in origin with a minor intermediate volcanic component. Plagioclase feldspar is also a major component of the sand comprising 20-27% of the rock (figure 4.1.10). The rock is made up of 9-13% matrix, and is therefore classed as a litharenite according to Pettijohn et al (1987). Quartz, mica and heavy minerals are present in minor amounts that range from 1-3%.

In this study the average Q:F:L ratio for the sandstone was found to be 3:26:71, differing slightly from the lithofacies 1 sandstone of Kirby's (1989) (6:45:48), possibly due to different point counting techniques (figure 4.1.9). Lithofacies 2 of Kirby (1989) is clearly different from either of the other data sets, with an average Q:F:L ratio of 29:60:11. These data fit into the arkose field of Pettijohn et al (1987), rather than the litharenite field of the other data (figure 4.1.9).

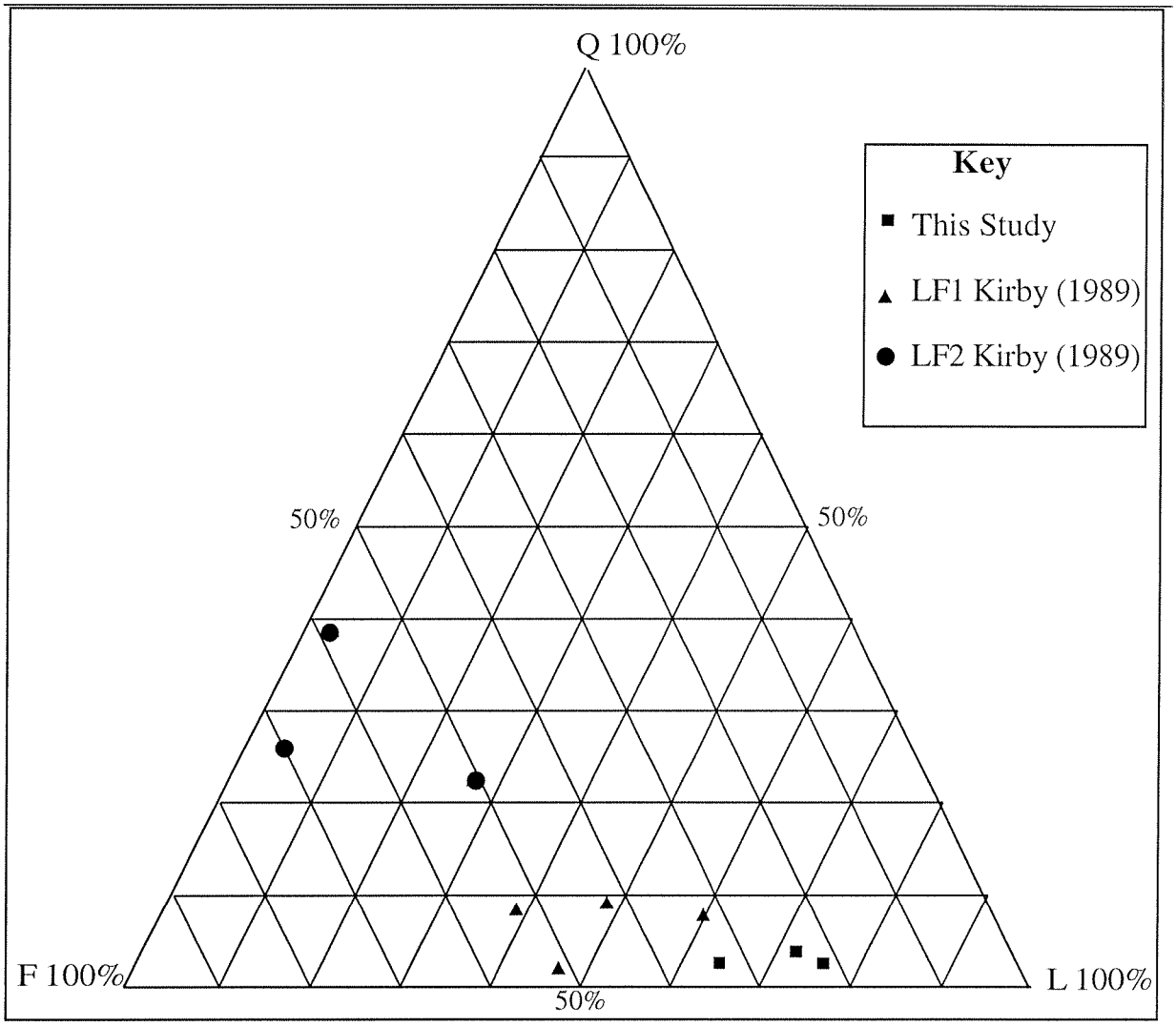

Figure 4.1.9 Q:F:L diagram for the Spear Peak Formation sandstone from this study as well as from Kirby (1989). This shows that the data from this study is similar to lithofacies 1 (LF1) of Kirby (1989), while lithofacies 2 (LF2) of Kirby (1989) is much more quartz and feldspar rich.

CONGLOMERATE PETROGRAPHY

Thin-sections of five pebbles from the Spear Peak Formation conglomerate facies A2 were analysed in order to classify them (appendix C, OU 73323-73327).

Pebble OU 73323 is a lithic-rich sandstone that has undergone prehnite-pumpellyite metamorphism, pebble OU 73324 is a volcanic breccia that has also undergone prehnite-pumpellyite metamorphism, pebble OU 73325 is a granitiod, and pebbles OU 73326 and OU 73327 are porphyritic andesites (see appendix C).

In the field, grey sandstone and siltstone of the Murihiku Terrane, and green sandstone from the Takitimu Group (pebble OU 73323), appear to make up most of the clasts in the conglomerates. Intermediate volcanic pebbles (pebbles OU 73324, OU 73326 and OU 73327) are the next most abundant, while granitoid pebbles (pebble OU 73325) are rare, with only a few seen over the duration of the study, all of them very weathered. The proportion of Murihiku Terrane derived pebbles increases to the north, and the type of pebbles that are present appears to be closely related to the basement rocks nearest the deposit.

HEAVY MINERALS

A thin section of the heavy mineral sample from the Spear Peak Formation (OU 73329) was analysed petrographically in order to identify the minerals present in the heavy fraction of the sandstone. All of the grains in the slide are low-grade metamorphic minerals, or lithic and feldspar grains that are extensively altered by low-grade metamorphism (figure 4.1.11). The minerals that are present are prehnite, pumpellyite and epidote (figure 4.1.11).

GEOCHEMISTRY OF THE SANDSTONE

Major and trace element geochemistry of the sandstone from the Spear Peak Formation has been analysed (appendix D, OU 73292-73295) using discriminant plots (see section 1.5.3). Data from this study plots in the arc field in both the silica versus K_2O/Na_2O (figure 4.1.12) and La/Y versus Ce/V plots (figure 1.4.13), and plots in the P2 field of the discriminant function diagram suggesting an intermediate volcanic source for the sediments.

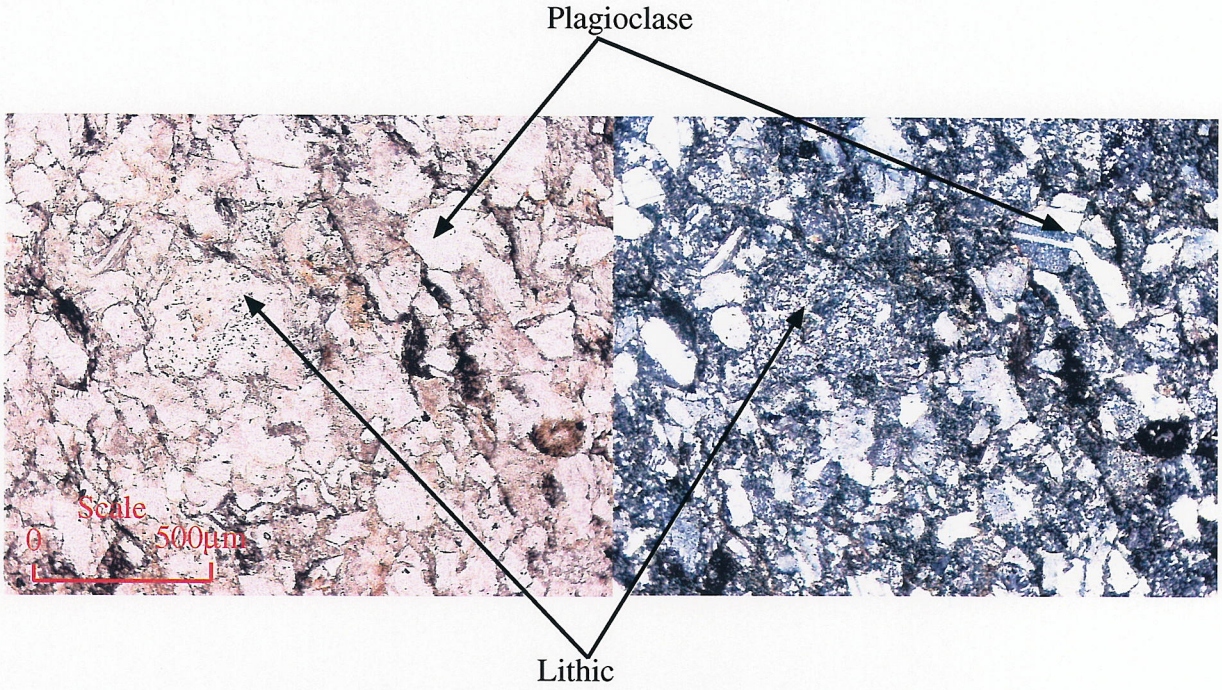

Figure 4.1.10 Photomicrograph of the Spear Peak Formation sandstone (OU 73207) (plane-polarised light on the left, cross-polarised light on the right), showing the major constituents of this unit. Note the smeared edges of some of the lithic grains, which may form pseudo-matrix.

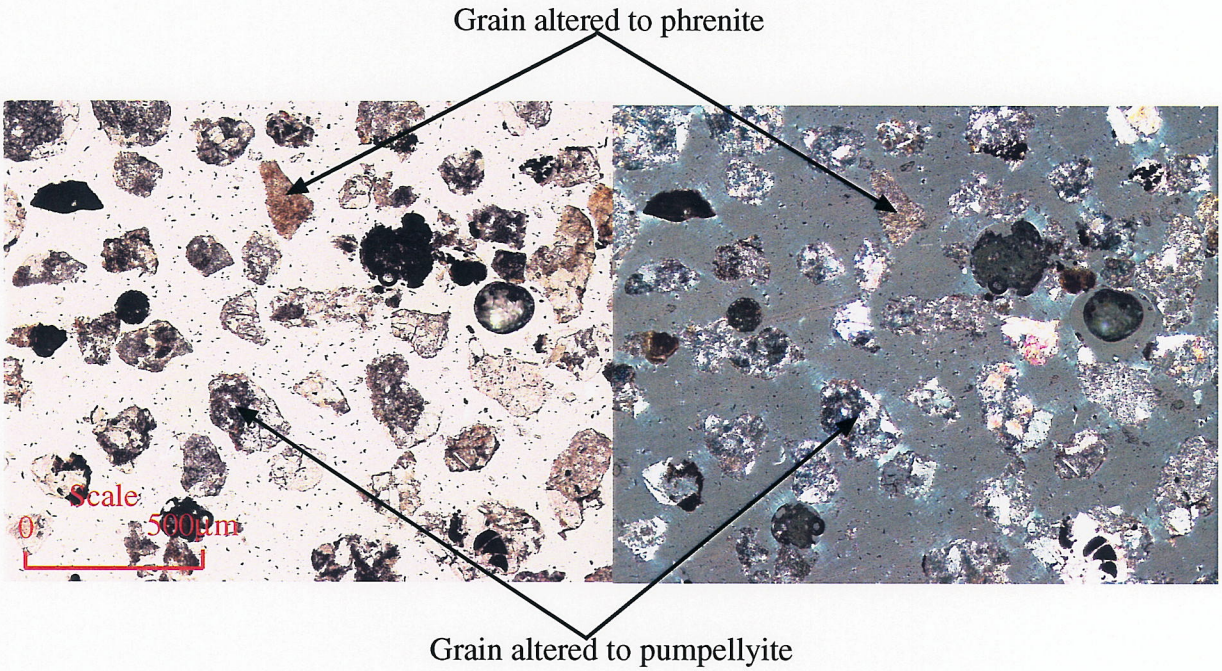

Figure 4.1.11 Photomicrograph of the heavy mineral sample from the Spear Peak Formation (OU 73329). This sample consists of grains that have been altered to various low-grade metamorphic minerals (phrenite, pumpellyite and epidote).

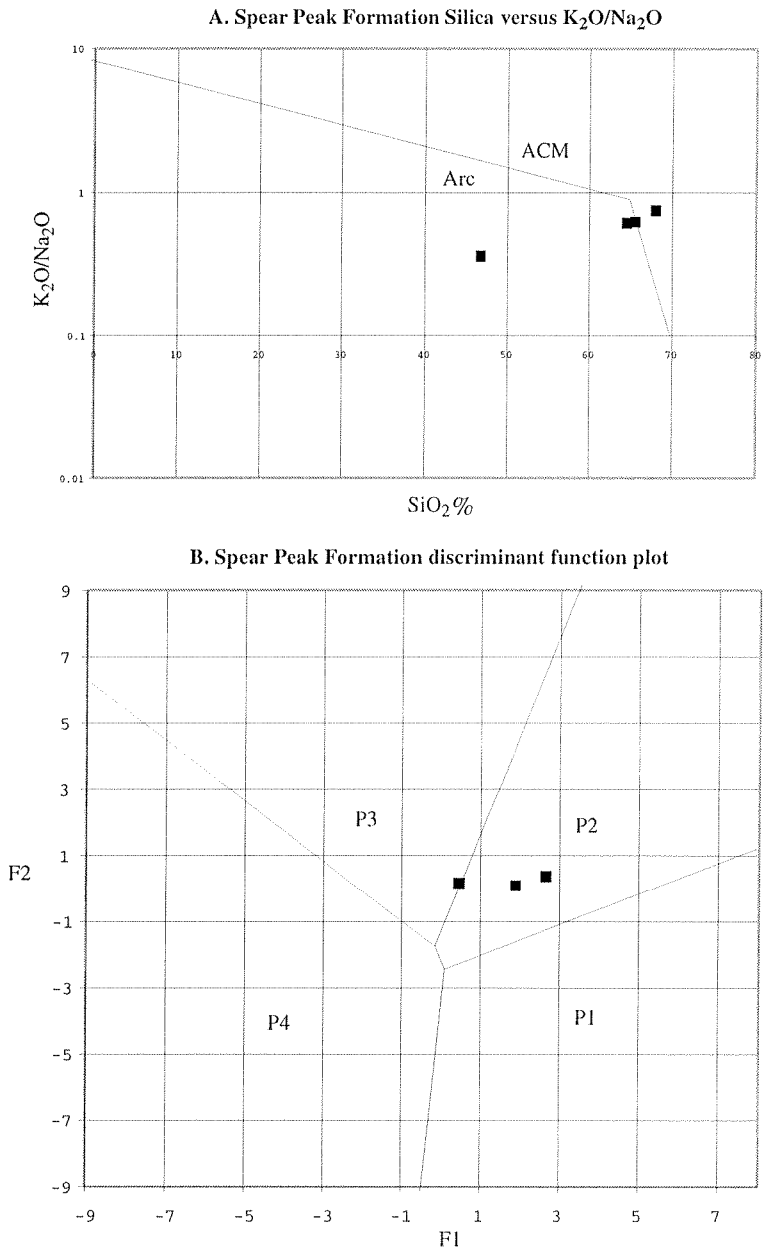

Figure 4.1.12 Major element discrimination plots. Plot A shows the simple SiO_2 vs K_2O/Na_2O plot, indicating an arc origin for the Spear Peak Formation sandstone. The more complex discriminant function plot B indicates that the sediments were derived from an intermediate volcanic source.

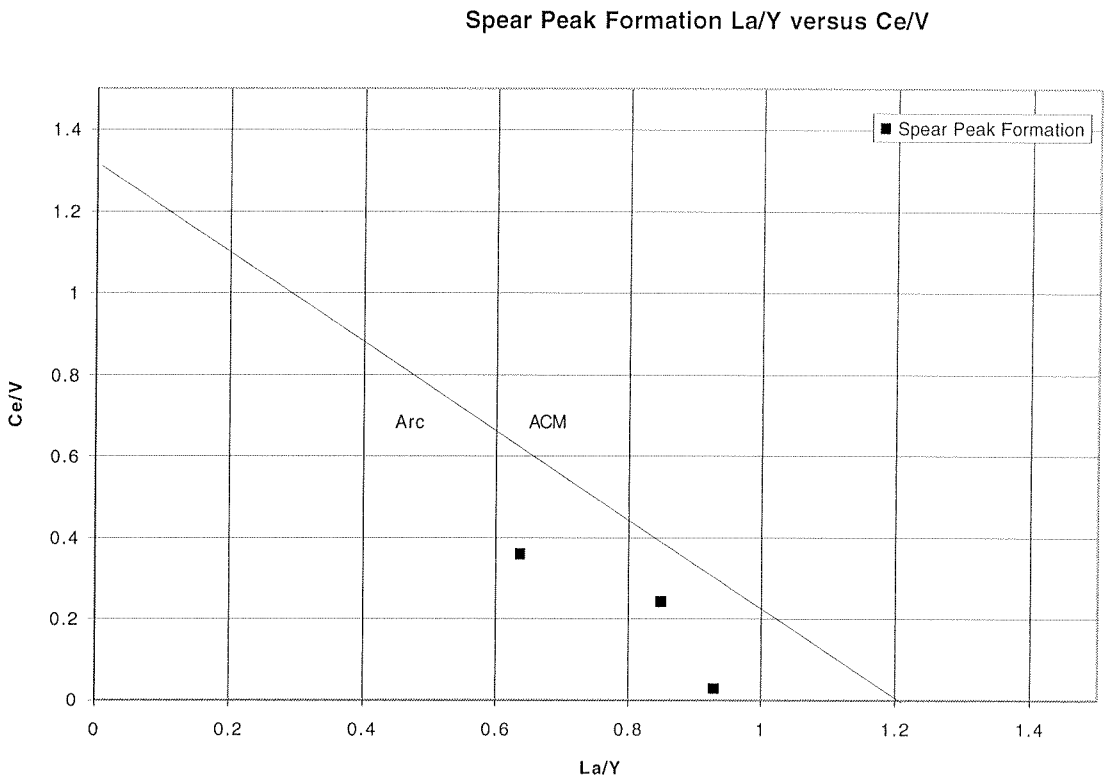

Figure 4.1.13 The La/Y vs Ce/V trace element discrimination plot shows that the Spear Peak Formation is derived from an arc type source.

4.1.5 SUMMARY

ENVIRONMENT OF DEPOSITION

Lithofacies present in the Spear Peak Formation indicate that it was deposited in a submarine environment, where the source of the sediment became more distal over time, as shown by the fining upward sequence. The base of the unit contains a number of debris flow channels (facies A2) and chaotic debris (facies F1), that formed as feeders to a submarine fan or fans (facies B2 and C1). The limestone breccia that is present indicates that these channels cut down into shelf sediments, which were able to build-up without being disturbed by a larger influx of sediment.

Rapid tectonic activity and undercutting of the shelf has formed the chaotic slump and olistolith facies F deposits. Between the channels, fan deposits (facies B2 and C1) dominate;

as the source became more distal the fans became the main depositional environment. The inner fan (facies B) is eventually succeeded by mid fan facies C deposits, and ultimately by the outer fan or basin plain deposits of the Waicoe Formation (facies G). Depositional processes changed along with the change in depositional environment. The proximal deposits (F1, A2 and B2) are almost entirely made up of debris flow deposits, while the more distal C1 facies is turbidite dominated.

The facies association within the Spear Peak Formation is almost identical to the proximal submarine ramp model of Heller and Dickinson (1985), although their model was for a sand-rich system. The architecture of the Spear Peak Formation submarine fan system is typical of the *channels with attached lobes* type 2 depositional system of Mutti (1985), or the multiple-source ramp of Reading and Richards (1994). These types of depositional systems, that are extensively channelized with coarse-grained sediments, are typical of areas with strong marginal tectonic uplift (Mutti, 1985; Reading and Richards, 1994). The tectonic uplift in the area would cause a rise in the relative sea level, leading to the infilling of the basin with alluvial sediments from adjacent fan deltas and river mouths (Mutti, 1985; Heller and Dickinson, 1985; Reading and Richards, 1994). As the amount of tectonic activity decreased in the area so did the sediment supply, resulting in deposition of more sand and mud-rich sediments, typical of ramps and fans in this type of setting (Mutti, 1985; Heller and Dickinson, 1985; Reading and Richards, 1994). The correlation between the composition of clasts in the conglomerate and the adjacent basement rocks, indicates that the channel deposits were formed close to the basin margin, and probably drained a relatively small area on land, making this a multiple source ramp (Reading and Richards, 1994).

Evidence from the sedimentology of the deposits and correlation with a number of models indicates that the Spear Peak Formation was deposited in an area of the basin on, or close to, the slope in a tectonically active area.

Provenance of the Spear Peak Formation

All of the petrology suggests that the bulk of the sediment that makes up this unit has been derived from the Takitimu Group and the Murihiku Terrane (in the Oligocene these formed a continuous block (Norris and Carter, 1982)). The evidence for this provenance includes: the high proportion of lithic grains in the sandstone, the presence of the low-grade metamorphic

minerals in the heavy mineral sample, and the abundance of pebbles in the conglomerate with the same petrology as Takitimu Group or Murihiku Terrane. Whole rock geochemistry of the sandstone indicates an intermediate volcanic arc provenance for the sediments, meaning that one of the volcanogenic Eastern Province terranes is the most likely source. The paleocurrent direction indicators clearly show that the sediment was transported from the south in a northerly direction.

To the west of the field area, Kirby (1989) found parts of the Spear Peak Formation that have a large granitoid component within the conglomerates and an arkose sandstone composition (lithofacies 2 in Kirby (1989)). Kirby (1989) suggests that this sediment was derived directly from Fiordland as part of a fan. Other possibilities are that these sediments have been reworked from the Beaumont Formation, which is much more granite rich to the west of the study area (Hall, 1989), or the sediments are infaulted parts of the Beaumont Formation.

4.2 WAICOE FORMATION

4.2.1 INTRODUCTION

TYPE SECTION

The type section for the Waicoe Formation is in Ligar Creek, from G.R. D44/962 816 upstream to G.R. D44/969 819. Additional reference localities are also given, one of which is at Gorge Hill (G.R. D43/212 048) within the study area (Turnbull et al, 1989).

DISTRIBUTION AND THICKNESS

The Waicoe Formation is present throughout the onshore western Southland basins, although unit thickness is variable, with a maximum thickness of about 1800 m in the Eglinton Valley (Turnbull et al, 1989). In the study area the Waicoe Formation is present at three horizons in the stratigraphic column (figure 2.2.1, appendix H). Repeated occurrence of the formation at different stratigraphic positions is due to the inter-fingering relationship it has with the other units in the Waiau Group. The only horizon where a complete unfaulted section is seen is between the Spear Peak Formation and the Weydon Formation (horizon A, appendix H). This section is approximately 400 m thick, while the total thickness of the Waicoe Formation in the study area could be 3-4 times this value.

PREVIOUS WORK

The Waicoe Formation was first mapped in the study area, as "Waitakian Marls" by McCraw (1947), whereas Carter and Norris (1977b) referred to the same unit as the Gorge Creek Mudstone. The name Waicoe Formation, formalised by Turnbull et al (1989), replaces these older terms and describes the "ubiquitous basinal mudstone of Western Southland" (Turnbull et al, 1989). This definition is necessary due to the mudstone being present throughout time and space in the western Southland basins. Within smaller areas such as the study area, the Waicoe Formation appears to be three separate formations. Instead of defining each of these horizons as separate units for this study, the Waicoe Formation is used in a regional context to avoid any confusion resulting from the unnecessary creation of new formations, and to show its regional relationships to the rest of the unit in western Southland.

4.2.2 AGE AND FOSSIL OCCURRENCE

Microfossils are the dominant fauna in the Waicoe Formation, and samples taken from each of the three horizons were analysed in order to determine the unit age, as well as to constrain the ages of the units above, below and within the Waicoe Formation. Foraminifera were also used to obtain depth information for each sample.

The age ranges of the foraminifera in the three horizons of Waicoe Formation are shown in figure 4.2.1. Horizon A (FRF D43 f 036) is lower Whaingaroan in age, as determined by the presence of *Globigerina angiporodies* and *Globigerina euaportura* (fossil identifications by R.E Fordyce). Horizon B (FRF D43 f 037) is Waitakian in age, based on the presence of *Globoquadrina dehisens*, *Globigerina woodi connecta*, *Notorotalia spinosa* and *Plectofrondicularia whaiangaroica* (fossil identifications by R.E Fordyce). Horizon C (FRF D43 f 038) is Otaian in age based on the other work done in the area by Harrington (1982) and Turnbull, Uruski et al (1993), this age is compatible with the foraminifera *Cibicides novozelandicus* that was found in this study (fossil identifications by R.E Fordyce). All these ages concur with the ages given in the stratigraphic column in Turnbull, Uruski et al (1993), also shown in figure 4.2.1.

The presence the genus *Notorotalia* in each of the three horizons of the Waicoe Formation suggests that the maximum possible depth for these sediments to have formed is approximately 200 m (figure 4.2.2) (fossil identifications by R.E Fordyce). Foraminifera present in the Waicoe Formation indicate that each time the sediment supply to the basin was low enough to allow the deposition of this mudstone, the depth of the basin was about 200 m, i.e. outer shelf-upper bathyal (Hayward, 1986).

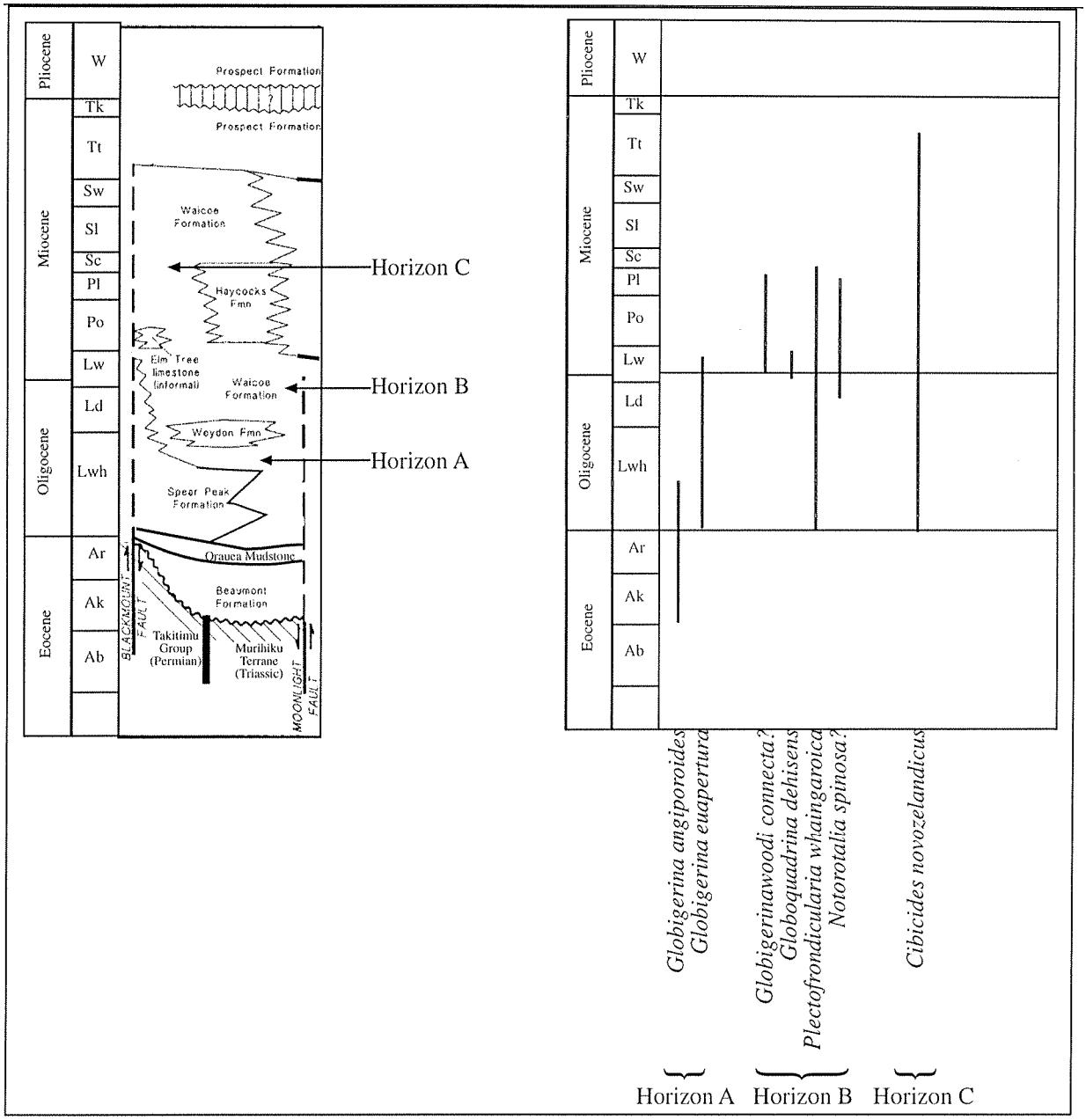

Figure 4.2.1 Stratigraphic column after Turnbull, Uruski et al (1993) showing the three horizons of Waicoe Formation present in the study area. The ages of these different horizons are shown by the age ranges of the different foraminifera on the right of the diagram.

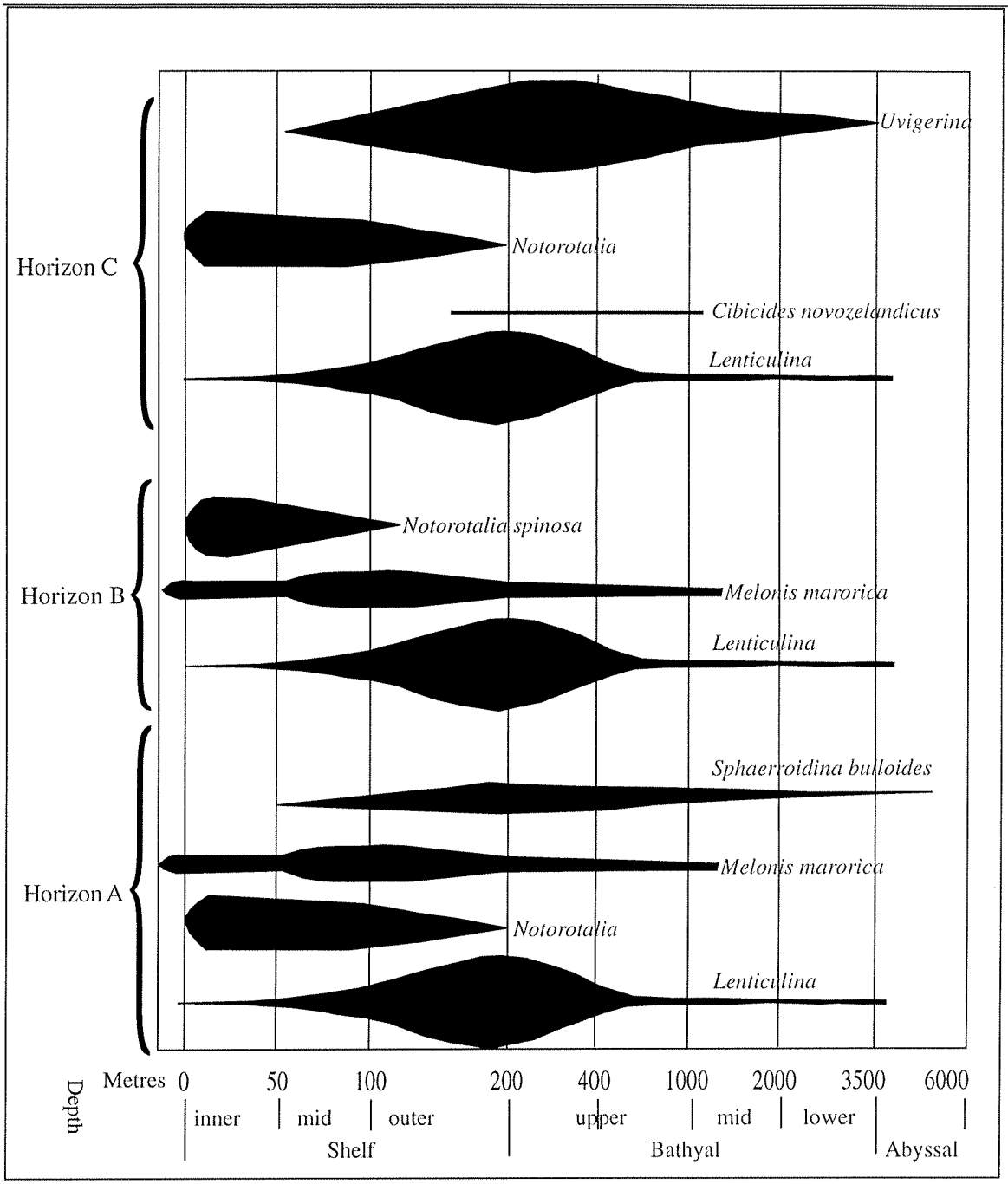

Figure 4.2.2 Depth ranges of the foraminifera found in each of the different Waicoe Formation horizons indicate that all the horizons formed in water depths of 150-300 m. The depth ranges for the different foraminifera are taken from Hayward (1986).

4.2.3 LITHOFACIES DESCRIPTION AND INTERPRETATION

The Waicoe Formation contains only one lithology, namely massive mudstone. This is described and interpreted in terms of the lithofacies of Ricci-Lucchi (1975) and Stow (1996). Other formations enclosed within the Waicoe Formation contain coarser sediments that are locally inter-fingered with the Waicoe Formation mudstones.

LITHOFACIES G DESCRIPTION

The Waicoe Formation consists entirely of facies G mudstone, and contains only about 1% of grains larger than 4ø (this was found during the separation of microfossils). The mudstone is generally massive, with small (centimetre scale) layers occasionally defined by a zone of intense bioturbation (e.g G.R. 2123300 5502700). The mudstone contains calcite, both as a constituent and as veins that cut it at various angles. Veins occur at every outcrop of Waicoe Formation (figures 4.2.4 and 4.2.5).

LITHOFACIES G INTERPRETATION

The massive, fine-grained, calcareous nature of the Waicoe Formation indicates that it has been deposited as rainfall from the surface layer of water in a deep-sea environment far removed from land (Stow, 1996). The sediment becomes dispersed through the water column as the fine-grained tail of turbidites, or by the action of normal currents, and settles slowly (Stow, 1996). The facies G mudstone accumulated slowly, so the presence of a mappable layer of it in the form the Waicoe Formation is indicative of a period of low sediment supply to the basin.

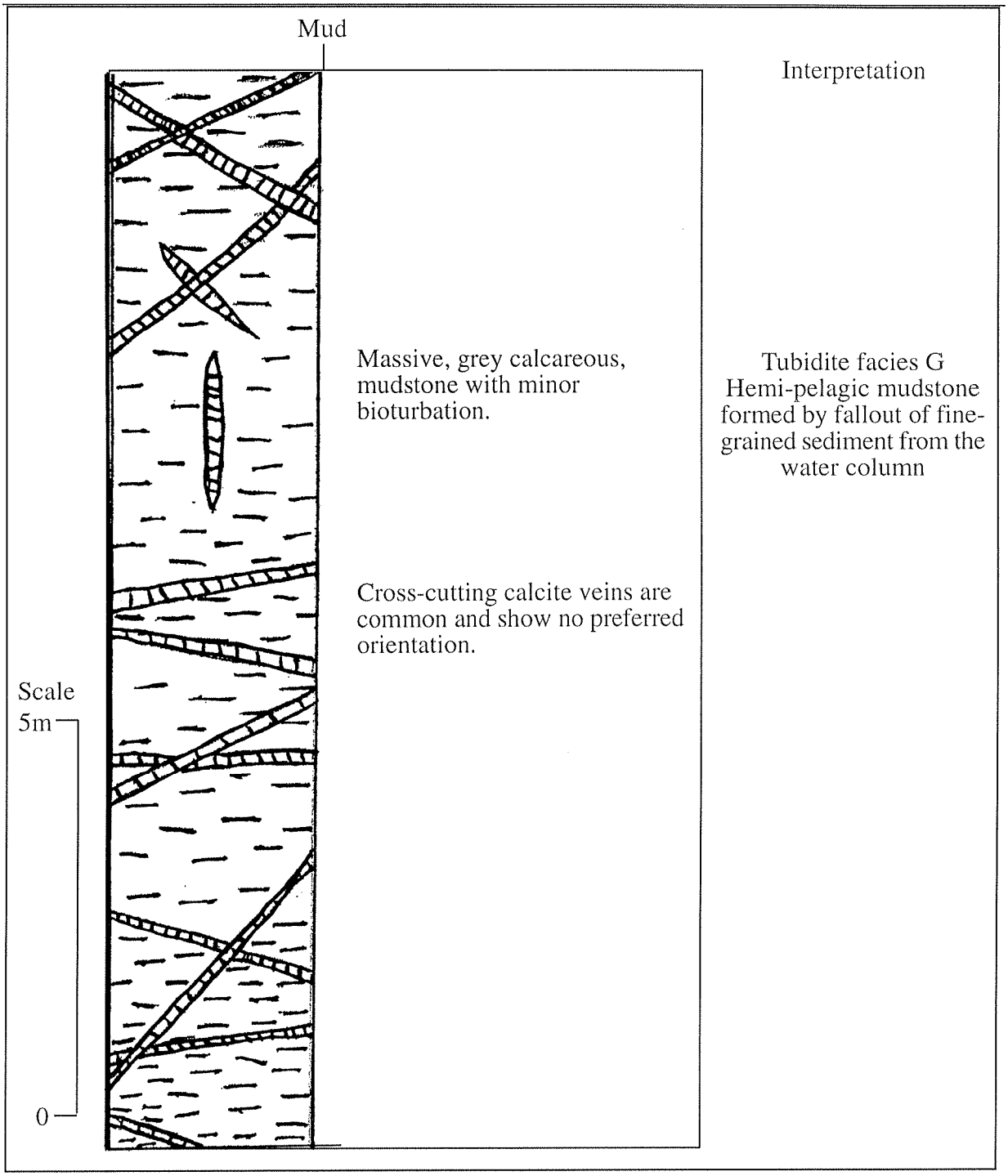

Figure 4.2.3 Measured section through the Waicoe Formation at G.R. 2121174 5504836 showing the homogeneous nature of the mudstone that is cut by calcite veins at various angles.

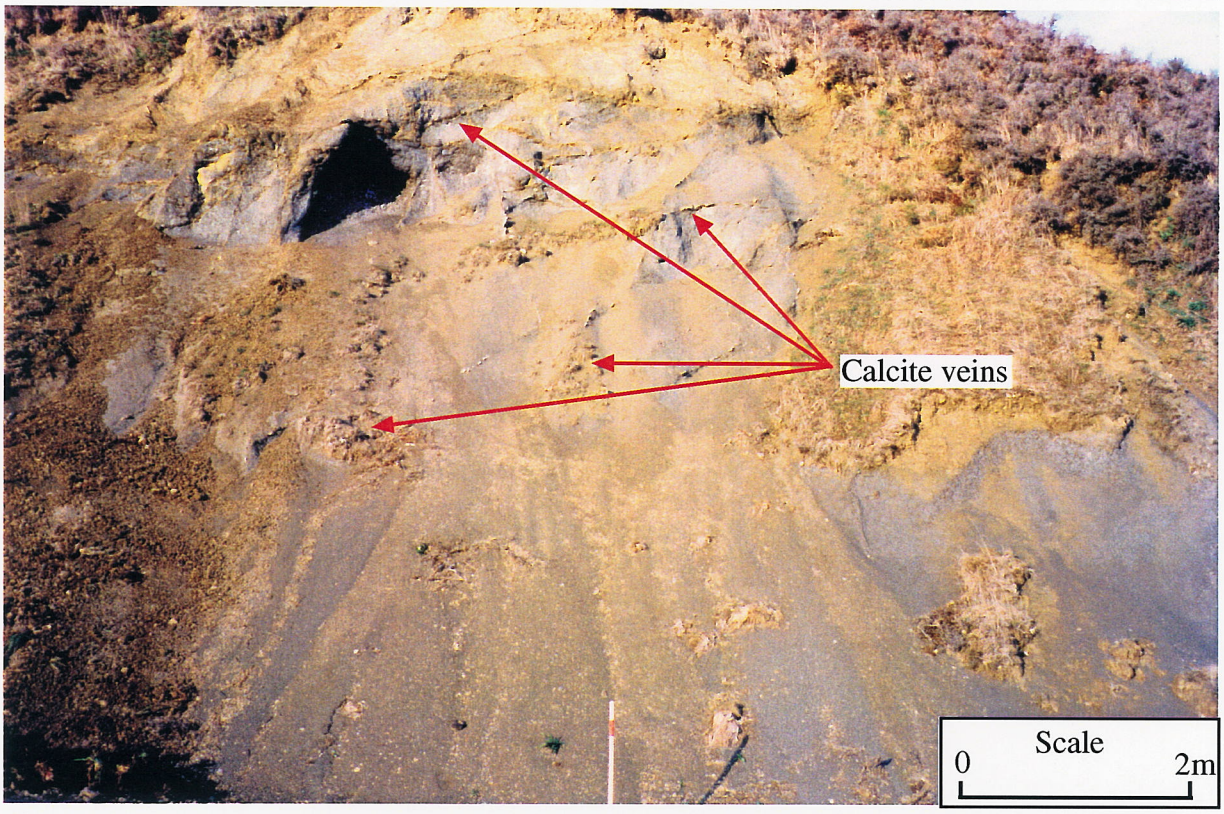

Figure 4.2.4 Waicoe Formation massive mudstone (G.R. 2121174 5504836) showing the calcite veins that are randomly orientated throughout the formation (close up figure 4.2.5).

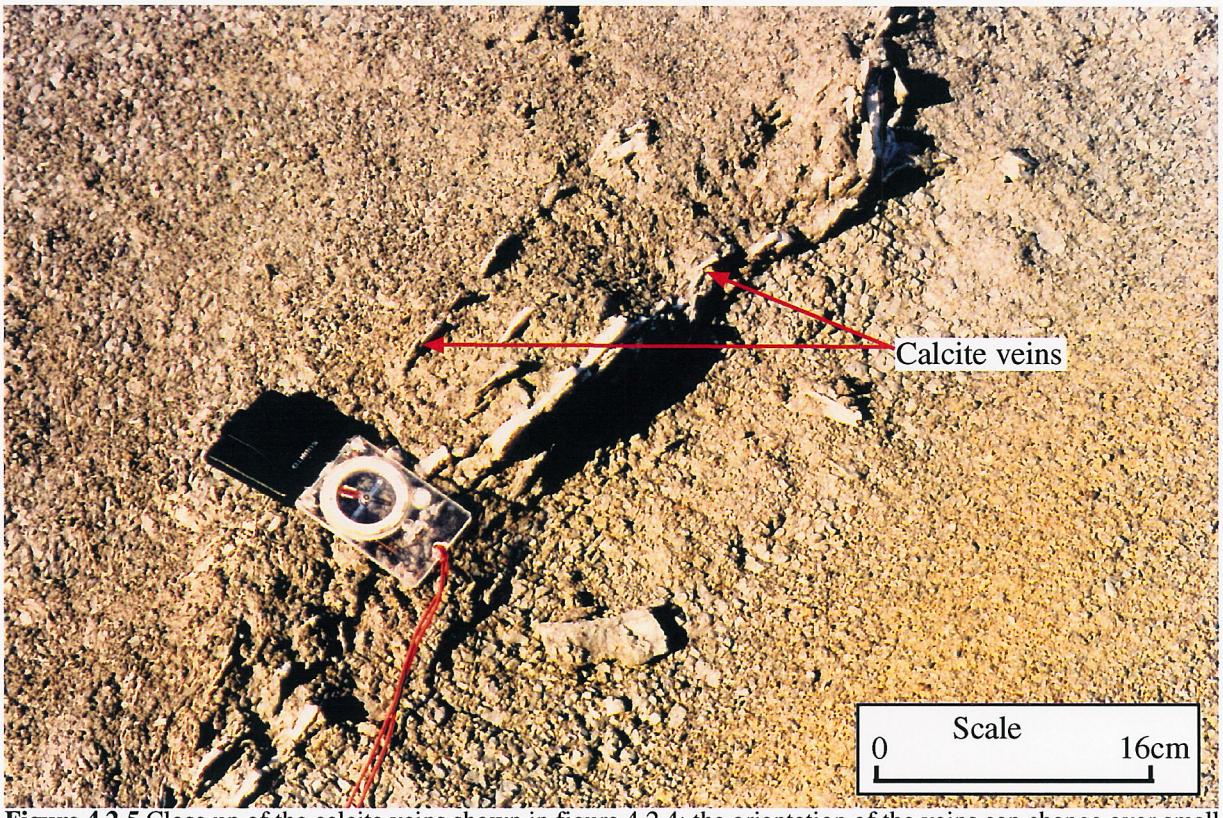

Figure 4.2.5 Close up of the calcite veins shown in figure 4.2.4; the orientation of the veins can change over small distances and there are no consistent crosscutting relationships.

4.3 WEYDON FORMATION

4.3.1 INTRODUCTION

TYPE SECTION

The type section for the Weydon Formation, as defined by Turnbull et al (1989), is in the Weydon Burn, from the basal contact with the Waicoe Formation (G.R. D43/246 044) to the centre of the syncline at G.R. D43/228 050. Mapping of the area reinterprets part of the type section as Waicoe Formation, and therefore the top of the type section has to be relocated at the upper contact between the Weydon Formation and the Waicoe Formation at G.R. D43/236 047.

DISTRIBUTION AND THICKNESS

The Weydon Formation is mapped in the Weydon Burn, Gorge Creek and Princhester Creek areas within the study area (appendix H) and may be present in the Aparima catchment to the south of the area (Turnbull et al, 1989). The thickness of the Weydon Formation in the study area is about 650 m and is relatively constant throughout the area.

PREVIOUS WORK

McCraw (1947) included the Weydon Formation in the "Duntroonian sandstones and conglomerates" together with the Spear Peak Formation. Carter and Norris (1977b) differentiated the Weydon Formation from the other Tertiary sediments on their sketch map before the formation was formally recognised by Turnbull et al (1989).

4.3.2 AGE AND FOSSIL OCCURRENCE

Fossils found in the Weydon Formation include fragmented bivalves and foraminifera that were too broken to identify species. Unit age has been estimated using foraminifera extracted from the Waicoe Formation above and below the Weydon Formation (section 4.2.2). The Waicoe Formation below the Weydon Formation includes the foraminifera *Globigerina euaportura* (Whaingaroan-Waitakian), *Globigerina angiporoides* (Kaiatan-top of lower Whaingaroan) (fossils identified by R.E Fordyce). The presence of *Globigerina angiporoides* means that the maximum age for the bottom of the Weydon Formation is middle

Whaingaroan (figure 4.2.1). Above the Weydon Formation *Globoquadrina dehisens*, *Globigerina woodi connecta*, *Notorotalia spinosa* and *Plectofrondicularia whaiangaroica* are present (fossils identified by R.E Fordyce). This indicates that the minimum age for the top of the Weydon Formation is Waitakian (figure 4.2.1). These two dates suggest that the Weydon Formation was deposited in the upper Whaingaroan-Duntroonian, which is the age given by Carter and Norris (1977b), Turnbull et al (1989), and Kirby (1989).

4.3.3 LITHOFACIES DESCRIPTION AND INTERPRETATION

The Weydon Formation is generally a fine-grained unit that ranges from mudstone to medium sandstone. Interbedded sandstone and mudstone makes up the prominent ridges typical of the formation and between the ridges, mudstone is the dominant lithology. These lithologies have been separated into different lithofacies based on the scheme of Ricci-Lucchi (1975) and Stow (1996) (see figure 4.1) in order to determine the environment of deposition of the unit.

LITHOFACIES D1

Facies D1 sediments are abundant in the resistant, ridge forming parts of the Weydon Formation. This facies is dominated by sandstone layers interbedded with mudstone and, averaged over the whole unit, the sand/pelite ratio is less than 1. Sandstone ranges in grain size from fine to medium with most beds being well-sorted and the grains generally angular in nature.

Facies D1 beds are very continuous and can be traced for hundreds of meters along the ridges that they have formed. Beds range in thickness from 5-50 cm, and in many cases the bases of these beds appear to be erosional, as shown by scour marks (figures 4.3.1, 4.3.3 and 4.3.4). Amalgamated beds occur rarely in this facies, but can reach up to 1.5 m in thickness and are generally composed of medium sand-sized grains. Coarsening and thickening upward sequences are apparent, with basal facies G mudstones giving way to the interbedded sandstone and mudstone of facies D1, with greater amalgamation near the top of the sequence (figures 4.3.1 and 4.3.3).

Sedimentary structures present in this facies include lamination, ripple marks, convolute beds, subtle grading, parting lineation, sole marks and bioturbation (figure 4.3.5). The most common of these is the fine lamination (1 mm scale) present in almost all of the sandstone

marks within the laminated sandstone are common in some beds but are absent in others. Ripples occur in the T_c part of the Bouma sequence (figure 4.3.4) and these were measured to determine the current direction (see paleocurrent analysis) (figure 4.3.1 and 4.3.5). The tops of many of the beds in this facies are convoluted (T_c) (figure 4.3.1), with the fold axes generally perpendicular to the flow direction measured from ripples, parting lineations and sole marks, indicating a down-slope flow. Most of the beds are normally graded, though this is subtle because of the small range of grain sizes in the beds, e.g fine sand grading into mud (figure 4.3.1). On the tops of some of the beds, faint parting lineations are present. Bioturbation is rare in this facies although it is seen on the top of some fine sand layers (figure 3.3.1). Full Bouma sequences are not seen in the Weydon Formation, and generally only the top parts (T_{bce}, T_{cde}, T_{de}) of the sequence are present.

LITHOFACIES D1 INTERPRETATION

The rock types, bed thickness and geometry, combined with the sedimentary structures present in this facies are all typical of turbidite facies, D1 and D2 of Ricci-Lucchi (1975) and Stow (1996). The main discriminating factors that indicate turbidite deposition of this facies are the presence of graded beds, and many of the features associated with the Bouma sequence, representative of sediment deposited from suspension. This facies is deposited by low density, mature turbidity currents, which may have an extremely high suspension volume (D2 of Ricci-Lucchi, 1975). Basu and Bouma (2000) describe similar deposits from the Tanqua Karoo and interpret them as levee-overbank and distal sheet deposits.

Alternative mechanisms that could have deposited the facies D1 sediments are bottom (Shanmugam, 2000) or contour currents (Stow and Lovell, 1979). The parallel relationship between the slumping direction of the convoluted beds and the current direction indicators shows that the current that deposited the sediment flowed down slope (appendix E3). This immediately discounts an interpretation of contour currents being the mechanism for deposition under the definition of Stow and Lovell (1979), which requires current flow to be parallel to the contours of the ocean floor. Shanmugam (2000) suggests that bottom currents don't necessarily flow parallel to the slope and sets out 17 criteria for the recognition of bottom currents. Many of the features are similar to those seen in facies D1 sediments (e.g fine-grained sand and silt, rhythmic occurrence of sand and mud layers, horizontal lamination,

and low-angle cross-lamination). features absent include very thin bedding <5 cm, 50 or more layers per 1 m, and lenticular bedding.

Mature turbidites are the favoured interpretation of the depositional processes that formed the facies D1 sediments in the Weydon Formation, despite the similarities with contourite deposits. This is based on the presence of sedimentary structures indicative of turbidity currents and the lack of features unique to debris flow or bottom current deposition. This interpretation fits in with the facies descriptions of Ricci-Lucchi (1975), Stow et al (1996) and Basu and Bouma (2000); it also fits the criteria set out by Shanmugam (2000) for the recognition of turbidites.

LITHOFACIES G DESCRIPTION (RICCI-LUCCHI 1975)

Facies G mudstones make up the non-resistant part of the Weydon Formation between the ridges formed by the facies D1 sediments. These sediments consist of mudstone that is generally massive, but is sometimes found to contain layers of broken shell material 5-10 cm thick (facies E2).

Sedimentary structures are not commonly seen in this facies due to the fine grain size, although bioturbation and fine lamination are sometimes observed especially where the sediments contain a silty layer.

LITHOFACIES G INTERPRETATION

Facies G sediments are formed mainly by hemi-pelagic settling of fine sediment from surface water (massive mudstone). The silty layers and broken shell layers are minor E2 deposits resulting from small debris flows within the mudstone.

LITHOFACIES DISCUSSION

Within the Weydon Formation 3-4 cycles are represented. Each cycle consists of a large thickness of facies G mudstone that was deposited in inter turbidite phases, followed by a thickening/coarsening upward sequence of facies D sediments that have formed in a outer fan environment (Mutti and Ricci Lucchi, 1972) (figure 4.3.2). The facies D deposits are sharply overlain by the bottom of the next cycle. The thin, sheet like nature of the beds in facies D suggests that the turbidite fan that deposited the sediments was probably of type 3 under the

classification of Mutti (1985), or a single point-source submarine fan of Reading and Richards (1994). Type 3 fans are relatively small, and are built up of unconfined sediments as shown by the sheet-like nature of the deposits (Mutti, 1985). While the model of Mutti and Ricci-Lucchi (1972) may no longer be popular (Shanmugam, 2000), an outer fan environment still appears likely, based on the sorting, grain-size and maturity of the sediment (Reading and Richards, 1994; Basu and Bouma, 2000).

The top of the Weydon Formation is located at the top of the last packet of facies D sediments, above this the mudstone becomes massive with no sign of turbidite deposition. While this distinction was good enough to map the separate units, the relationship between the turbidites and hemi-pelagic mudstones could be better studied using mineralogical and geochemical criteria, as described by Sighinolfi and Tateo (1998).

PALEOCURRENT DIRECTION

Ripple marks, scour marks and parting lineations within the facies D sediments were used to find the current direction of the fans that deposited the Weydon Formation (figure 4.3.3; appendix E3). The results indicate that the currents flowed approximately from east to west, with the possibility of some deviation due to the flows spreading out on the basin floor in a semi-circular pattern.

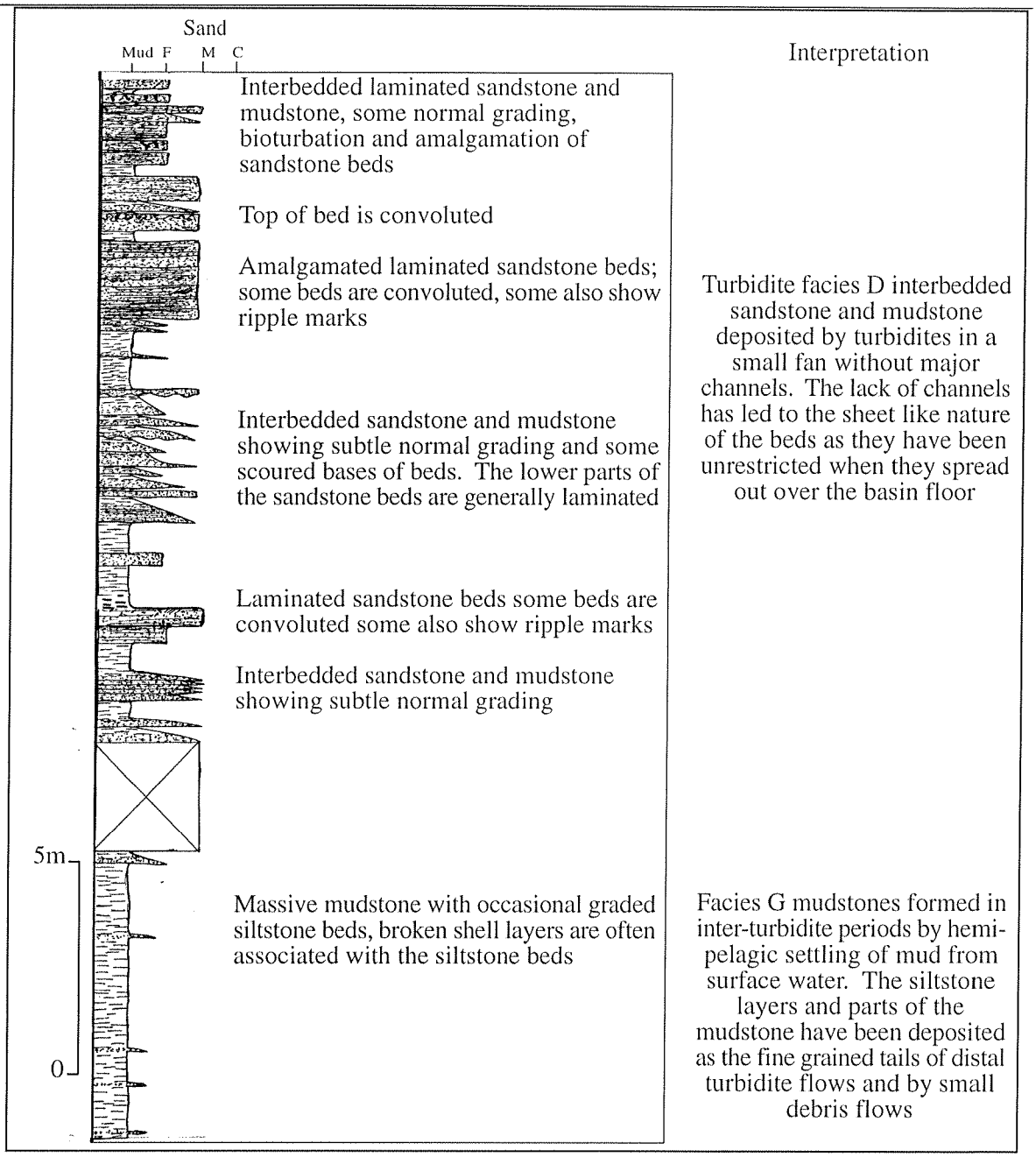

Figure 4.3.1 Measured section through the Weydon Formation at G.R. 2124300 5504700. This section shows the upper (turbidite dominated) part of the cycle represented by the facies D sediments. The facies G sediments are the top of a much thicker sequence of inter-turbidite non-resistant mudstones.

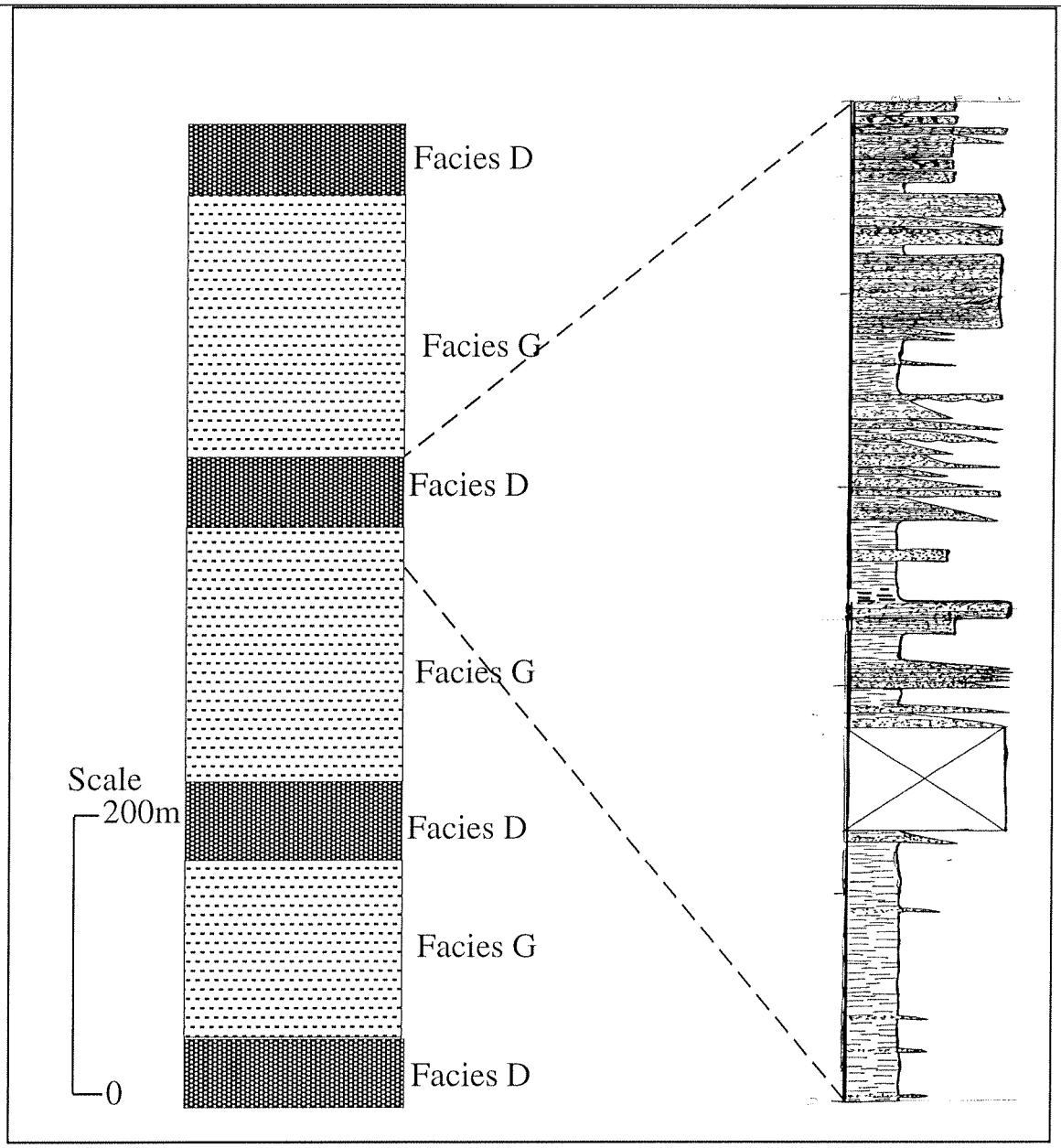

Figure 4.3.2 Schematic section of the Weydon Formation showing the interbedded facies D and G sediments. The section from figure 3.1.1 correlates to part of the section as shown.

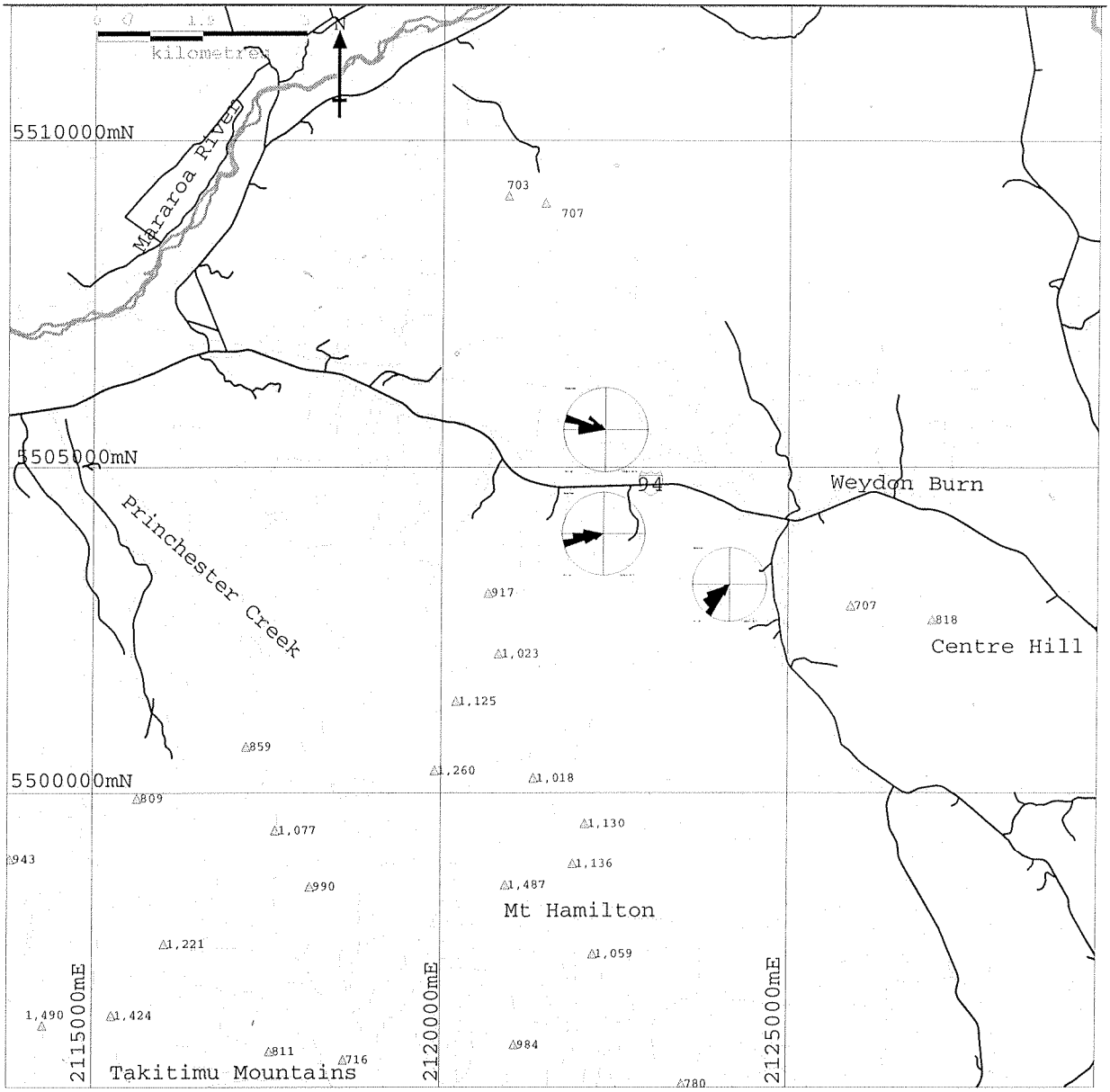

Figure 4.3.3 Current direction map for the Weydon Formation showing that the flow direction was broadly to the west, with some deviation probably due to the flows spreading out on the basin floor.

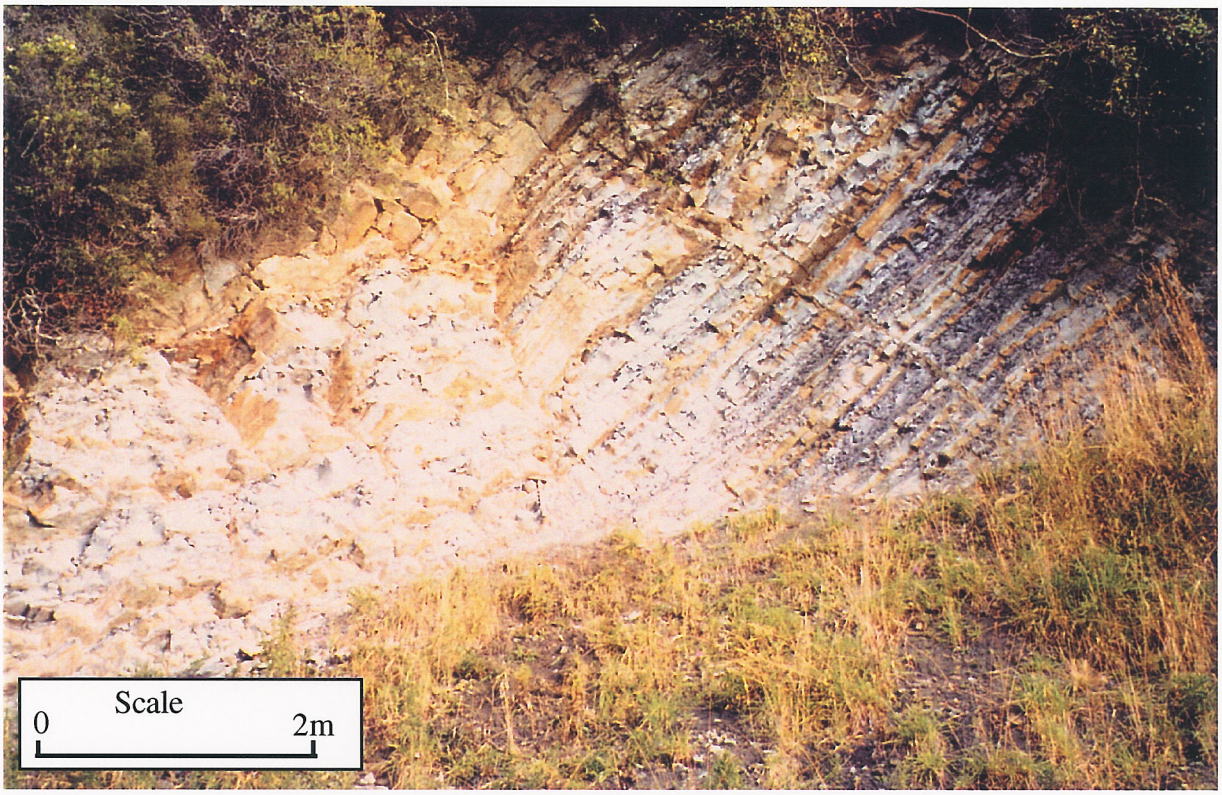

Figure 4.3.4 An outcrop of Weydon Formation at G.R. 2124100 5502300 showing the interbedded mudstone (grey) and sandstone (brown) that is typical of the facies D sediments forming the resistant ridges in the area. The outcrop also displays the coarsening and thickening upward sequence typical of the Weydon Formation and other outer fan deposits.

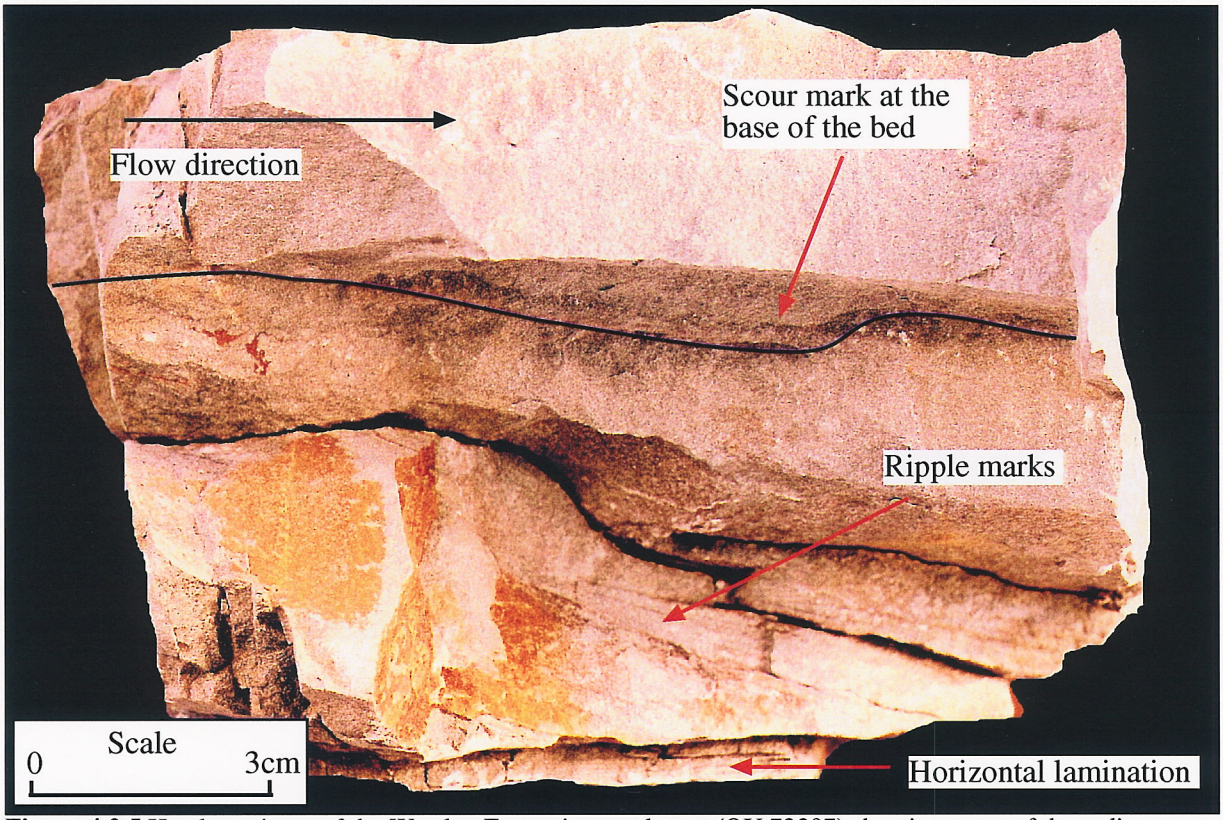

Figure 4.3.5 Hand specimen of the Weydon Formation sandstone (OU 73297) showing some of the sedimentary structures that are present in this formation and how they can be used to find the current direction.

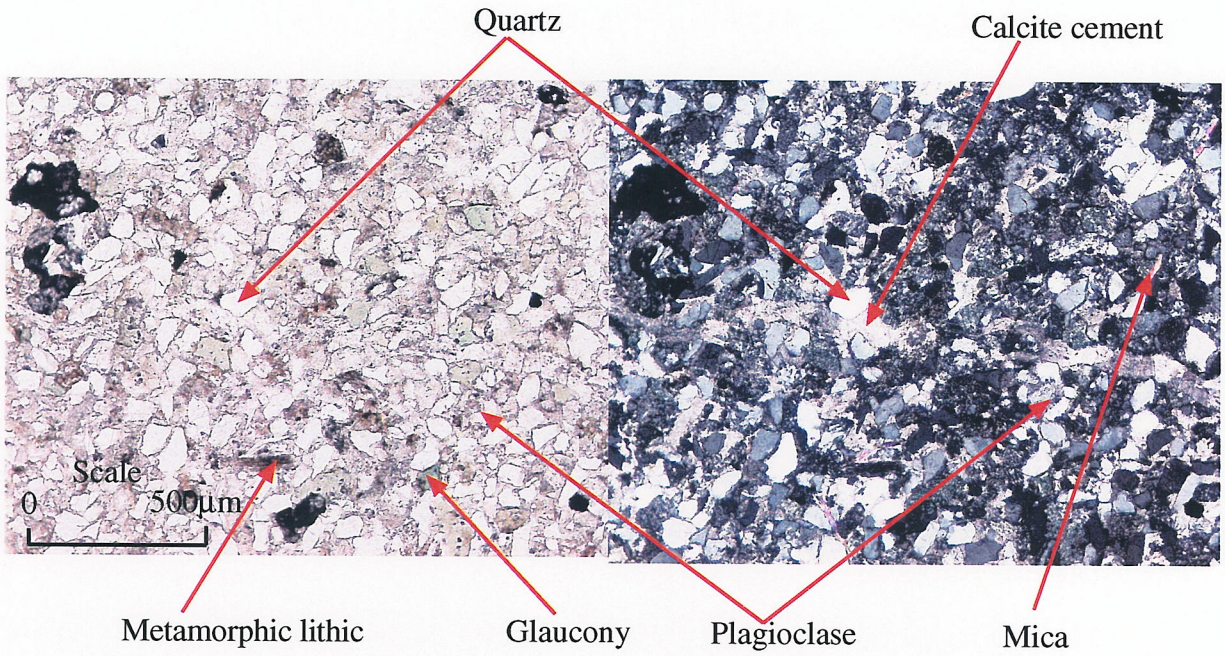

Figure 4.3.6 Photomicrograph of the Weydon Formation sandstone (OU 73297) (plane-polarised light on the left, cross-polarised light on the right) showing many of the constituents.

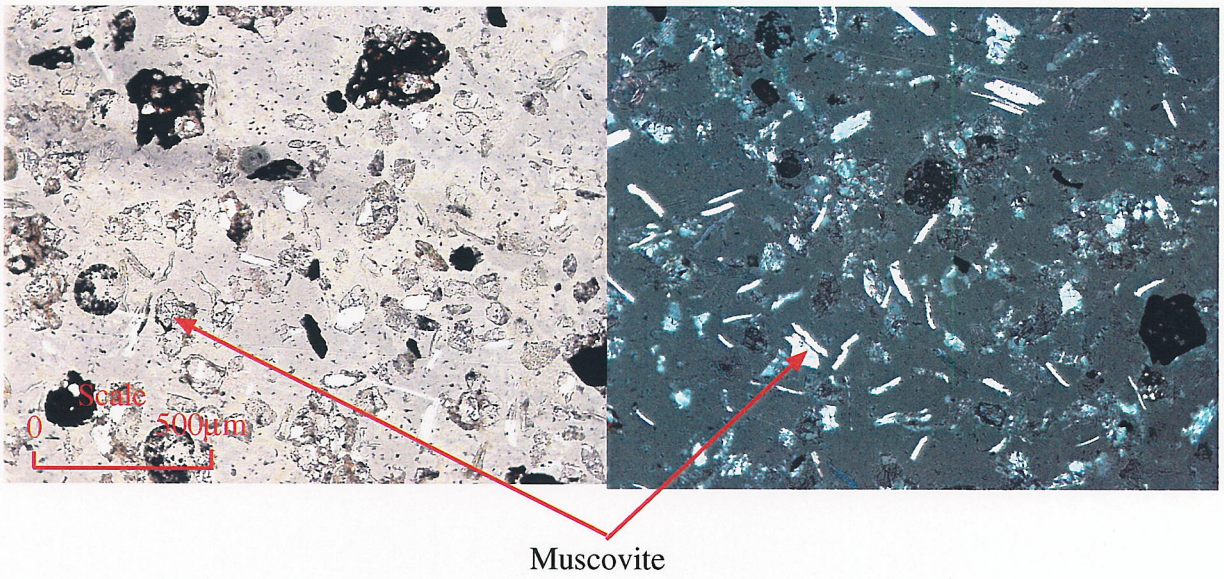

Figure 4.3.7 Photomicrograph of the heavy mineral sample from the Weydon Formation (OU 73330) (plane-polarised light on the left, cross-polarised light on the right), the majority of this sample is muscovite, despite it being close to the density of the heavy liquid.

4.3.4 PETROLOGY

INTRODUCTION

Petrological techniques were used in order to find the provenance and aid in the identification of the sedimentary processes that formed the Weydon Formation. Sandstone petrography was used to identify the mineral proportions in the unit, with sandstone whole rock geochemistry and heavy mineral samples used in order to decipher the provenance.

SANDSTONE PETROLOGY

Six sandstone slides from the Weydon Formation were examined petrographically and point counted (appendix B, OU 73296, OU 73297, OU 73298, OU 73299, OU 73308, OU 73309) using the method described in section 1.5.6. The grains are angular, and around 0.1 mm in diameter. The sandstone is well sorted, and the clasts are surrounded by calcite cement.

The Weydon Formation sandstone is predominantly quartz rich (40-50%) (figure 4.3.6). Lithics account for 20-27% of the grains, and comprise equal proportions of sedimentary and metamorphic grains (figure 4.3.6). Other constituents include 5-15% calcite cement, 8-9% feldspar and minor mica, heavy minerals and glaucony (1-3%) (figure 4.3.6).

The average Q:F:L ratio for the sandstone from the Weydon Formation is 58:11:31 (figure 4.3.8). While the data from Kirby (1989) is also plotted on the graph, they show a lot of variation and are not useful. The sandstone fits into the litharenite field of Pettijohn et al (1987) although it is in the quartz-rich part of the field.

HEAVY MINERALS

A thin section of the heavy mineral sample from the Weydon Formation was analysed petrographically (OU 73330). Muscovite is the dominant mineral, despite some of it not having been collected due to density similarities between the liquid and the muscovite (figure 4.3.7). Minor amounts of pumpellyite are also present. While these minerals do not exclusively indicate a provenance for the sediments, the lack of minerals such as garnet, zircon and opaque minerals may discount a Median Tectonic Zone or Western Province origin.

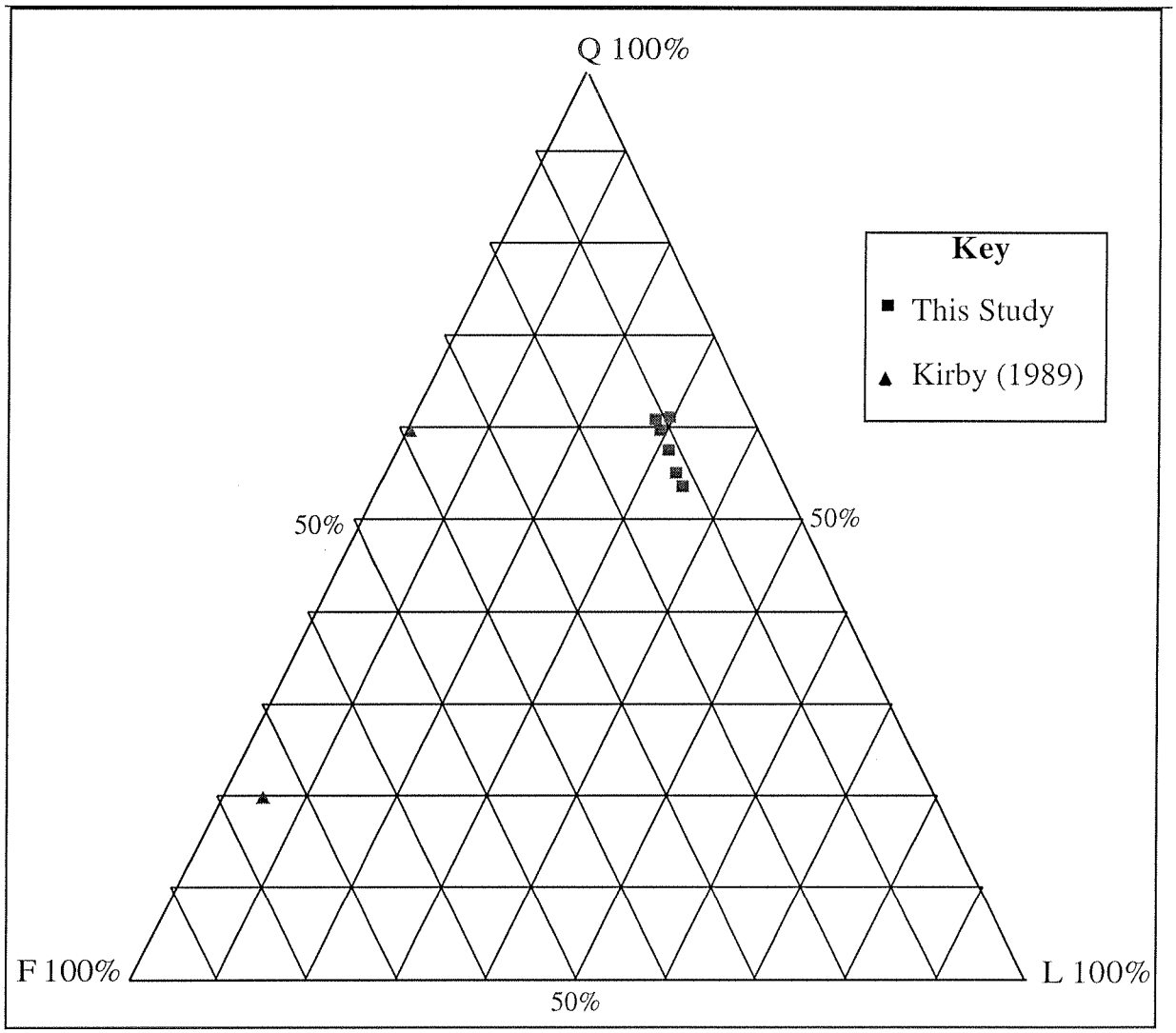

Figure 4.3.8 Q:F:L diagram for the Weydon Formation sandstone from this study as well as from Kirby (1989). The data from this study and Kirby (1989) are obviously different, although the reasons for this are unclear.

GEOCHEMISTRY OF THE SANDSTONE

Major and trace element geochemistry of the sandstone from the Weydon Formation has been analysed (appendix D, OU 73296-73299) using discriminant plots (section 1.5.3). Data from the Weydon Formation fall mainly in the arc field on the discriminant function plot (figure 4.3.10 B), and in the active continental margin field in the trace element plot and silica versus K_2O/Na_2O (figures 4.3.9 and 4.3.10A), illustrating the problems that may occur with recycled sediments. The sandstone petrology, major element chemistry and the heavy minerals, indicate that the sediments are derived from an arc terrane, but they have undergone extensive reworking to become quartz-rich. The sand has become more silica rich with respect to

potassium and sodium due to the break down of feldspar minerals during the weathering process. Trace element concentrations in the sandstone have probably been altered, due to the minerals containing the arc type trace elements being heavier than the other minerals in the sand (Roser et al, 2002). Sorting of the sand in the littoral belt along basin margins and to a lesser degree by turbidity currents, results in it becoming more mature and losing some of its provenance identifying characteristics, such as these heavy minerals (Ricci-Lucchi, 1985; Morton, 1985). The lack of true heavy minerals and the relatively low percentage of lithic grains in the sand shows that these types of sorting processes have occurred.

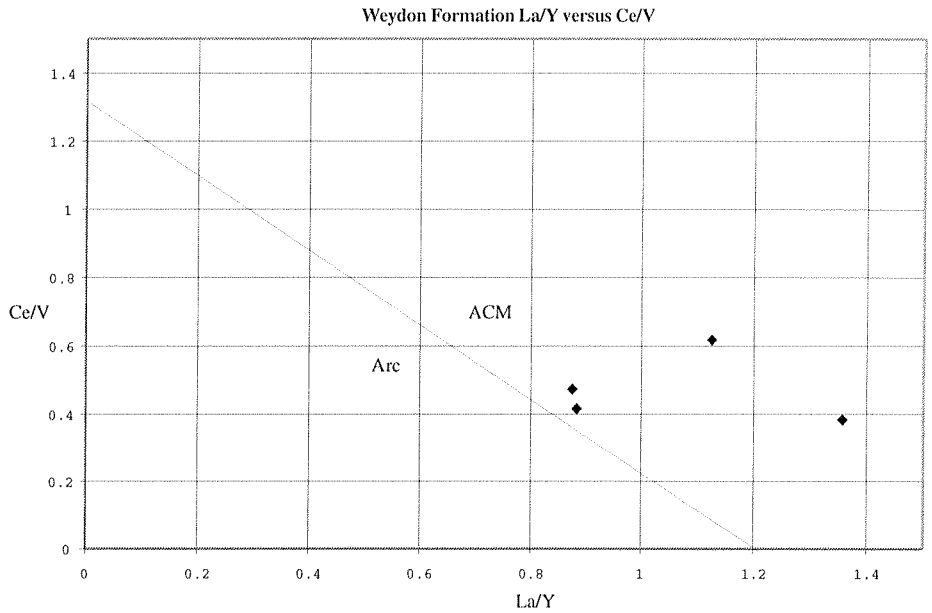

Figure 4.3.9 In this La/Y vs Ce/V trace element plot, all the Weydon Formation sandstone samples plot in the active continental margin field, based on other petrographical and geochemical data described in this section. This apparent enrichment in light rare-earth elements (La/Y) is probably due to sorting and deposition of heavy minerals prior to the deposition of deep sea facies, rather than being a real artefact present in the rock from which the sediment is derived.

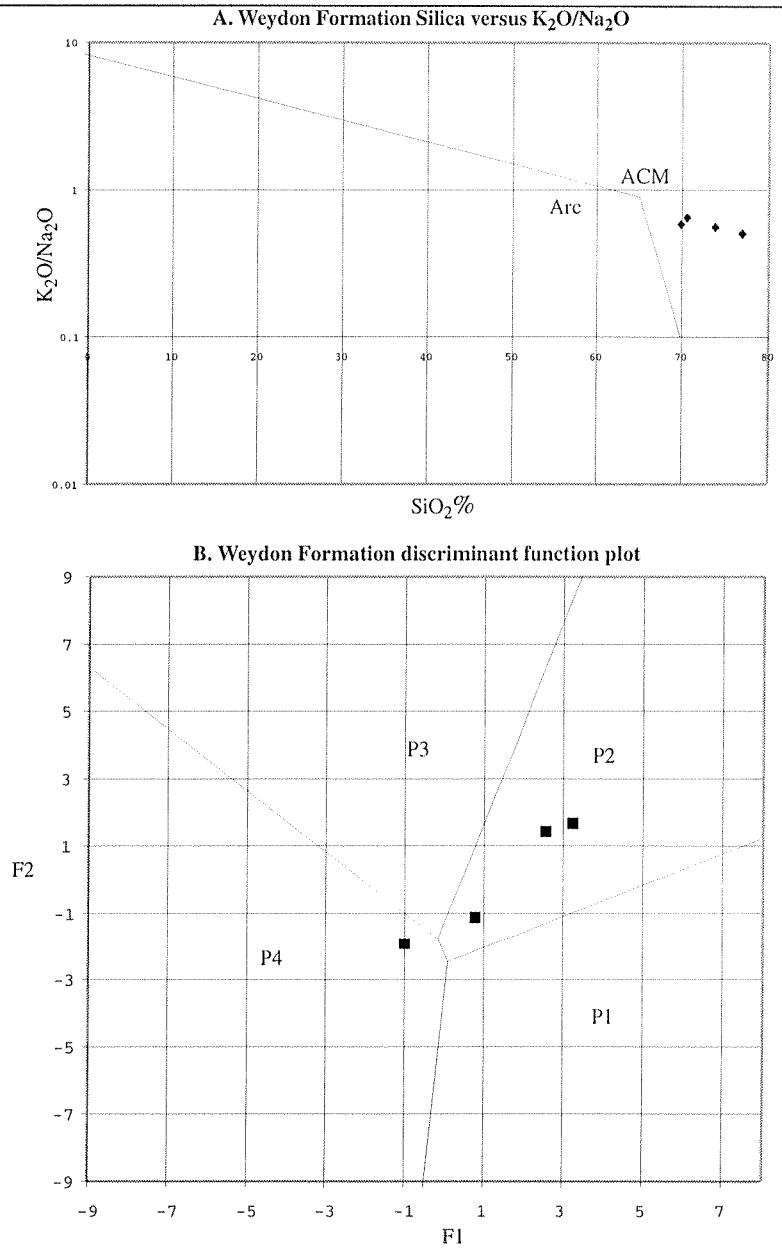

Figure 4.3.10 **(A)** On this simple SiO_2 vs K_2O/Na_2O graph the Weydon Formation sandstones mainly plot in the active continental margin field, probably due to weathering of the sand during reworking causing the breakdown of feldspar. **(B)** The discriminant function plot shows that most of the Weydon Formation sandstone samples plot in the intermediate volcanic section (P2), indicative of an arc type origin for the sediment. The one sample that plots in the P4 section is indicative of recycling.

4.3.5 SUMMARY

ENVIRONMENT OF DEPOSITION

Lithofacies present in the Weydon Formation show that the accumulation of turbidites (facies D1) and hemi-pelagic mudstones (facies G) resulted in the formation of this unit. The nature of the sandstone facies suggests that they were deposited in a small fan with no major channels. The sand was deposited as thin continuous sheets to build up the fan, as in a type 3 depositional system of Mutti (1985), or a single point-source submarine fan of Reading and Richards (1994). The lithofacies associations in the Weydon Formation show that there were 3-4 major turbidite-dominated fan building episodes during deposition of the unit, as shown by the facies D packets that now form distinctive ridges in the area. Between these phases of turbidite deposition, hemi-pelagic mud (facies G) and silty minor debris flows (facies E2) were deposited without being swamped by the coarser grained turbidites of facies D1. This cyclic nature of sedimentation during deposition suggests episodic variations in sea level or sediment supply, caused either by climate change or by local tectonic activity (Mutti, 1985).

PROVENANCE OF THE WEYDON FORMATION

The petrology of the Weydon Formation combined with the current direction measurements, suggest that this unit was derived from the Caples Terrane and its metamorphic equivalent within the Otago Schist, situated to the northeast of the study area (figure 1.4.1). Evidence for this provenance comes from the paleocurrent direction indicators, large proportions of sedimentary and metamorphic lithic grains in the sandstone, the muscovite and low-grade metamorphic minerals in the heavy mineral sample, and the arc-type geochemistry of some of the sandstone samples (Kawachi, 1974; Turnbull, 1979; Roser and Korsch, 1988; Mortimer and Roser, 1992). Deviations in the geochemistry from this interpretation can be explained by sorting processes (Roser at al, 2002), or by the break down of feldspar.

All other reports on the provenance of the Weydon Formation (Turnbull et al, 1989; Kirby, 1989; Turnbull et al, 1993) suggest that it was derived from Fiordland, due to the quartz-rich nature of the sand. The evidence given above, as well as the lack of any distinctive Fiordland heavy minerals such as garnet, zircon and opaque minerals, shows that this is not the case.

4.4 HAYCOCKS FORMATION

4.4.1 INTRODUCTION

TYPE SECTION

No complete section is seen through the Haycocks Formation. The type section designated by Harrington (1982) and Turnbull et al (1993) is along the road at G.R. D43/230 137.

DISTRIBUTION AND THICKNESS

The Haycocks Formation has been mapped at the Haycocks (appendix H) and across the Mararoa River to the northwest (Harrington, 1982). The base of the unit is not seen due to faulting, and the top is gradational into the Waicoe Formation. A minimum thickness for this unit is 2500 m (Harrington, 1982; Turnbull et al, 1989).

PREVIOUS WORK

The name Haycocks Formation was informally suggested by Carter and Norris (1977b). Harrington (1982) made a full description of the unit, including sedimentology, petrology, provenance and age. The Haycocks Formation was formalised by Turnbull et al (1989) with much of the information coming from Harrington (1982). Turnbull, Uruski et al (1993) briefly mention the provenance of the Haycocks Formation and its relationship to other units in the Te Anau Basin.

3.4.2 AGE AND FOSSIL OCCURRENCE

Some bivalve shells were seen in the Haycocks Formation during the study but were not identified due to their broken nature. Harrington (1982) noted the presence of the bivalve *Parvamussium* in the Haycocks formation suggesting that the basin was at leat 500 m deep at the time of formation, although foraminifera samples from the Waicoe Formation directly above the Haycocks Formation indicate that the depth at this time was only about 200 m (figure 4.2.2).

The age of the Haycocks Formation has been determined from the ages of the Waicoe Formation horizons on either side of it (figure 4.2.1). The presence of *Globoquadrina*

dehisens, *Globigerina woodi connecta*, *Notorotalia spinosa* and *Plectofrondicularia whaiangaroica* below the Haycocks Formation and *Cibicides novozelandicus* above the unit suggests an age of Waitakian to Otaian, concurring with the ages given in Harrington (1982) and Turnbull, Uruski et al (1993) (fossil identifications by R.E Fordyce).

4.4.3 LITHOFACIES DESCRIPTION AND INTERPRETATION

The Haycocks Formation consists of interbedded sandstone and mudstone, grading from a sandstone-dominant base, through a mudstone-dominant top, and eventually grading into the Waicoe Formation. The unit has been separated into a number of lithofacies in order to define the depositional environments. Outcrop is scarce, so facies relationships are difficult to ascertain on a regional scale.

LITHOFACIES C DESCRIPTION

Lithofacies C sediments dominate the lower part of the Haycocks Formation. This facies is made up mainly of medium sandstone interbedded with mudstone and has a sandstone/mudstone ratio that is >> 1. The sediment is generally well sorted.

The beds are continuous over large distances resulting in the strike-parallel ridge topography that is typical of this unit. Thickness of the beds ranges from 50 cm up to a few metres. The thickest beds show no signs of amalgamation, although it is possibly not seen because of extensive outcrop weathering. Normal grading is present in some beds whereas others appear massive, with sharp upper contacts on some sandstone beds.

Sedimentary structures in this facies include sole marks, load casts and lamination. Complete Bouma sequences are rare, T_{ae} and T_{be} and T_{abe} being the most common sequences seen.

LITHOFACIES C INTERPRETATION

The continuous nature of the beds combined with the sedimentary structures that are present suggest that this facies formed as part of a submarine fan and was deposited by turbidites with a contribution from debris flows possible. Ricci-Lucchi (1975) and Stow (1996) suggest that facies C sediments such as these are typical of a middle fan environment, where most sediment is deposited as lobes of the fan rather than in channels. This is supported by the

laterally continuous nature of the beds, suggesting that they were unconfined as they were deposited.

Shanmugam (2000) suggests that ungraded beds can only be formed by debris flows however the amalgamation of a number of sandstone beds during turbidite deposition could also form ungraded beds. The presence of non-graded, non-laminated beds in this facies suggests that debris flows could have deposited a significant proportion of the sediment. Unfortunately, a lack of evidence supporting debris flow deposition, due to both the absence of fresh outcrop and the similarities between C1 and C2 sediments, means that there are no typical features such as reverse grading, floating clasts, armoured mud balls etc (figure 4.1).

LITHOFACIES D DESCRIPTION

Facies D sediments become more abundant toward the top of the Haycocks Formation. Like facies C this facies also consists of interbedded, well-sorted, medium sandstone and mudstone, but the sandstone/mudstone ratio is approximately 1.

The beds range in thickness from 5-40 cm and are continuous, adding to the distinctive topography created by this unit. Amalgamated beds are not seen in this facies. Normal grading is common with beds fining from medium sandstone up to siltstone or mudstone, although ungraded beds are also present.

Sedimentary structures include sole marks, ripple marks and lamination. No full Bouma sequences were present in the facies; graded T_{ce} and graded T_{de} are the most common sequences observed.

LITHOFACIES D INTERPRETATION

Facies D sediments contain more mudstone than facies C suggesting that they were formed in a more distal part of the fan, or as the amount of sediment was decreasing. Ricci-Lucchi (1975) and Stow (1996) suggest that facies D sediments like these are typical of a middle-outer fan environment where most sediment is deposited as lobes of the fan rather than in channels. This is supported by the laterally continuous nature of the beds which are thinner than in facies C, suggesting that they were unconfined as they were deposited, but more distal than facies C.

LITHOFACIES DISCUSSION

The two different facies in the Haycocks Formation tend to form packets that are repeated throughout the unit (figure 4.4.2). Each packet consists of facies C sediments overlain by facies D sediments as seen in figure 4.4.1. These packets are essentially fining and thinning upward sequences but do not appear to fine all the way to mudstone (i.e lithofacies G). The Haycocks Formation forms a distinct topography that consists of small ridges and gullies, where the ridges are formed by the resistant sandstone of the facies C sediments and the gullies are formed by the more mud-rich facies D sediments. Overall the Haycocks Formation fines and thins upwards until it eventually grades into the Waicoe Formation (figure 4.4.2).

Most facies models indicate that fining and thinning upward sequences are typical of migrating lobes, however work on present day submarine fans shows that these models are too simplistic (Shanmugam, 2000). While migrating lobes may cause the fining upward sequence, it may also be due to tectonic uplift, or changes in sea level in the source area. Uplift would result in more erosion in the source area, as well lowering the relative sea level, resulting in movement of sediments from the littoral areas to the heads of submarine canyons. The packets of sandy sediments could be related to incremental uplift in the source area, while the large scale fining upward sequence could be due to an overall decrease in tectonic activity (e.g Takano, 2002).

PALEOCURRENT ANALYSIS

Scour marks from both of the lithofacies at the outcrop G.R. 2122900 5513700 were measured using the techniques described in section 1.5.5. The results are shown in figure 4.4.3 and show that the turbidites that make up the Haycocks Formation flowed from the northwest to southeast (appendix E4).

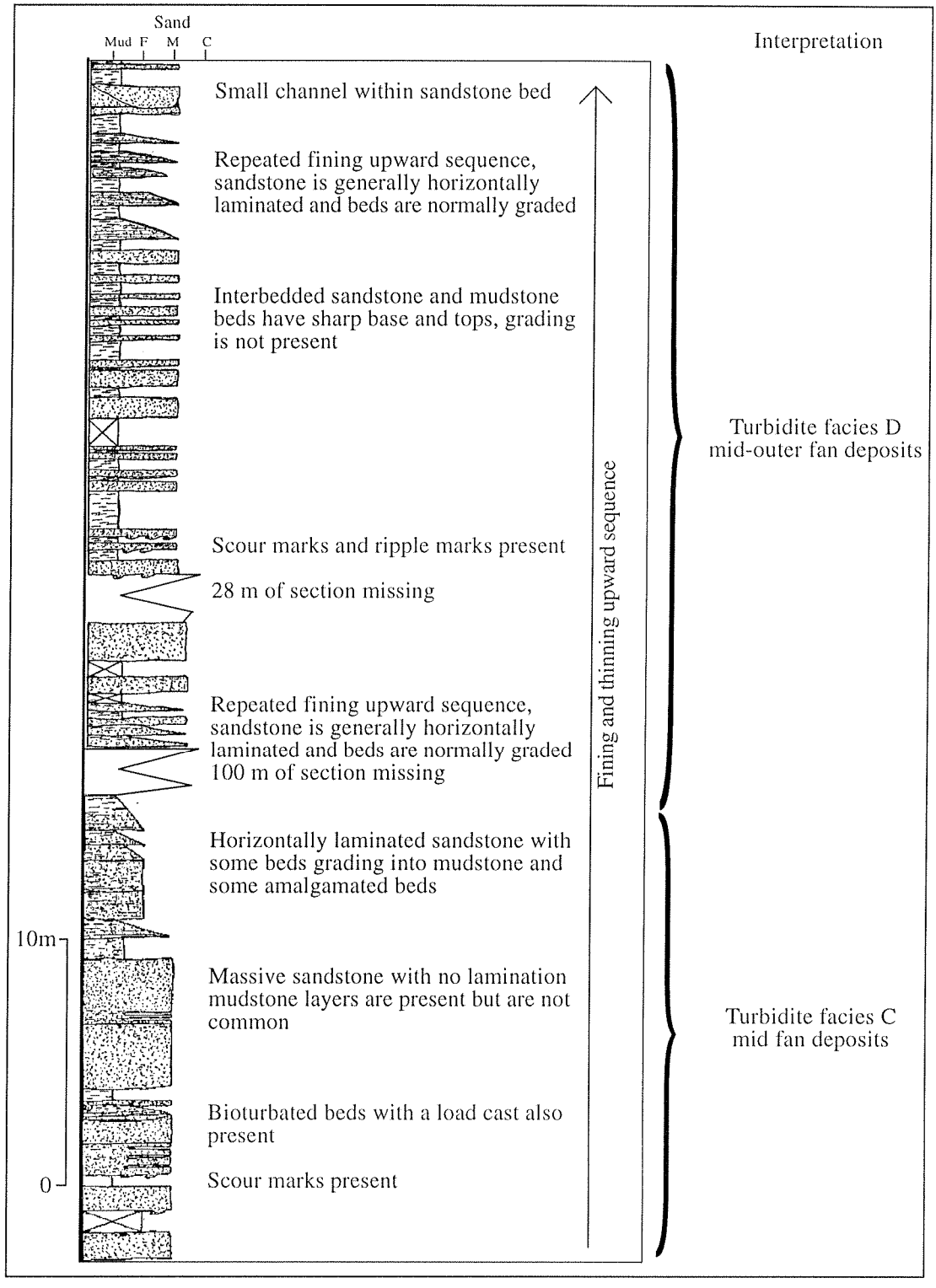

Figure 4.4.1 This section, which starts at G.R. 2122900 5513700, shows the two main lithofacies that are present in the Haycocks Formation. This sequence represents a packet of beds from the upper part of the unit; each packet grades from facies C sediment up into facies D sediment leading to a cyclic fining and thinning upward sequence.

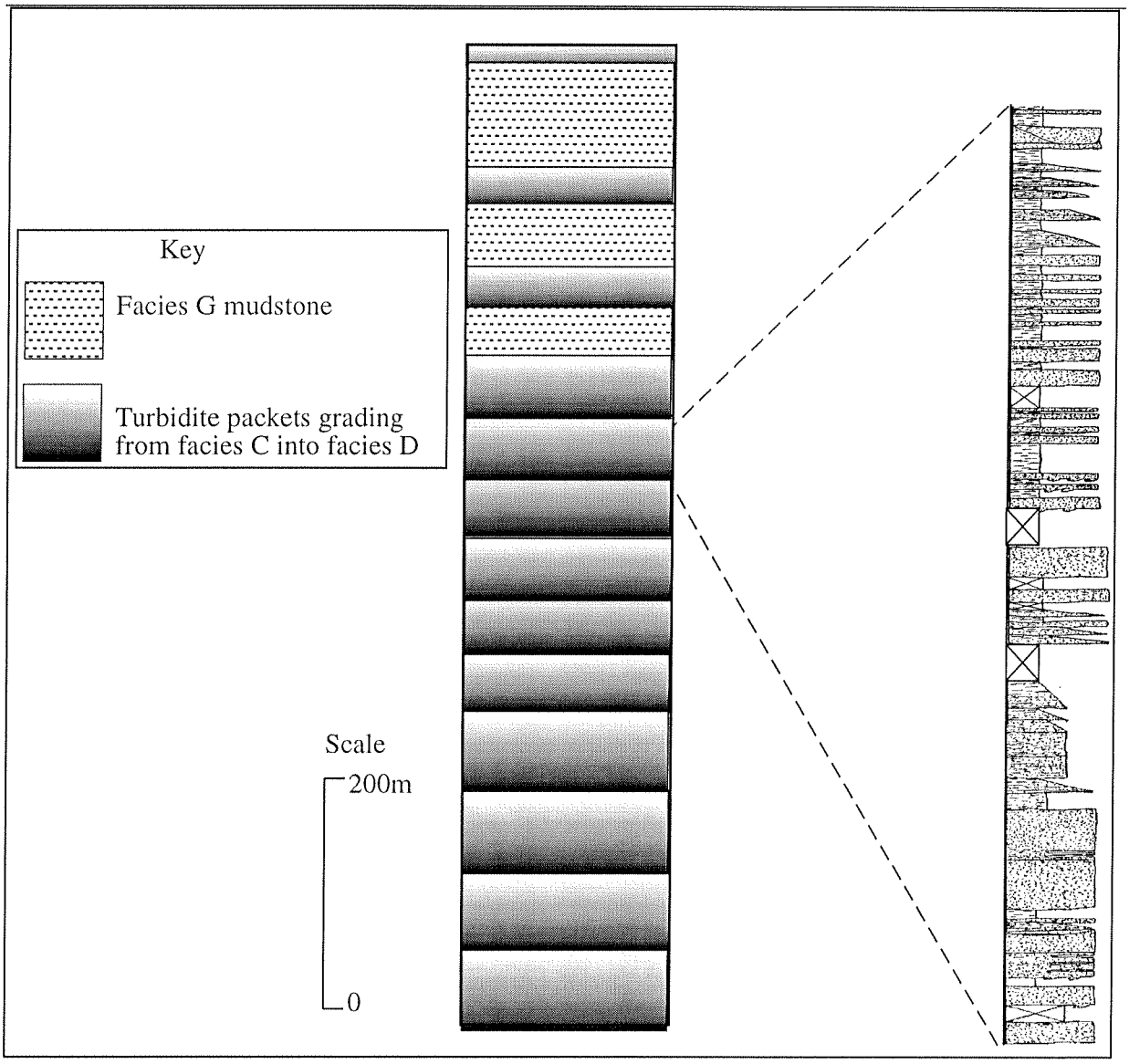

Figure 4.4.2 Schematic section through the Haycocks Formation showing the repeated fining upward sequence that is typical of the unit. The section from figure 3.4.1 represents one of these cycles, as shown in this figure.

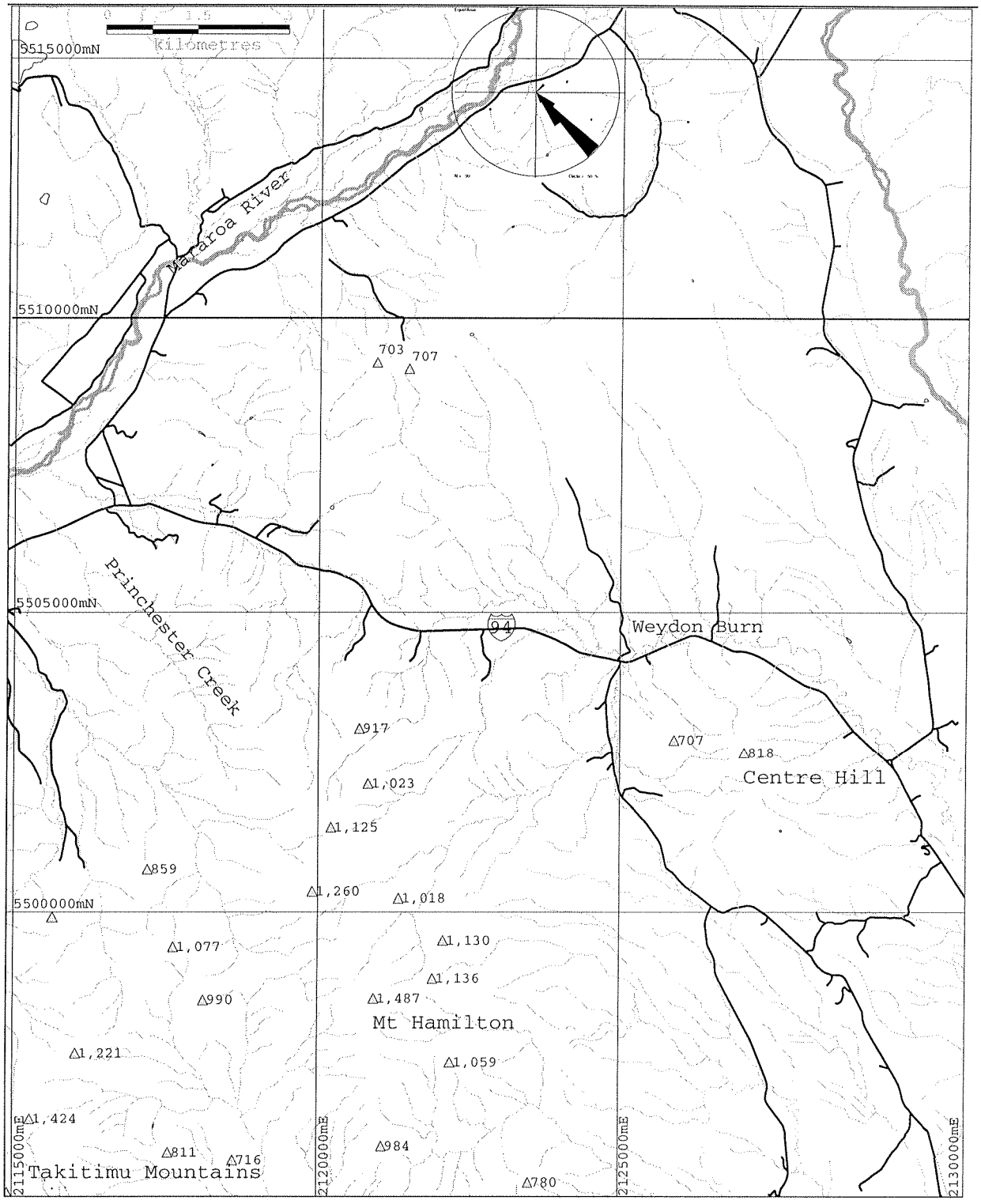

Figure 4.4.3 Current direction map for the Haycocks Formation showing that the current that deposited this unit flowed from the northwest to southeast.

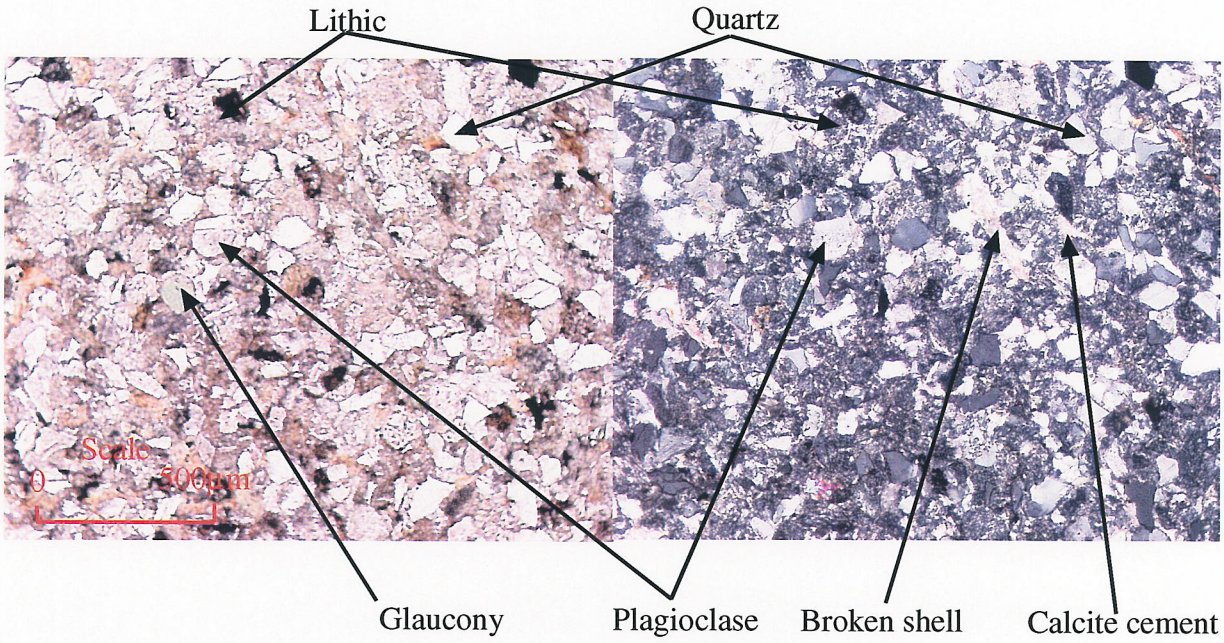

Figure 4.4.4 Photomicrograph the Haycocks Formation sandstone (OU 73301) (plane-polarised light on the left, cross-polarised light on the right) showing the main constituents. The glaucony and broken shell fragments suggest that this sediment has been reworked from a shelf environment.

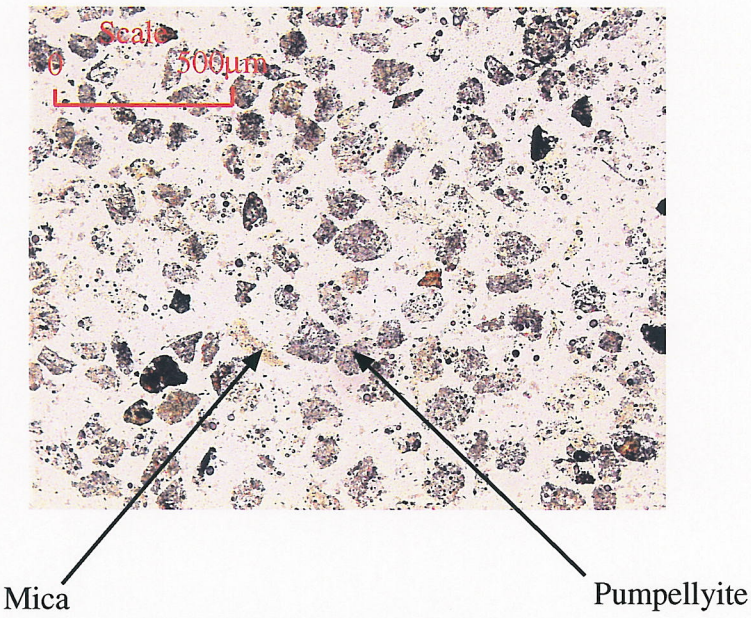

Figure 4.4.5 Photomicrograph of the heavy mineral slide from the Haycocks Formation (OU 73331). This sample consists of low grade metamorphic minerals, mainly pumpellyite and mica (muscovite and biotite) with minor amounts of chlorite also present.

4.4.4 PETROLOGY

INTRODUCTION

The same petrological techniques used on the other units were used to determine provenance and describe the petrology of this unit. These include hand specimen observations, petrography of sandstone and heavy minerals, and whole-rock geochemistry. Data from Harrington (1982) have also been incorporated into this study in order to increase the sample size.

SANDSTONE PETROGRAPHY

Three sandstone slides from the Haycocks Formation were investigated petrographically using general observations and the point count method described in section 1.5.6 (appendix B, OU 73300-73302). The grains in the sandstone are angular and average 0.3 mm in diameter. The sand is well sorted, and grains are clast supported with calcite cement infilling all of the pore space.

The sandstone is lithic-rich, with lithic grains making up 40-50% of the rock (figure 4.4.4). The lithics are dominantly sedimentary (greywacke) with minor amounts of metamorphic (schist) grains also present (figure 4.4.4). Quartz is the second most common constituent in the Haycocks Formation sandstone, making up 20-30% of the rock, while feldspar comprises 10-14% (figure 4.4.4). Minor amounts of mica and heavy minerals are also present along with about 10% calcite cement.

In this study the average Q:F:L ratio for the sandstone was found to be 31:14:55, similar to the results of Harrington (1982), who found an average Q:F:L of 21:35:44 (figure 3.4.6). The discrepancy between the two data sets is probably due to different point counting techniques. Most of the data falls in the litharenite field of Pettijohn et al (1982).

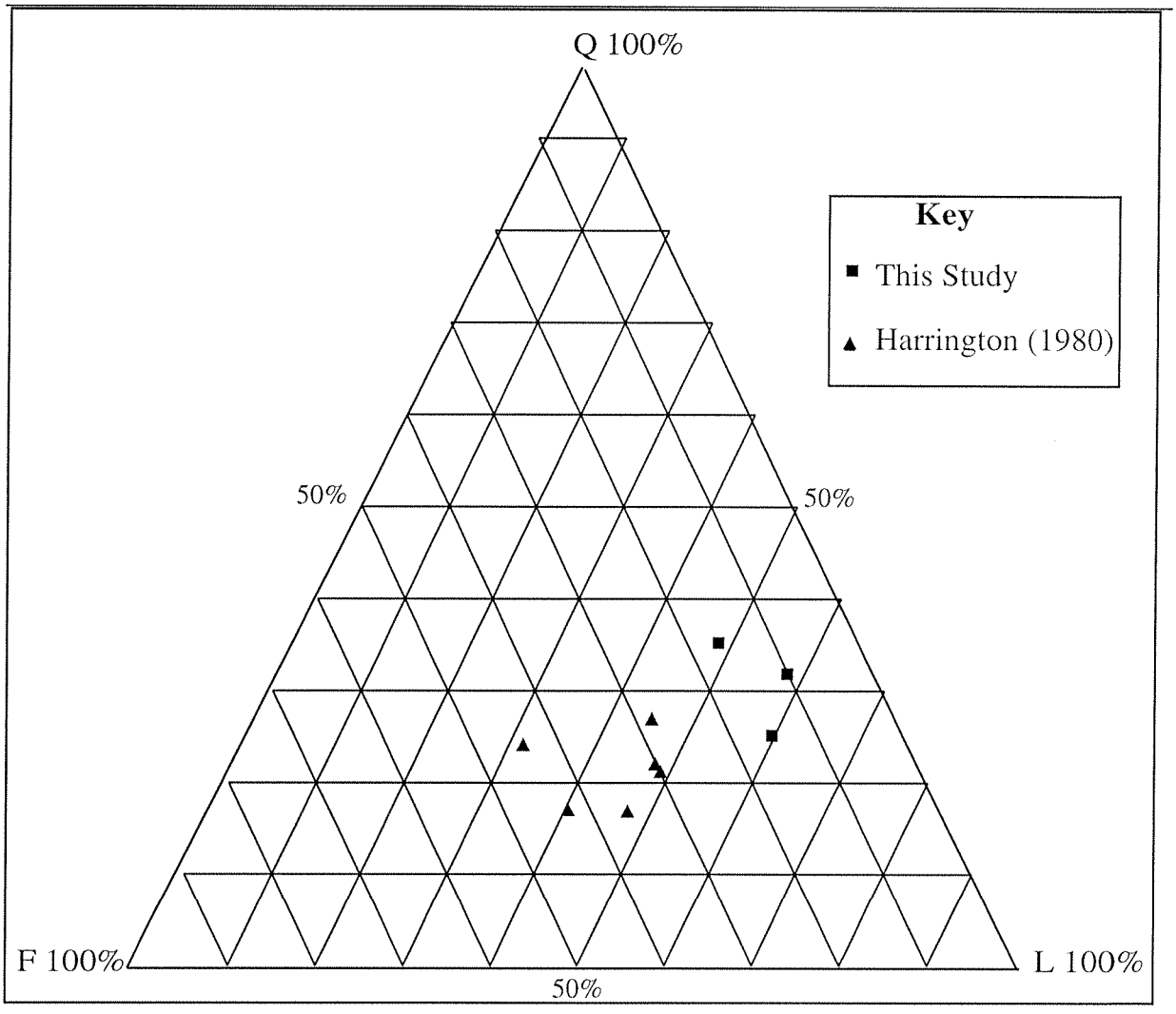

Figure 4.4.6 Q:F:L diagram for the Haycocks Formation sandstone from this study as well as from Harrington (1982). The data is similar for both studies and falls in the litharenite field of Pettijohn et al (1987). The difference between the two sample sets may result from differences in the composition of the rock or, more likely, due to a difference in the point counting technique.

HEAVY MINERALS

A thin section of the heavy mineral sample extracted from the Haycocks Formation (OU 73331) was petrographically examined to identify the minerals present. In this sample, muscovite, chlorite and pumpellyite are present (figure 4.4.5). All of these minerals are metamorphic minerals of greenschist facies or lower.

GEOCHEMISTRY OF THE SANDSTONE

Major and trace element whole rock geochemistry of the Haycocks Formation sandstone has been analysed (appendix D, OU 73300-73306) using the discriminant function plots described in section 1.5.3. The geochemistry of the Haycocks Formation shows a similar trend to the Weydon Formation. All the samples plot in the intermediate volcanic P2 field of the discriminant function plot (figure 4.4.8B). On the SiO_2 versus K_2O/Na_2O (figure 4.4.8A) graph the data plot in the arc field, while in the La/Y versus Ce/V graph (figure 4.4.7) all the data plot in the active continental margin field. The trace element concentrations in the sandstone have probably changed during the reworking process, resulting in the deposition of the heavy mineral grains in the littoral zone (Ricci-Lucchi, 1985; Morton, 1985). Heavy minerals often contain trace elements that are not contained in the other grains in the rock, therefore preferential deposition of heavy minerals results in different trace element signatures in the reworked sediment than in the original rock (Roser et al, 2002).

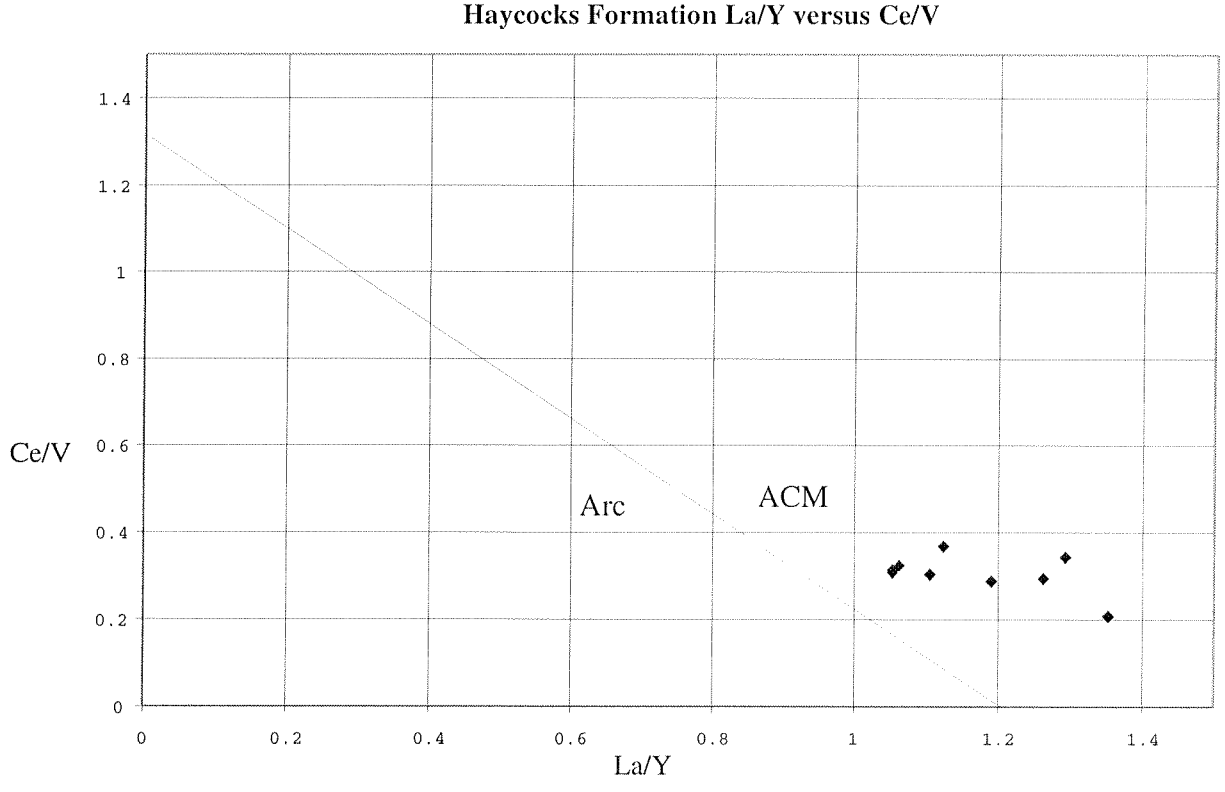

Figure 4.4.7 All these data pot in the active continental margin field suggesting that reworking has removed the minerals that contain many of the trace elements.

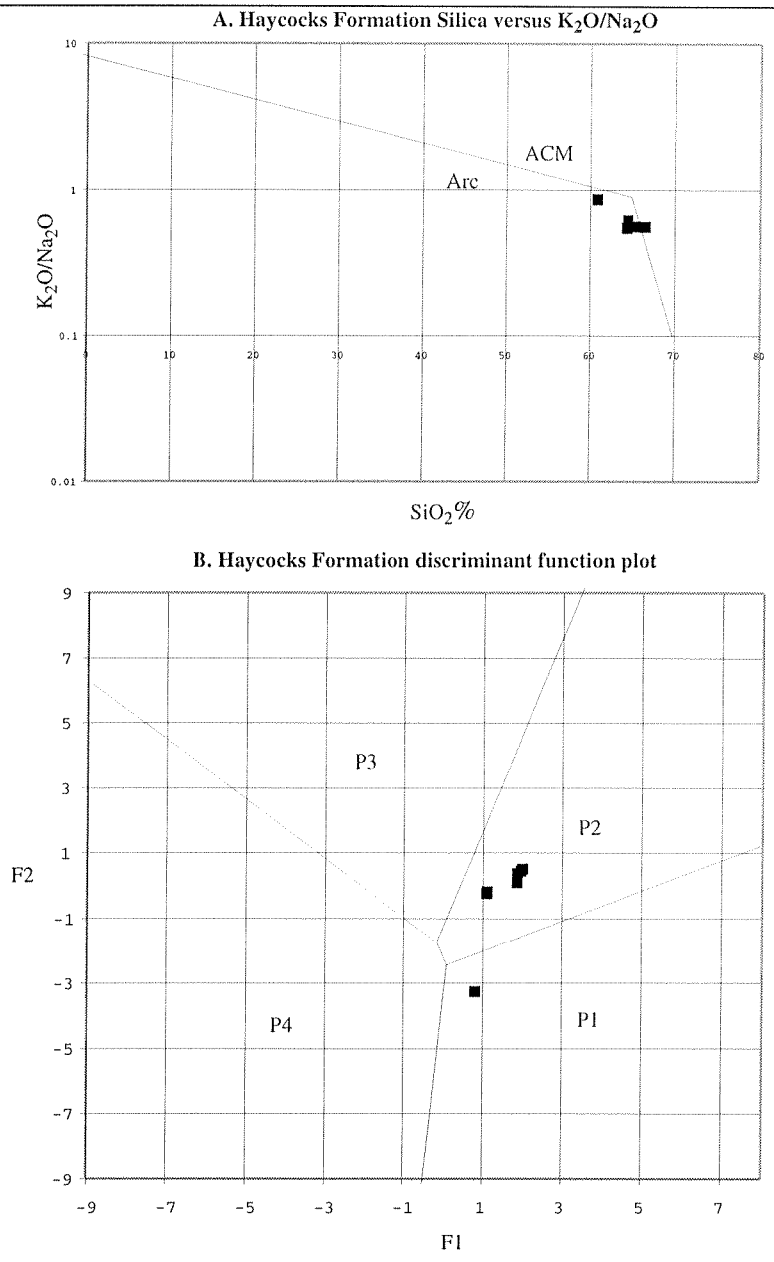

Figure 4.4.8 Both the silica versus K_2O/Na_2O graph and the discriminant function plot indicate an arc origin for the Haycocks formation sandstone.

4.4.5 SUMMARY

ENVIRONMENT OF DEPOSITION

Lithofacies that are present in the Haycocks Formation show that it formed as a large submarine fan with migrating lobes depositing thick sheets of sediments, mainly by turbidity currents (Mutti, 1985; Reading and Richards, 1994). The fan has been built up through the accumulation of many phases of turbidite activity that initially deposited a lot of sand (facies C), and then finer grained sediments as sediment supply dissipated (facies D). The thick-bedded nature of the sandstone and the thickness of the unit overall, suggest that the Haycocks Formation formed as a type 2 depositional system of Mutti (1985), or as a sand-rich submarine fan (Reading and Richards, 1994; Richards et al, 1998). The sheet-like nature of these deposits is indicative of unconfined deposition in the distal part of a fan (Reading and Richards, 1994; Richards et al, 1998; Saito and Ito, 2002).

The thinning and fining upward sequence that is present on a large scale within the whole unit could represent an overall migration and abandonment of the lobes that formed the fan (Mutti, 1985). This sequence could also be indicative of a change in tectonic activity in the source area. An example of where tectonics control the sedimentation rate is in the Niigata-Shin'etsu basin Japan (Takano, 2002). Takano (2002) shows how changes in the tectonic regime directly relate to changes in the depositional systems. The early Miocene was when the Moonlight Fault System changed from dominantly transtensional to transpressional (Carter and Norris, 1976) and this may have caused a decrease in sediment supply to the fan that deposited the Haycocks Formation. Small scale thinning and fining upward sequences seen as the individual packets described above, may again be caused by migrating fan lobes (Mutti, 1985) or the result of increased sediment due to tectonic activity (Takano, 2002).

PROVENANCE OF THE HAYCOCKS FORMATION

The petrological data from the Haycocks Formation suggests that it is derived from the Caples Terrane. Specific evidence is the high proportion of sedimentary lithic grains in the sandstone, the presence of metamorphic minerals that are greenschist facies or lower in the heavy mineral sample, and the major element sandstone geochemistry. This petrological data is supported by the paleocurrent data that indicates that the currents depositing the unit flowed

from the northwest where the Caples Terrane is located (figure 1.4.1). Carter and Norris (1977b), Harrington (1982), Turnbull et al (1989) and Turnbull, Uruski et al (1993) have all indicated that the Haycocks Formation is derived from the Caples Terrane and data from this study confirms this.

5 QUATERNARY SEDIMENTS

5.1 PLEISTOCENE SEDIMENTS

5.1.1 INTRODUCTION

Two different types of sediments were deposited during the Pleistocene and these now cover much of the study area, although this is not shown on the geological map (appendix H), in order that the underlying units can be seen more easily. Pleistocene sediments do not outcrop well in the area although topographic features show their extent.

5.1.2 FLUVIAL TERRACES

Between the main road and the Mararoa River lies a horizontal terrace at 50-100 m above the present day river (figure 5). The terrace is covered by a veneer of gravel that is 1-10 m thick in outcrop. This flat lying gravel unconformably overlies the Tertiary units in the area.

The gravel is poorly sorted and clast supported, with clasts ranging in diameter from 5-30 cm. Surrounding the gravel is a poorly sorted matrix of sand and granule sized material. Clasts in the gravel are generally well rounded, with some slightly angular clasts that have broken along foliation planes. Clast composition is dominantly schist and metabasite, and many have numerous quartz veins. Greenish coloured greywacke is common, and rare granitoid clasts are also present. The schist and greywacke are most likely derived from the Caples Terrane, and the metabasite is derived from the Dun Mountain Ophiolite in the north, while the granitoid clasts are from Fiordland.

These fluvial terraces were deposited in the Pleistocene, when much of the surrounding area was covered by glacial ice. They have been deposited by sediment flowing from the north, as glacial outwash. McKellar (1973) called these deposits the Mavora outwash gravels and indicated that they were deposited before the last glaciation.

5.1.3 TALUS FANS

Along the edges of the Takitimu Mountains and Centre Hill lie many old fan surfaces that dip moderately away from the adjacent hills (figure 5). Outcrop of the fan gravels is generally absent, but where present the fan gravels appear to be a few metres in thickness and bedding tends to dip parallel to the main surfaces.

The fans consist of poorly sorted breccia, with angular clasts ranging in size from coarse sand up to 10 cm diameter cobbles. The dip of the beds and the resulting upper surface is sub-parallel to the slope, which is typical of fans. Some beds contain cross-beds, indicating that the sediment flowed from the mountains adjacent to the fan (in this case mainly to the north). In some outcrops reverse grading is present, suggesting a mass flow deposit origin. Clasts in the fans are composed of adjacent country rocks such as the Murihiku Supergroup and some of the harder Tertiary units.

5.2 HOLOCENE SEDIMENTATION

Sedimentation patterns in the Holocene have changed slightly since the Pleistocene. The retreat of the glaciers has allowed the Mararoa River, which still flows from the north carrying Caples Terrane and Dun Mountain Ophiolite Belt derived clasts, to cut down through the terrace gravels and create a large river valley in the area (figure 5). Other major drainage systems such as Princhester Creek also deposit fluvial sediments in the area (figure 5). In the area around Mount Hamilton large talus scree slopes are common (figure 5).

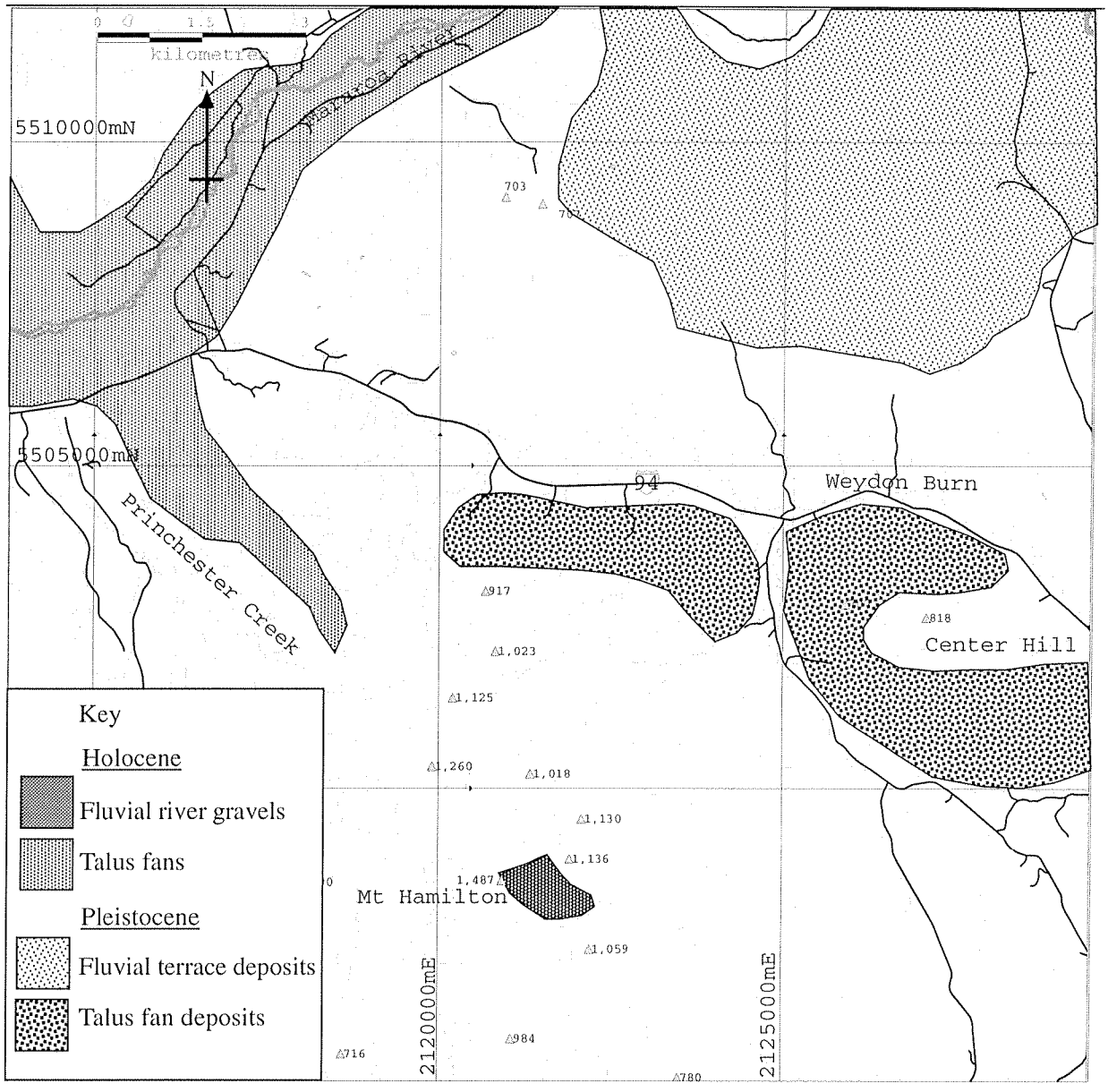

Figure 5 Map showing the extent of the Pleistocene sediments in the study area. The fluvial terrace deposits form a flat surface, while the talus fan deposits form sloping surfaces. This map was created from observations of the type of surface in the study area, rather than from mapping outcrops due to a lack there of.

6 STRUCTURE

6.1 INTRODUCTION

Outcrop scale faults and folds are rarely seen, but large scale structures can be identified on aerial photographs and can be inferred from relationships between rock units and bedding orientations. Two major regional structures, namely the Moonlight Fault System and the Southland Syncline, occur in the area. Smaller structures (figure 6.1), are likely to be geometrically and kinematically related to these two major structures given their orientations. Detailed studies of the structures and sedimentary bedding orientations in the field area have been used to gain a better understanding of the regional structures in terms of their kinematics and timing of activity.

6.1.1 MOONLIGHT FAULT SYSTEM

The name Moonlight has been applied to a number of faults and fault systems in western Southland and Central Otago. Park (1909) named a fault near Lake Wakatipu the Moonlight Fault, forming part of what was initially the Moonlight Fault Zone (Turnbull et al, 1975). Since then Norris et al (1978) have defined the Moonlight Fault System as a number of sub-parallel faults that run from near the Alpine Fault, through the Wakatipu area, towards the south. This system defines the edges of, and separates, the Te Anau and Waiau Basins onshore, and the Solander and Balleny Basins offshore.

The faults that make up the Moonlight Fault System tend to be steeply dipping features that have generally undergone oblique slip (Turnbull et al, 1975; Norris et al, 1978). The fault system as a whole has moved in several episodes, each involving different types of motion, with the initial phase probably having occurred during the Cretaceous (Turnbull et al, 1975). The Moonlight Fault System was reactivated in the Eocene-Oligocene in an extensional environment, forming sedimentary basins adjacent to it (Turnbull et al, 1975; Carter and Norris, 1976; Norris et al, 1978; Norris and Carter, 1980, 1982; Norris and Turnbull, 1993; Turnbull, Uruski et al, 1993). In the mid Oligocene the fault system became transtensional with much of the deformation caused by strike-slip faulting (Norris and Turnbull, 1993). In

the Miocene the Moonlight Fault System became transpressional and a number of high angle reverse faults were activated (Turnbull et al, 1975; Carter and Norris, 1976; Norris et al, 1978; Norris and Carter, 1980, 1982; Norris and Turnbull, 1993; Turnbull, Uruski et al, 1993).

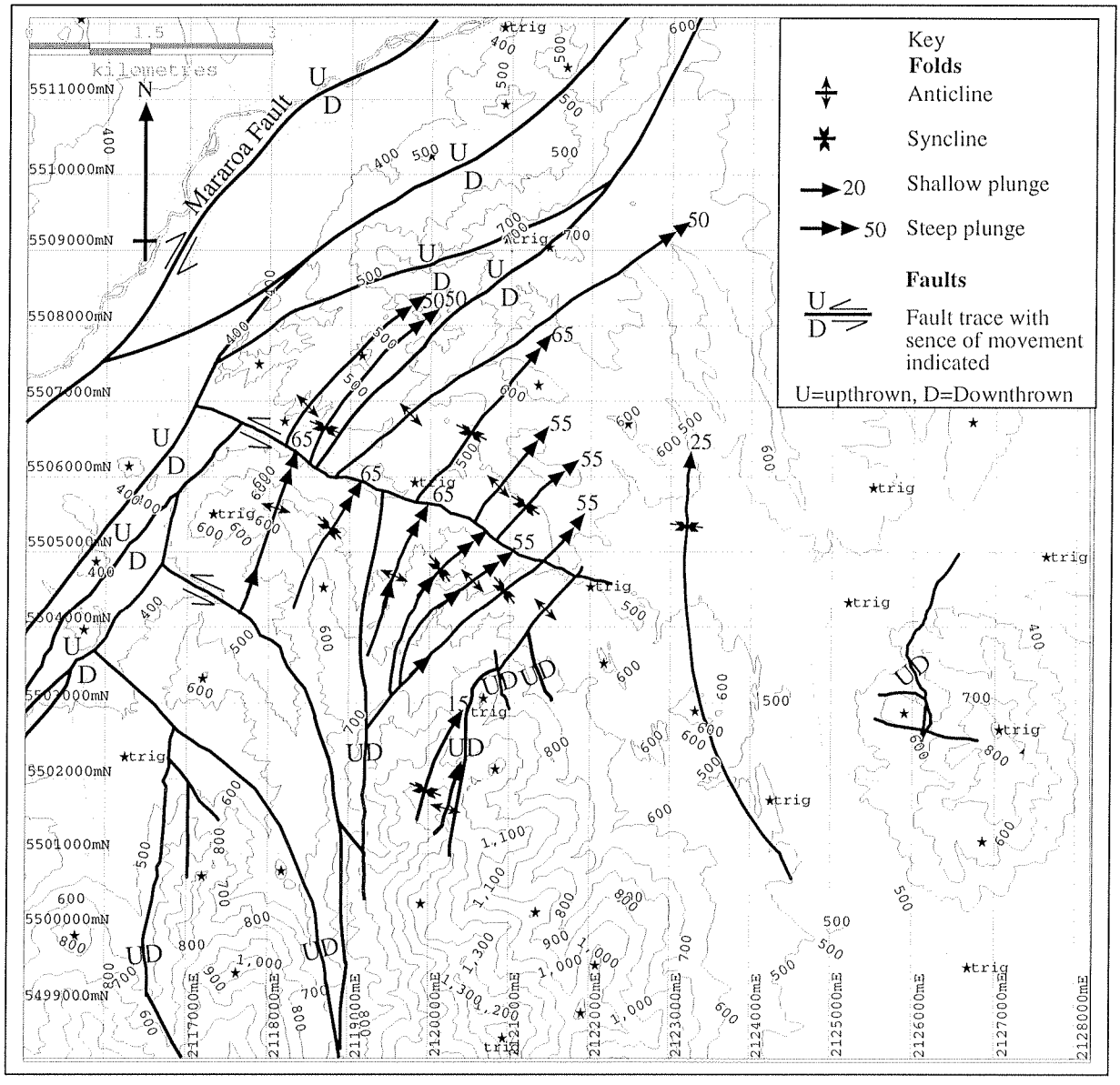

Figure 6.1 Map of the structures in the study area showing the main Moonlight Fault System (Mararoa Fault in this area). Faults in the area are either parallel to this system, perpendicular to it or strike north-south. Fold trends of the folds curve toward the fault system indicating that there is dextral shear across the area.

The strike-slip component of the fault system is dextral south of lake Wakatipu (Norris et al, 1978; Norris and Carter, 1980; Constantine, 1988; Uruski, 1992), and although north of the lake the most recent activity (Miocene) was also dextral some sinistral movement occurred

prior to the Miocene (White, 1998). The amount of strike-slip displacement on the fault is variable, with at least 2 km offset (depending on the dip of the Dun Mountain Ophiolite Belt) where the fault system cuts the Dun Mountain Ophiolite Belt north of the field area (Coombs et al, 1976; Carter and Norris, 1977b), and 18-30 km offset in the Waiau and offshore basins (Norris and Carter, 1980; Constantine, 1988, Uruski 1992).

Off the south coast of New Zealand faults along the same trend as Moonlight Fault System are still active, and Anderson (1991) describes an earthquake that occurred 800 km to the south of New Zealand on the Macquarie Ridge. This earthquake occurred on a steeply dipping plane along strike from the onland expression of the Moonlight Fault System and had dextral strike-slip movement on it (Anderson, 1991). The strike-slip faults south of New Zealand are directly linked to the Moonlight Fault System, although they are more active than those onshore as plate motion here is taken up by subduction under Fiordland rather than on the strike-slip faults (Lamarche and Lebrun, 2000).

6.1.2 SOUTHLAND SYNCLINE

The Southland Syncline is a regional structure that can be traced from the coast in South Otago to the study area on the eastern side of the Alpine Fault (Wellman, 1955; Speden, 1959; Turnbull, in prep.). The syncline folds the Triassic and Jurassic strata of the Murihiku Terrane and is thought to have been formed during Cretaceous terrane accretion (Coombs et al, 1976; Bishop, et al 1985).

Between the south coast and the Hokonui Hills the axis of the syncline trends between 105° and 115° (Speden, 1959; Boles, 1974). From the Hokonui Hills to the study area the syncline begins to trend in a more north-south direction (160° in the study area) (Coombs, 1950; Wellman, 1955; Boles, 1974; Turnbull in prep.). Further northwest, the syncline is not well defined but elements of it trend north-south (Bishop et al, 1990).

6.2 FAULT DESCRIPTIONS

The field area contains many faults of various different scales, the smallest occurring along bedding planes in folded strata (figures 6.2 and 6.3), the largest forming part of the Moonlight

Fault System with displacements on the kilometre scale. Three different orientations of faults are recognised in the study area: north-south, northeast-southwest and northwest-southeast each occurring in defined zones, with some overlap (figure 6.1)

6.2.1 NORTH-SOUTH STRIKING FAULTS

In the south of the area the Murihiku Supergroup and the Beaumont Formation are offset by a number of north-south striking faults (figure 6.1; appendix H). From the geological map of the area (appendix H) cross-sections were produced. These allowed an estimate of the amount of vertical offset on the faults to be made in areas where the outcrop is substantially continuous, the largest fault having vertical offset of approximately 1200m. The horizontal offset along these faults is difficult to estimate and appears to be insignificant compared to the vertical displacement. Only a few hundred meters sinistral separation on the faults, can be accounted for by vertical movement. The topographic expression of these faults suggests that they are very steeply dipping. Due to the steep dips of the faults, defining the movement as normal or reverse is difficult. However the amount of shortening, shown by the repetition of the stratigraphic sequence associated with these faults, suggest that they are high angle reverse faults (cross-sections and map, appendix H).

The north-south striking faults in the south of the area include the terrane boundary fault between the Murihiku Terrane and the Takitimu Group rocks of the Brook Street Terrane. The similar orientation and relative movement on the reactivated terrane boundary fault and the other faults in this area suggests that they were formed during terrane accretion. Subsequent movement has been the result of reactivation, evident from the Murihiku Supergroup being faulted over the Beaumont Formation in places. This reactivation occurred post early Whaingaroan as theses faults cut parts of the Spear Peak Formation. It is likely movement would have been synchronous with the folding of the Tertiary sediments in the late Miocene.

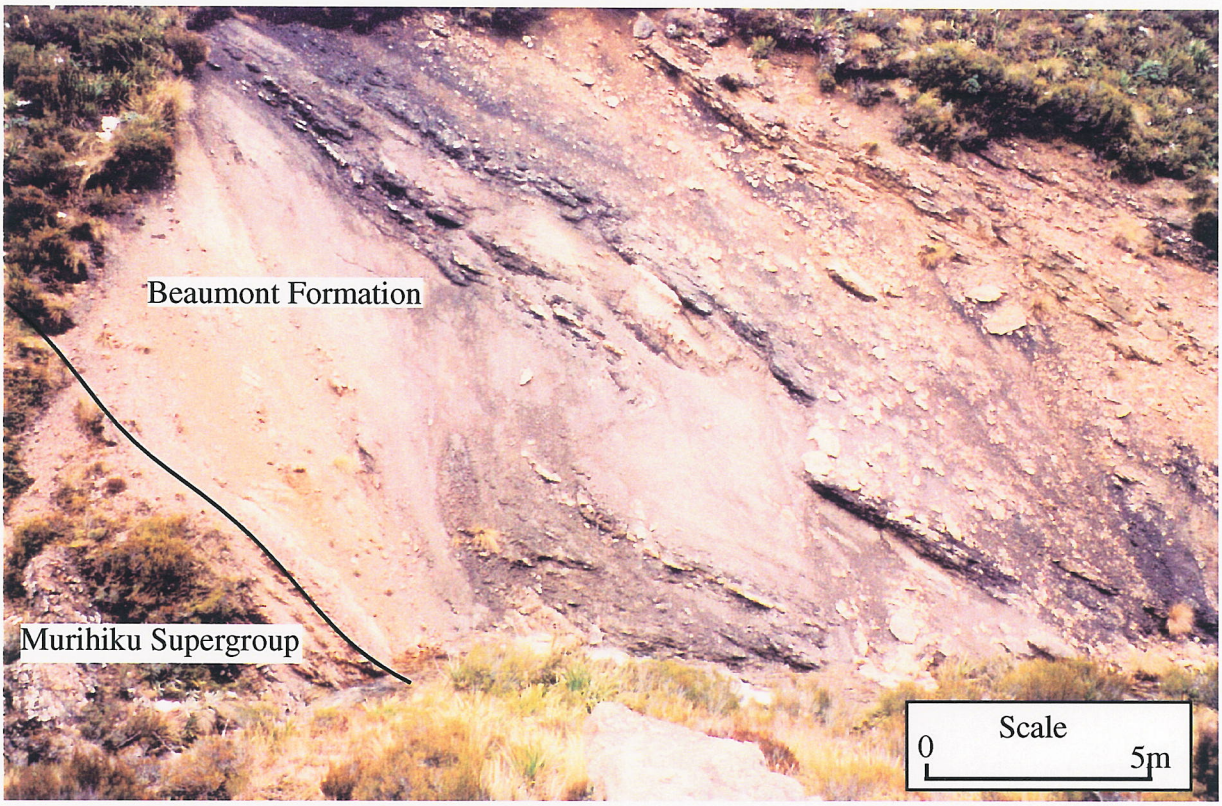

Figure 6.2 The unconformity between the Murihiku Supergroup and the Beaumont Formation at G.R. 2120900 5503200 showing the deformation that has been concentrated in this area during folding. The localised deformation is due to the change from the rigid basement rock to the mud-rich basal part of the Beaumont Formation. Note that both units have a similar dip, indicating that the west limb of the Southland Syncline was flat untill the Miocene.

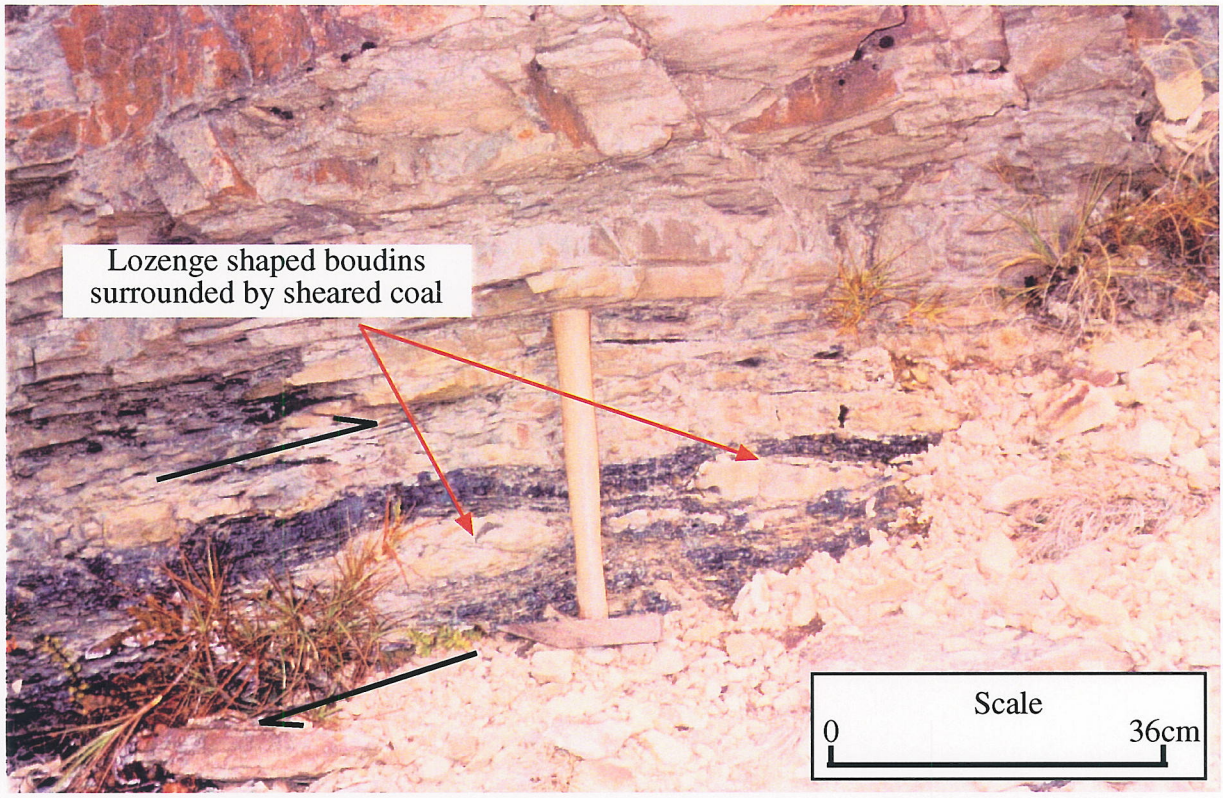

Figure 6.3 Flexure caused by the folding has been taken up along the weak layers in the Beaumont Fomation such as this coal layer (G.R. 2121190 5503030).

6.2.2 NORTHEAST-SOUTHWEST STRIKING FAULTS

In the west and north of the field area a number of faults striking 030°–065° cut the Waiau Group sediments (figure 6.1; appendix H). These faults have vertical displacements of a few hundred metres up to an unknown but probably kilometre scale vertical displacement, juxtaposing the Weydon and Haycocks Formations, and tilting the Haycocks Formation to approximately 80° (appendix H). No estimate of any strike-slip movement that has occurred can be made due to the lack of good offset markers. These faults are all parallel to the Mararoa Fault that runs along the west side of the Mararoa River (Harrington, 1982), suggesting that the smaller northeast-southwest striking faults in the study area are on the edge or part of the Moonlight Fault System.

The topographic expression of the faults suggests that they are very steeply dipping. Seismic profiles of the Te Anau Basin that cut the edge of the study area show steeply dipping faults that dip to the east and the west (Turnbull, Uruski et al, 1993). Offset of the faults shown in the seismic profile is normal, although the oldest units identified are Oligocene and the faults don't reach the surface (Turnbull, Uruski et al, 1993). Actual movement on these faults has probably been similar to that of the Moonlight Fault System with the faults being formed as normal faults, and changing to high angle reverse faults, although no evidence for this is seen in the study area. These faults were most active in the late Miocene and possibly more recently as shown by the steeply dipping Prospect Formation on the west of the Mararoa River (Harrington, 1982). Some movement is still occurring along these faults to the southwest of the area, as shown by offsets in Pleistocene sediments (Carter and Norris, 1977b; Hall, 1989).

6.2.3 NORTHWEST-SOUTHEAST STRIKING FAULTS

A small number of faults striking 115°-135° occur throughout the study area (figure 6.1). These faults tend to be short, dying out within 5-6 kilometres to the east of the Mararoa River Quaternary alluvium, cutting all units except for the Haycocks Formation. All these faults exhibit a dextral separation of units and structures that occur across them. The fact that these faults are linear features that crosscut topography indicates that they are close to vertical.

6.2.4 FAULT DISCUSSION

The faults that are present in the study area are generally oblique high angle reverse faults, most likely related to the Moonlight Fault System. The orientations of the faults contradict the general rules of Andersonian faulting (Anderson, 1905) due to the fact that they have been reactivated as high angle reverse faults rather than Andersonian thrusts.

The north-south striking faults are not only steeply dipping, they also formed at an oblique angle to the nearby Moonlight Fault System. These faults are most likely reactivated structures formed during the Cretaceous terrane accretion, supported by an orientation similar to the axis of the Southland Syncline and the terrane boundary. Reactivation of these structures has since occurred due to them being weak discontinuities in the Murihiku Terrane basement. The northeast-southwest striking structures have the same orientation as the main Moonlight Fault System. They are much steeper than the predicted orientation of reverse faults in the Andersonian model (Anderson, 1905), possibly due to their formation as normal faults, followed by their reactivation as planes of weakness within stronger rock. The northwest-southeast striking faults are also probably reactivated structures. The discontinuous nature of these structures, the spatial relationships between them and the other two sets of faults in the area, and their apparently high angle to the stress field (almost perpendicular to the Moonlight Fault System), suggests that they may link north-south striking faults to the northeast-southwest striking faults.

6.3 FOLD DESCRIPTIONS

There are a number of folds in the study area, ranging in size from small drag folds on the edges of faults to the regional Southland Syncline. This section describes the folds that have been mapped in the area with wavelengths of hundreds of meters to kilometres.

6.3.1 SOUTHLAND SYNCLINE

As the regional significance of the Southland Syncline is explained at the start of this chapter, this section describes in detail the structure as seen in the study area. The axis of the Southland Syncline runs between Centre Hill and Mount Hamilton in the southeast part of the

study area. The axial line of the fold trends 160° and is horizontal, the fold is asymmetrical, with a steeper eastern limb (figures 6.4 and 6.5).

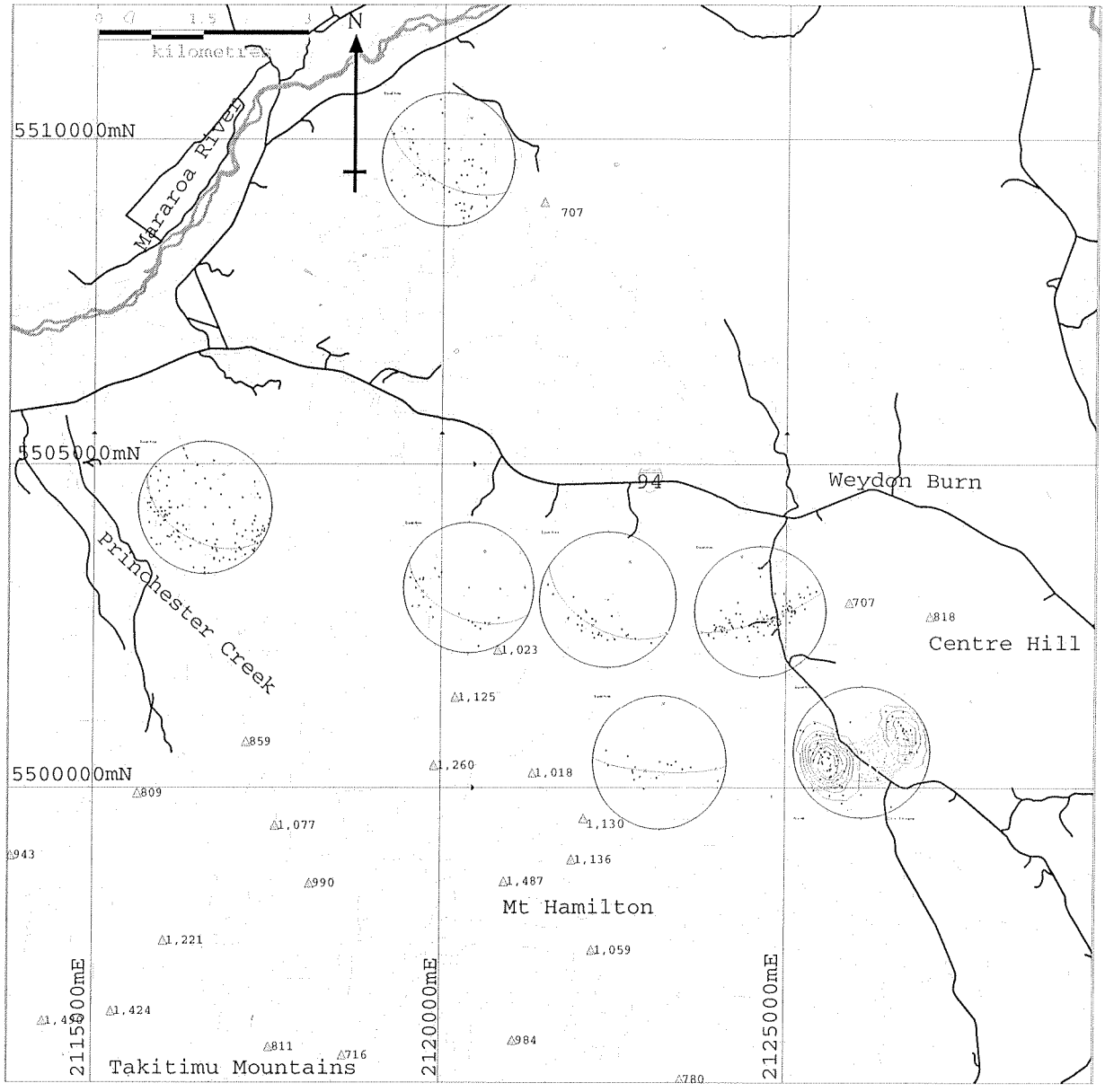

Figure 6.4 Stereonets from different parts of the study area showing bedding measurements of Tertiary sediments, with a best-fit great circle and associated pi pole. These show that the sediments are folded with the axis of these folds sub-parallel to the Southland Syncline in the east, and becoming sub-parallel to the Moonlight Fault System in the west. Also shown is the contour plot from figure 6.5 near the middle of the Southland Syncline.

The timing of the folding can be constrained by measuring the unconformity between the Murihiku rocks and the Tertiary sediments. Figure 6.5 shows bedding measurements from the Murihiku rocks plotted alongside the Tertiary sediments from the area between the limbs

of the syncline. This figure shows that if the bedding is unfolded until the unconformity is horizontal, the Murihiku rocks are sub-horizontal on the west limb but dip 40° on the east limb of the Southland Syncline. This indicates that west limb of the Southland Syncline was flat lying until the late Miocene, while the east limb dipped at a much shallower angle than it does at present, similar to its orientation south of the study area (e.g Boles, 1974). The Southland Syncline has been tightened as the overlying sediments have been folded, probably during the late Miocene as the deformation has also tilted the late Miocene Prospect Formation north of the area (Harrington, 1982; Manville, 1994) (figure 6.5).

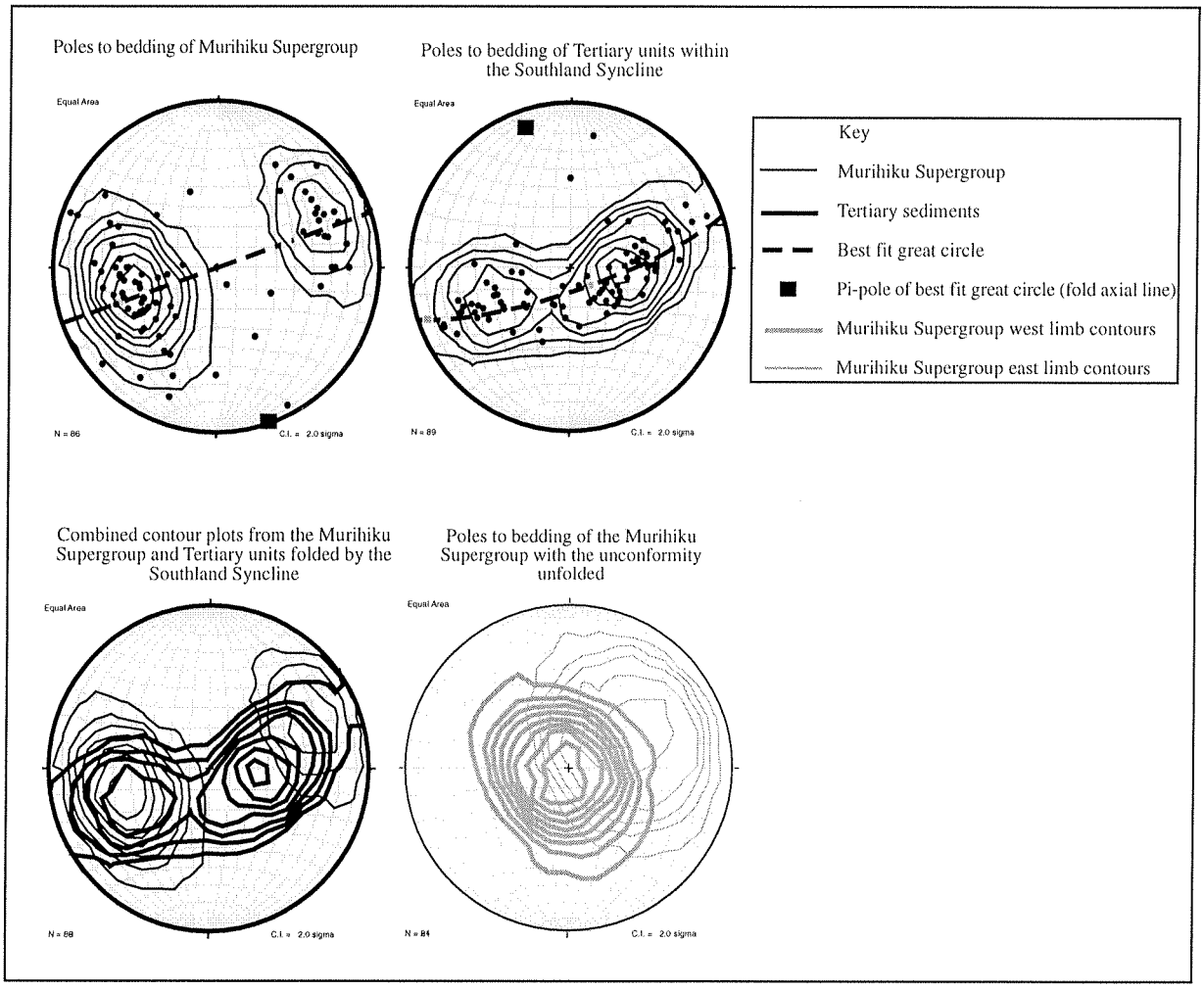

Figure 6.5 Stereonets showing strike and dip measurements from the Murihiku Supergroup (top left), with the pi pole to a best fit great circle indicating that the axis of the syncline in the area is close to horizontal on a trend of approximately 160°. The plot on the top right has data from the Tertiary sediments between the limbs of the Southland Syncline, showing that they also form a shallow plunging syncline along the same trend as the Southland Syncline. The combined data (bottom left) and the Murihiku Supergroup bedding with the unconformity unfolded (bottom right) show that if the unconformity was unfolded the dip of Murihiku Supergroup would be 0° on the west limb and 40° on the east limb.

6.3.2 TERTIARY FOLDING

All of the Tertiary units in the area (as well as the Murihiku basement discussed above) have been folded during the later part of the Tertiary some time after the deposition of the Haycocks Formation (figure 6.1). Plotting the large data set of bedding measurements on stereonets has allowed analysis of the folds in the study area (appendix F). In order to make sense of the data, the area was divided up into segments for which the data was plotted on a stereonet, as shown in figure 6.4.

Figure 6.4 shows that in the east the folds are generally more cylindrical than in the west of the area where the stereonet plots show more scatter. The orientation of the fold axis also changes across the study area. The trends of the fold axis go from north-northeast in the southeast of the area to northeast in the west (figure 6.1). In the east they plunge shallowly to the north-northwest whereas on the west side of the study area, the axes plunge more steeply in a northeasterly direction (figure 6.1).

Folding of the Beaumont Formation has been taken up by shear along weak planes such as coal seams and the unconformity (figures 6.2 and 6.3). In the upper part of the Tertiary sequence the movement is taken up along the weak mudstone planes common to these units.

6.3.3 FOLD DISCUSSION

SHEAR ASSOCIATED WITH THE MOONLIGHT FAULT SYSTEM

The change in the orientation of the folds in the area suggests that they have been influenced by transpression related to the Moonlight Fault System (figure 6.1). The trends of the fold axes have been dragged subparallel to the fault system due to dextral shear adjacent to the fault system, while they have been steepened by the reverse shear on the fault system (figures 6.1 and 6.3). There are two possible ways for this type of deformation to have occurred: (1) the folds formed in the Tertiary units as a direct result of transpressive strain across the shear zone with the axis rotating towards the fault system as they were formed, in the same way as the long axis of a strain ellipse (Sanderson and Marchini, 1984); or (2) the folds formed in the shear zone associated with basement structures and have been rotated as rigid blocks along with the basement (e.g Jamison, 1991; Jonk and Biermann, 2002).

Figure 6.1 shows that the folds to the east are at angles of more than 45° to the fault system while the western folds trend about 20° from the strike of the fault system. Folds formed by transpressional strain initiate at angles of less than 45° (Ramsay and Huber, 1983; Fossen and Tikoff, 1993; Tikoff and Peterson, 1998), this is evidence that the folds in the east have formed as a result of folding and faulting of the basement along pre-existing structures, while the folds in the west of the area may have deformed in the manner suggested by the strain ellipse concept. Using the angles between the fold axes and the Moonlight Fault System the amount of shear strain across the area could be calculated using the formula $\gamma = \cot\theta_2 - \cot\theta_1$, where θ_1 is the inital angle of the fold axis (45° in the case of simple shear) and θ_2 is the angle of the axis after shear (20° in the study area). This simple equation does not adequately describe the fold axis rotations in the study area due to the contraction that has accompanied shear (transpression) as suggested by the increasing plunge of the fold hinges (Tikoff and Peterson, 1998). Transpression causes the fold axis to rotate much faster than in a simple shear situation, therefore using the simple shear equation results in a value for shear that is too high. Also it predicts too much shortening across the folds. By measuring the shortening and the fold orientation the amount of shear can be constrained.

Figure 6.6 is a cross-section perpendicular to the fault system with the units reconstructed to their pre-folded lengths, indicating that there has been 30% shortening across the study area. To calculate the shear in the area resulting from the transpression, the method of Fossen and Tikoff (1993) was used as this method assumes simultaneous simple shear and volume change (i.e pure shear with vertical extension). On figure 6.7 the intersection of the line of 30% shortening and 20° angle from the shear zone gives a value for shear strain of 0.5. This value of shear strain equates to a dextral shear of approximately 5 km distributed across the study area, and seems consistent with the magnitude of strike-slip expected in this area.

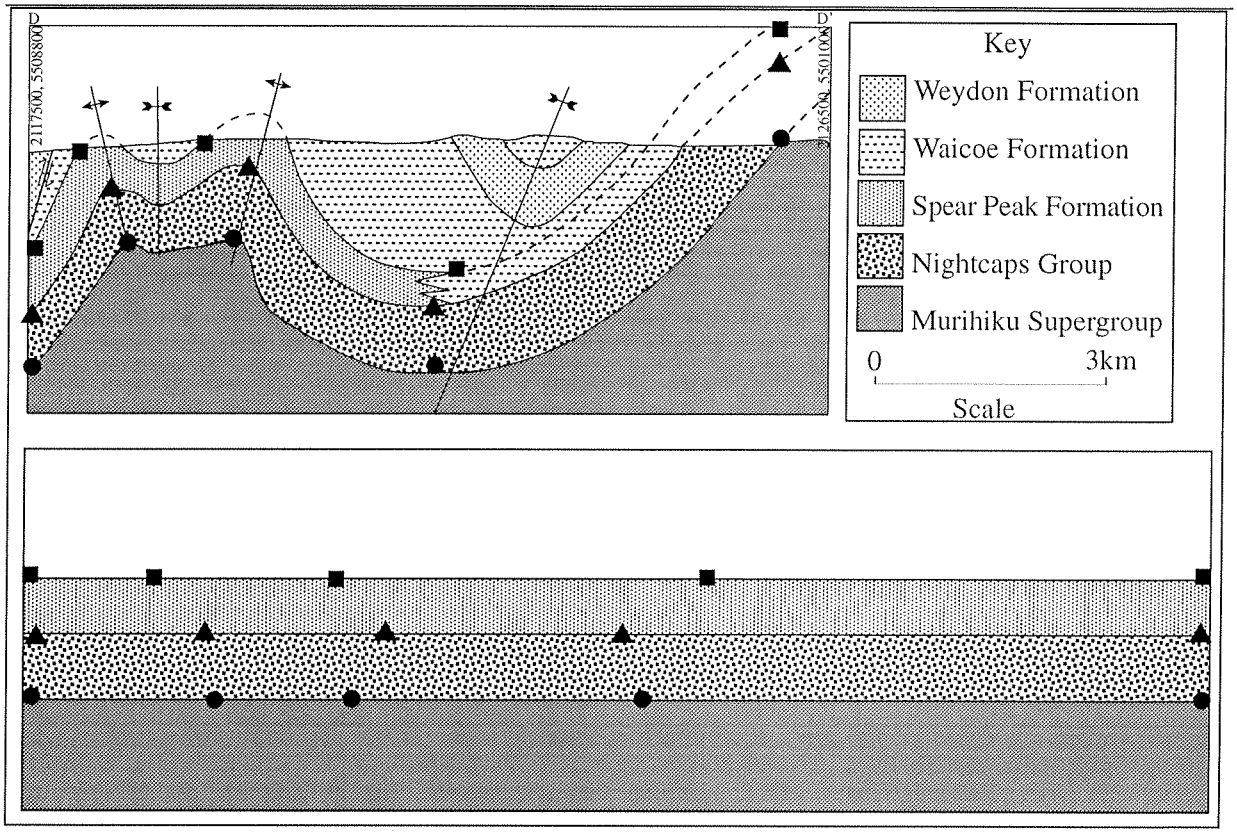

Figure 6.6 The top cross-section D-D' (see map: appendix H) is perpendicular to the Moonlight Fault System (NW-SE), the bottom section is reconstructed with the shortening component removed. This shows that there has been about 30% shortening across the study area perpendicular to the Moonlight Fault System.

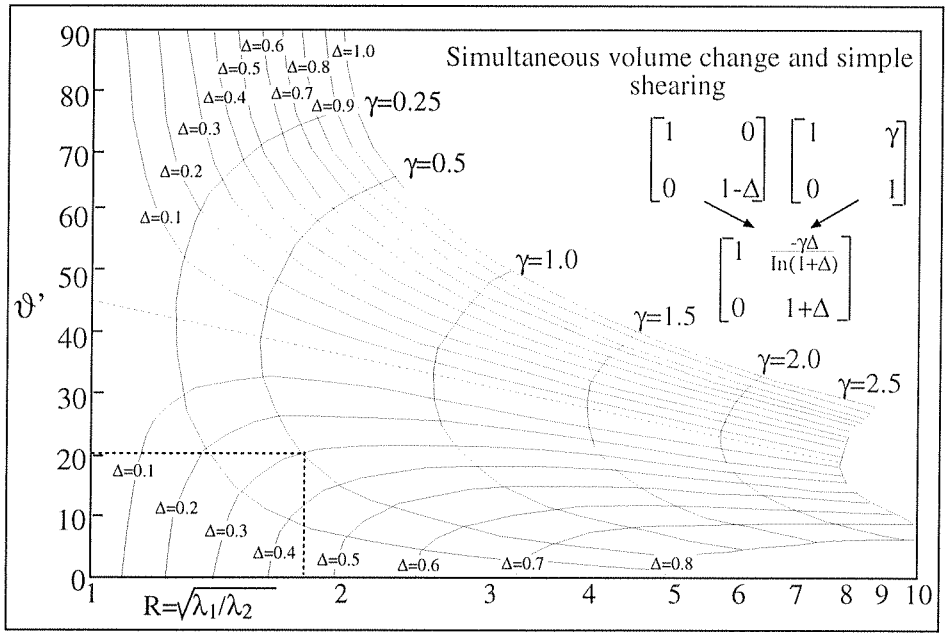

Figure 6.7 Diagram from Fossen and Tikoff (1993) showing the relationship between the angle of the long axis of the strain ellipse (θ') and the ellipticity (R) for different values of shear strain (γ) and dilation (Δ). The dotted lines shows that the shear strain in the area is 0.5, where θ' is the angle between the Moonlight Fault System and the fold axis' and Δ is approximated by the shortening in the area.

DISHARMONIC FOLDING

The relationships between the structures in the study area indicate that the basement rocks tend to be faulted while the Beaumont Formation contains both faults and small folds (figures 6.8 and 6.10). The structure in the rest of the sequence is dominated by disharmonic folding with the Spear Peak Formation tightly folded with wavelengths of about 2km, and the Waicoe and Weydon Formations broadly folded with wavelengths of up to 15km (figure 6.8). The differences in the structures throughout the vertical sequence can be explained in terms rock behaviour. The basement Murihiku rocks and to a lesser extent the Beaumont Formation, are made up of well-indurated sandstone. As it is difficult to tightly fold these rocks, they are forced to fault often along pre-existing structures in the Murihiku (6.11). Further up the sequence the sediments become more mud-rich making accommodation of folding much easier. The Orauea Mudstone dampens some of the faulting and enables space created by the folding of the Spear Peak Formation to be accommodated, made possible due to the mudstone layers within this unit (figure 6.8). The Waicoe Formation forms another layer where space created by disharmonic folding is able to be in-filled; the presence calcite veins suggesting that this has occurred (chapter 4.2). The Weydon and Waicoe Formation are quite mud-rich and have been folded without any associated faulting.

This pattern of disharmonic folding is consistent with the experiments of Williams (1980) in which a model with competent layers embedded in an incompetent host were folded at the base. It was found that if the distance between the layers is 1.5 times the wavelength of the small folds, disharmonic folding would occur, while at smaller distances the folds are harmonic (Williams, 1980). The stratigraphic sequence in the study area is similar to the model in that it has a number of competent sandstone-rich layers in an incompetent mudstone unit (Waicoe Formation). The Beaumont and Spear Peak Formations are less than the wavelength of the small folds (about 1000m) from the basement, so they deform in harmony with the it, while the Weydon Formation is approximately 1500m from the basement and deforms in a disharmonic manner with respect to the underlying units and basement.

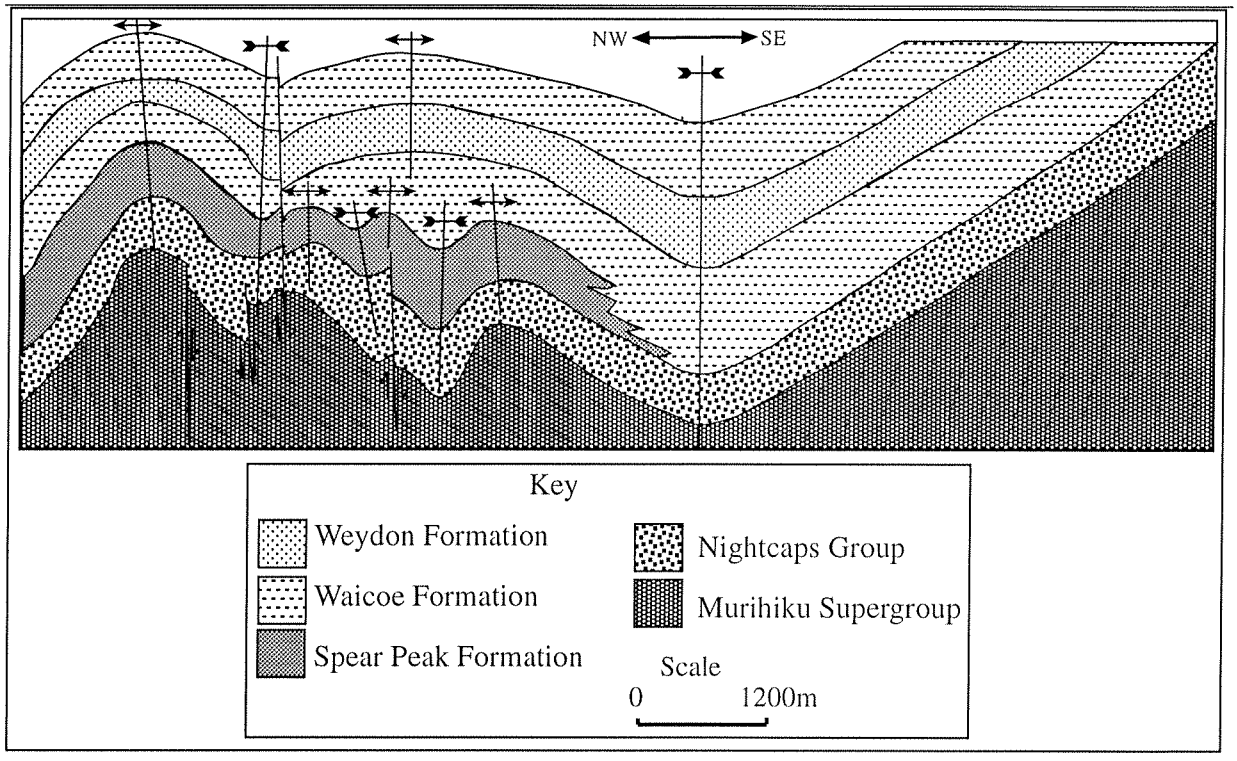

Figure 6.8 Idealised cross-section created by stacking cross-sections from different parts of the sequence. It shows that the basement rocks are folded into the large Southland Syncline but apart from this the deformation has been caused by faulting, the Tertiary sequence shows disharmonic folding.

Another example of disharmonic folding is described by Searle (1994) in the southeastern Palmyride fold belt, Syria. The stratigraphy and structure in this area has many similarities to that of this study. The stratigraphy consists of Triassic and Jurassic gypsum (equivalent to the Beaumont and Spear Peak Formations) that form tightly folded cores of the broader overlying folds (Searle, 1994) (figure 6.9) Upper Cretaceous limestone and sandstone overlain by Tertiary marl with occasional chert and limestone layers, form the broader parts of the folds (equivalent to the Waicoe and Weydon Formations) (Searle, 1994) (figure 6.9). The area has later undergone dextral transpression resulting in the formation of the folds and other structures similar to those described here (Searle, 1994). Comparing figures 6.8 and 6.9 shows similarities between the disharmonic folding in the two areas, although the example of Searle (1994) shows a much more tightly folded core than that seen in this study.

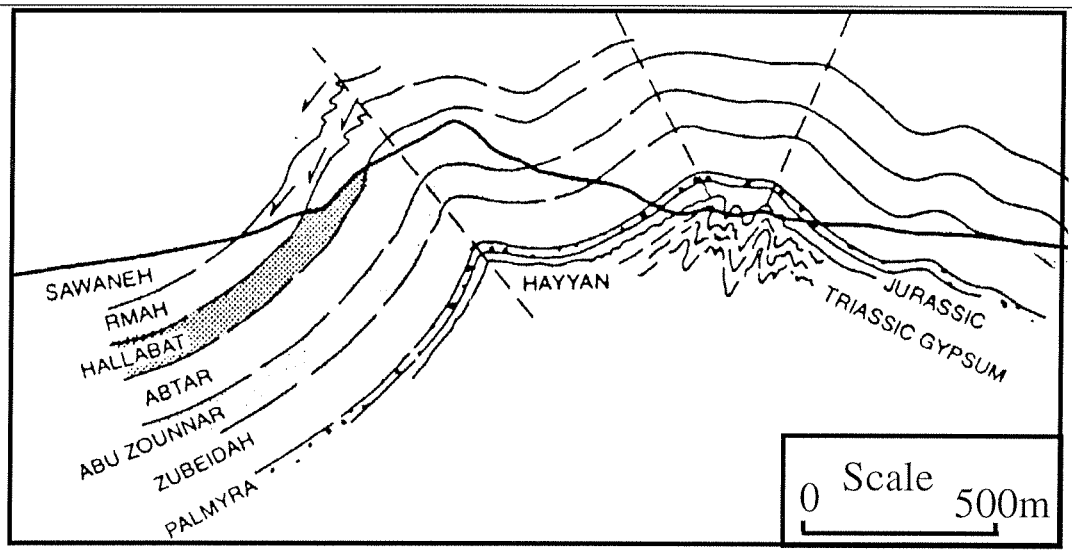

Figure 6.9 Cross-section B-B' from Searle (1994) showing disharmonic folding, the Triassic-Jurassic units form tightly folded cores of broader folds. The units that overlie the tightly folded core consist of interbedded competent rocks such as limestone and incompetent marls.

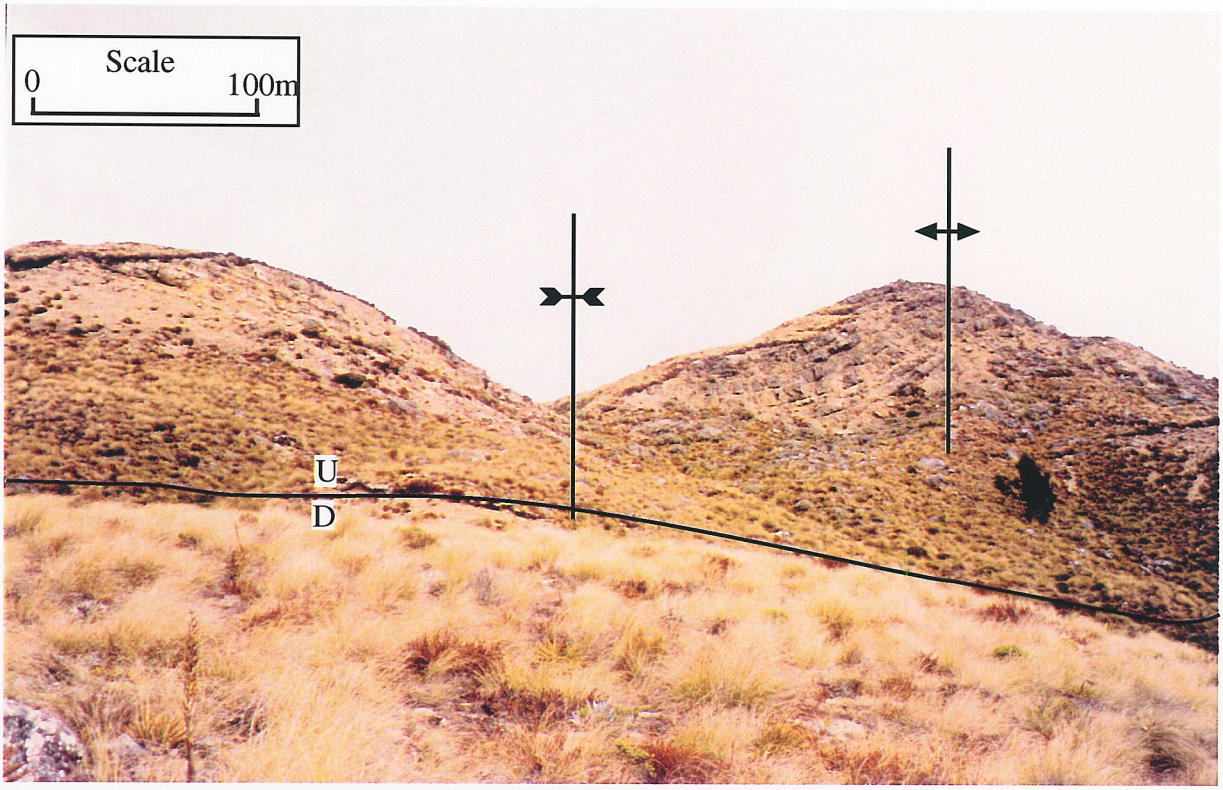

Figure 6.10 Beaumont Formation folded into a syncline-anticline pair looking southeast from G.R. 2120200 5502200 in response to the fault in the foregroundwhich has uplifted the Beaumont formation over the Murihiku Supergroup.

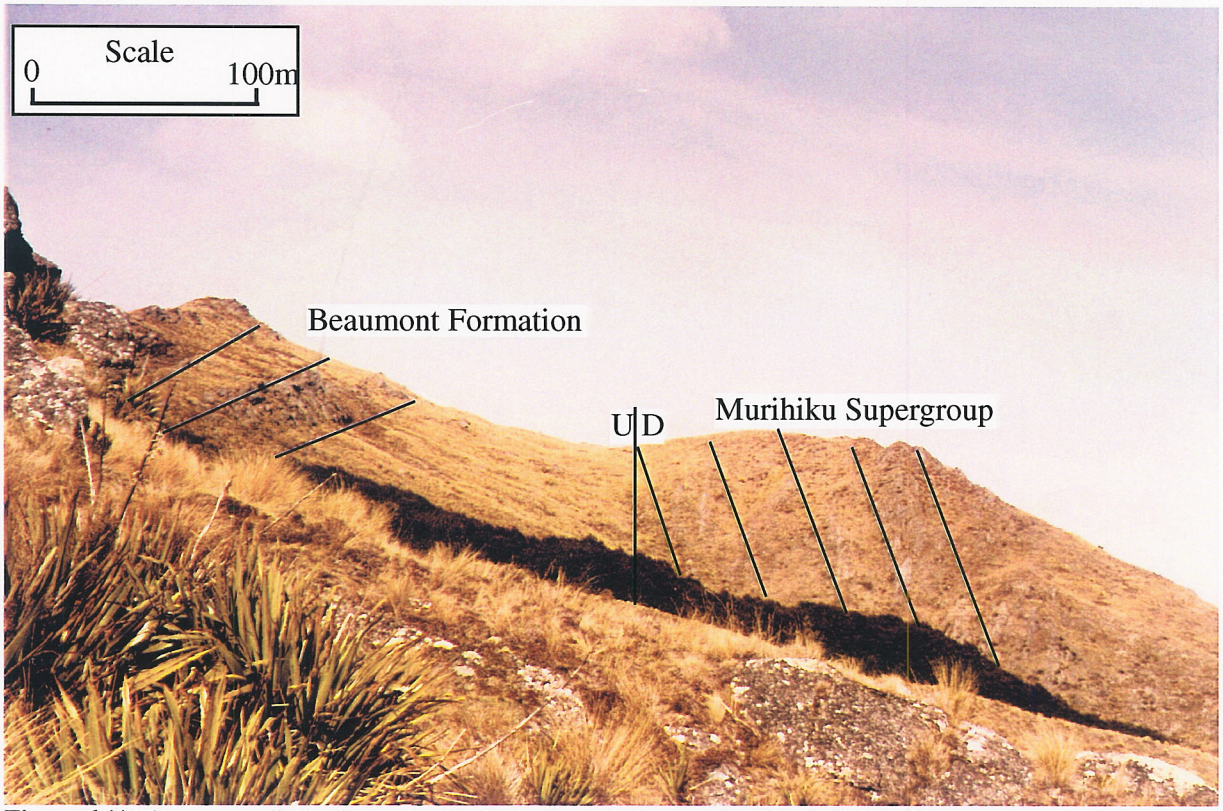

Figure 6.11 The western limb of the syncline looking north from G.R. 2121500 5501300. The Beaumont Formation has been folded in this area while the Murhiku Supergroup has been faulted below it. The black lines show the differences in the dips of the different units.

6.4 STRUCTURE CONCLUSIONS

Despite the major effect of the Moonlight Fault System in the study area, relict basement structures such as the Southland Syncline and faults associated with terrane accretion, have been reactivated in the late Tertiary. These structures are dominant in the south and east of the study area, while the Moonlight Fault System structures are most abundant in the west. Analysis of the fold axes and overall shortening in the study area shows that there is about 5km of dextral shear dispersed throughout the area that is related to the Moonlight Fault System and about 30% shortening normal to the fault system. Estimates of the amount of displacement across the Moonlight Fault System, made by measuring the offset of the Dun Mountain Ophiolite belt substantially underestimate the displacement. This is due to the amount of movement that is occurring as shear adjacent to the fault system. The shear indicates that this fault system is a major structure in the area that affects all the units including the basement, and that it has undergone dextral reverse movement on it in this area.

The different lithologies that form the stratigraphic sequence in the study area have resulted in the folds being disharmonic, with the rigid basement rocks and some of the Beaumont Formation being faulted. In the overlying Weydon and Waicoe Formations broader folds occur above the more tightly folded Spear Peak Formation (figure 6.8)

The data clearly show that, during the time of Tertiary sediment deposition, the Southland Syncline had a flat western limb and a moderately dipping east limb, rather like the syncline further to the east in central Southland. Steepening of the west limb occurred following deposition of the Tertiary sediments and appears associated with shear and rotation across the Moonlight Fault System. All the structures parallel to the Dun Mountain Ophiolite Belt are rotated into a north-south orientation across this zone, as part of the regional bending of the South Island terranes adjacent to the Alpine Fault (Norris, 1979; Sutherland, 1999). The data from the study area clearly show that this bending was a late Cenozoic occurrence.

7 GEOLOGICAL HISTORY AND PALAEOGEOGRAPHY

7.1 INTRODUCTION

Combining all the information collected during the study enables a geological history of the study area to be constructed, and also gives an idea of the changes in the geography of the area. This chapter discusses in chronological order the structural and sedimentary changes that have occurred in the study area over time. The geological history of the area is split into two sections: Mesozoic and Tertiary. During the Mesozoic a multiple of geological processes formed and deformed the Murihiku Terrane. Due to the regional extent of the Murihiku Terrane, information from the literature has been used to provide a regional, geological and geographic context in which to interpret observations from the study area. The second section in this chapter discusses the Tertiary geology of the area. Much of the information in this section can be found in the study area, and this is the main focus of the chapter.

7.2 MESOZOIC GEOLOGICAL EVENTS

7.2.1 TRIASSIC-MIDDLE JURASSIC

Throughout the Triassic-Jurassic most of the Murihiku Supergroup basement rocks were deposited in a fore-arc basin (Campbell and Coombs, 1966), with minor deposition during the late Permian-early Cretaceous (Roser et al, 2002), fed by volcanic material from an arc near the Gondwanaland margin (Balance and Campbell, 1993). As the arc was still active, juvenile ash was deposited intermittently over the basin (chapter 2), and most of the volcanic material eroded from the onshore part of the arc was resedimented in the deep-water basin (chapter 2). The arc that fed the basin was dominantly andesitic and parts of it were dissected, resulting in granitic material being exposed (chapter 2). Rivers feeding the basin were large enough to carry boulder-sized material that was subsequently redeposited by mass flows into the marine basin, shown by facies A sediments (chapter 2). Most of the sediment that is seen in the study area has been reworked by contour parallel currents, with minor amounts of turbidite deposited sediment still preserved (chapter 2).

7.2.2 MIDDLE JURASSIC-LATE CRETACEOUS

Between the mid-Jurassic and the late-Cretaceous the Murihiku and the Brook Street Terranes were thrust together during accretion at the active margin of the Gondwanaland super continent (Coombs et al, 1976; Bishop et al, 1985; Landis et al, 1999). This caused the Murihiku Terrane to be folded into the broad Southland Syncline, and the Takitimu Group was tilted, almost vertically (Coombs et al, 1976; Houghton, 1981; Landis et al, 1999). During this time similar sediments were deposited on both terranes suggesting that they were joined, or at least close to each other (Landis et al, 1999).

By the late Cretaceous most of the terrane accretion had ceased and the basement rocks of New Zealand were in place (Coombs et al, 1976; Bishop et al, 1985; Landis et al, 1999). In the late Cretaceous western Southland underwent a period of extension, and an erosion surface was cut across the Murihiku Terrane during this period (Norris and Carter, 1980), as a result no sediments from this era are preserved in the study area. However non-marine sediments are preserved in western Southland at Ohai (Bowen, 1964; Sykes, 1988; Turnbull, Uruski et al, 1993) and Puysegur Point (Turnbull, Uruski et al, 1993).

7.3 TERTIARY GEOLOGICAL EVENTS

7.3.1 PALAEOCENE

The erosion that began in the Cretaceous continued on into the Palaeocene as shown by the lack of sediment in the area, and little or no deformation occurred with west limb of the Southland Syncline remaining sub-horizontal in the Eocene (chapter 6).

7.3.2 EOCENE

The period of erosion continued in the study area until the late Eocene (Kaiatan) when a large braided river system that flowed from the southwest, draining a basement high that separated the Te Anau and Waiau Basins entered the area, depositing the Beaumont Formation (chapter, 3.1; figure 7.1). The Beaumont Formation shows that there were two main sedimentary environments associated with the fluvial system: a river dominated environment that included conglomerate and sandstone; and a swamp or backswamp environment composed of

mudstone and coal seams (chapter 3.1). Flora were present on the river plain, as indicated by the presence of leaf imprints in the sandstone (chapter 3.1).

During the latest Eocene (Runangan) the river that deposited the Beaumont Formation was replaced by the Orauea Lake, due to continued extension in the area creating a topographically low area on the eastern side of the Te Anau and Waiau Basins (Turnbull, Uruski et al, 1993). The Orauea Mudstone was deposited in Lake Orauea by settling of mud and carbonaceous material (chapter 3.2).

River and lake systems were controlled by the formation of the Te Anau Basin due to the northward propagating extensional zone, where northeast-southwest striking faults ruptured as normal faults related to the Moonlight Fault System (Turnbull et al, 1975; Carter and Norris, 1976; Norris and Turnbull, 1993). This tectonic activity uplifted parts of Median Tectonic Zone, as shown by the detritus present in some of the sediments. Tectonic activity also generated the uplift of some of the Takitimu Group causing it to be deposited in the Beaumont Formation. Apart from the Takitimu Group component of the Beaumont Formation no evidence of syn-sedimentary deformation is seen in the area, indicating that it either didn't occur, or that it is not recognisable due to later deformation.

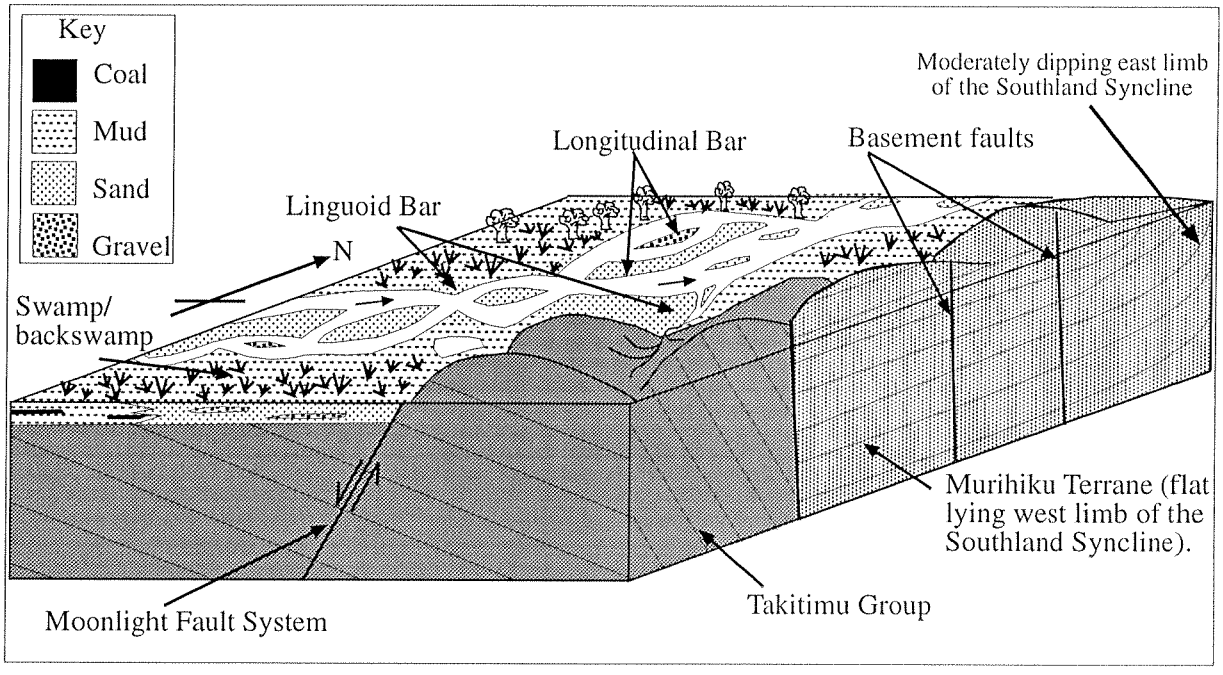

Figure 7.1 Cartoon reconstruction of the study area during the mid-Eocene, showing the braided river system that deposited the Beaumont Formation flowed from the southwest carrying Fiordland derived material. Sediment is also derived from the slightly uplifted Takitimu block to the southeast. In areas away from the actual river, swamp and backswamp environments prevail with some vegetation growing in these areas.

7.3.3 OLIGOCENE

Most of the sediment exposed in the study area accumulated during the Oligocene-Miocene due to transtensional tectonics and associated marine transgression. The large amount of sediment that has accumulated seems unusual considering that this side of the Moonlight Fault System was uplifted relative to the main Te Anau Basin at the time, this subsidence was probably due to reactivation of older faults in the basement rocks now exposed in the Takitimu Mountains. In the study area these faults combined with the Moonlight Fault System to form the basin margin. As the main zone of extension moved north the source of the sediment also moved north as shown by the change in the provenance of the sediment in the units in the study area (chapters 3 and 4).

EARLY OLIGOCENE (EARLY WHAINGAROAN)

Continuing propagation of the extensional zone resulted in further subsidence of the Te Anau Basin, and a marine transgression swept over the area (Carter and Norris, 1976; Norris and Carter, 1980; Norris and Turnbull, 1993). Tectonic activity resulted in the rapid uplift of the Takitimu Group and the associated Murihiku Supergroup. Sediment eroded from these uplifted units was deposited as a number of small submarine fans that form the Spear Peak Formation (chapter 4.1). Conglomerate and breccia in the Spear Peak Formation indicate that the fans formed close to the source (chapter 4.1; figure 7.2). Gravel-rich proximal fans and ramps are indicative of rapid uplift that may exceed 250m/m.y (Heller and Dickinson, 1985; Mutti, 1985). The Spear Peak Formation shows a fining upward sequence that is typical of submarine fans, and shows that the source of the sediment was becoming more distal with time, due either to a slowing in the rate of uplift of a more rapid marine transgression (chapter 4.1).

Sedimentology of the Spear Peak Formation shows that the area to the south-east of the study area was rapidly uplifted at this time (chapter 4.1). The only major fault that has been recognised in the study area to the south-east of the outcrops of Spear Peak Formation is the terrane boundary fault between the Murihiku Terrane and the Takitimu Group, which has infaulted some tertiary sediments, other structures parallel to this are present throughout the area (appendix H; chapter 6). The Moonlight Fault System is to the west of the uplifted area

but distributed strain across an area to the east of the fault system could have reactivated a number of the faults formed during terrane accretion (north-south striking faults).

Deposition of the Spear Peak Formation was relatively short lived and by the middle of the Whaingaroan, the continued marine transgression resulted in the Waicoe Formation mudstone covering the entire study area. This indicates that the topography in the Takitimu Group associated with the Spear Peak Formation was submerged and the basin was starved of sediment leading to the deposition of the hemi-pelagic mudstone. Foraminifera from the Waicoe Formation indicate that the depth of the basin at this time was about 200-400 m (upper bathyal).

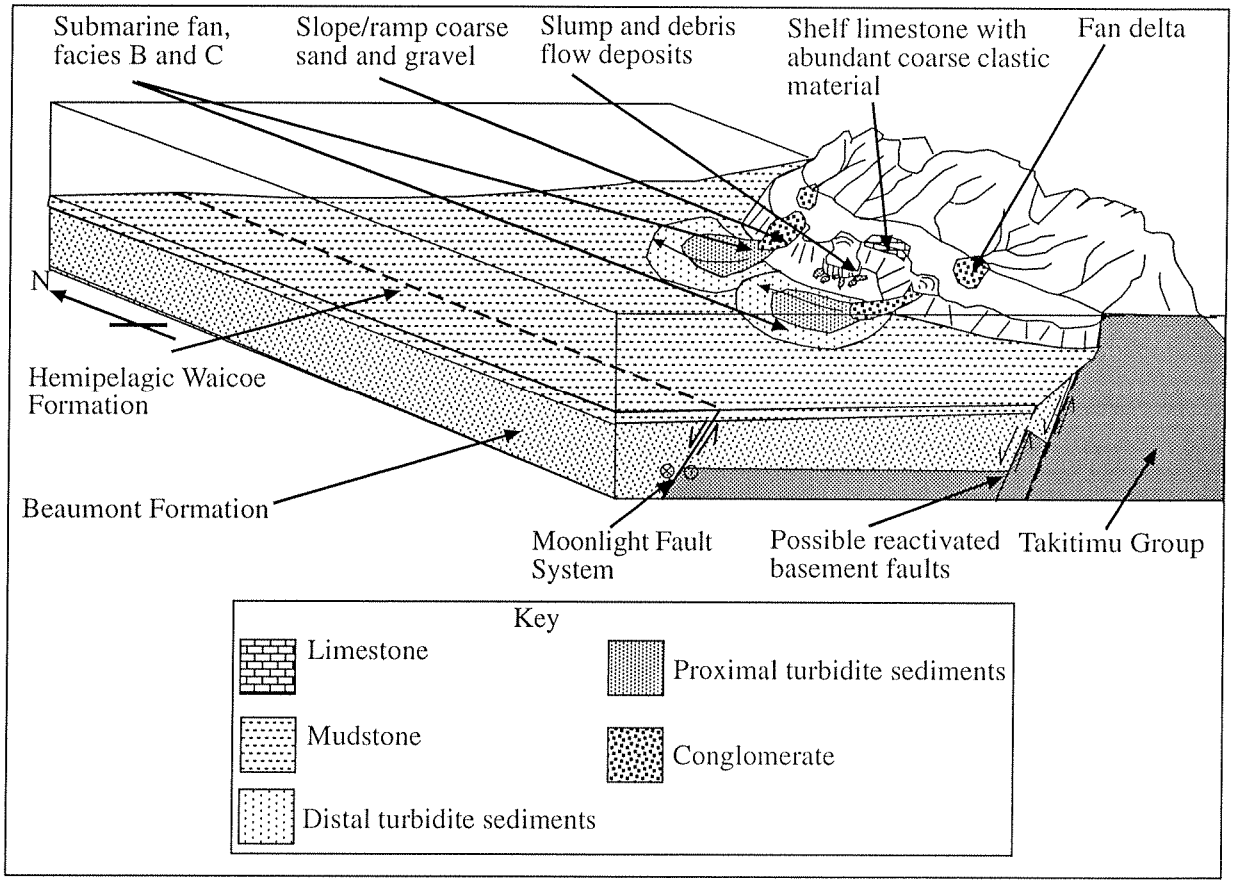

Figure 7.2 Cartoon reconstruction of the study area during the early Oligocene showing the uplifted Takitimu Group and Murihiku Supergroup in the east feeding a number of small, coarse, submarine fans that make up the Spear Peak Formation with hemi-pelagic mudstone of the Waicoe Formation deposited outside of these fans. The uplifted area is to the east of the Moonlight Fault System.

MIDDLE-LATE OLIGOCENE (LATE WHAINGAROAN-DUNTROONIAN)

Uplift of the Caples Terrane and associated schist to the north of the study area began at this time. Shelf sediments and fossils recognised near Lake Wakatipu give evidence for a shelf environment fringing the uplifted area (Turnbull et al, 1975). In the study area the distal turbidites of the Weydon Formation are derived from the shelf (shown by the shell fragments, reworked glaucony and Caples detritus) that was present in the north (chapter 4.3; figure 7.3). Sandstone rich facies in the Weydon Formation were deposited in about four pulses of turbidite deposition in an outer fan, separated by hemi-pelagic mud deposition (chapter 4.3). The fan consisted of one major lobe deposited as a number sheets with no major feeder channels (chapter 4.3).

Continuation of the early Oligocene transtension resulted in the tectonic regime that formed a marine basin in the late Whaingaroan. The presence of Caples detritus in the Weydon Formation suggests that an area to the north had been uplifted at the tip of the propagating transtensional zone, while in the study area subsidence was occurring, forming a depression within the transtensional zone. The depression in the study area lead to a water depth of 150-200 m (outer shelf).

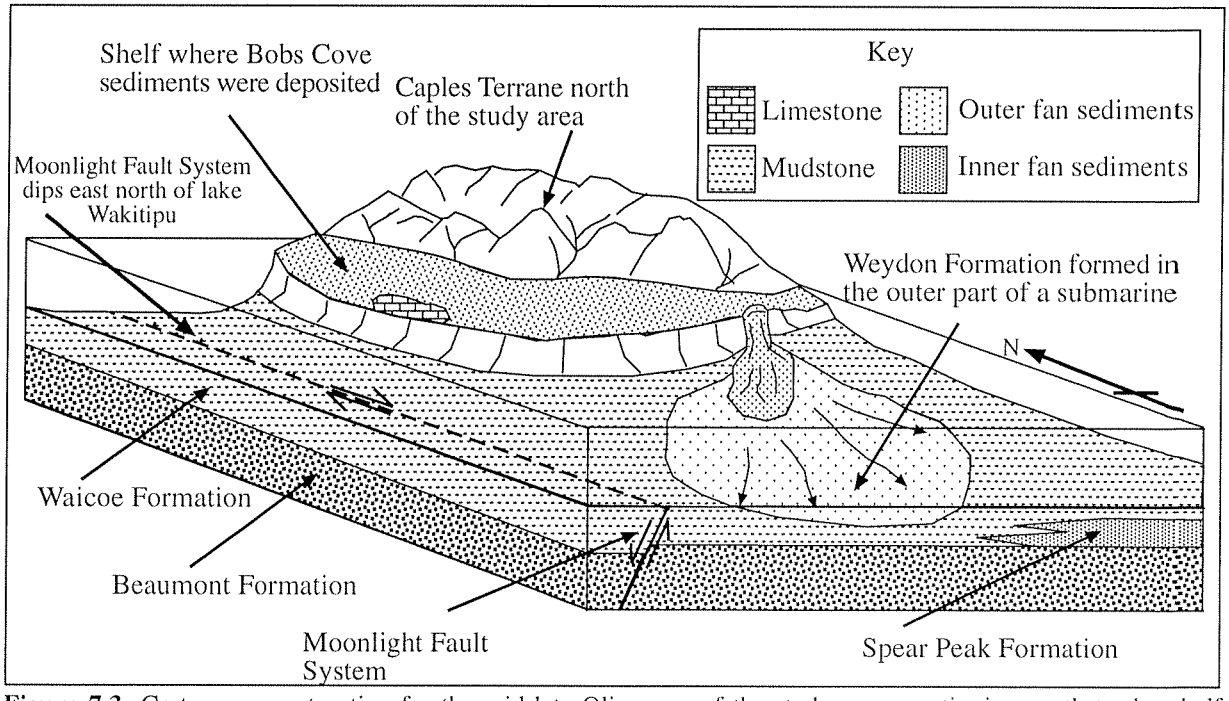

Figure 7.3 Cartoon reconstruction for the mid-late Oligocene of the study area, continuing north to the shelf described in Turnbull et al (1975) and Central Otago. The uplifted Caples Terrane supplies the sediment to the shelf from where it is redeposited by a small submarine fan into the study area as the Weydon Formation.

The last part of the Oligocene is the Duntroonian stage, when the basin again became starved of sediment and the hemi-pelagic mud of the Waicoe Formation was able to be deposited.

7.3.4 MIOCENE

EARLY-MIDDLE MIOCENE (WAITAKIAN-OTAIAN)

The early part of the Miocene resulted in the transtensional tectonic regime of the Oligocene being replaced by transpression on the Moonlight Fault System and Alpine Fault (Turnbull, Uruski et al, 1993). This resulted in a second phase of uplift of Caples Terrane sediments to the north of the study area on the Moonlight and Hollyford Fault Systems (Norris and Carter, 1982). Sediment that was eroded from this uplifted area was deposited in a number of fans in western Southland (e.g Carter and Norris, 1977a), with Haycocks Formation deposited in the study area (chapter 4.4). The Haycocks Formation formed as a large outer fan, mainly as sheets of sand deposited on the basin plain unconfined by channels (chapter 4.4). The Haycocks Formation thins and fines upward back into the Waicoe Formation mudstone due to decreases in sediment supply (chapter 4.4).

Despite the change in tectonic regime subsidence continued in the study area is evident from a water depth of approximately 200 m, yet large amounts (up to 2500 m) of sediment were able to accumulate (chapter 4.4).

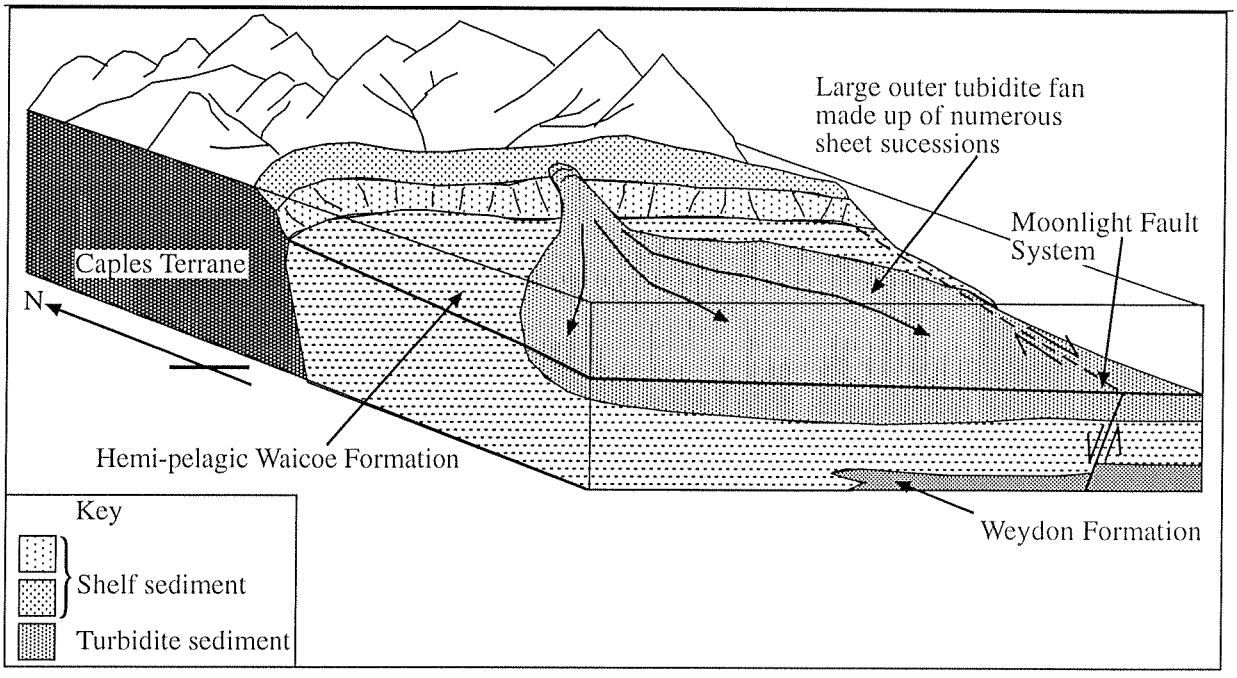

Figure 7.4 Cartoon reconstruction of the study area and Central Otago during the early Miocene. The Caples Terrane is uplifted in the north, forming the source for the Haycocks Formation sediment into the basin.

LATE MIOCENE-PLIOCENE

The late Miocene was a time of substantial change in the tectonic regime of the South Island of New Zealand, generating a change in the environment and type of sedimentation. At the beginning of the late Miocene (c. 11-12 Ma) the slip rate on the Alpine Fault increased and subduction beneath Fiordland was initiated, and toward the end of the late Miocene (6.4 Ma) the Alpine Fault changed from a completely strike-slip fault to one with a considerable convergent component (Norris and Carter, 1980; 1982; Sutherland, 1995; Walcott, 1998). These changes lead to major uplift across most of the South Island, and as a result marine transgression ceased and regression began. In the study area this phase resulted in the inception of a major river system that flowed from the Caples Terrane in the north. This river and fan-delta system deposited large quantities of conglomerate across the Te Anau Basin known as the Prospect Formation (Manville, 1994).

At this time the motion on the Moonlight Fault System changed to oblique compression causing most of the faults in the system to become high angle reverse faults (Norris and Carter, 1980; 1982). This stage of accelerated deformation is when many of the structures, such as the folds and reverse faults were most active, although they may have begun to form

prior to this (chapter 6). Deformation in the area caused uplift and erosion of all of the units in the basin.

LATE PLIOCENE

In the late Pliocene, activity on the Moonlight Fault System and associated structures continued, uplifting and tilting all of the rocks in the study area. Shear associated with this deformation, combined with the bending of the terranes also resulted in folding of all the Tertiary units. Uplift has resulted in the removal of the Prospect Formation from the study area and tilted it where it is present to the west (Manville, 1994). In the zone of faults near the Moonlight Fault System the Tertiary units are faulted into slivers between different fault strands.

7. 4 QUATERNARY

In the Pleistocene much of the Te Anau Basin was eroded by glaciers, stripping off most of the Prospect Formation, and depositing large volumes of outwash gravel (McKellar, 1973). The glacial outwash gravels present in the study area pre-date the last glaciation (McKellar, 1973). Prospect Formation is no longer present here, but there is little evidence for glacial activity. Instead it is likely that fluvial and mass flow processes were responsible for most of the erosion in the area. Old talus surfaces are common features along the edge of the Takitimu Mountains and Centre Hill. The raised terrace that is present in the north of the study area was formed at this time with outwash gravel from glaciers further north being deposited in this area (appendix H). Since the deposition of the glacial outwash gravels, the Mararoa River has cut down through the rocks in the area along the Moonlight Fault System and still drains areas to the north.

Undeformed fan deposits and outwash gravels, coupled with a lack of recent fault traces, shows that the amount of deformation has decreased during the Quaternary. It has not ceased entirely however, as a fault trace south of the study area (Carter and Norris, 1977b; Hall, 1989) cuts glacial outwash gravel, indicating that deformation continues still.

8 SUMMARY AND CONCLUSIONS

8.1 SEDIMENTOLOGY OF THE BURWOOD SUB-BASIN

8.1.1 DEPOSITIONAL ENVIRONMENTS AND PROCESSES

Sedimentary facies within the study area show that a range of different sedimentary environments developed in response to changes in the tectonic environment. Non-marine environments include a gravel-rich braided river that deposited the Beaumont Formation, flowing northeast through a swamp area with plants and ponds (chapter 3.1), and lake that covered most of western Southland (Turnbull, Uruski et al, 1993), in which the Orauea Mudstone was deposited (chapter 3.2). Many of the sediments in the study area were deposited in a dominantly deep-water marine environment, with four main deep-water depositional processes represented in the area: debris flows, turbidity currents, bottom currents and hemi-pelagic settling. Small submarine fans built up by deposition from mainly debris flows and minor turbidity currents are seen in the Spear Peak Formation (chapter 4.1). The outer parts of two sandy, turbidite-dominated submarine fans are seen in the Weydon Formation (chapter 4.3) and Haycocks Formation (section 4.4). Hemi-pelagic mudstone was deposited in the basin at times when there was low sedimentation, forming the Waicoe Formation (chapter 4.2).

8.1.2 PROVENANCE OF THE SEDIMENTS

Provenance of the sediments in the study area has changed over time in response to the changing tectonic conditions in the western Southland area. The late Eocene Beaumont Formation has a mixed provenance of distal Median Tectonic Zone material (from the basement high of Zink (2000) or from Fiordland) and local Takitimu Group and Murihiku Supergroup detritus (chapter 3.1). The early Oligocene Spear Peak Formation is derived from the local Takitimu Group and Murihiku Supergroup material (chapter 4.1). The Weydon Formation (chapter 4.3) and Haycocks Formation (chapter 4.4) contain sediment derived from the Caples Terrane to the north of the study area.

8.1.3 UPLIFT AND SEDIMENTATION RATES

Work done during this study has not improved on the sedimentation rate plots given in Turnbull, Uruski et al (1993) (figure 8.1.1) due to the low resolution dating systems used. Submarine fans such as those in the study area have built up faster than dating with microfossils can resolve. A qualitative interpretation of the sedimentation rate would show three peaks relating to the three submarine fans in the area, with associated dips representing the periods of limited sediment input in the basin when the Waicoe Formation was deposited. Unfortunately a lack of outcrop in the area, especially within the Waicoe Formation, makes constraining the age of the units difficult.

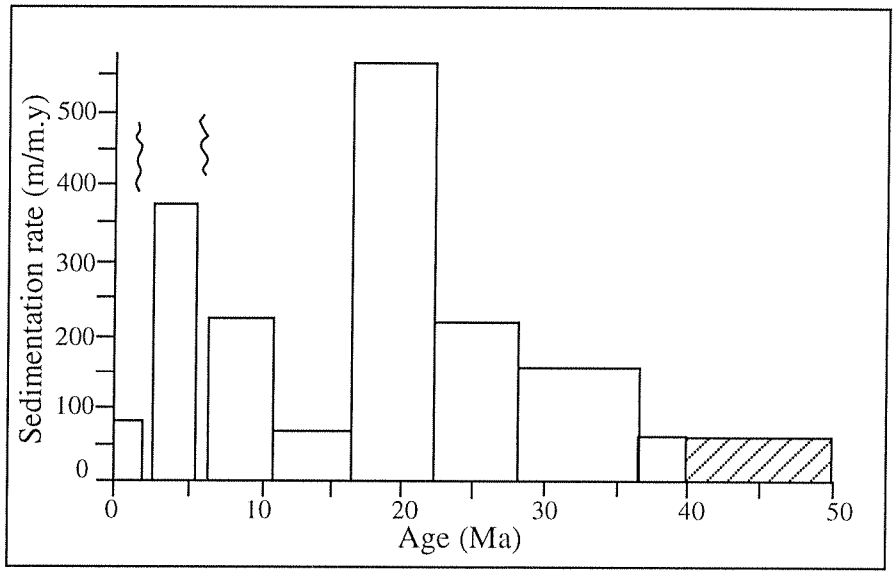

Figure 8.1.1 Sedimentation rate plot for the Burwood sub-Basin from Turnbull, Uruski et al (1993). This plot shows a very simplistic view of the sedimentation rate in the area due to the poor age constraints.

Uplift rates in the area are also hard to quantify, although investigations of the sediments in the area give a qualitative record of the uplift. The main phase of uplift in the area started in the late Eocene and by the early Oligocene the area that now makes up the Takitimu Mountains was being rapidly uplifted (>250m/m.y) (chapter 4.1). The area then underwent a period of subsidence until the late Miocene.

8.2 TECTONIC HISTORY OF THE BURWOOD SUB-BASIN

8.2.1 GEOMETRY OF THE BASIN

Contraction of the Burwood sub-Basin in the late Miocene has destroyed much of the original basin architecture. Nevertheless, a picture of the development of the basin can be built up by looking at the sediments in the area.

In the late Eocene the study area was of low relief, extending west to a basement high separating the Waiau and Te Anau Basins (Zink, 2000), with an eastern edge in what is now the Takitimu Mountains, and a basin floor that sloped to the northeast. This low area was formed in an extensional environment (Sutherland, 1995), probably as a half-graben (Zink, 2000) (chapter 3). In the early Oligocene the area that now forms the Takitimu Mountains was rapidly uplifted forming the edge of the Burwood sub-Basin. The basin was probably narrow, elongated in a north south direction (parallel to the edges of the main basins) and still sloped to the north (chapter 4.1). From this period until the middle Miocene the sedimentary sequence in the Burwood sub-Basin differed from those in the Te Anau and Waiau Basins (Turnbull, Uruski et al, 1993). In the late Oligocene and early Miocene, the study area formed a subsiding, open part of the Burwood sub-Basin, with the major basin margin north of the study area in the Caples Terrane (chapter 4.3 and 4.4). In the late Miocene the basin was shortened in an east-west direction as a result of transpressional folding and high angle reverse faulting of the basin sediments resulting in their uplift (chapter 5).

The Burwood sub-Basin has recorded all the main tectonic events in western Southland, from the extensional rifting in the Eocene, through the transtensional to transpressional phase from the Oligocene-early Miocene, and finally to the late Miocene compression of the area. The changes in the basin architecture described above can be attributed to the changing tectonic regime in the area given in Carter and Norris (1976), Sutherland (1995) and Walcott (1998).

8.2.2 OBLIQUE REVERSE-DEXTRAL SHEAR RELATED TO THE MOONLIGHT FAULT SYSTEM

The late Miocene phase of compression that occurred in the South Island of New Zealand resulted in the reversal of the movement on the Moonlight Fault System (Carter and Norris, 1976; Norris and Turnbull, 1993). Within the Burwood sub-Basin, the Moonlight Fault

System is not a single feature and a large amount of the movent is taken up in a shear zone adjacent to the fault itself (chapter 6). In the study area the basin has been shortened by more than 30% perpendicular to the fault system, and displaced about 5km dextrally (chapter 6). This zone of shear is regionally important, as it is more than double the amount of displacement seen across the actual fault north of the area where it crosses the Dun Mountain Ophiolite Belt (Coombs et al, 1976; Carter and Norris, 1977b; Norris and Turnbull, 1993). It also helps to explain the discrepancy between the amount of movement on the Moonlight Fault System to the south of the area, and to the north where it crosses the Dun Mountain Ophiolite Belt (Coombs et al, 1976; Cater and Norris, 1977b; Norris and Carter, 1980; Constantine, 1988). Structures investigated in the study area show that most of the bending of the South Island terranes has occurred in the late Cenozoic (chapter 6), which fits with the tectonic models of Walcott (1998) and Sutherland (1999).

8.3 Relationship between the Burwood sub-Basin and other western Southland Basins

While the Burwood sub-Basin shares a similar deformation history to the Te Anau and Waiau Basins, sedimentation patterns show that through much of its history it has been a separate basin. Sedimentation of the oldest unit shows similarities to the Waiau Basin while the youngest sediments are related to those in the Te Anau Basin. The Beaumont Formation shows that the study area was connected to the Waiau Basin in the Eocene (chapter 3.1). The southwest-northeast flow direction of the current indicators (chapter 3.1) shows that the sediment flowed from the basement high of Zink (2000) rather than Fiordland as the sediment in the Te Anau Basin was all being transported to the south at the time (Zink, 2000).

In the early Oligocene (early Whaingaroan) the Burwood sub-Basin shows no sedimentary record of being attached to either the Waiau or the Te Anau Basins. The location of the basin margin to the east, coupled with northward sediment transport (chapter 4.1) indicates that the Burwood sub-Basin was not joined to the Te Anau Basin and it opened to the south (Zink, 2000). At this time the Burwood sub-Basin may have been part of the Waiau Basin to the south as its the eastern margin was also depositing sediment (Carter and Norris, 1977a.).

In the mid-late Oligocene (late Whaingaroan-Duntroonian) the Burwood sub-Basin began receiving sediment from the north (chapter 4.3) and was most likely joined to the shelf where the Bobs Cove Beds of Turnbull et al (1975) were being formed. The Burwood sub-Basin was probably still separated from the Te Anau Basin by a basement high at this time as the Turret Peaks Formation (Turnbull, 1985) was being deposited from a Fiordland source but failed to reach to the study area. During the early Miocene, the Burwood sub-Basin was fed from the same basin margin as the main Te Anau Basin. This margin was in the north and drained the Caples Terrane (Turnbull, Uruski et al, 1993; Zink, 2000) (chapter 4.4), which must have been undergoing uplift at this time. Although the margin was in the same area, two separate basins must have existed at this time as coarse sediment was able to by-pass most of the Te Anau Basin and be deposited in the Monawai sub-Basin in the south (Carter and Norris, 1977a), while in the Burwood sub-Basin, a large submarine fan made up of entirely sand-sized material was deposited (chapter 4.4). During the late Miocene the Te Anau Basin and Burwood sub-Basin finally joined as the Prospect Formation was deposited in both basins at this time (Manville, 1994).

Throughout the evolution of the Burwood sub-Basin, the Moonlight Fault System probably controlled its spatial relationships with the other basins in the area. It appears that the Te Anau Basin margin moved northwards overtime, especially during the Oligocene-Miocene transtensional-transpressional tectonic regime, controlling the provenance of sediment in the sub-basin (chapter 6). The differences between the sediments in the main basin compared with the sub-basin can be explained by the basement high that separated them, preventing the units being deposited in both basins. This northward movement of the margin has resulted in similarities with the Waiau Basin in the older (Eocene) tertiary rocks and similarities with Te Anau Basin sediments in the younger tertiary (late Miocene) parts of the basin.

8.4 TECTONIC CONTROLS ON SEDIMENTATION

Throughout this thesis sedimentation rates have been discussed in terms of the tectonic regime in the area, while other factors have generally been discounted as major controls on the sedimentation rate. Zink (2000) discusses in detail the controls on sedimentation in the Te Anau Basin, and subsequently this section intends only to compare the results of this study to

that of Zink (2000) in order to show that the main control on sedimentation was the tectonic regime in western Southland.

The controlling factors of basin evolution are: tectonic signal, climatic signal, local structural signal and eustatic signal (Zink, 2000). Of these the climatic and eustatic signals can be discounted as major contributors to the basin evolution as Hornibrook, (1992) indicates that the New Zealand climate was quite stable and warm during the Eocene-Miocene, and LeMasurier and Landis (1996) show that the sea level transgressed until the Oligocene and then regressed. The deposition of three submarine fans in the Oligocene-Miocene (chapter 4) is sporadic rather than a transgression regression sequence. Sedimentology of the Spear Peak Formation is also indicative of deposition adjacent to a tectonically active zone (chapter 4.1).

Of the five aspects regarded by Zink (2000) as features related to tectonic signal, four are represented in the Burwood sub-Basin. Fault-block tilting parallel to the basin axis is seen especially in the south of the study area, for example the Murihiku has been titled parallel to reactivated structures (see map and cross-section A-A', appendix H). The basin formed an elongate shape as shown by the narrow fans deposited as the Spear Peak Formation, although this has been altered by later deformation (see chapters 4.1 and 7, and map and cross-sections, appendix H). Fluctuating sediment input is shown by the interbedded submarine fan and hemi-pelagic mudstone layers in the Waiau Group (chapter 4) . The Burwood sub-Basin as a whole is indicative of a pull-apart basin in that it it has subsided throughout its history.

The remaining feature mentioned by Zink (2000) is the overall half-graben shape of the basin. This feature is not seen in the Burwood sub-Basin, although it could have been destroyed by later deformation as the area has been extensively deformed in the late Cenozoic (chapter 6, map and cross-sections, appendix H). As within the rest of the Te Anau Basin, some older structures have controlled the shape of the sub-basin during its formation, although these features have been reactivated in the stress field associated with the opening of the basin (Zink, 2000). Overall the tectonic signal suggested by Zink (2000) for the Te Anau Basin is also observed in the Burwood sub-Basin.

REFERENCES

Adams, C. J., Bishop, D. G. & Gabites, J. E. 1985. Potassium-argon age studies of a low-grade progressively metamorphosed greywacke sequence, Dansey Pass South Island, New Zealand. *Journal of the Geological Society of London* **142**, 339-349.

Aitchison, J. C., Landis, C. A. & Turnbull, I. M. 1988. Stratigraphy of Stephens Subgroup (Maitai Group) in the Countess Range-Mararoa River area, northwestern Southland, New Zealand. *Journal of the Royal Society of New Zealand* **18**(3), 271-284.

Allen, J. R. L. 1963. The classification of cross-stratified units, with notes on their origin. *Sedimentology* **2**, 93-114.

Anderson, E. M. 1905. The dynamics of faulting. *Edinburgh Geological Society Transactions* **8**(3), 387-402.

Anderson, H. J. 1991. Focal mechanisms of some recent large New Zealand earthquakes. *New Zealand Journal of Geology and Geophysics* **34**, 103-109.

Arafin, M. S. 1982. Tertiary geology of the Birchwood area. Unpublished MSc thesis, University of Otago.

Ballance, P. F. & Campbell, J. D. 1993. The Murihiku Arc-Related Basin of New Zealand (Triassic-Jurassic). In: *South Pacific Sedimentary Basins* (edited by Ballance, P. F.). *Sedimentary Basins of the World* **2**. Elsevier.

Basu, D. & Bouma, A. H. 2000. Thin-bedded turbidites of the Tanqua Karoo; physical and depositional characteristics. In: *Fine-grained turbidite systems* **72;**. American Association of Petroleum Geologists, Tulsa, OK, United States, 263-277.

Beanland, S. 1980. Geology of the Princhester area. Unpublished BSc thesis, University of Otago.

Begg, J. G. 1981. The Basement Geology and Palaeontology of the Wairaki Hills, Southland. Unpublished PhD thesis, University of Otago.

Begg, J. G. & Ballard, H. R. 1991. An Early Permian fauna from the Mantle Volcanics Formation, Skippers Range, Northwest Otago. *New Zealand Journal of Geology and Geophysics* **34**(2), 145-155.

Bishop, D. G. 1986. Puysegur. Geological Map of New Zealand. Department of Scientific and Industrial Research, Wellington.

Bishop, D. G., Blattner, P. & Landis, C. A. 1990. Sheet 16-Hollyford Miscellaneous map of New Zealand. Department of Scientific and Industrial Research, Wellington.

Bishop, D. G., Bradshaw, J. D. & Landis, C. A. 1985. *Provisional Terrane Map of South Island, New Zealand.* Circum-Pacific Council for Energy and Mineral resources Houston, Texas, U.S.A.

Blake, M. C. & Landis, C. A. 1973. The Dun Mountain ultramafic belt-Permian oceanic crust and upper mantle in New Zealand. *U.S. Geological Survey Journal of Research* **1**, 529-534.

Boggs, S. 2001. *Principles of sedimentology and stratigraphy.* Prentice-Hall Inc., New Jersey.

Boles, J. R. 1974. Structure, Stratigraphy and Petrology of mainly Triassic rocks, Hokonui Hills, Southland, New Zealand. *New Zealand Journal of Geology and Geophysics* **17**(2), 337-374.

Boles, J. R. & Coombs, D. S. 1977. Zeolite facies alteration of sandstones in the Southland Syncline, New Zealand. *American Journal of Science* **277**, 982-1012.

Bouma, A. H. 1964. Turbidites. In: *Turbidites (Developments in Sedimentology 3).*

Bowen, F. E. 1964. Geology of Ohai Coal Field. New Zealand Geological Survey Bulletin.

Bradshaw, J. Y. 1990. Geology of crystalline rocks of northern Fiordland; details of the granulite facies western Fiordland Orthogneiss and associated rock units. *New Zealand Journal of Geology and Geophysics* **33**(3), 465-484.

Campbell, J. D. & Coombs, D. S. 1966. Murihiku Supergroup (Triassic-Jurassic) of Southland and South Otago. *New Zealand Journal of Geology and Geophysics* **9**, 393-398.

Carlson, J. & Grotzinger, J. P. 2001. Submarine fan inferred from turbidite thickness distributions. *Sedimentology* **48**, 1331-1351.

Carter, L. & Carter, R. M. 1988. Late Quaternary development of left-bank-dominant levees in the Bounty Trough, New Zealand. *Marine Geology* **78**(3-4), 185-197.

Carter, R. M., Hicks, M. D., Norris, R. J. & Turnbull, I. M. 1978. Sedimentation patterns in an ancient arc-trench-ocean basin complex: Carboniferous to Jurassic Rangiatata Oregen, New Zealand. In: *Sedimentation in Submarine Canyons, Fans and Trenchs.* (edited by Stanley, D. J. & Kelling, G.). Dowden Hutchinson and Ross, Stroudsburg, 340-361.

Carter, R. M. & Norris, R. J. 1976. Cainozoic history of southern New Zealand: an accord between geological observations and plate tectonic predictions. *Earth and Planetary Science Letters* **31**, 85-94.

Carter, R. M. & Norris, R. J. 1977a. Redeposited conglomerates in a Miocene flysch sequence at Blackmount, western Southland, New Zealand. *Sedimentary Geology* **18**(4), 289-319.

Carter, R. M. & Norris, R. J. 1977b. Post-conference excursion to Blackmount, Waiau Basin. *Geological Society of New Zealand Conference Tour Notes.*

Carver, R. E. 1971. *Procedures in Sedimentary Petrology.* John Wiley & Sons, Inc., New York.

Carver, R. E. 1971. Heavy-Mineral Separation. In: *Procedures in Sedimentary Petrology* (edited by Carver, R. E.). John Wiley & Sons, New York, 427-452.

Challis, G. A. & Lauder, W. R. 1977. Pre-Tertiary geology of the Longwood Range (Parts NZMS 1 Sheets S167, S168, S175, S176). New Zealand Geological Survey Miscellaneous Series. Department of Scientific and Industrial Research, Wellington.

Collinson, J. D. 1978a. Alluvial Sediments. In: *Sedimentary Environments and Facies* (edited by Reading, H. G.) **1**. Blackwell Science Publications, Oxford.

Collinson, J. D. 1978b. Lakes. In: *Sedimentary Environments and Facies* (edited by Reading, H. G.). Blackwell Scientific Publications, Oxford.

Collinson, J. D. 1996. Alluvial sediments. In: *Sedimentary environments; processes, facies and stratigraphy* (edited by Reading, H. G.). Blackwell Science, Oxford, United Kingdom, 37-82.

Constantine, A. 1988. Stratigraphy and Provenance of Tertiary Sediments at Lake Hauroko, with Reference to Dextral Strike-Slip Movement on the Moonlight Fault System. Unpublished BSc(Hons) thesis, University of Otago.

Coombs, D. S. 1950. The geology of the northern Taringatura hills, Southland. *78, Part 4; Pages 426-448.*

Coombs, D. S. 1954. The nature and alteration of some Triassic sediments from Southland, New Zealand. *Transactions of the Royal society of New Zealand* **82**, 65-106.

Coombs, D. S., Cook, N. D. J., Kawachi, Y., Johnstone, R. D. & Gibson, I. L. 1996. Park Volcanics, Murihiku

Terrane, New Zealand: petrology, petrochemistry, and tectonic significance. *New Zealand Journal of Geology and Geophysics* **39**, 469-492.

Coombs, D. S., Ellis, A. J., Fyfe, W. S. & Taylor, A. M. 1959. The zeolite facies with comments on the interpretation of hydrothermal syntheses. *Geochimica et Cosmochimica* **17**, 53-107.

Coombs, D. S., Landis, C. A., Norris, R. J., Sinton, J. M., Borns, D. J. & Craw, D. 1976. The Dun Mountain ophiolite belt, New Zealand, its tectonic setting, constitution, and origin, with special reference to the southern portion. *American Journal of Science* **276**(5), 561-603.

Couples, G. D. & Lewis, H. 2000. Effects of interlayer slip in model forced folds. In: *Forced folds and fractures* **169;**. Geological Society of London, London, United Kingdom, 129-144.

Cowden, A., Ruddock, R., Reay, A., Nicolson, P., Waterman, P. & Banks, M. J. 1990. Platinum mineralisation potential of the Longwood igneous complex, New Zealand. In: *Proceedings of the Fifth international platinum symposium* **42; 1-4**. Springer-Verlag, Vienna, Austria, 181-195.

Cox, S. H. 1878. Report on the geology of the Te Anau district. *New Zealand Geological Survey Reports of geological explorations 1877-78* **11**, 110-118.

Dabrio, C. J. 1990. Fan-delta facies associations in late Neogene and Quaternary basins of southeastern Spain. In: *Coarse-grained deltas* **10;** (edited by Colella, A. & Prior, D.B.) Blackwell, Oxford, International, 91-111.

Dabrio, C. J. & Polo, M. D. 1988. Late Neogene fan deltas and associated coral reefs in the Almazora Basin Almeria Province. In: *Fan Deltas: Sedimentology and tectonic Settings* (edited by Nemec, W. & Steel, R.J). Blackie and Son, London, 354-367.

Dickinson, W. R. 1985. Interpreting Provenance Relations From Detrital Modes of Sandstones. In: *Provenance of arenites* (edited by Zuffa, G. G.). D. Reidel Publishing Company, 333-361.

Field, B. D., Browne, G. H. & others. 1989. Cretaceous and Cenozoic sedimentary basins and geological evolution of the Canterbury region, South Island, New Zealand. *New Zealand Geological Survey Basin Studies* **2**.

Fitzharris, C. A. 1967. Geology of the Elm Tree Creek area Southland. Unpublished BSc thesis, University of Otago.

Folk, R. L. 1980. *Petrology of Sedimentary Rocks*. Hemphill Publishing Co, Austin, Texas.

Force, E. R., Force, L. M. & Thyne, M. L. 1970. Quaternary Warping at Gorge Saddle, Western Southland. *Earth Science Journal* **4**(2), 141-144.

Fossen, H. & Tikoff, B. 1993. The deformation matrix for simultaneous simple shearing, pure shearing and volume change, and its application to transpression-transtention tectonics. *Journal of Structural Geology* **15**, 413-422.

Frost, C. D. & Coombs, D. S. 1989. Nd isotope character of New Zealand sediments: implications for terrane concepts and crustal evolution. *American Journal of Science* **289**, 744-770.

Galehouse, J. S. 1971. Point Counting. In: *Procedures in Sedimentary Petrology* (edited by Carver, R. E.). John Wiley & Sons, New York, 385-407.

Grindley, G. W. 1958. The Geology of the Eglinton Valley, Southland. *New Zealand Geological Survey Bulletin* **58**.

Hall, C. 1989. Geology of Elmwood Station, Western Southland with emphasis on Stratigraphy and Provenance

of Cenozoic Sediments. Unpublished BSc(Hons) thesis, University of Otago.

Harrington, W. M. A. 1982. The Geology of Haycocks-Snowdown Forest, Western Southland. Unpublished BSc(Hons) thesis, University of Otago.

Harwood, G. 1988. Microscopic techniques: 2 Principles of sedimentary petrography. In: *Techniques in Sedimentology* (edited by Tucker, M.). Blackwell Scientific Publications, London, 108-173.

Hayward, B. W. 1986. A guide to paleoenvironmental assessment using New Zealand Cenozoic foraminiferal faunas. New Zealand Geological Survey, Lower Hutt, 73.

Hector, J. 1863. Geological expedition to the west coast of Otago New Zealand. *Otago Provincial Government Gazette* **6**.

Hector, J. 1864. On the Geology of the Province of Otago, New Zealand. *Geological Magazine* **233**(1).

Heller, P. L. & Dickinson, W. R. 1985. Submarine Ramp Facies Model for Delta- Fed, Sand-Rich Turbidite Systems. *The American Association of Petroleum Geologist Bulletin* **69**(6), 960-976.

Hickson, T. A. & Lowe, D. R. 2002. Facies architecture of submarine fan channel-levee complex: the Juniper Ridge Conglomerate, Coalinga, California. *Sedimentology* **49**, 335-362.

High Jr, L. R. & Picard, M. D. 1971. Mathematical Treatment of Orientation Data. In: *Procedures in Sedimentary Petrology* (edited by Carver, R. E.). John Wiley & Sons, New York, 21-45.

Hornibrook, N. d. B. 1992. New Zealand Cenozoic marine paleoclimates; a review based on the distribution of some shallow water and terrestrial biota. In: *Pacific Neogene; environment, evolution, and events.* (edited by Tsuchi, R. & Ingle Jr, J.-C.). University of Tokyo Press, Tokyo, Japan., 83-106.

Hornibrook, N. d. B., Brazier, R. C. & Strong, C. P. 1989. Manual of New Zealand Permian to Pleistocene foraminiferal biostartigraphy. *New Zealand Geological Survey Paleontological Bulletin.* **56**.

Houghton, B. F. 1981. Lithostratigraphy of the Takitimu Group, central Takitimu Mountains, western Southland, New Zealand. *New Zealand Journal of Geology and Geophysics* **24**(3), 333-348.

Houghton, B. F. & Landis, C. A. 1989. Sedimentation and volcanism in a Permian arc-related basin, southern New Zealand. *Bulletin of Volcanology* **51**(6), 433-450.

Hoyt, J. H. 1971. Measurement of Sedimentary Structure Orientation. In: *Procedures in Sedimentary Petrology* (edited by Carver, R. E.). John Wiley & Sons, New York, 3-20.

Hutton, F. W. 1871. Reports on the Geology of Southland, New Zealand. *Reports of the Geological Explorer* **7**.

Ingersoll, R. V., Bullard, T. F., Ford, R. L., Grim, J. P., Puckle, J. D. & Sares, S. W. 1984. The effect of grain size on detrital modes: atset of the Gazzi-Dickinson point-counting method. *Journal of Sedimentary Petrology* **54**, 103-116.

Jamison, W. R. 1991. Kinematics of compressional fold development in convergent wrench terranes. *Tectonophysics* **190**, 209-232.

Jonk, R. & Biermann, C. 2002. Deformation in Neogene sediments of the Sorbas and Vera Basins (SE Spain): constraints on simple-shear deformation and rigid body rotation along major strike-slip faults. *Journal of Structural Geology* **24**, 963-977.

Kawachi, Y. 1974. Geology and petrochemistry of weakly metamorphosed rocks in the upper Wakatipu District, southern New Zealand. *New Zealand Journal of Geology and Geophysics* **17**(1), 169-208.

Kimbrough, D. L., Tulloch, A. J., Coombs, D. S., Landis, C. A., Johnson, M. R. & Mattison, J. M. 1993. Isotopic ages from the Nelson region of South Island, New Zealand: crustal structure and definition of the

Median Tectonic Zone, New Zealand. *Tectonophysics* **225**, 433-448.

Kimbrough, D. L., Tulloch, A. J., Coombs, D. S., Landis, C. A., Johnston, M. R. & Mattison, J. M. 1994. Uranium-lead zircon ages from the Median Tectonic Zone, New Zealand. *New Zealand Journal of Geology and Geophysics* **37**, 393-419.

King, R. J., Jameison, B. S. & Turnbull, I. M. 1985. Fiordland complex. In: *Sheet D42AC & part of D43-Te Anau Downs. Geological map of New Zealand.* (edited by Turnbull, I. M.). Department of Scientific and Industrial Research, Wellinton, 7-11.

Kirby, M. 1989. Structure, Stratigraphy and Provenance of Cenozoic Sediments in the Princhester Creek area Northern Takitimu Mountains. Unpublished BSc(Hons) thesis, University of Otago.

Kuenen, P. H. & Migliorini, C. I. 1950. Turbidity currents as a cause of graded bedding. *Journal of Geology* **58**, 91-127.

Laird, M. G. 1993. Cretaceous Continental Rifts: New Zealand Region. In: *Sedimentary Basins of the World: South Pacific Sedimentary Basins* (edited by Ballance, P. F.) **2**. Elsevier.

Lamarche, G. & J-F, L. 2000. Transition from strike-slip faulting to oblique subduction: active tectonics at the Puysegur Margin, south New Zealand. *Tectonophysics* **316**, 67-89.

Landis, C. A. 1974. Stratigraphy, lithology, structure, and metamorphism of Permian, Triassic, and Tertiary rocks between the Mararoa River and Mount Snowdon, western Southland, New Zealand. *Journal of the Royal Society of New Zealand* **4**(3), 229-251.

Landis, C. A., Campbell, H. J., Aslund, T., Cawood, P. A., Douglas, A., Kimbrough, D. L., Pillai, D. D. L., Raine, J. I. & Willsman, A. 1999. Permian-Jurassic strata at Productus Creek, Southland, New Zealand: implications for terrane dynamics of the eastern Gondwanaland margin. *New Zealand Journal of Geology and Geophysics* **42**, 255-278.

LeMasurier, W. E. & Landis, C. A. 1996. Mantle Plume activity recorded by low relief surfaces in west Antarctica and New Zealand. *Geological Society of America Bulletin* **108**, 1450-1466.

Lindholm, R. 1987. *A Practical Approach to Sedimentology.* Allen & Unwin, London.

Lindsay, N. M. 1980. Geology of the Dunton Range, Te Anau. Unpublished BSc (Hons) thesis, University of Otago.

Lowe, D. R. 1982. Sediment gravity flows: II-depositional models with special reference to the deposits of high density turbidity currents. *Journal of Sedimentary Petrology* **52**, 279-297.

MacKinnon, T. C. 1983. Origin of the Torlesse Terrane and coeval rocks, South Island, New Zealand. *Geological Society of America Bulletin* **94**, 967-985.

Maejima, W. 1988. Marine transgression over an active alluvial fan; the Early Cretaceous Arida Formation, Yuasa-Aridagawa Basin, southwestern Japan. In: *Fan deltas; sedimentology and tectonic settings.* Blackie and Son, Glasgow, United Kingdom.

Manville, V. 1994. The Prospect Formation Sedimentology, Stratigraphy and Significance: Late Miocene-Pliocene syntectonic sediment of the Te Anau Basin western Southland, New Zealand. Unpublished PhD thesis, University of Otago.

Massari, F. & Colella, A. 1988. Evolution and Types of fan delta systems in some major tectonic settings. In: *Fan Deltas: Sedimentology and Tectonic settings* (edited by Nemec, W. & Steel, R.J). Blackie and Son.

Mattinson, J. M., Kimbrough, D. L. & Bradshaw, J. Y. 1986. Western Fiordland orthogneiss; Early Cretaceous

arc magmatism and granulite facies metamorphism, New Zealand. *Contributions to Mineralogy and Petrology* **92**(3), 383-392.

McCraw, J. D. 1947. Geology of the Northern Takitimu Mountains. Unpublished MSc thesis, University of Otago.

McKellar, I. C. 1973. Te Anau-Manapouri (1st ed.) New Zealand Geological Survey Miscellaneous series map 4. Department of Scientific and Industrial Research, Wellington, 19.

Miall, A. D. 1977. A review of the braided river depositional environment. *Earth Science Reviews* **13**, 1-62.

Miall, A. D. 1978. Summary of Braided River Deposits. In: *Fluvial sedimentology* (edited by Miall, A. D.). Canadian Society of Petroleum Geologists, Calgary, 597-604.

Miall, A. D. 1999. In defense of facies classifications and models. *Journal of Sedimentary Research* **69**(1), 2-5.

Mitchell, A. H. G. & Reading, H. G. 1978. Sedimentation and Tectonics. In: *Sedimentary environments and Facies* (edited by Reading, H. G.). Blackwell Scientific Publications, Oxford.

Morris, W. & Busby-Spera, C. 1990. A submarine-fan valley-levee complex in the upper Cretaceous Rosario Formation: Implication for turbidite facies models. *Geological Society of America Bulletin* **102**, 900-914.

Mortimer, N. & Roser, B. P. 1992. Geochemical evidence for the position of the Caples- Torlesse boundary in the Otago Schist, New Zealand. *Journal of the Geological Society of London* **149**, 967-977.

Mortimer, N., Tulloch, A. J., Spark, R. N., Walker, N. W., Ladley, E., Allibone, A. & Kimbrough, D. L. 1999. Overview of the Median Batholith, New Zealand; a new interpretation of the geology of the Median Tectonic Zone and adjacent rocks. In: *Gondwana-10; event stratigraphy of Gondwana; proceedings Volume 1* **29; 1**. Pergamon, London-New York, International, 257-268.

Morton, A. C. 1985. Heavy minerals in provenance studies. In: *Provenance of arenites* (edited by Zuffa, G. G.) **Series C: Mathematical and Physical Sciences. 148;**. D Reidel Publishing Company, Dordrecht-Boston, International, 249-277.

Morton, A. C. 1991. Geochemical studies of detrital heavy minerals and their application to provenance research. In: *Developments in sedimentary provenance studies* **57;**. Geological Society of London, London, United Kingdom, 31-45.

Mutti, E. 1985. Turbidite systems and their relations to depositional sequences. In: *Provenance of Arenites* (edited by Zuffa, G. G.). D.Reidel Publishing Company, Dordrecht.

Mutti, E. & Ricchi Lucchi, F. 1972. Le torbiditi dell'Apennino settentrionale: introduzione all'-analisi di facies. *Mem. Soc Geol. Italia* **11**, 161-199.

Nauman, C. R. 1973. Alabaster Group Rocks (Lower Permian) in southern Skippers Range, north-west Otago, New Zealand. *Journal of the Royal Society of New Zealand* **32**, 527-544.

Nemec, W. 1990. Aspects of sediment movement on steep delta slopes. In: *Coarse-grained deltas* **10;**. (edited by Colella, A. & Prior, D.B.) Blackwell, Oxford, International, 29-73.

Nemec, W. 1990. Deltas; remarks on terminology and classification. In: *Coarse-grained deltas* **10;**. (edited by Colella, A. & Prior, D.B.)Blackwell, Oxford, International, 3-12.

Nemec, W. & Postma, G. 1993. *Quaternary alluvial fans in southwestern Crete: sedimentation processes and geomorphic evolution*. Special Publication of the International Association of Sedimentologists.

Nemec, W. & Steel, R. J. 1988. What is a fan delta and how do we recognize it? In: *Fan deltas; sedimentology*

and tectonic settings. (edited by Nemec, W. & Steel, R.J) Blackie and Son, Glasgow, United Kingdom.

Normark, W. R. 1991. Turbidite elements and the obsolescence of the suprafan concept. *Giornale di Geologia, ser 3ª* **53**(2), 1-10.

Norris, R. J. 1979. A geometrical study of finite strain and bending in the South Island. In: *The origin of the Southern Alps* (edited by Walcott, R. I. & Cresswell, M. M.) **18**. Royal Society of New Zealand Bulletin.

Norris, R. J. & Carter, R. M. 1980. Offshore sedimentary basins at the southern end of the Alpine Fault, New Zealand. In: *Sedimentation in oblique-slip Mobile Zones* (edited by Ballance, P. F. & Reading, H. G.). Blackwell Scientific Publications, Oxford, 237-265.

Norris, R. J. & Carter, R. M. 1982. Fault-bounded blocks and their role in localising sedimentation and deformation adjacent to the Alpine Fault, southern New Zealand. *Tectonophysics* **87**, 11-23.

Norris, R. J., Carter, R. M. & Turnbull, I. M. 1978. Cainozoic sedimentation in basins adjacent to a major continental transform boundary in southern New Zealand. *Journal of the Geological Society of London* **135**, 191-205.

Norris, R. J., Koons, P. O. & Cooper, A. F. 1990. The obliquely- convergent plate boundary in the South Island of New Zealand: implications for ancient collision zones. *Journal of Structural Geology* **12**, 715-725.

Norris, R. J. & Turnbull, I. M. 1993. Cenozoic basins adjacent to an evolving transform plate boundary, southwest New Zealand. In: *South Pacific Sedimentary Basins: Sedimentary Basins of the World* (edited by Ballance, P. F.). *Sedimentary Basins of the World* **2**. Elsevier.

Oliver, G. J. H. & Coggon, J. H. 1979. Crustal structure of Fiordland, New Zealand. *Tectonophysics* **54**(3-4), 253-292.

Park, J. 1909. The geology of the Queenstown subdivision. *New Zealand Geological Survey Bulletin* **7**.

Park, J. 1921. Geology and mineral resources of western Southland. *New Zealand Geological Survey Bulletin* **23**.

Pettijohn, F. J., Potter, P. E. & Siever, R. 1987. *Sand and Sandstone*. Springer-Verlag, New York.

Pilaar, W. F. H. & Wakefield, L. L. 1984. Hydrocarbon Generation in the Taranaki Basin, New Zealand. In: *Petroleum Geochemistry and Basin Evaluation* (edited by Demaison, G. & Morris, R. J.). The American Association of petroleum Geologists, Tulsa.

Piper, D. J. W. & Kontopoulos, N. 1994. Bed forms in submarine channels: comparison of ancient examples from Greece with studies of recent turbidite systems. *Journal of Sedimentary Research* **64**(2), 247-252.

Pocknall, D. T. & Turnbull, I. M. 1989. Paleoenvironmental and stratigraphic significance of palynomorphs from Upper Eocene (Kaiatan) Beaumont Coal Measures and Orauea Mudstone, Waiau Basin, western Southland, New Zealand. *New Zealand Journal of Geology and Geophysics* **32**, 371-378.

Postma, G., Nemec, W. & Kleinspehn, K. L. 1988. Large floating clasts in turbidites: a mechanism for their emplacement. *Sedimentary Geology* **58**, 47-61.

Potter, P. E. & Pettijohn, F. J. 1977. *Paleocurrents and Basin Analysis*. Springer-Verlag, New York.

Ramsay, J. G. & Huber, M. I. 1983. *The Techniques of Modern Structural Geology Volume 1: Strain Analysis*. Academic Press, London.

Reading, H. G. & Richards, M. 1994. Turbidite Systems in Deep-Water Basin Margins Classified by Grain Size and Feeder System. *American Association of Petroleum Geologists, Bulletin* **78**, 792-822.

Ricchi Lucchi, F. 1985. Influence of transport processes and basin geometry on sand composition. In:

Provenance of Arenites (edited by Zuffa, G. G.) **Series C: Mathematical and Physical Sciences. 148;**. D Reidel Publishing Company, Dordrecht-Boston, International, 19-47.

Ricci-Lucchi, F. 1975. Depositional cycles in two Turbidite Formations of northern Apennies (Italy). *Journal of Sedimentary Petrology* **45**(1), 3-43.

Richards, M., Bowman, M. & Reading, H. G. 1998. Submarine-fan systems I: characterization and stratigraphic prediction. *Marine and Petroleum Geology* **15**, 689-717.

Roser, B. P., Coombs, D. S., Korsch, R. J. & Campbell, J. D. 2002. Whole rock geochemical variations and evolution of the arc-derived Murihiku Terrane, New Zealand. *Geological Magazine* **139**(6), 665-685.

Roser, B. P. & Korsch, R. J. 1988. Provenance signatures of sandstone-mudstone suites determined using discriminant function analysis of major-element data. *Chemical Geology* **67**(1-2), 119-139.

Roser, B. P., Mortimer, N., Turnbull, I. M. & Landis, C. A. 1993. Geology and Geochemistry of the Caples Terrane, Otago, New Zealand: Compositional variations near a Permo-Triassic Arc Margin. In: *South Pacific Sedimentary Basins* (edited by Ballance, P. F.). *Sedimentary Basins of the World* **2**. Elsevier.

Rupke, N. A. 1978. Deep Clastic Seas. In: *Sedimentary environments and Facies* (edited by Reading, H. G.). Blackwell Scientific Publications, Oxford.

Saito, T. & Ito, M. 2002. Deposition of sheet-like turbidite packets and migration of channel-overbank systems on a sandy submarine fan: and example from the Late Miocene-Early Pliocene forearc basin, Boso Peninsula, Japan. *Sedimentary Geology* **149**, 265-277.

Sanderson, D. J. & Marchini, W. R. D. 1984. Transpression. *Journal of Structural Geology* **6**, 449-458.

Searle, M. P. 1994. Structure of the intraplate eastern Palmyride Fold Belt, Syria. *Geological Society of America Bulletin* **106**, 133-1350.

Shanmugam, G. 2000. 50 years of the turbidite paradigm (1950s-1990s): deep-water processes and facies models-a critical perspective. *Marine and Petroleum Geology* **17**, 285-342.

Sighinolfi, G. P. & Tateo, F. 1998. Mineralogical and geochemical criteria for distinguishing turbidite and hemipelagic pelites- the Maastrichtian of the northern Apennines, Italy. *Sedimentary Geology* **115**, 301-313.

Sinton, J. M. 1980. Petrology and evolution of the Red Mountain ophiolite complex, New Zealand. In: *The Jackson volume* **Vol. 280-A, Part 1;**. Kline Geology Laboratory Yale University, New Haven, CT, United States, 296-328.

Smale, D. 1985. Heavy minerals in Tertiary Sandstones of the Te Anau Basin. New Zealand Geological Survey, Dunedin.

Smale, D. 1990. Distribution and provenance of heavy minerals in the South Island: A review. *New Zealand Journal of Geology and Geophysics* **33**, 557-571.

Smale, D. & Morton, A. C. 1987. Heavy mineral suites of core samples from the McKee Formation (Eocene-Lower Oligocene), Taranaki: Implications for provenance and diagenesis. *New Zealand Journal of Geology and Geophysics* **30**, 299-306.

Speden, I. G. 1959. The alignment of fold axis in the Jurassic of south eastern Otago and southern Southland. *New Zealand Journal of Geology and Geophysics* **2**, 448-460.

Stow, D. A. V., Faugeres, J.-C., Adriano, V. & Gonthier, E. 1998. Fossil contourites: a critical review. *Sedimentary Geology* **115**, 3-31.

Stow, D. A. V. & Johansson, M. 2000. Deep-water massive sands: nature, origin and hydrocarbon implications. *Marine and Petroleum Geology* **17**.

Stow, D. A. V. & Lovell, J. P. B. 1979. Contourites: Their Recognition in Modern and Ancient Sediments. *Earth-Science Reviews* **14**, 251-291.

Stow, D. A. V. & Mayall, M. 2000. Deep-water sedimentary systems: New models for the 21st century. *Marine and Petroleum Geology* **17**, 125-135.

Stow, D. A. V., Reading, H. G. & Collinson, J. D. 1996. Deep seas. In: *Sedimentary environments; processes, facies and stratigraphy.* (edited by Reading, H.G.) Blackwell Science, Oxford, United Kingdom, 395-453.

Stow, D. A. V. & Shanmugam, G. 1980. Sequence of structures in fine-grained turbidites: comparison of recent deep-sea and ancient flysch sediments. *Sedimentary Geology* **25**, 23-42.

Sutherland, R. 1995. Cenozoic plate tectonics in the SW Pacific; evolution of the Macquarie Ridge, Puysegur subduction zone, and South Island, New Zealand. In: *New Zealand Geophysical Society symposium 1995; Subduction systems and processes in New Zealand; programme and abstracts* **Symposium, Abstracts. 1995;**. New Zealand Geophysical Society, Wellington, New Zealand, ; unpaginated.

Sutherland, R. 1999. Cenozoic bending of New Zealand basement terranes and Alpine Fault displacement; a brief review. *New Zealand Journal of Geology and Geophysics* **42**(2), 295-301.

Sykes, R. 1988. The Morley Coal Measures, Ohai Coalfield, Southland. New Zealand energy research and development committee, Wellington, 85.

Sylvester, A. G. 1988. Strike-slip faults. *The Geological Society of America Bulletin* **100**, 1666-1703.

Takano, O. 2002. Changes in depositional systems and sequences in response to basin evolution in a rifted and inverted basin: and example from the Neogene Niigata-Shin'etsu basin, Northern Fossa Magna, central Japan. *Sedimentary Geology* **152**, 79-97.

Thomas, L. 1992. *Handbook of Practical Coal Geology.* John Wiley & Sons, Chichester.

Tikoff, B. & Peterson, K. 1998. Physical experiments of transpressional folding. *Journal of Structural Geology* **20**(6), 661-672.

Tucker, M. G. 1991. *Sedimentary Petrology: An introduction to the origin of Sedimentary Rocks.* Blackwell Sciences, Oxford.

Turnbull, I. M. 1979. Stratigraphy and sedimentology of the Caples terrane of the Thomson Mountains, northern Southland, New Zealand. *New Zealand Journal of Geology and Geophysics* **22**(5), 555-574.

Turnbull, I. M. 1985. Sheet D42AC & part of D43-Te Anau Downs. Geological map of New Zealand. Department of Scientific and Industrial Research, Wellington.

Turnbull, I. M. 1986. Sheet D42BD & part of D43-Snowdon. Geological map of New Zealand. Department of Scientific and Industrial Research, Wellington.

Turnbull, I. M. 2000. Geology of the Wakatipu Area. Institute of Geological and Nuclear Sciences, Lower Hutt.

Turnbull, I. M. in prep. Geology of the Murihiku. Institute of Geological and Nuclear Sciences, Lower Hutt.

Turnbull, I. M., Barry, J. M., Carter, R. M. & Norris, R. J. 1975. The Bobs Cove beds and their relationship to the Moonlight fault zone. *Journal of the Royal Society of New Zealand* **5**(4), 355-394.

Turnbull, I. M., Lindqvist, J. K., Norris, R. J., Carter, R. M., Cave, M. P., Sykes, R. & Hyden, F. M. 1989. Lithostratagraphic nomenclature of the Cretaceous and Tertiary sedimentary rocks of Western

Southland, New Zealand. New Zealand Geological Survey.

Turnbull, I. M., Uruski, C. I. & others. 1993. *Cretaceous and Cenozoic Sedimentary Basins of western Southland, South Island, New Zealand.* Institute of Geological and Nuclear Sciences Limited.

Uruski, C. I. 1992. Seismic evidence for dextral wrench faulting on the Moonlight Fault System. *New Zealand Geological Survey Record* **44**, 69-76.

van der Lingen, G. J. 1969. The turbidite problem. *New Zealand Journal of Geology and Geophysics* **12**, 7-50.

Walcott, R. I. 1998. Modes of oblique compression: Late Cenozoic tectonics of the South Island of New Zealand. *Reviews of Geophysics* **36**(1), 1-26.

Walker, R. G. 1975. Generalized facies models for resedimented conglomerates of turbidite association. *Geological Society of America Bulletin* **86**, 737-747.

Walker, R. G. 1978. Nested submarine-fan channels in the Capistrano Formation, San Clemente, California. *Geological Society of America Bulletin* **86**, 915-924.

Walker, R. G. 1992. Turbidites and submarine fans. In: *Facies models: response to sea level change* (edited by Walker, R. G. & James, N. P.). Geological Association of Canada, 239-263.

Ward, C. M. 1984. Geology of the Dusky Sound area, Fiordland. Unpublished PhD thesis, University of Otago.

Weissel, J. K., Dennis, E. H. & Herron, E. M. 1977. Plate tectonics synthesis: the displacements between Australia, New Zealand, and Antarctica since the late Cretaceous. *Marine Geology* **25**, 231-277.

Wellman, H. W. 1956. Structural outline of New Zealand. *New Zealand department of industrial and scientific research bulletin* **121**.

White, S. R. 1998. The Mid-Cenozoic Siberia Fault Zone (SFZ) in Northwest Otago, New Zealand and a study of Greenschist Facies metamorphism in the Haast Schist. Unpublished PhD thesis, University of Otago.

Williams, J. R. 1980. Contact strain, circulation cells and disharmonic folding. *Tectonophysics* **64**, 17-31.

Wood, B. L. 1962. Wakatipu Geological Map of New Zealand 1:250 000. Department of Scientific and Industrial Research, Wellington.

Zink, C. 2000. Middle Eocene to middle Miocene evolution of the Te Anau basin, western Southland, New Zealand. Unpublished PhD thesis, University of Otago.

Sample number	VR_0 %
OU 73285	23.57
OU 73281	19.54
OU 73282	27.59
OU 73283	28.73
OU 73287	32.08
OU 73284	34.08
OU 73286	27.81

Appendix B

Piont Count Data

Formation	OU number	Quartz	Feldspar	VL	SL	ML	Mica	Heavy Minerals	Matrix	Glaucony	Calcite	Other	Total	Q	F	L
Beaumont	73290	59.2	11	5.2	12.5	0.2	0.2	0.7	10.7	0	0	0	99.7	67.196	12.486	20.32
Beaumont	73291	51.7	20.7	5.2	13	0.2	0.5	1.2	7.2	0	0	0	99.7	56.938	22.797	20.26
Beaumont	73289	49.7	20.2	2.7	16.5	0	0.5	1	9.2	0	0	0	99.8	55.78	22.671	21.55
Spear Peak	73307	2	26.5	1.2	43	7.2	0.7	2	13.2				95.8	2.5031	33.166	64.33
Spear Peak	73293	3.2	20.5	0.5	58.2	2.7	1.2	2.2	11.2				99.7	3.7603	24.089	72.15
Spear Peak	73292	2.2	19.5	1.2	64.7	2	0.2	1	9				99.8	2.4554	21.763	75.78
Weydon	73308	42.5	9.2	0.5	12.5	14.7	1.2	2	16	1.2	1	0	100.8	53.526	11.587	34.89
Weydon	73298	47.2	7.2	0.7	10	12.2	2.2	4.7	10	2.7	2.7	0	99.6	61.061	9.3144	29.62
Weydon	73296	40.2	8.5	2.5	10.7	11.2	1.5	3	0.5	2.7	19	0	99.8	54.993	11.628	33.38
Weydon	73297	49.5	9	0.7	12.2	10	1	1	0.5	0.7	15.2	0	99.8	60.811	11.057	28.13
Weydon	73299	49.7	9.7	0	14	13	2	1.5	9.7	0.4	0	0	100	57.523	11.227	31.25
Weydon	73309	45.7	8.5	0.2	12	10.2	1.5	0.5	7.2	2.2	11.7	0	99.7	59.661	11.097	29.24
Haycocks	73301	20.7	12.5	0	46.7	2.5	3.5	1.7	0.5	0	11.7		99.8	25.121	15.17	59.71
Haycocks	73300	27.5	8.7	0	49	1.2	0.7	2	0	0	10.7		99.8	31.829	10.069	58.1
Haycocks	73302	30.2	14	0	35.5	6	1.2	2.5	0	0	10.5		99.9	35.239	16.336	48.42

B

	Quartz(%)	Feldspar(%)	Lithic(%)	Biotite(%)	Hornbend	Cement(%)	Other	Matrix(%)
Muirihiku Sandstone								
OU73288	5%	50% (An42)	35%(Lv&Ls)	3%	minor	6%(zeolite?)	zircon	
OU73310	10%	50%(plag)	15%(Lv&Ls)	minor				25%
OU73311	7%	50%(plag)	20%(Lv&Ls)		minor			25%
Murihiku Tuff								
OU73312		15%(plag crystals)						
OU73313		40% (plag crystals)	10%(Lv)					
Murihiku conglomerate clasts								
OU73314		Present(An54)			Present (Fe rich)			
OU73315	Present	Present		Present (Fe rich)	Present (Fe rich)			
OU73316	Present	Dominantly plag.,some K-spar		Present (Fe rich)	Present (Fe rich)			
OU73317	Present	Over 50% microcline		Present (Fe rich)	Present (Fe rich)			
OU73318	Present	Dominantly plag.,some K-spar		Present (Fe rich)	Present (Fe rich)			
Beaumont Formation conglomerate clasts								
OU73319	20%	60% (plag), 20%(k-spar)						
OU73320	10%	90%(plag)						
OU73321	3%	80% (k-spar) 17%(plag)		minor				
OU73322	20%	20%	60%					
Spear Peak Formation conglomerate clasts								
OU73323		Plag	Lv	minor				present
OU73324		Plag	Large (Lv)					
OU73325	Present	Plag and k-spar		Present	Present		Magnitite?	
OU73326		Plag		Present	Present			
OU73327		Plag		Present	Present		Opaque mineral	

(continued over page)

	Glass(%)	Alteration	Q:F:L	Grain/crystal Size	Sorting
Muirihiku Sandstone					
OU73288			,24:51:25	0.5mm average	poor-moderate
OU73310			.13:67:20	.08mm max.	poor
OU73311			,9:65:26	.08mm max.	poor
Murihiku Tuff					
OU73312	85%(vitric shards)	Zeolite (heulandite)		.1mm	mderately(bimodal)
OU73313	50%(vitric shards)	Zeolite (heulandite)		.5mm	poor
Murihiku conglomerate clasts					
OU73314		hornblend altered and weathered out		5mm phenocrysts, cryptocrystalline groundmass	n/a
OU73315		feldspar altered		2-6mm phenocrysts, up to .5mm groundmass	n/a
OU73316		feldspar altered to epidote, hornblend & biotite very altered and weathered		few mm	n/a
OU73317		feldspar altered to epidote, hornblend & biotite very altered and weathered		few mm	n/a
OU73318		feldspar altered to epidote, hornblend & biotite very altered and weathered		few mm	n/a
Beaumont Formation conglomerate clasts					
OU73319		felspar altered to epidote		1-2mm	n/a
OU73320				1-2mm phenocrysts, .1mm groundmass	n/a
OU73321		plag. altered to epidote		2-3mm	n/a
OU73322		lithics altered to epidote and pumpellyite	,20:20:60	.5-4mm	poor
Spear Peak Formation conglomerate clasts					
OU73323		Epidote alteration		up to 2mm	poor
OU73324		Plag altered to epidote		up to cm	poor
OU73325		feldspar altered to epidote, hornblend & biotite very altered and weathered		few mm	n/a
OU73326				5mm phenocrysts, cryptocrystalline groundmass	n/a
OU73327		Feldspar altered to epidote		5mm phenocrysts, cryptocrystalline groundmass	n/a

(continued over page)

	Roundedness	Texture	Classification
Muirihiku Sandstone			
OU73268	sub-angular	Sedimentary	Lithic arkose
OU73310	angular	Sedimentary	Feldspathic siltstone-greywake
OU73311	angular	Sedimentary	Feldspathic siltstone-greywake
Murihiku Tuff			
OU73312	Angular (glass shows conchoidal fracture shapes)	Sedimentary	Vitric tuff
OU73313	Angular (glass shows conchoidal fracture shapes)	Sedimentary	Vitric/crystal tuff
Murihiku conglomerate clasts			
OU73314	n/a	Porphyritic volcanic	Andesite
OU73315	n/a	Porphyritic volcanic with aligned crystals	Flow ryolite
OU73316	n/a	Equigranular plutonic	granitoid
OU73317	n/a	Equigranular plutonic	granitoid
OU73318	n/a	Equigranular plutonic	granitoid
Beaumont Formation conglomerate clasts			
OU73319	n/a	Equigranular plutonic	granitoid
OU73320	n/a	Porphyritic volcanic	Porphyritic andesite
OU73321	n/a	Equigranular plutonic	granitoid
OU73322	sub-angular	Sedimentary	Litharenite/greywake
Spear Peak Formation conglomerate clasts			
OU73323	angular	Sedimentary	Greywake
OU73324	angular	Breccia with plag groundmass	Vlocanic breccia
OU73325	n/a	Equigranular plutonic	granitoid
OU73326	n/a	Porphyritic volcanic	Porphyritic andesite
OU73327	n/a	Porphyritic volcanic	Porphyritic andesite

Appendix D1

-ID-	Ou Number	SiO_2	TiO_2	Al_2O_3	$Fe_2O_3^t$	MnO	MgO	CaO	Na_2O	K_2O	P_2O_5	Loi %	Total	Recalculated to 100% total SiO_2	TiO_2	Al_2O_3	$Fe_2O_3^t$	MnO	MgO	CaO	Na_2O	K_2O	P_2O_5	Total	F1	F2	K2O/Na2(
MMD Mir295	73288	63.73	0.79	16.54	5.71	0.07	1.61	2.02	3.35	2.53	0.14	2.75	99.24	66.048	0.819	17.142	5.918	0.073	1.6686	2.0935	3.472	2.622	0.145	100	1.705	1.095	0.7552239
MMD Bm072	73289	83.21	0.48	8.10	2.05	0.09	0.37	0.08	1.48	1.55	0.03	1.88	99.32	85.396	0.493	8.3128	2.104	0.092	0.3797	0.0821	1.519	1.591	0.031	100	-5.01	-2.47	1.0472973
MMD BM 312/1	73290	76.50	0.39	11.54	2.26	0.01	0.35	0.15	2.62	2.66	0.05	2.09	98.62	79.25	0.404	11.955	2.341	0.01	0.3626	0.1554	2.714	2.756	0.052	100	-3.21	1.157	1.0152672
MMD BM 312/2	73291	75.58	0.46	12.30	2.34	0.02	0.40	0.16	3.07	2.65	0.05	1.81	98.84	77.893	0.474	12.676	2.412	0.021	0.4122	0.1649	3.164	2.731	0.052	100	-2.65	1.797	0.8631922
MMD Sp251	73292	60.99	0.81	15.14	6.47	0.11	1.98	3.55	3.30	2.02	0.11	4.81	99.29	64.553	0.857	16.025	6.848	0.116	2.0957	3.7574	3.493	2.138	0.116	100	2.653	0.383	0.6121212
MMD SP 322	73293	65.03	0.72	15.54	5.90	0.06	1.74	0.70	3.34	2.49	0.11	3.09	98.72	68.002	0.753	16.25	6.17	0.063	1.8195	0.732	3.493	2.604	0.115	100	0.44	0.176	0.745509
MMD SP 346	73294	38.30	0.50	10.54	5.41	0.12	2.50	21.79	1.84	0.66	0.12	17.15	98.93	46.833	0.611	12.888	6.615	0.147	3.057	26.645	2.25	0.807	0.147	100	14.66	5.308	0.3586957
MMD SP 347	73295	59.91	0.56	12.46	4.54	0.11	2.47	7.07	2.58	1.61	0.08	7.24	98.63	65.554	0.613	13.634	4.968	0.12	2.7027	7.7361	2.823	1.762	0.088	100	1.867	0.102	0.624031
MMD Wd	73296	69.70	0.45	10.48	4.88	0.05	1.24	3.74	2.41	1.34	0.09	4.90	99.28	73.85	0.477	11.104	5.171	0.053	1.3138	3.9627	2.554	1.42	0.095	100	0.767	-1.14	0.5560166
MMD Wd 019	73297	63.45	0.43	10.67	3.52	0.13	1.00	7.79	2.35	1.37	0.09	8.20	99.00	69.879	0.474	11.751	3.877	0.143	1.1013	8.5793	2.588	1.509	0.099	100	3.253	1.672	0.5829787
MMD Wd 148	73298	64.01	0.47	10.06	3.51	0.06	1.05	7.83	2.19	1.42	0.08	7.83	98.51	70.589	0.518	11.094	3.871	0.066	1.1579	8.6348	2.415	1.566	0.088	100	2.562	1.434	0.6484018
MMD Wd 197	73299	73.56	0.41	10.39	4.26	0.03	1.27	1.76	2.53	1.27	0.08	3.18	98.74	76.978	0.429	10.873	4.458	0.031	1.329	1.8418	2.648	1.329	0.084	100	-1	-1.93	0.5019763
MMD Hc	73300	59.47	0.71	13.25	4.70	0.09	2.63	7.04	2.67	1.64	0.10	7.08	99.38	64.431	0.769	14.355	5.092	0.098	2.8494	7.6273	2.893	1.777	0.108	100	1.852	0.1	0.6142322
MMD HC5	73301	59.88	0.71	13.38	4.81	0.09	2.67	6.76	3.00	1.64	0.11	6.90	99.95	64.352	0.763	14.379	5.169	0.097	2.8694	7.2649	3.224	1.762	0.118	100	1.869	0.367	0.5466667
MMD HC20	73302	59.65	0.71	13.31	4.75	0.09	2.64	7.03	2.97	1.64	0.10	6.90	99.79	64.216	0.764	14.329	5.114	0.097	2.8421	7.5681	3.197	1.766	0.108	100	2.004	0.507	0.5521886
MMD HC318	73303	55.96	0.87	16.74	7.71	0.07	3.60	2.27	2.51	2.16	0.11	7.20	99.20	60.826	0.946	18.196	8.38	0.076	3.913	2.4674	2.728	2.348	0.12	100	0.813	-3.28	0.8605578
MMD HC342	73304	62.09	0.57	12.86	4.74	0.09	2.64	5.83	2.95	1.64	0.09	6.30	99.80	66.406	0.61	13.754	5.07	0.096	2.8235	6.2353	3.155	1.754	0.096	100	1.095	-0.23	0.5559322
MMD HC342b	73305	61.65	0.56	12.76	4.66	0.08	2.59	5.75	2.93	1.63	0.08	6.40	99.09	66.512	0.604	13.766	5.028	0.086	2.7943	6.2035	3.161	1.759	0.086	100	1.102	-0.19	0.556314
MMD HC347	73306	60.39	0.57	12.57	4.62	0.11	2.51	7.06	2.88	1.61	0.09	7.30	99.71	65.35	0.617	13.602	4.999	0.119	2.7162	7.6399	3.117	1.742	0.097	100	1.958	0.442	0.5590278

Field no.	OU no.	Sc	V	Cr	Ni	Cu	Zn	Ga	As	Rb	Sr	Y	Zr	Nb	Ba	La	Ce	Nd	Pb	Th	U	La/Y	Ce/V
MMD Mir295	73288	16	134	40	18	24	99	19	12	77	168	28	194	8	464	26	56	20	18	12	5	0.928571429	0.417910448
MMD BM 312/1	73290	9	78	14	5	8	30	11	2	74	87	11	126	4	400	13	13	10	9	9	3	1.181818182	0.166666667
MMD BM 312/2	73291	12	84	20	9	8	35	12	8	73	100	12	152	5	355	12	9	8	10	8	4	1	0.107142857
MMD Bm072	73289	7	63	33	8	5	35	10	2	45	35	11	134	5	285	9	28	6	8	7	4	0.818181818	0.444444444
MMD SP 322	73293	21	167	35	25	20	86	17	11	70	119	22	170	7	438	14	60	19	20	9	3	0.636363636	0.359281437
MMD SP 346	73294	27	138	67	31	25	46	10	8	18	398	14	59	5	174	13	4	14	0	3	1	0.928571429	0.028985507
MMD Sp251	73292	21	173	48	28	25	84	17	5	56	138	33	162	6	451	28	42	21	9	8	5	0.848484848	0.242774566
MMD SP 347	73295	15	99	223	84	17	60	14	4	49	218	17	117	4	293	22	34	25	11	8	4	1.294117647	0.343434343
MMD Wd	73296	11	81	110	25	5	60	12	4	44	152	16	208	5	251	18	50	16	12	6	4	1.125	0.617283951
MMD Wd 019	73297	18	93	175	25	7	50	12	6	48	164	24	186	5	250	21	44	22	7	7	3	0.875	0.47311828
MMD Wd 148	73298	17	101	160	25	7	57	12	8	45	178	17	230	6	217	15	42	17	11	8	3	0.882352941	0.415841584
MMD Wd 197	73299	16	107	85	17	7	56	12	4	49	164	14	176	5	233	19	41	21	11	8	3	1.357142857	0.38317757
MMD Hc	73300	18	130	394	85	14	68	14	8	48	234	19	170	6	313	20	40	19	8	7	4	1.052631579	0.307692308
MMD HC5	73301	18	122	556	89	16	63	14	9	49	235	19	170	3	293	21	37	17	10	5	3	1.105263158	0.303278689
MMD HC20	73302	17	121	382	87	22	64	15	8	49	235	19	167	3	291	20	38	15	10	5	3	1.052631579	0.314049587
MMD HC318	73303	19	174	141	89	37	92	19	17	79	239	21	153	5	408	25	50	24	19	9	4	1.19047619	0.287356322
MMD HC342	73304	14	106	219	92	17	63	14	6	50	214	16	117	3	301	18	39	15	11	4	3	1.125	0.367924528
MMD HC342b	73305	15	105	203	88	16	62	14	5	50	213	16	117	4	300	17	34	15	11	5	3	1.0625	0.323809524
MMD HC347	73306	21	125	202	79	15	61	13	4	49	212	17	119	5	295	23	26	15	9	7	2	1.352941176	0.208

G.R 2119328 5502754		Bedding030/40/E	2119548 5502441		Bedding320/30/NE		G.R 2121195 5503037		Bedding330/30/NE		G.R 2129530 5502108 Bedding335/43/NE		
Strike	Dip	Dipdirection	Strike	Dip	Dipdirection	Sed.Strcture	Strike	Dip	Dipdirection	Sed.Strcture	Strike	Dip	Dipdirection	Sed.Strcture
330	40	NE	330	50	NE	Cross-bedding	130	30	NE	Cross-bedding	325	70	NE	Cross-bedding
315	30	NE	280	50	NE	Cross-bedding	155	40	NE	Cross-bedding	355	70	NE	Cross-bedding
0	60	E	295	50	NE	Cross-bedding	170	40	E	Cross-bedding	335	80	NE	Cross-bedding
320	30	NE	310	50	NE	Cross-bedding	180	50	E	Cross-bedding	310	40	NE	Cross-bedding
325	40	NE	330	70	NE	Cross-bedding	145	30	NE	Cross-bedding	270	70	N	Cross-bedding
355	40	NE	315	70	NE	Cross-bedding	165	40	NE	Cross-bedding	320	70	NE	Cross-bedding
340	40	NE	340	50	NE	Cross-bedding	170	35	NE	Cross-bedding	355	70	NE	Cross-bedding
350	40	NE	310	50	NE	Cross-bedding	175	45	NE	Cross-bedding	5	40	NE	Cross-bedding
325	45	NE	260	60	NE	Cross-bedding	150	40	NE	Cross-bedding	340	70	NE	Cross-bedding
320	40	NE	320	45	NE	Cross-bedding	140	45	NE	Cross-bedding	295	80	NE	Cross-bedding
350	45	E	0	70	NE	Cross-bedding	40	50	NW	Cross-bedding	315	40	NE	Cross-bedding
355	40	E	10	50	NE	Cross-bedding	60	30	NW	Cross-bedding	260	80	NE	Cross-bedding
335	40	NE	310	70	NE	Cross-bedding	160	30	NE	Cross-bedding	325	70	NE	Cross-bedding
310	60	NE	305	45	NE	Cross-bedding	82	45	N	Cross-bedding				
315	40	NE	325	50	NE	Cross-bedding	175	50	E	Cross-bedding				
290	65	NE	280	80	NE	Cross-bedding	125	60	NE	Cross-bedding				
320	40	NE	340	90	NE	Cross-bedding	160	30	NE	Cross-bedding				
			250	45	NE	Cross-bedding	145	40	NE	Cross-bedding				
							175	40	NE	Cross-bedding				
							178	30	E	Cross-bedding				
							110	30	NE	Cross-bedding				
							120	35	NE	Cross-bedding				
							160	50	NE	Cross-bedding				
							140	45	NE	Cross-bedding				
							145	50	NE	Cross-bedding				
							130	40	NE	Cross-bedding				
							150	40	NE	Cross-bedding				
							130	35	NE	Cross-bedding				
							120	30	NE	Cross-bedding				
							145	30	NE	Cross-bedding				

Spear Peak Formation

GR 2121500 5503400 Bedding150/41/W

Strike	Dip	Dipdirection	Sed.Strcture
86	30	N	Cross-bedding
86	30	N	Cross-bedding
123	30	N	Cross-bedding
99	25	N	Cross-bedding
136	30	N	Cross-bedding
107	30	N	Cross-bedding
106	20	N	Cross-bedding
64	30	N	Cross-bedding
354	35	N	Cross-bedding
354	20	N	Cross-bedding
33	30	N	Cross-bedding
9	30	N	Cross-bedding
46	30	N	Cross-bedding
17	25	N	Cross-bedding
16	25	N	Cross-bedding
336	30	N	Cross-bedding

Trend	Plunge	
356	40	Channel axes
357	40	Channel axes
26	40	Channel axes
296	40	Channel axes

G.R 2127367 5505879 Bedding230/60/W

Strike	Dip	Dipdirection	Sed.Strcture
70	90	N	Cross-bedding
120	60	NE	Cross-bedding
150	60	NE	Cross-bedding
120	40	NE	Cross-bedding
125	80	NE	Cross-bedding
150	60	NE	Cross-bedding
120	30	NE	Cross-bedding
150	90	NE	Cross-bedding
70	30	N	Cross-bedding
160	70	NE	Cross-bedding
100	90	NE	Cross-bedding
130	60	NE	Cross-bedding
120	70	NE	Cross-bedding
135	40	NE	Cross-bedding
70	70	N	Cross-bedding
150	20	NE	Cross-bedding
150	70	NE	Cross-bedding
180	90	NE	Cross-bedding
120	90	NE	Cross-bedding
170	70	NE	Cross-bedding

G.R 2128674 5504900 Bedding140/65/NE

Strike	Dip	Dipdirection	Sed.stucture
120	50	NE	Imbrication
130	60	NE	Imbrication
150	60	NE	Imbrication
145	50	NE	Imbrication
160	60	NE	Imbrication
110	50	NE	Imbrication
170	50	NE	Imbrication
175	50	NE	Imbrication
120	40	NE	Imbrication
160	40	NE	Imbrication
150	40	NE	Imbrication
105	40	NE	Imbrication
150	60	NE	Imbrication
140	40	NE	Imbrication
155	60	NE	Imbrication
140	60	NE	Imbrication
110	60	NE	Imbrication
115	40	NE	Imbrication
125	50	NE	Imbrication
145	40	NE	Imbrication
160	40	NE	Imbrication
120	60	NE	Imbrication
115	60	NE	Imbrication

G.R 2123589 5504658 Bedding210/40/W

Strike	Dip	Dipdirection	Sed.Structure
185	45	W	Ripple
175	35	W	Ripple
230	20	W	Ripple
190	40	W	Ripple
195	40	W	Ripple
185	30	W	Ripple
200	30	W	Ripple
200	20	W	Ripple
210	30	W	Ripple
190	40	W	Ripple
185	40	W	Ripple
170	40	W	Ripple
170	30	W	Ripple
210	40	W	Ripple
210	35	W	Ripple

Trend	Plunge	
280	30	Flute
280	40	Flute
260	40	Partingineation
280	40	Partingineation
260	40	Partingineation
340	20	Convolute beds axis
350	30	Convolute beds axis
335	40	Convolute beds axis
330	30	Convolute beds axis

G.R 2127671 5506260 Bedding160/30/W

Strike	Dip	Dipdirection	Sed.Structure
140	40	SW	Ripple
130	40	SW	Ripple
145	45	SW	Ripple
145	40	SW	Ripple
145	50	SW	Ripple
180	30	W	Ripple
160	40	SW	Ripple
150	30	SW	Ripple
120	40	SW	Ripple
120	40	SW	Ripple
135	50	SW	Ripple
135	40	SW	Ripple
170	30	SW	Ripple
170	40	SW	Ripple
130	45	SW	Ripple
160	30	SW	Ripple
135	40	SW	Ripple
135	30	SW	Ripple
155	30	SW	Ripple
145	40	SW	Ripple
145	30	SW	Ripple
165	30	SW	Ripple
180	30	W	Ripple

Trend	Plunge	
240	30	Flute
260	30	Flute
250	30	Flute

G.R 2122002 5504628 Bedding160/80/W(OT)

Strike	Dip	Dipdirection	Sed.Structure
150	30	E	Ripple
155	60	E	Ripple
140	40	E	Ripple
150	40	E	Ripple
150	40	E	Ripple
145	30	E	Ripple
145	50	E	Ripple
150	50	E	Ripple
155	40	E	Ripple
160	40	E	Ripple
160	40	E	Ripple
160	40	E	Ripple

G.R 2122916 5513661 Bedding 220/70/NW

Trend	Plunge	Sed. Structure
340	70	Flute
330	50	Flute
350	50	Flute
335	70	Flute
340	70	Flute
330	70	Flute
350	70	Flute
290	70	Flute
300	70	Flute
350	70	Flute
320	70	Flute
330	70	Flute
340	70	Flute
0	70	Flute
330	70	Flute
332	70	Flute
330	70	Flute
350	70	Flute
345	70	Flute
355	70	Flute
285	70	Flute
320	70	Flute
305	70	Flute
310	70	Flute
330	70	Flute
0	70	Flute
325	70	Flute

Field No.	Lattitude	Longitude	Strike	Dip (right hand rule)	Measuremnet
1	-45.5962	168.032	100	70	Bedding
2	-45.5971	168.032	296	35	Bedding
3	-45.5974	168.032	290	40	Bedding
4	-45.5977	168.032	90	45	Bedding
5	-45.5993	168.03	292	60	Bedding
6	-45.6002	168.028	302	50	Bedding
7	-45.6035	168.028	337	40	Bedding
8	-45.606	168.027	345	40	Bedding
9	-45.6076	168.026	355	50	Bedding
10	-45.6065	168.031	12	55	Bedding
11	-45.605	168.031	0	46	Bedding
12	-45.6044	168.033	5	50	Bedding
13	-45.6019	168.036	160	90	Bedding
14	-45.6015	168.037	130	50	Bedding
15	-45.5999	168.037	335	55	Bedding
16	-45.5976	168.039	130	30	Bedding
17	-45.5957	168.038	0	0	None
18	-45.5848	168.055	170	40	Bedding
19	-45.5847	168.054	170	55	Bedding
20	-45.584	168.054	172	40	Bedding
21	-45.5857	168.053	168	38	Bedding
22	-45.5865	168.052	178	40	Bedding
23	-45.5881	168.052	178	36	Bedding
24	-45.5894	168.052	182	44	Bedding
25	-45.5903	168.052	176	58	Bedding
26	-45.5911	168.052	23	30	Bedding
27	-45.5917	168.052	242	10	Bedding
28	-45.5936	168.053	230	20	Bedding
29	-45.5935	168.052	295	20	Bedding
30	-45.5919	168.051	202	20	Bedding
31	-45.5875	168.05	180	20	Bedding
32	-45.5877	168.05	205	10	Bedding
33	-45.5881	168.048	275	25	Bedding
34	-45.5901	168.044	338	52	Bedding
35	-45.591	168.045	330	40	Bedding
36	-45.5917	168.045	320	30	Bedding
37	-45.5937	168.044	0	0	None
38	-45.5948	168.043	322	30	Bedding
39	-45.5957	168.054	290	10	Bedding
40	-45.5947	168.055	292	20	Bedding
41	-45.5913	168.056	188	40	Bedding
42	-45.5894	168.055	160	40	Bedding
43	-45.5905	168.029	200	20	Bedding
44	-45.5903	168.028	2	50	Bedding
45	-45.589	168.026	340	30	Bedding
46	-45.5896	168.025	320	50	Bedding
47	-45.5909	168.024	340	55	Bedding
48	-45.5923	168.022	320	80	Bedding
49	-45.5922	168.021	340	55	Bedding
50	-45.5908	168.018	330	40	Bedding
51	-45.5921	168.016	22	60	Bedding
52	-45.5932	168.013	338	40	Bedding
53	-45.5931	168.012	325	62	Bedding
54	-45.5923	168.01	342	50	Bedding
55	-45.5924	168.007	330	48	Bedding
56	-45.5912	168.005	22	55	Bedding
57	-45.5911	168.004	209	30	Bedding
58	-45.5927	168.006	310	45	Bedding
59	-45.5936	168.006	330	43	Bedding
60	-45.5943	168.006	0	0	None
61	-45.595	168.007	350	60	Bedding
62	-45.596	168.007	362	64	Bedding
63	-45.5902	168.007	40	40	Bedding
64	-45.5881	168.006	180	20	Bedding
65	-45.5878	168.006	330	35	Bedding
66	-45.5876	168.006	5	17	Bedding
67	-45.5864	168.007	310	32	Bedding
68	-45.5854	168.009	350	30	Bedding
69	-45.5842	168.012	350	42	Bedding
70	-45.5835	168.015	0	52	Bedding
71	-45.5836	168.016	355	38	Bedding
72	-45.5836	168.021	345	40	Bedding
73	-45.5881	168.042	328	40	Bedding
74	-45.5887	168.04	340	40	Bedding
75	-45.5876	168.039	335	50	Bedding
76	-45.5876	168.034	0	0	none
77	-45.5841	168.031	350	44	Bedding
78	-45.5763	168.024	334	40	Bedding
79	-45.5772	168.021	312	44	Bedding
80	-45.5777	168.02	318	30	Bedding
81	-45.5778	168.017	332	55	Bedding
82	-45.5802	168.015	320	40	Bedding
83	-45.5813	168.015	348	40	Bedding
84	-45.5833	168.011	350	42	Bedding
85	-45.5866	168.005	0	0	none
86	-45.5861	168.004	190	40	Bedding
87	-45.5866	168.004	198	10	Bedding
88	-45.5882	168.005	195	15	Bedding
89	-45.5894	168.004	197	30	Bedding
90	-45.5898	168.022	335	50	Bedding
91	-45.5878	168.025	345	55	Bedding
92	-45.6122	168.023	0	45	Bedding
93	-45.6143	168.022	358	60	Bedding
94	-45.6149	168.02	352	48	Bedding
95	-45.6151	168.017	32	70	Bedding
96	-45.6159	168.014	356	50	Bedding
097KH	-45.6162	168.01	352	25	Bedding

Field No.	Lattitude	Longitude	Strike	Dip (right hand rule)	Measuremnet
98	-45.6157	168.009	240	40	Bedding
99	-45.6146	168.007	290	72	Bedding
100	-45.6141	168.007	242	84	Bedding
101	-45.6135	168.006	345	50	Bedding
102	-45.6115	168.007	320	48	Bedding
103	-45.6103	168.007	298	50	Bedding
104	-45.6083	168.008	270	55	Bedding
105	-45.6084	168.004	310	45	Bedding
106	-45.6059	168.003	198	82	Bedding
107	-45.6054	168.002	0	0	none
108	-45.6051	168.001	358	38	Bedding
109	-45.6031	167.998	180	70	Bedding
110	-45.5981	168.001	300	38	Bedding
111	-45.5966	168.002	338	35	Bedding
112	-45.5938	168.005	330	45	Bedding
113	-45.5855	168.05	178	43	Bedding
114	-45.5866	168.046	280	20	Bedding
115	-45.5867	168.044	354	25	Bedding
116	-45.5844	168.041	335	50	Bedding
117	-45.5821	168.038	340	60	Bedding
118	-45.5813	168.037	340	55	Bedding
119	-45.5778	168.036	0	0	none
120	-45.5774	168.035	330	25	Bedding
121	-45.5772	168.036	330	70	Bedding
122	-45.5766	168.035	328	50	Bedding
123	-45.575	168.033	340	42	Bedding
124	-45.5718	168.031	358	60	Bedding
125	-45.5702	168.031	344	62	Bedding
126	-45.5682	168.03	336	75	Bedding
127	-45.5654	168.029	338	64	Bedding
128	-45.5629	168.028	338	62	Bedding
129	-45.5625	168.029	160	80	Bedding
130	-45.563	168.03	335	75	Bedding
131	-45.5645	168.034	0	0	none
132	-45.5665	168.04	356	30	Bedding
133	-45.5723	168.048	162	35	Bedding
134	-45.5729	168.049	166	30	Bedding
135	-45.5744	168.049	172	35	Bedding
136	-45.5751	168.051	175	32	Bedding
137	-45.5746	168.052	178	28	Bedding
138	-45.5771	168.052	178	44	Bedding
139	-45.5768	168.054	175	35	Bedding
140	-45.5794	168.054	180	45	Bedding
141	-45.563	168.058	220	30	Bedding
142	-45.5625	168.056	205	28	Bedding
143	-45.5602	168.054	222	25	Bedding
144	-45.5599	168.058	214	20	Bedding
145	-45.561	168.059	215	30	Bedding
146	-45.5582	168.056	230	30	Bedding
147	-45.5587	168.052	220	20	Bedding
148	-45.5631	168.049	210	25	Bedding
149	-45.5639	168.052	200	26	Bedding
150	-45.5602	168.018	0	0	none
151	-45.5601	168.022	320	48	Bedding
152	-45.5581	168.022	335	54	Bedding
153	-45.5556	168.022	5	42	Bedding
154	-45.5539	168.023	6	70	Bedding
155	-45.5515	168.023	310	30	Bedding
156	-45.5501	168.022	14	80	Bedding
157	-45.5465	168.018	0	0	none
158	-45.5444	168.019	0	0	none
159	-45.5412	168.02	0	0	none
160	-45.5372	168.019	0	0	none
161	-45.5367	168.018	40	90	Bedding
162	-45.5359	168.014	195	30	Bedding
163	-45.5355	168.014	215	55	Bedding
164	-45.5316	168.018	268	40	Bedding
165	-45.5296	168.018	243	68	Bedding
166	-45.5282	168.017	256	88	Bedding
167	-45.5277	168.016	35	70	Bedding
168	-45.5366	168.012	222	50	Bedding
169	-45.5383	168.007	250	30	Bedding
170	-45.543	168.007	0	0	Bedding
171	-45.5465	168.005	270	42	Bedding
172	-45.5486	168.009	320	60	Bedding
173	-45.5519	168.012	30	50	Bedding
174	-45.5525	168.012	0	0	none
175	-45.5506	168	145	55	Bedding
176	-45.5392	167.973	40	60	Minor fold trend & plunge
177	-45.5383	167.977	50	90	Bedding
178	-45.5388	167.979	40	90	Bedding
179	-45.5392	167.98	280	35	Bedding
180	-45.5389	167.982	75	20	Bedding
181	-45.5358	167.985	230	25	Bedding
182	-45.5349	167.987	315	7	Bedding
183	-45.5356	167.989	195	42	Bedding
184	-45.5341	167.99	10	40	Bedding
185	-45.5334	167.991	250	60	Bedding
186	-45.5342	167.994	155	45	Bedding
187	-45.5326	167.995	340	80	Bedding
188	-45.5313	167.997	320	75	Bedding
189	-45.5309	168.002	82	60	Bedding
190	-45.5312	168.001	200	50	Bedding
191	-45.5339	167.999	25	80	Minor fold trend & plunge
192	-45.5351	167.999	82	80	Overturned bedding
193	-45.5374	167.999	255	80	Bedding
194	-45.5405	167.998	230	80	Bedding
195	-45.5436	167.996	198	50	Bedding

(continued over page)

Field No.	Lattitude	Longitude	Strike	Dip (right hand rule)	Measuremnet
196	-45.5428	167.985	330	35	Bedding
197	-45.54	167.979	225	70	Minor fold trend & plunge
198	-45.4983	168.023	235	45	Bedding
199	-45.4985	168.024	238	60	Bedding
200	-45.4994	168.026	240	48	Bedding
201	-45.5006	168.028	230	55	Bedding
202	-45.5046	168.03	0	0	Bedding
203	-45.5054	168.031	245	70	Bedding
204	-45.5077	168.035	90	13	Bedding
205	-45.5106	168.034	180	30	Bedding
206	-45.5169	168.033	0	0	Bedding
207	-45.522	168.023	0	0	Bedding
208	-45.5218	168.021	70	90	Bedding
209	-45.5212	168.018	0	0	Bedding
210	-45.5228	168.011	250	80	Bedding
211	-45.5232	168.008	255	57	Bedding
212	-45.5241	168.005	260	58	Bedding
213	-45.5232	168	255	68	Bedding
214	-45.5071	168.003	228	50	Bedding
215	-45.5124	168.02	252	70	Bedding
216	-45.515	168.024	84	50	Overturned bedding
217	-45.5165	168.024	70	50	Overturned bedding
218	-45.5158	168.024	255	70	Bedding
219	-45.5523	168.007	7	70	Bedding
220	-45.567	168.06	168	28	Bedding
221	-45.5698	168.065	0	0	none
222	-45.5721	168.022	240	50	Bedding
223	-45.5729	168.021	245	40	Bedding
224	-45.5735	168.019	243	50	Bedding
225	-45.5729	168.017	352	35	Bedding
226	-45.574	168.015	335	30	Bedding
227	-45.575	168.012	355	50	Bedding
228	-45.5737	168.012	335	42	Bedding
229	-45.5744	168.01	305	70	Bedding
230	-45.5764	168.01	120	60	Bedding
231	-45.5775	168.009	350	42	Bedding
232	-45.5787	168.007	320	30	Bedding
233	-45.5788	168.004	324	38	Bedding
234	-45.581	168.001	10	40	Bedding
235	-45.5831	168.001	342	35	Bedding
236	-45.5834	167.998	12	70	Bedding
237	-45.5826	167.997	322	30	Bedding
238	-45.5803	167.995	348	30	Bedding
239	-45.5787	167.994	280	20	Bedding
240	-45.5766	167.988	356	65	Bedding
241	-45.5734	167.987	267	42	Bedding
242	-45.5706	167.987	218	60	Bedding
243	-45.5622	167.986	348	48	Bedding
244	-45.5599	167.985	350	45	Bedding
245	-45.5549	167.983	318	45	Bedding
246	-45.5528	167.983	322	60	Bedding
247	-45.5532	167.985	330	40	Bedding
248	-45.5528	167.986	322	50	Bedding
249	-45.5517	167.987	312	50	Bedding
250	-45.5513	167.994	182	40	Bedding
251	-45.5515	167.998	260	80	Bedding
252	-45.5517	168	225	55	Bedding
253	-45.5537	168.005	348	60	Bedding
254	-45.5558	168.006	354	70	Bedding
255	-45.5555	168.008	10	80	Bedding
256	-45.5879	168.068	0	0	none
257	-45.5888	168.076	200	40	Bedding
258	-45.5884	168.077	162	60	Bedding
259	-45.5897	168.08	150	60	Bedding
260	-45.5906	168.081	164	58	Bedding
261	-45.5926	168.081	162	55	Bedding
262	-45.5954	168.082	152	58	Bedding
263	-45.5978	168.083	158	48	Bedding
264	-45.5936	168.085	165	60	Bedding
265	-45.5909	168.085	170	70	Bedding
266	-45.5905	168.088	154	62	Bedding
267	-45.59	168.09	140	60	Bedding
268	-45.5938	168.092	130	60	Bedding
269	-45.59	168.091	0	0	none
270	-45.5856	168.092	150	60	Bedding
271	-45.5834	168.09	156	58	Bedding
272	-45.5815	168.091	180	62	Bedding
273	-45.5802	168.089	135	75	Bedding
274	-45.5786	168.088	190	55	Bedding
275	-45.5766	168.084	145	60	Bedding
276	-45.5737	168.081	180	60	Bedding
277	-45.5713	168.08	152	70	Bedding
278	-45.5718	168.078	142	38	Bedding
279	-45.5729	168.077	210	30	Bedding
280	-45.5753	168.074	260	30	Bedding
281	-45.5766	168.074	230	30	Bedding
282	-45.5775	168.075	160	55	Bedding
283	-45.579	168.078	205	30	Bedding
284	-45.5811	168.081	240	10	Bedding
285	-45.5827	168.079	70	40	Bedding
286	-45.5855	168.077	220	30	Bedding
287	-45.5866	168.074	0	0	none
288	-45.5848	168.069	0	0	none
289	-45.581	168.074	160	70	Bedding
290	-45.5801	168.074	155	68	Bedding
291	-45.5805	168.076	160	68	Bedding
292	-45.5807	168.067	0	0	none
293	-45.5809	168.065	180	40	Bedding

Field No.	Lattitude	Longitude	Strike	Dip (right hand rule)	Measuremnet
294	-45.5811	168.064	190	30	Bedding
295	-45.5656	168.084	155	55	Bedding
296	-45.5638	168.076	240	20	Bedding
297	-45.5682	168.02	300	30	Bedding
298	-45.5782	168.025	330	30	Bedding
299	-45.5807	168.018	0	0	none
300	-45.5795	168.02	325	40	Bedding
301	-45.5702	168.017	310	50	Bedding
302	-45.5712	168.01	255	20	Bedding
303	-45.5719	168.009	260	50	Bedding
304	-45.571	168	290	35	Bedding
305	-45.5683	167.996	0	70	Bedding
306	-45.5676	167.988	340	70	Bedding
307	-45.5616	167.986	350	50	Bedding
308	-45.5809	168.086	310	50	Bedding
309	-45.5802	168.088	0	0	none
310	-45.5802	168.088	0	0	none
311	-45.5736	168.02	332	41	Bedding
312	-45.5764	168.017	330	30	Bedding
313	-45.5771	168.016	175	5	Bedding
314	-45.5777	168.014	335	30	Bedding
315	-45.5798	168.009	0	0	none
316	-45.58	168.008	20	80	Bedding
317	-45.5787	168.007	20	85	Bedding
318	-45.5045	167.977	0	0	none
319	-45.5706	168.036	0	0	none
320	-45.5819	168.065	0	0	none
321	-45.5675	168.019	315	45	Bedding
322	-45.5673	168.017	325	40	Bedding
323	-45.5666	168.015	285	42	Bedding
324	-45.5676	168.012	280	45	Bedding
325	-45.5688	168.011	235	60	Bedding
326	-45.5705	168.008	225	80	Bedding
327	-45.5705	168.007	285	45	Bedding
328	-45.5702	168.005	290	50	Bedding
329	-45.5689	168.004	264	45	Bedding
330	-45.5685	168.005	15	80	Bedding
331	-45.5669	168.003	10	60	Bedding
332	-45.566	168.004	12	60	Bedding
333	-45.5645	168.006	350	80	Bedding
334	-45.5638	168.007	260	50	Bedding
335	-45.563	168.008	180	75	Bedding
337	-45.5622	168.004	254	55	Bedding
338	-45.5643	168.001	333	55	Bedding
339	-45.5617	168.001	342	80	Bedding
340	-45.5568	168.008	10	65	Bedding
341	-45.5779	168.009	20	40	Bedding
342	-45.4802	168.047	217	66	Bedding
343	-45.4994	168.004	0	0	none
344	-45.5655	168.04	0	0	none
345	-45.5701	167.966	250	50	Bedding
346	-45.5661	167.947	30	70	Bedding
347	-45.5436	167.967	40	60	Bedding
348	-45.5467	167.97	30	90	Bedding
349	-45.5472	167.97	230	60	Bedding
350	-45.5439	167.974	270	80	Bedding
351	-45.571	168.008	0	0	none
352	-45.572	168.006	320	75	Bedding
353	-45.5737	168.003	270	50	Bedding
354	-45.5723	167.999	295	45	Bedding
355	-45.574	167.995	245	50	Bedding
356	-45.5763	167.993	30	40	Bedding
357	-45.5792	167.996	320	30	Bedding
358	-45.5818	167.996	345	40	Bedding
359	-45.5823	167.995	335	43	Bedding
360	-45.5831	167.995	245	45	Bedding
361	-45.5839	167.993	315	45	Bedding
362	-45.5845	167.993	330	40	Bedding
363	-45.5843	167.995	310	30	Bedding
364	-45.584	167.996	355	55	Bedding
365	-45.5848	167.998	15	50	Bedding
366	-45.5853	167.999	0	0	none
367	-45.5853	167.999	10	90	Bedding
368	-45.5864	168	305	30	Bedding
369	-45.5869	168.001	220	30	Bedding
370	-45.5883	168.002	185	20	Bedding
371	-45.5829	168.003	180	25	Bedding
372	-45.5815	168.004	25	50	Bedding
373	-45.5711	168.019	0	0	none
374	-45.5506	167.99	180	30	Bedding
375	-45.5567	167.986	320	45	Bedding
376	-45.5587	167.986	320	55	Bedding
377	-45.555	167.989	320	35	Bedding
378	-45.554	167.99	310	50	Bedding
379	-45.5529	167.99	10	45	Bedding
380	-45.545	167.988	0	0	none

Field no.	OU no.	Easting	Northing	sample type
299	73281	2121303	5502554	Bm (coal)
315/s	73282	2120559	5502667	Bm (coal)
315/n	73283	2120559	5502667	Bm (coal)
357	73284	2129548	5502441	Bm (coal)
72	73285	2121555	5502255	Bm (coal)
357a	73286	2129548	5502441	Bm (coal)
87	73287	2120243	5501832	Bm (coal)
295	73288	2126335	5504548	Mr (sandstone)
312/3	73289	2121195	5503037	Bm (sandstone)
312/1	73290	2121195	5503037	Bm (sandstone)
312/2	73291	2121195	2121195	Bm (sandstone)
251	73292	2129551	5505702	Sp (sandstone)
322	73293	2121163	5504039	Sp (sandstone)
346	73294	2125657	5503667	Sp (sandstone)
347	73295	2127119	5506256	Sp (sandstone)
wd1	73296	2123076	5501780	Wd (sandstone)
19	73297	2124098	5502285	Wd (sandstone)
148	73298	2123589	5504658	Wd (sandstone)
197	73299	2127952	5506883	Wd(sandstone)
Hc	73300	2122900	5513700	Hc (sandstone)
Hc 5	73301	2122900	5513700	Hc (sandstone)
Hc 20	73302	2122900	5513700	Hc (sandstone)
318	73303	2127610	5508240	Hc (sandstone)
342	73304	2122916	5513661	Hc (sandstone)
342b	73305	2122916	5513661	Hc (sandstone)
347	73306	2127119	5506256	Hc (sandstone)
223	73307	2121504	5503444	Sp (sandstone)
ID2	73308	2120214	5505662	Wd (sandstone)
129	73309	2122002	5504628	Wd (sandstone)
Msilt	73310	1211943	5499090	Mr (sandstone)
Mss	73311	2121836	5498847	Mr (sandstone)
tuff1	73312	2124030	5505570	Mr (tuff)
tuff2	73313	2120559	5502617	Mr (tuff)
MP1	73314	2114700	5487420	Mr (pebble)
MP4	73315	2114700	5487420	Mr (pebble)
MP2	73316	2114700	5487420	Mr (pebble)
MP3	73317	2114700	5487420	Mr (pebble)
MP5	73318	2114700	5487420	Mr (pebble)
BmP1	73319	2121555	550225	Bm (pebble)
BmP2	73320	2121555	550225	Bm (pebble)
BmP3	73321	2121555	550225	Bm (pebble)
BmP4	73322	2121555	550225	Bm (pebble)
SpP1	73323	2121500	5503400	Sp (pebble)
SpP2	73324	2121500	5503400	Sp (pebble)
SpP3	73325	2121500	5503400	Sp (pebble)
SpP4	73326	2121500	5503400	Sp (pebble)
SpP5	73327	2121500	5503400	Sp (pebble)
Bm Hm	73328	2121195	2121195	Bm (heavym ineral)
Sp Hm	73329	2117300	5505900	Sp (heavym ineral)
Wd Hm	73330	2124098	5502285	Wd (heavymineral)
Hc Hm	73331	2122900	5513700	Hc (heavymineral)
	Fossil record forms			
Horizon A	FRF D43 f 036	2124900	5502950	Waicoe foram
Horizon B	FRF D43 f 037	2123050	5500450	Waicoe foram
Horizon C	FRF D43 f 038	2117600	5518500	Waicoe foram

Appendix H

The geology of the Burwood sub -Basin Mount Hamilton - Mararoa River western Southland

1:25 000
Geological Map

By
Michael P. McDonnell

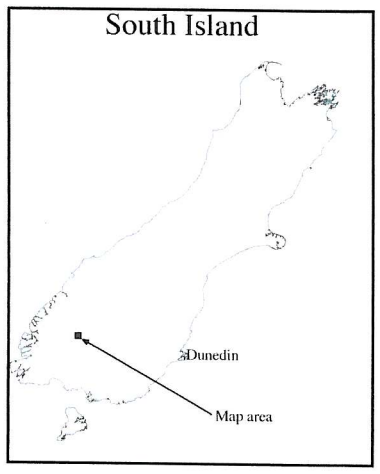

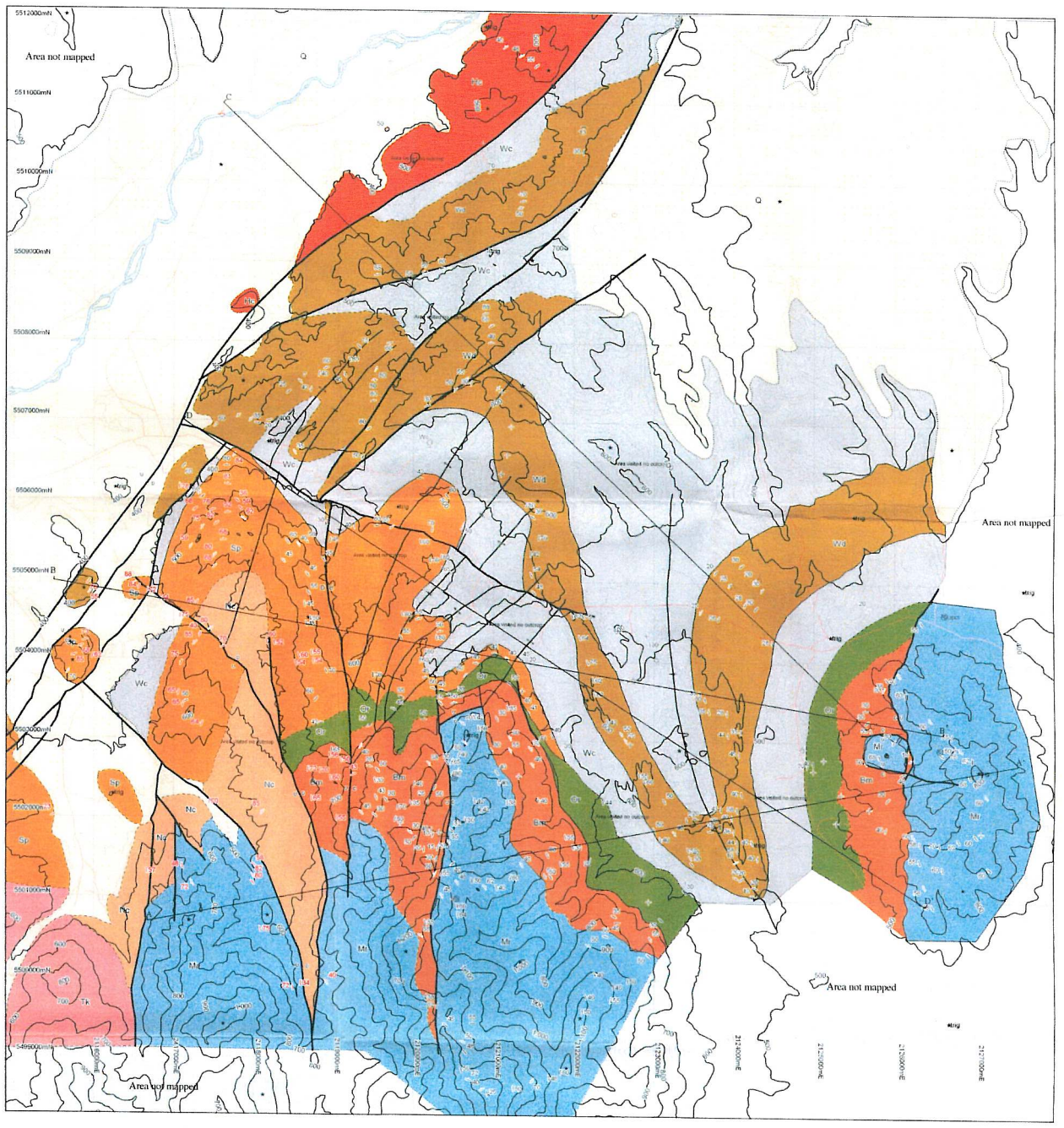

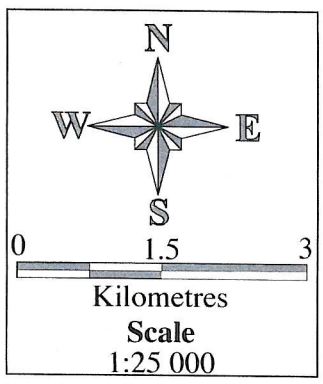

Bedding data shown in red are from Kirby (1989)

Fossil localities labelled JDC were collected by Dr J.D Campbell.

Topographic information is from the Map Info database

Grid is New Zealand Map Service grid

Cross-section D-D' is shown in figure 6.4

A full list of bedding data is presented in appendix F

Legend

Topographic symbols

- High point
- 20m contour
- 100m contour
- Road
- River

Geological Symbols

- Micro-fossil locality
- Leaf fossil
- Macro-fossil locality
- Outcrop (no bedding measurements taken)
- Strike and dip
- Overturned bedding (strike and dip)
- Minor s-fold
- Anticline axis
- Syncline axis
- Fault
- Inferred contact
- Appoximate contact
- Accurate contact

Geological units

	Q	**Quaternary sediments** - Coarse clastic glacial outwash gravel, talus fan and river plain deposits.	Quaternary
		Unconformity	
Waiau Group	Wc	**Waicoe Formation** - Massive grey calcareous mudstone.	Miocene
	Hc	**Haycocks Formation** - Interbedded sandstone and mudstone in a generally thinning and fining upward sequence.	
		Fault contact	
	Wc	**Waicoe Formation** - Massive grey calcareous mudstone.	
	Wd	**Weydon Formation** - Interbedded graded sandstone and mudstone, forming a number of thickening upward "packets" within massive grey calcareous mudstone.	Oligocene
	Wc	**Waicoe Formation** - Massive grey calcareous mudstone.	
	Sp	**Spear Peak Formation** - Dominantly interbedded sandstone and mudstone with lenses of conglomerate and breccia near the base, forms a generally fining upward sequence.	
		Conformable contact	
Nightcaps Group	Undifferentiated Nightcaps Group. Nc Or	**Orauea Mudstone** - Massive brown carbonaceous mudstone.	Eocene
	Nc Bm	**Beaumont Formation** - Carbonaceous grey mudstone overlain by thin to thick bedded sandstone and conglomerate, contains minor coal seams.	
		Unconformity	
	Mr	**Murihiku Supergroup** - Thick bedded grey siltstone, with interbedded conglomerate and graded sandstone beds.	Triassic
		Fault contact	
	Tk	**Takitimu Group** - Arc volcanic rocks and volcaniclastic sediment.	Permian